

**GENERATION OF AN INTEGRATED KARYOTYPE OF THE HONEY BEE  
(*Apis mellifera* L.) BY BANDING PATTERN AND FLUORESCENT *IN SITU*  
HYBRIDIZATION**

A Dissertation

by

GILDARDO AQUINO PEREZ

Submitted to the Office of Graduate Studies of  
Texas A&M University  
in partial fulfillment of the requirements for the degree of

DOCTOR OF PHILOSOPHY

December 2007

Major Subject: Entomology

**GENERATION OF AN INTEGRATED KARYOTYPE OF THE HONEY BEE  
(*Apis mellifera* L.) BY BANDING PATTERN AND FLUORESCENT *IN SITU*  
HYBRIDIZATION**

A Dissertation

by

GILDARDO AQUINO PEREZ

Submitted to the Office of Graduate Studies of  
Texas A&M University  
in partial fulfillment of the requirements for the degree of

DOCTOR OF PHILOSOPHY

Approved by:

Chair of Committee, J. Spencer Johnston

Committee Members, Craig Coates

Robert N. Coulson

David M. Stelly

Head of Department, Kevin Heinz

December 2007

Major Subject: Entomology

## ABSTRACT

Generation of an Integrated Karyotype of the Honey Bee (*Apis mellifera* L.) by Banding Pattern and Fluorescent *In Situ* Hybridization. (December 2007)

Gildardo Aquino Perez, B.S. Universidad Autónoma Chapingo;

M.S., Colegio de Postgraduados,

Texcoco, Estado de México, México

Chair of Advisory Committee: Dr. J. Spencer Johnston

To enhance the scientific utility and practical application of the honey bee genome and assign the linkage groups to specific chromosomes, I identified chromosomes and characterized the karyotype of the sequenced strain DH4 of the honey bee. The primary analysis of the karyotype and ideogram construction was based on banding and Fluorescence In Situ Hybridization (FISH) for rDNA detection. FISH confirmed two locations for the NOR on telomeric regions of chromosomes 6 and 12 plus an additional less frequent signal on chromosome 1, all three of which were confirmed with silver staining (AgNO<sub>3</sub>), 4',6-diamidino-2phenylindole (DAPI), and C-Banding methods were used to construct the primary ideograms that served as a basis to further identify the chromosomes and locate important structures. The primary map was compared with Giemsa banding, AgNO<sub>3</sub>-banding, Trypsin banding, and R-banding. The karyotype of the honey bee was established as two metacentric chromosomes (1 and 10), two submetacentric with ribosomal organizer (6 and 12), four submetacentric heterochromatic chromosomes (16, 15, 4 and 13), four euchromatic subtelocentric chromosomes (2, 8, 11 and 14) and four acrocentric chromosomes (3, 5, 7 and 9). *In situ* nick-translation banding methods were used to verify the heterochromatin distribution. The cytogenetic maps of the honey bee karyotype represented in the ideograms were subsequently used to place 35 mapped BACs (Solignac et. al. 2004) of Solignac's BAC library. As the BACs hybridized to multiple sites, the mapping was based on strength and frequency of the signals. Location and position of the BACs was compared with

those published in the different version of Map Viewer of the NCBI and BeeBase web sites. 10 BACs were confirmed with the last version of Map Viewer V4, 12 BACs were mapped based on high frequency and agreement with the earlier version of Map Viewer. 14 BACs were mapped as confirmed based on moderate frequency of the signal and agreement with the last version of MVV, most of these BACs hits as a secondary signal.

## DEDICATION

To my Children: Verónica Donají, Elisa Aurora, and Marco Antonio

To my Wife: Bertha López Santiago

To my Father, Luis Rey Aquino Figueroa,  
To my Mother, Elisa Aurora Pérez Bláz (†)

To God, who is Hope for everyone who suffers from injustice, abandon and contempt; the Source of forgiveness and hope of new life for the hopeless and repentant; the Glory of those who even without knowing Him but because of their actions are righteous people.

## ACKNOWLEDGEMENTS

I am very grateful to Drs. Kim Jeong-Soon and Nurul Islam-Faridi from the Dept. of Crop and Soil Sciences, Texas A&M University, College Station, TX, and Dr. M. Mandrioli from Dipartimento di Biologia Animale, Università di Modena, Italy, for their kind recommendations spread preparations, to Dr. P. Klein from the Institute for Plant Genomics and Biotechnology of Texas A&M University for providing the BDG-512 rDNA clone, to Dr. Tanya Pankiew for providing the biological material for DNA extraction, to Danny Weaver Apiaries of Navasota, TX, for providing the DH4 strain drones, and to Dr Hong-bin Zhang of the Department of Plant and Soil Science of Texas A&M University for his valuable help in the DNA extraction and purification. My special thanks to Dr. David Stelly for his friendship and support in the microscope facilities, and comments and suggestions during the experimental and writing work, and Dr. Robert Coulson, Dr. Craig Coates, and Dr. Patricia Pietrantonio, current and former members of my committee, for their support, suggestions and commentaries on my work. For their friendship and important logistic support, I am grateful to Dr Benjamin Figueroa, Dr. Felix Gonzalez, Dr Nina M. Barcenaz, Fransisco Morales, Erasmo Rubio, Ivan Ramirez, Alma Solís, and Beatriz Rodriguez. Special thanks go to Miss Caroline Jones for her important support to my family, including friendship and valuable teaching. I would like to express my appreciation to my father and mother (†), sisters and brothers, who with their hard work supported my education. Above all, my gratitude goes to my family, who are my life, the reason to face the challenges of every day. To all I missed, my apologies and thanks.

I am deeply grateful and indebted to my advisor and Chair of my Committee, Dr J. Spencer Johnston and his wife Diane, for their remarkable approachability and patience. To Dr. Johnston, for his support as I pursued my PhD in the Department of Entomology of Texas A&M University, and who provided not only the important economic support through an assistantship but also by his constructive comments and suggestions to gain experience in my novel field of molecular cytogenetics.

## TABLE OF CONTENTS

	Page
ABSTRACT .....	iii
DEDICATION .....	v
ACKNOWLEDGEMENTS .....	vi
TABLE OF CONTENTS .....	vii
LIST OF FIGURES.....	viii
LIST OF TABLES .....	x
 CHAPTER	
I    INTRODUCTION .....	1
II   CHARACTERIZATION OF THE KARYOTYPE OF DRONES OF STRAIN DH4 OF <i>Apis mellifera</i> L .....	9
Introduction.....	9
Materials and Methods .....	12
Results.....	17
Discussion.....	51
III  MAPPING 35 CLONES FROM SOLIGNAC’S BAC LIBRARY ON THE KARYOTYPE OF HONEY BEE .....	57
Introduction.....	57
Materials and Methods .....	60
Results.....	64
Discussion.....	96
IV <i>IN SITU</i> NICK-TRANSLATION BANDING IN DH4 HONEY BEE DRONE CHROMOSOMES .....	103
Introduction.....	103
Materials and Methods .....	105
Results.....	107
Discussion.....	116
V    CONCLUSIONS AND FUTURE WORK .....	120
REFERENCES .....	125
APPENDIX .....	150
VITA .....	186

## LIST OF FIGURES

FIGURE		Page
1	Standard deviation for three files and stages of prophase .....	20
2	Means for (a) Arm ratio, (b) chromosome, (c) short and (d) long arm length of individual chromosome at four stages of prophase, and stained with DAPI.....	24
3	Chromosome classification at different stages of prophase.....	27
4	Means for (a) Relative length and (b) arm ratio of chromosomes of honey bee stained with six methods .....	28
5	Number of bands detected in honey bee chromosomes using DAPI staining method at four stages of prophase.....	30
6	Number of bands detected in honey bee chromosomes.....	31
7	Banding pattern of honey bee chromosomes based on Ba(OH) <sub>2</sub> .....	34
8	Relative content of heterochromatin in honey bee chromosomes .....	36
9	Comparative ideograms and banding classification of chromosomes of honey bee stained with DAPI (D), Ba(OH) <sub>2</sub> (C), giemsa (G), trypsin (T), AgNO <sub>3</sub> (nr), and R-banding (R) at different stages of prophase .....	49
10	Examples of count plots and histograms for detecting location and position of the BACs on the chromosomes of honey bee.....	68
11	Examples of plots to map the BACs in the chromosomes of honey bee .	69
12	Examples of FISH experiments for mapping 35 BACs of Soliganc library.....	70
13	Examples of FISH experiments for mapping 35 BACs of Soliganc library for multiple experiments .....	71
14	Map references of 35 BACs of Soliganc library by chromosomes .....	78
15	Position of the signals on the chromosomes represented by the Ba <sub>2</sub> OH-C-banding ideogram (up), and map location with BAC names (down), Group 1 .....	84



FIGURE	Page
16	Position of the signals on the chromosomes represented by the Ba <sub>2</sub> OH-C-banding ideogram (up), and map location with BAC names (down), Group 2 ..... 85
17	Position of the signals on the chromosomes represented by the Ba <sub>2</sub> OH-C-banding ideogram (up), and map location with BAC names (down), Group 3 ..... 86
18	Cases of BACs synteny on the chromosomes of honey bee..... 93
19	Cases of synteny of the Solignac BACs in honey bee chromosomes..... 95
20	Preliminary test with in situ biotin-nick translation mix kit (Roche Applied Science) on honey bee chromosomes at 15°C and developed with streptavidin-Cy3 conjugate..... 109
21	Banding evidence obtained from use of the biotin and digoxigenin nick translation mix (Roche Applied Science) on prophase chromosomes of honey bee ..... 110
22	Comparative nick translation banding pattern with Ba(OH) <sub>2</sub> -C- and DAPI banding ..... 114
23	Number of bands of honey bee chromosomes digested by the nick translation mix (Roche Diagnostic GmbH, Penzberg, Germany) system ..... 116

## LIST OF TABLES

TABLE		Page
1	Mean and standard deviation for chromosome length ( $\mu\text{m}$ and %) and arm ratio for different data files .....	19
2	Analysis of variance (ANOVA) for arm ratio .....	21
3	Chromosome classification based on arm ratio .....	26
4	Average length and arm ratio of honey bee chromosomes.....	27
5	Means of number of bands read per staining method and stage of prophase for DAPI method .....	29
6	Heterochromatin content in honey bee chromosomes based on $\text{Ba}(\text{OH})_2$ and DAPI staining methods.....	35
7	List of the Solignac BACs worked with Fluorescence In Situ Hybridization (FISH).....	66
8	Mapped signals, places confirmed, places suggested and places for secondary signals for 35 FISHed BACs .....	74
9	Number of BAC signals observed in the FISH experiments, location and position on the chromosome grouped by coincidences with the different versions of NCBI Map Viewer .....	88
10	Approximate relative distances between pairs of BACs in four chromosomes of honey bee.....	96

## CHAPTER I

### INTRODUCTION

Based on the small genome and the impact of the honey bee in the human life and activities, the National Human Genome Research Institute (NHGRI) selected the honey bee as a high priority organism for sequencing (Evans and Gundersen-Rindal, 2003). Complete sequencing of the genome was carried out by the Human Genome Sequencing Center at Baylor College of Medicine (BCM-HGSC) supported by the Honey Bee Genome Sequencing Project (HBGSP), and the last version of the sequence (Amel\_4.0) was released in March 2006 (HBGSP, 2006). The sequence is currently available at the National Center for Biotechnology Information (NCBI) and BeeBase-TAMU web sites (HBGSP, 2006). Amel\_4.0 is primarily based on a whole genome shotgun (WGS) assembly strategy. The final assembly is partially supported by the physical BACs because of instability of the clones used (HBGSP, 2006, Supplementary Notes and Methods). The availability of a cytogenetic map based on a karyotype characterization is vital to integrate information generated for the genome project and enhance the reliability and robustness of the different maps [recombinational maps based on RAPDs by Hunt and Page (1995), microsatellites by Solignac et al. (2004) and the sequence map (HBGSP, 2006)] now available. Although the sequence was assembled with the aid of mapped molecular markers, the order and location of the markers on a physical cytogenetic map are yet to be established. The molecular cytogenetic characterization and identification of chromosomes are an important and necessary parts of a complete genome project, and have been carried out in this study.

Currently, molecular cytogenetic mapping and chromosome identification without a traditional karyotype characterization have been carried out in insect species and plants with a small genome and correspondingly small chromosomes (Guzzo et al., 2000; Cheng et al., 2002; Kim, et al., 2003; Jiang and Gill, 2006; Shoguchi et al., 2004,

---

This dissertation follows the style of Cytogenetic and Genome Research.

2005 and 2007). Small chromosomes usually exhibit little information in metaphase chromosomes banding; they usually are very highly packed. Even so, the availability of this resource is invaluable. It is important to correlate the morphology of the karyotype with the available genetic and physical maps in order to increase the accuracy, and diagnostic value with regard to chromosomal abnormalities (Taucher et al., 1996). Chromosomes structures are landmarks that unambiguously can track the molecular markers and determine the final and correct organization and order in the maps (Shoguchi et al., 2005). Chromosomal banding patterns and *in situ* hybridization of fluorescently labeled DNA (FISH) provide additional landmarks for preparation of cytological maps. The importance of banding and physical chromosome markers generated interest in producing specific chromosome band probes to overcome limitations in resolution of M-FISH and SKY (Liehr and Clausen 2002) to detect subtle rearrangements in the chromosomes.

The centromeres, nucleolus organizers (NORs), banding patterns and constrictions have been the most reliable cytogenetic markers. They help not only to orient and validate the physical and genetic maps, they also provide important background information. The centromere, heterochromatin bands and telomeres have a definitive influence on recombination and gene expression. They are related not only to phylogenetics but also to the ontogenetic history of the organism (Sullivan et al., 2001; Straub and Becker 2007). Knowledge of the cytogenetic map becomes invaluable to study the interaction of the macro and micro-organization of the genome and understand its consequences in characteristics of interest such as productivity, evolution, disease resistance, and fitness improvement (Sumner 2003). It is general knowledge that imprinting, an extremely important mechanism, is dependant on heterochromatin and chromosome banding. Related with heterochromatin and chromosome banding are gene and chromosome inactivation, as in the X chromosome in mammals and marsupials, sex determination in insects [coccids and some parasitic wasp (Nur 1980, Herrick and Seger, 1999)], and gene regulation and expression in plants (Baroux et al., 2002; de la Casa-Esperon and Sapienza, 2003), animals (Chandra and Brown 1975; O'Neil et al., 2000;

Killian et al., 2001), and other insects (Lloyd, 2002; de la Casa-Esperon and Sapienza, 2003; Field et al., 2004). In mammals, banding patterns have a remarkable importance because imprinting appears to rely on differential chromatin structure. Aberrant imprinting has been implicated in various human cancers and, in a number of cloned mammals, potentially limits the usefulness of somatic nuclear transfer (Lloyd et al., 2002).

Knowledge of the banding distributions on chromosomes of the honey bee is considered particularly important to address questions about gene regulation and expression in caste determination and division of labor (Drupeau, 2006). In social insects such as honey bee, the imprinting mechanism is thought to be related to the gene expression that determines caste and social organization (Queller, 2003). Support of this hypothesis relies on the existent literature on the genes that reside in constitutive and facultative heterochromatin and the regulation of these genes by juxtaposition (Tulin et al., 1998), heterochromatic gene expression (Schulze et al., 2006; Shi et al., 2006), and position of the genes in relation to heterochromatin (Dimitri, 1995; Gvozdev et al., 1999; Tulin et al., 1998; Schotta et al., 2003). Cis and trans influences of heterochromatin, and in ON and OFF regulation of advancing and retiring heterochromatinization have also reported (Dimitri et al., 1995; Gvozdev et al., 1999; Roshchina et al., 2005). An imprinting and banding relationship has been documented in Prader-Willi and Angelman syndromes (Lalande, 1997), mosaics and imprinting polymorphisms (Jinno et al., 1994). In *Drosophila* the relation between heterochromatin banding, imprinting and gene silencing is very well documented (Tulin et al., 2002, Yasuhara and Wakimoto, 2006).

It is well known that adult worker honeybees typically shift from working in the hive to foraging for nectar and nurses activities (HBGPC, 2006). Genomics and proteomics related to these changes have been documented (Corona et al., 1999; Evans and Wheeler, 1999, 2000; Chan et al., 2006; Adam et al., 2006), and hypotheses about the possible mechanism of social behavior include chromosome organization (Robinson and Ben-Shahar, 2002). The latter suggest “evolution via gene duplication and diversification that result in changes in protein coding or regulatory sequence”. It is

probable that those changes are based, at least in part, on genes expression regulated by heterochromatin plasticity.

It isn't enough to know the genome at the molecular and recombination level; it is important to know the structure and organization of the genome at the cytological level and know the macro organization of the heterochromatin in the honey bee genome. Knowledge of the location and position of the genes or gene clusters on morphologically different chromosomes and different region of the chromosome helps to understand the function and expression pattern of those genes. For example, the major royal jelly (MRJP) cluster, a cluster of genes that encodes for protein substances responsible for castes differentiation (Drapeau et al, 2006) was assigned a subtelomeric position in chromosome 11 in the Map Viewer of NCBI, although the genomic clone (57E10) that carries this cluster was mapped on chromosome 4 in this study. This cluster, whether on chromosome 11 or 4, is located in an overlapping facultative band region, suggesting heterochromatin band regulation. Thus, the cytogenetic characterization of the honey bee genome through the banding pattern of the karyotype can easily be justified.

Cytological characterization of the banding pattern of chromosomes also helps with the mapping and assembly, detecting regions of conflict between the genetic and physical maps. Included are large repetitive sequence regions that in cytogenetic studies (and depending on staining method) are detected as dark bands. In the current physical and genetic maps, these region are detected as gaps, due to absence or reduced levels of recombination or because repetitive sequence are usually difficult to clone and sequence (Adams et al., 2000; Hosking et al., 2000; Topp and Dawe 2006). Many times, repetitive fragments are cloned as part of large unique sequences; in other cases those fragments integrate into a chimeric clone that detrimentally influence the mapping process (Yasuhara, et al., 2003; HBGPC, 2006) and reduce the reliability of those maps. Linkage maps and cytogenetic maps can help to reduce those problems; however, the resolution of linkage maps is frequently lower than the cytogenetic map, and frequently are non linear due to the inherent problem of differential recombination rates between gene rich and gene poor region, between C/G rich and A/T rich regions and at the cytogenetic

level, between heterochromatin and euchromatin (Kim et al., 2005b; Granau et al., 2006). The literature in this subject is vast, one of the most recent reviews is Corradini et al. (2007). It is very well documented that recombination in euchromatin is higher than in heterochromatin. The low rate of recombination in heterochromatin is not only because of the tightly packed nature but also for the frequent inverted repeats that prevent recombination, most of these inversions are derived from mobile elements. The rate varies greatly with the structure and composition of heterochromatin, while transposable elements have contributed to the plasticity of heterochromatin by stimulating chromosome rearrangement or gene transfer into a particular environment (Yasuhara et al., 2003; Fu et al., 2002; Corradini et al., 2007). Physical maps potentially have a very high level of resolution because they are based on overlapping clonal relationships, which enable effective usage of cloned libraries for sequencing, molecular analysis and comparative studies. However, increasing kinds of evidence suggest a poor relationship of the physical map with linkage maps. When this relationship fails, physical maps become a fragmented collection of ordered sequences (Kim, 2003). A cytogenetic map alone is limited in utility because of the resolution; and that limitation is greatest for small chromosomes and genomes. However, molecular cytogenetics resolution assisted by FISH typically will exceed the resolution of linkage maps in large, low-recombination regions (Kim, 1993).

Cytogenetic maps based on karyotype characterization (arm ratio, position of constrictions, banding pattern) that are enriched with FISHed molecular markers enable comparative studies, detection of changes in chromosomal structures, patterns in mitosis and meiosis, and provides elements to assess recombination and physical map relationships (Kim, 1993; Harper and Cande, 2000). Fluorescence *in situ* hybridization (FISH) has become the most reliable technique for physical mapping. However, its resolution is limited by the size of the probes. With use of antibodies, detection is possible for fragments as small as 5 KB, but with the consequently annoying background (Bentley, 1990). Probes of 1-3 KB long, in some cases < 1 KB, have been detected but the frequency of detection and reproducibility is very low (Jiang and Gill, 2006). In

general, FISH cannot resolve signal separation beyond 130 KB (0.2-3  $\mu\text{m}$ ) in interphase nuclei (G2) and 1Mb (0.4 $\mu\text{m}$ ) in metaphase chromosomes (Bentley, 1990, Cheng et al., 2002). Using two-color FISH to metaphase chromosomes; the resolution between signals cannot be increased beyond 750 kb (Bentley, 1990). However, with fiber-FISH the resolution can be increased (to 3.21 kb/ $\mu\text{m}$  in rice chromosome analysis Cheng et al., 2002). Detection and correct location of probes can also be affected by the size and phase of the chromosomes, as well as occurrence of repetitive DNA in the probes and genomes, all of which necessitate high levels of assessment (Cheng et al., 2002; Jiang and Gill, 2006).

Currently, FISH techniques have been diversified to fit almost every necessity. FISH has been used to determine chromosomes number and structure (Davison et al., 2002; Kearney 2006; Jiang and Gill 2006), changes in ploidy and introgression (Dong et al., 2001; Eastmond et al., 1995), genome evolution (Tönnies et al., 2001; Wienberg, 2005), transgenesis and dynamics of mobile elements (Dong et al., 2001; Krustaleva and Kik, 2001), karyotyping and chromosome identification (Geigl et al., 2006), changes in chromosome structure and abnormalities (Boggs and Chinault, 1997; Slotter et al., 2000; Natarajan and Boei, 2003), microbiology detection (Moter and Göbel, 2000; Bottari et al., 2006), DNA-peptide association detection (Bottari et al., 2006), chromosome banding (Liehr et al. 2006), and genetic improvement (Oleszczuk et al., 2002). *Ciona intestinalis* has very small chromosomes and a small genome, and its sequencing maps and scaffold alignments are supported by FISH landed BACs (Shoguchi et al., 2005 and 2007). The FISH procedure has been routinely used to verify the genome sequence maps in human and *Drosophila* (The International Human Genome Mapping Consortium 2001), to characterize the genes of *Drosophila* that resides in heterochromatin regions (Rossi et al., 2007), to map genome heterochromatin sequencing (Hosking et al., 2002), and to determine structural chromosome organization using mobile elements (Yan et al., 2002), to detect and differentiate of sex chromosomes, as in several species of Lepidoptera (Traut et al., 1999). In *Aedes aegypti*, FISH is used to integrate the genetic linkage groups and the physical maps (Brown, 2001; Sallam et al., 2005; Severson et al.,



2004), In *Bombyx mori* FISH is applied to assign the small, holocentric chromosomes to linkages groups using a BAC library (Yoshido et al., 2005) and comparative analysis (Yasucochi et al., 2006).

In the honey bee, FISH of repetitive sequence has been used to characterize ribosomal organizer regions (Beye and Moritz, 1993), centromeres (Beye and Moritz, 1994), different honey bee chromosomes types (Beye and Moritz, 1995), and telomeres (Sahara et al., 1999; Frydrychová et al., 2004). FISH to metaphase chromosomes and to small chromosomes in some insects has been a big challenge. However in some dipteran that form polytene chromosomes, including many Drosophilidae and mosquitoes, and in some Lepidoptera species, the polytene chromosomes have been successfully used for FISH. In insects having small chromosomes and genomes but no polytene chromosomes, FISH to mitotic prophase and meiotic chromosomes without the benefit of a reliable karyotype has been used with limited success. Chromosome identification can be a limiting factor, especially in those cases where the linkage map and physical map are still incomplete. In the latter case, the combination of banding pattern and FISH could be a solution to improve the reliability and agreement between the recombinational and physical map. This approach has been routinely used in the study of chromosome abnormalities in animals. Giemsa staining and C-banding are frequently used in FISH experiments, and this technique could be used to provide chromosome identification and karyotype characterization in the honey bee, and to support the previously mentioned maps.

Any approach that differentially characterizes the structure and organization in a small chromosome is of potential value for the study of the honey bee. *In situ* incorporation of labeled dUTP-biotin or dUTP-digoxigenin on spread chromosomes by polymerase I can be produced wherever a nick is induced by DNase I. When this incorporation is followed by subsequent development of signals using fluorochromes, the process is known as nick banding or mapping of hypersensitive sites in the chromatin. This technique was developed and extensively used during the 1980 and 1990 decades and differs from the more recently developed FISH-banding. The latter

uses chromosome microdissection and PCR to obtain probes, subsequently performing FISH on chromosomes spreads. FISH banding is considerably more expensive than *in situ* nick banding, although the increased cost of FISH banding is certainly justified in detection of human chromosome abnormalities (Liehr and Claussen, 2002; Liehr et al., 2002 and 2006). Here we show the value of nick banding with the small chromosomes of the honey bee, compare that to other banding approaches and suggest that the insights gained here make this method of general utility for other organisms with small chromosomes.

## CHAPTER II

### CHARACTERIZATION OF THE KARYOTYPE OF DRONES OF STRAIN DH4 OF *Apis mellifera* L.

#### Introduction

The honeybee is an important model organism to study social behavior, communication, response strategies against parasitism and diseases, responses to disasters, and medical applications of royal jelly (RJ) in cancer and neurological disturbances. Because of that importance the honey bee genome was selected for sequencing [The Honey Bee Genome Sequencing Consortium (HBGSC), 2006]. As part of that effort, the complete karyotype of the sequenced strain was produced and the banding patterns (position of heterochromatin), centromere position, and other chromosomal landmarks were described. The goal was to make it possible to subsequently locate on the karyotype the molecular markers generated for the honey bee genome sequence project.

The chromosomes of the honey bee have been studied since 1901, when the haploid chromosome number was established,  $n = 16$  (Fahrenhorst, 1977; Beye and Moritz, 1994). The haplo-diploid chromosome numbers were confirmed by Hoshihara (1978) and Hoshihara et al. (1981). Karyology studies were published for *A. mellifera* (Hoshihara and Kusanagi, 1978; Hoshihara 1984 a and b; Hoshihara and Imai, 1993; Hoshihara and Okada 1986; Stanimirovic et al., 2005) and for the related genera *Bombus* (Hoshihara, 1995) and *Melipona* (Rocha and Pompolo, 1998; Rocha et al., 2002; and 2003). Based on arm-length ratio, Hoshihara and Kusangi (1978) classified honey bee chromosomes into 8 metacentric and 8 submetacentric chromosomes. Later, Hoshihara (1984a), using the Sumner *et al.* (1972) C- banding method and Levan et al. (1964) chromosome classification, reported that the karyotype of honey bee consists of 4 metacentrics

(chromosomes 1-4) and 12 submetacentric or subtelocentric chromosomes. C-bands were found in all chromosomes except 1 and 9. Hoshiya and Okada (1986) reported the same karyotype for *Apis cerana* and *A. mellifera ligustica*, with one difference, presumably associated with ribosomal DNA sequence (NOR), in *A. cerana* chromosome 2. In all prior studies, chromosomes 1 and 16 were the only ones consistently and correctly identified; the rest of the chromosomes usually were classified in groups based on similarity of characteristics, such as banding pattern and centromere position.

Analyses of the prior chromosome classifications demonstrated inconsistencies among the classification schemes (Beye and Moritz, 1994, 1995). Attempting to overcome those difficulties, Beye and Moritz (1993, 1994, and 1995) carried out a series of studies using molecular markers, including rDNA, telomeric (*Alu I*) and centromeric (*Ava I*) sequence probes. According to Beye and Moritz (1993), rDNA probes from pD103 clone coding for 28S, 18S, 5.8S and 2S of *Drosophila melanogaster* (Tautz et al., 1988) tag two chromosomes at telomeric positions, no chromosome classification was given in this study. A honey bee centromere-specific probe isolated by CsCl-bisbenzimidazole gradient and cloned in *E. coli* using the pUC19 vector, tagged the centromere position in at least 14 chromosomes, in this study two metacentric, four submetacentric, two subtelocentric and eight telocentric chromosomes were classified (Beye and Moritz, 1994). Later, Beye and Moritz (1995) using the repetitive sequence *Alu I* [*Alu I* family from pSAM clone containing telomeric repeats (Tares, 1993)] identified telomeric positions in 11 of the 16 chromosomes. In the same study, Beye and Moritz (1995) combined the three probes to classify the chromosome set of honey bee into three groups; the first and third group included the largest and the four shortest chromosomes, respectively. The remaining eight chromosomes were in the second group. They also described chromosomes individually and characterized the karyotype based on positive signals for the three probes. Since the description was based on position of the probes, the classification based on arm ratio was not clear. Using the ideogram provided, the probable classification is, one metacentric (C1), three sub-metacentric (C2, C6, C5), five sub-telocentric (C4, C8, C11-C13) and seven telocentric (C3, C9, C10, C13-C16)

chromosomes. The signal at centromeric and telomeric positions was very heterogeneous. The probe used for centromeric detection is not specific for this structure, since the signals comes from constitutive heterochromatin which is probably not only present in pericentromeric heterochromatin but in several other parts of the chromosomes as well. Additionally, there are at least two chromosomes with low or no pericentromeric heterochromatin (Hoshiba, 1984a) and others with only one whose positions varies, thus identification of the centromere with repetitive elements from constitutive heterochromatin is inaccurate. They also used a cocktail with all the probes mixed, but they did not use different labels for the probes in order to identify each probe. Because the ideogram, karyotype characterization and chromosome identification were based on metaphase and overlapped chromosomes; therefore, it is difficult to contrast the banding with the signals of the probes. Besides, the probes used by Beye and Moritz (1995) were not available to repeat the experiment in the present study. Stanimirovic et al. (2005), worked with different ecotypes of *A. mellifera carnica* from Yugoslav regions using trypsin-giemsa banding (GTG), and described chromosome length and banding pattern differences between ecotypes. However, the studies were for comparative purposes and lack a complete karyotype characterization.

For the reasons given above, it was not possible to use the heretofore described karyotypes to locate the molecular markers generated for the honey bee genome sequence project. Even so, the published results were a very good starting point and were used as such to help generate a correct and complete karyotypic characterization of honey bee chromosomes. In this study we present the karyotype characterization based on a large number of cells of the sequenced DH4 strain of European honey bee; and we describe banding patterns generated for BaOH<sub>2</sub> (C-banding; Sumner, 1972), DAPI banding, AgNO<sub>3</sub> NOR banding pattern (Howell and Black 1980), Giemsa banding, and trypsin banding (Seabright, 1971; Stanimirovic et al., 2005). The resulting cytogenetic map is used to locate some of the BAC-DNA generated by the Solignac (2004) library. Those same BACs were used to support the recombination map sequence utilized in the reconstruction of the completed honey bee genome.

## **Material and Methods**

### **Animals**

All drones used in this study come from the DH4 queen. Drones from that same queen were used to construct the physical genomic sequence. The DH4 drones were obtained from Danny Weaver of BeeWeaver Apiaries, Navasota TX. Individual drones were collected in the morning, placed in tubes and transported to the Insect Genetics Laboratory in the Department of Entomology, Texas A&M University, without any specific pre-treatment.

### **Chromosome preparation**

Testes were obtained from white-eye DH4 pupae drones by dissections that were carried out in physiological saline supplemented with 5% sucrose and 0.01 % colchicine. Washed and cleaned testes were placed into 1.5mL plastic tubes containing fresh supplemented physiological solution and incubated at 36°C for 35-40 min. Following incubation, testes were washed with double distilled water three times before incubation in double distilled water, for 7 minutes or until the follicles show a grainy appearance. The testes were next sucked in and out (aspirated) with an insulin 1mL syringe. The resulting macerate was centrifuged 3 min at 3000rpm, the pellet was dissolved in Methanol:Acetic Acid (3:1) for 30 min and centrifuged for three times. This final cell solution was examined for chromosomes before being applied onto RITE-ON Micro slides. From 5 to 8  $\mu$ L per slides was applied on each slide. Before the applied fixative solution evaporates, one drop of additional fresh fixer was applied on the slides to remove debris. It was very difficult to get consistently good chromosomal preparations, although it was possible to obtain 40 to 60 slides with only one pair of testes. Slide preparations were dried overnight and treated with an alcohol series (70%, 80% 100%) then stored at -80°C. The chromosome preparations eventually used for banding studies were more than 2 years old. When a slide preparation was required for use, it was placed

in cold alcohol series and fixed with a drop of Methanol:Acetic Acid (3:1) and let dry at room temperature 30 min to 2 hours, and finally were placed on a hot plate at 52°C overnight.

### **Giemsa-banding (G)**

The slides were equilibrated in 2xSSC buffer for 20 min at 65°C, and then the slides were incubated in Giemsa stain [2 mL of Gurr's Giemsa Improved R66 (BDH) in 50 mL of buffer] dissolved in Gurr buffer pH 6.8 for 45 min at room temperature (RT). The slides were finally briefly washed in distilled water and allowed to drain until dried. Once dry, slides were mounted in Kleermount® xylene solution permanent mounting media. ISCN (2005) identifies this method as G.

### **C-banding (CBG)**

The method of Sumner (1972) with some modification for chromosomes fixed with methanol:acetic acid (3:1) was used. The slides were predigested in 0.2N hydrochloric acid for 20 min, then washed with ddH<sub>2</sub>O before applying a 5% Ba(OH)<sub>2</sub>.8H<sub>2</sub>O solution and incubating for 3 min at 45°C. The slides were then washed in 2xSSC buffer for 20 min at 65°C and stained in Giemsa as specified in the Giemsa banding protocol. The stained slides were briefly washed in distilled water, blotted, dried and mounted in Kleermount® xylene solution permanent mounting media. ISCN (2005) identifies this method as CBG.

### **Trypsin-banding (GTG)**

Denatured slides were equilibrated for 5 min in PBS pH 6.8 before incubation in 0.25 % trypsin (Trypsin-EDTA, SIGMA cat T4174) for 15 sec and stained according to Seabright (1971) and Sumner (1994). The stain utilized was the same as specified for G- and C-banding. After air drying, slides were mounted in Kleermount® xylene solution permanent mounting media. ISCN (2005) identifies this method as GTG.

**R-banding (RHG)**

The slides were incubated in 1M NaH<sub>2</sub>PO<sub>4</sub> solution pH 5.5 for 20 min at 88°C, washed with pre-warmed distilled water at 36°C and equilibrated with Gurr buffer before staining with Giemsa solution according to Sumner (1994). After air drying, slides were mounted in Kleermount® xylene solution permanent mounting media. ISCN (2005) identifies this method as RHG.

**Nucleolus organizer (AgNO<sub>3</sub>-NOR)**

The methods of Howell and Black (1980) and Bilinski and Bilinska (1996) gave very good results. The first was preferred because that technique does not include any additional staining, renders better resolution in old chromosome preparations of honey bee, and allows analysis of the banding pattern generated by AgNO<sub>3</sub>. Briefly, 4 g of silver nitrate dissolved in 8 mL of deionized mili-Q water as aqueous solution, and 2 % of gelatin U.S.P. G-7 (Fisher cat # 383309) as colloidal developer were utilized. Just before use, 200 µL of developer and 400 µL of aqueous solution were mixed in a 1.5 mL plastic tube. Immediately 100 µL of the mixed solution was applied to the slides and covered with a 22x40mm plastic coverglass. Each slide with its coverglass was placed on a hot plate at 70°C and held there until the solution turned golden-brown. Then, the slide was rinsed off and washed with deionized water; air dried and mounted in Kleermount® xylene solution permanent mounting media. ISCN (2005) identifies this method as AgNO<sub>3</sub>-NOR.

**DAPI-banding and FISH hybridization**

To correct imprecision because of variation in size of the chromosomes in different stages of prophase of mitosis and meiosis, rDNA was used as marker in the DAPI banding technique. According to Beye and Moritz, (1993), rDNA tags chromosomes 4 and 11. Because the RNA marker used by Beye and Moritz (1993, 1994, and 1995) was not available for this work, we used the clone BDG-512 carrying a



plasmid p3629 with a 1750pb insert of *S. cerevisiae* 18S rDNA kindly provided by Dr. P. Klein of the Institute for Plant Genomics and Biotechnology at Texas A&M University. Conventional DNA hybridization was performed based on Pinkel et al. (1986), Beye and Moritz (1995) and Sahara et al. (1999). Detection, enhancing and postwashing was done according to Schubert et al., (2001). Bovine Serum Albumin (BSA, protease free, Jackson Immuno Research cat 001-000-162) and Normal Goat Serum (NGS, Roche cat 03117839001) were used instead of Boehringer blocking reagents, as the former protocol recommend.

Slides treated for fluorescence hybridization (FISH) detection were counterstained. The slides were briefly equilibrated in 4xSCC plus 0.2% Tween 20, then 250 $\mu$ L of 5 $\mu$ g/mL of 4' 6-diamidino-2phenylindole (DAPI, Sigma, Cat# D-9542) in McIlvaine's buffer (9 mM citric acid, 80 mM Na<sub>2</sub>HPO<sub>4</sub>·H<sub>2</sub>O, 2.5 mM MgCl<sub>2</sub>, pH 7.0) was applied and the slide incubated for 30 min at room temperature. After a brief wash in 4xSCC plus 0.2% Tween-20, 25  $\mu$ L of home-prepared antifade solution was applied to slides. The antifade was prepared following Trask (1980) recommendations. The slides were stored at -20°C for a week before microscope analysis.

### **Microscope analysis**

The slides treated for G-, C-, R-, NOR-, and trypsin banding were examined with a light Zeiss microscope equipped with phase contrast and pictures were taken with a Nikon Coolpix 45000 adapted camera (Edmund Scientific). The DAPI stained slides were examined with a motorized epi-florescence microscope Olympus AX-70 and pictures were digitalized with a Peltier-cooled 1.3 M pixel Sensys camera (Roper Scientific) and MacPro v. 4.2.3 digital image system (Applied Imaging Corp., Santa Clara Cal., USA) located in the Laboratory for Plant Molecular Cytogenetics, Soil and Crop Science Texas AM University. The pictures from DAPI staining were converted to black and white negatives using the Irfanview V3.98 (Irfan Skiljan, 2006) program in order to reveal the banding pattern. In the rest of the banding treatments, the pictures were contrast enhanced in the same program and processed in Adobe Photoshop V 6.0.

### **Data recording and analysis**

The data recording was based on prophase, where, even given the instability across prophase, the banding pattern is clear and measurable. Different stages of prophase for DAPI staining were determined by visual characteristics following the general observation of Kireeva et al. (2004). Thus, four stages were considered, prophase I (early prophase), prophase II (middle prophase), prophase III (Late prophase) and prophase IV (Pre-metaphase). The banding recording for DAPI experiments were based on the bands of prophase I (early prophase) and prophase II (middle prophase). Measurements were made when the bands were clearly distinguished and separated, and it was possible to measure from the telomere of the short arm to the telomere of the long arm. Beginning at the telomere of the short arm, the start of each band and the end of the band were measured, obtaining a couple of values for each band, which values represented the range and length of the band. Using only prophase I and prophase II, the bands were arrayed in rows by chromosome and columns by similar range, using the length and the middle point of the range. Prophase III and prophase IV were included in the band sorting. Typically, when several bands were fused, the measurement of the end or start of one band matched with the end or start of the bands in the chromosomes where there was no overlap. The coincidences allowed location of the block at the correct position. These same block were further subdivided into the correspondent bands whenever evidence of the fused bands were clearly observed as the slight constrictions that delimiting the edges. When subdivision was not possible, the band was considered as a block in the correspondent stage of prophase, which was frequently the case for late prophase and prophase IV. This procedure not only helped to sort the bands, it also verified the chromosome identifications.

Subsequently the measurements sorted by phase, to see if bands are consistent through the phases, appear several times in a single stage of prophase or appear (five times) in all stages. When a band was present only one to three times in all stages of prophase, it was considered a possible artifact. However, if the three bands appear in a

single stage of prophase, it was considered enough to include it in the map. When a band was present only once at every stages of prophase it also was mapped, because overlapped bands in late prophase typically showed evidence of that band.

To allow comparisons between chromosomes at different mitotic phases and between the different chromosomes in each stage, relative values (position relative to total chromosome length) were used to locate the bands and all other characteristic of the karyotype of the honey bee. To assign a relative size to each chromosome, we considered the haploid complement total 100%. To locate chromosome characteristics, each chromosome's total length was considered 1.0, and a fraction of this number was used to locate the positions of characters of interest on that chromosome (ISCN, 2005).

Since the banding and chromosome size throughout prophase is variable, large sample sizes, and a step-by-step process in chromosome classification and identification were carried out. In each step a file of data was generated to improve the chromosome classification and identification in the next step. For the final file, the data was sorted according to length, arm ratio and band position.

## **Results**

### **Data description**

The BDG-512 yeast rDNA clone consistently hybridized at a telomeric position in the short arm of two chromosomes. These chromosomes, when classified by size, were assigned the numbers 6 and 12; this result was used for all subsequent chromosome classification and identification. To obtain the ultimate karyotypic description of honey bee chromosomes, a step-by-step procedure was used. Three reasons obligated us to follow this procedure. First, it was very difficult to identify individually the chromosomes in the absence of a prior, correct description of the karyotype. Second, the irregular morphology at prophase and the very heterochromatic and reduced size of the chromosomes at metaphase changes the morphology. Third and most problematic was that during the mapping process additional information became available. The new

information frequently contradicted our current results, obligating us to reanalyze our data. For example, Baudry et al. (2004) using half-tetrad analysis concluded that chromosomes 2 and 4 are telocentric - a result that was not confirmed in the third iteration of analysis of our data. The Honeybee Genome Sequencing Consortium (HBGSC), states that the genome of the honey bee chromosomes is arranged in 15 telocentric and one metacentric chromosome (HBGSC, 2006). However, the supplementary information of that same publication states that there are probably three metacentric chromosomes instead of two - again a result that was not confirmed in the third iteration of our data.

As evidence of improved, repeatable chromosomal identification, we briefly compared 3 data files (also called trials) obtained during this process. Compared were file 1 (21 cells analyzed), file 2 (60 cells analyzed) and file 3 (166 cells analyzed). File 2 was produced using the arm ratios, total length and band position information gleaned from File 1. File 3 took into account the conclusions from the analysis of File 2. And, finally, to generate the ideogram for the honey bee karyotype, a fourth file was generated which was the file 3 improved. File 3 was three times reviewed to verify the new published information, including that in Baudry et al. (2004) and HBGSC (2006). File 3 consisted of measurements from 166 cells and 2656 chromosomes read from 18 slides that came from testes of a single drone. A complementary file from five banding methods (BaOH<sub>2</sub>-C-banding, trypsin-banding, AgNO<sub>3</sub>-NOR-banding, giemsa-banding and R-banding) consisted of measurement of bands from 54 cells on 15 slides, with at least three pictures per slides. The slides also came from a single drone - but a different individual than was used for DAPI experiments. The two drones were from the DH4 queen and were collected in the same day and hour. When completed, files 1, 2, and 3, without the complementary file, were used to show the improvement in the chromosome classification. In this comparative study only mitotic chromosomes were used because the size of the chromosomes was more measurable and resolution of banding pattern was better than in meiotic and metaphase chromosomes.

Overall, the haploid size of the genome was assumed to be 100%, the average chromosome size was 6.25% and individual sizes ranged from 12.15 % to 3.5 % depending on the chromosome and phase (Table 1). Absolute values ( $\mu\text{m}$ ) were used to express general comparisons among trials and stages of prophase. Comparison among chromosomes and their characteristics were expressed in relative values. Only when necessary were absolute values reported.

**Table 1.** Mean and standard deviation for chromosome length ( $\mu\text{m}$  and %) and arm ratio for different data files. The means represent the average size of all chromosomes. There are two independent comparisons; one between the three files (Trials) and the other between stages of prophase (prophase I - prophase IV).

Length (Rel)	Absolute Length ( $\mu\text{m}$ )	Standard Deviation	Relative Length (%)	Standard Deviation	Arm Ratio	Standard Deviation	N
Files (Trials)							
Trial-1	2.453a	1.029	6.231a	1.855	2.860b	1.520	337
Trial-2	2.288b	1.083	6.257a	1.900	2.278a	1.378	960
Trial-3	2.114c	0.982	6.241a	2.097	3.201c	1.363	2657
Stages of prophase							
Prophase-I	3.366a	1.535	6.268a	2.465	3.292d	1.641	407
Prophase-II	2.485b	0.973	6.234a	2.118	3.114c	1.546	945
Prophase-III	2.024c	0.741	6.239a	2.003	2.956b	1.326	1563
Prophase-IV	1.640d	0.566	6.250a	1.861	2.822a	1.366	1036
Tukey's test: Means for groups in homogeneous subsets are displayed. These are based on Type III Sum of Squares. The group sizes are unequal and the harmonic mean of the group sizes is used. Type I error levels are not guaranteed to equal $\alpha = 0.05$ .							

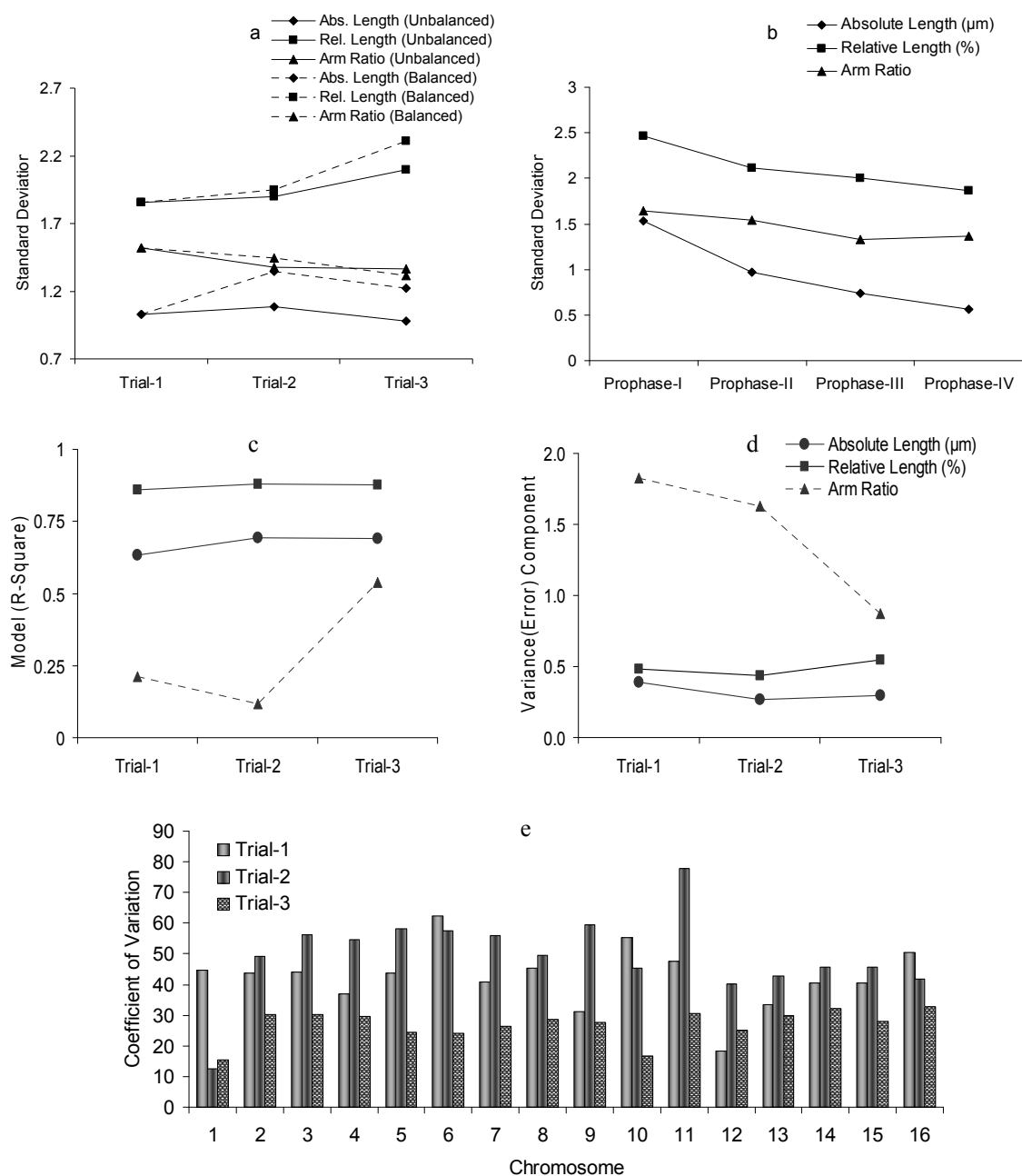


**Fig. 1.** Standard deviation for three files and stages of prophase. (a) Standard deviation for relative length (%), absolute length ( $\mu\text{m}$ ), and arm ratio for balanced (solid lines) and unbalanced (dotted lines) data. for a balanced data set with sample size  $N = 21$  cells (4 Prophase I, 5 Prophase II, 8 Prophase III, and 4 Prophase IV; solid lines) per trial, and for the actual unbalanced data set ( $N = 21$  for trial 1,  $N = 60$  for trial 2, and  $N = 166$  for trial 3; dotted lines), (b) Standard deviation for the same variable for unbalanced data file 3 in four stages of prophase. (c) R-Square and (d) variance component of error for three files (trials), (e) per chromosome coefficients of variation.

A nested analysis of variance for arm ratio finds highly significant differences across trials, stage of prophase; and chromosomes but no higher order effects (Table 2).

### Files comparisons

Phase and file (trial) are not correlated to relative chromosome length ( $-0.008$ ,  $p < 0.601$  and  $0.021$ ,  $p < 0.138$ ), but are correlated with absolute length and arm ratio ( $r = -0.121$ ,  $r = -0.487$ ,  $p < 0.000$  and  $r = 0.273$ ,  $r = -0.088$ ,  $p < 0.000$  respectively). Because the later trials include more early phases, where chromosomes are longer, the correclation makes it difficult to demonstrate the expected improvement in the data in the successive data files Fig. 1a, b. However, the model R-square fit is clearly better for the third trial Fig. 1C) and the mean square error (Variance (Error) Component) is significantly reduced for all but the absolute length, as expected (Fig. 1d),

**Table 2.** Analysis of variance (ANOVA) for arm ratio. ANOVA assuming that each trial variable is nested under the model  $Y_{ijk} = \mu + \text{Trial}(\alpha_i) + \text{Chromosome}(\beta_j) + \text{Phase}(\gamma_k) + \beta_j(i) + \beta_i(j) + \beta_j(i*j) + E_{ijk}$

Dependant variable: Arm Ratio Source	Type III Sum of Squares	df	Mean Square	F	Sig.
Corrected Model	4920.624	191	25.762	24.129***	0
Trial	549.0978	2	274.549	257.146***	1.3E-106
Phase	24.62773	3	8.209	7.689***	4.02E-05
Chromosome	879.2951	15	58.620	54.904***	5.4E-152
Error	4923.054	4611	1.068		
Chromosome(Trial*Phase)	695.9451	90	7.733	0.777 NS	2.74
Chromosome(Trial)	982.8938	30	32.763	1.789 NS	19.4
Chromosome(Phase)	962.6656	45	21.393	0.384 NS	3.06

The improvement of the arm ratio in each chromosome is shown in Fig. 1e. Clearly, all chromosomes show a reduced coefficient of variation in the last file (Trial-3) compared with the previous ones. The highest coefficients of variation suggest that chromosomes 6, 9, 10 and 11 were the most difficult chromosomes to identify, while 1,

2, 8 and 13 were the most consistently identified. An unexpected result is the consistently high variability observed in the short chromosomes 13-16; some characteristics of these chromosomes explain this variability. The presence of a euchromatic band in the p arm of C14, the loss of a telomeric satellite in the p arm in C15, which with a centromere-like structure in the middle of the C15 not only add variation but also make this chromosome more metacentric and easy confounded with C10. The variation of C16 comes from difficulty identifying the centromere because most of the short arm of C16 is heterochromatic from early prophase. Variation in the arm ratio for C4, C8, and C11 comes from the euchromatic band in the short arm. In C2, variation is explained by the presence of two additional centromere-like structures, one of at a sub-telomeric position. Examples of these characteristics can be observed in the karyograms of Fig. A.1.

Variation in the lengths of the chromosomes was affected by the presence of structures such as the constrictions in the large arms of chromosomes 3, 4, 5, 7, 8, 9 and 13, missing fragments in C1, and satellites in the short arms of chromosomes C3, C5, C11 and C15, some of which can be observed in Fig. A.1.

### **Chromosome condensation**

Although later paragraphs explain how the different kinds of chromatin were determined, the result first mentioned refers to DAPI staining method that later will be compared against Ba(OH)<sub>2</sub>, a more specific method for constitutive heterochromatin. The relative length of chromosomes, short and long arms were negatively correlated with heterochromatin content ( $r = -0.329, -0.248, -0.321$ ;  $p < 0.000$  respectively), which means more heterochromatin equates to shorter chromosomes and arms. However, the same variables (length of chromosomes and arms) were positively correlated with number of bands ( $r = 0.437, 0.246, \text{ and } 0.446$ ,  $p < 0.0001$  respectively). The pericentromeric heterochromatin was negatively correlated with length of chromosomes and arms ( $r = -0.530, \text{ and } -0.521$ ;  $p < 0.000$  respectively). Also negatively correlated were long and short arms length and amount of constitutive heterochromatin ( $r = -0.514$



and -0.271,  $p = 0.000$  respectively). The above correlations are explained by the progressive condensation and heterochromatinisation during successive prophase stages. The correlation also occurs because as the arms become shorter more heterochromatin is detected. DAPI in later stages of the honey bee prophase does not differentiate clearly between different kind of heterochromatin and  $Ba(OH)_2$  does. This difference identifies the facultative heterochromatin that was positively correlated with the total length, short arm and long arm length ( $r = 0.270, 0.084, \text{ and } 0.293; p < 0.000$  respectively). Thus, condensation seems to be significantly influenced by facultative and constitutive heterochromatin of the chromosome during prophase.

### **General karyotype description**

To facilitate reading, the chromosomes and stages of prophase will be subsequently shortened to the letter C and P followed by an Arabic number for each chromosome and a roman number for each stages of prophase, for example chromosomes 1 and 7, will be referred as C1 and C7 and PI, PII, PIII, and PIV will reference prophase I, prophase II, prophase III and prophase IV, respectively.

As explained in detail in appendix A.2, the arm ratio and the length of the chromosomes decrease through prophase, except for C1, C6, C8, C10 that shows not significant changes through stages of prophase in arm ratio (Fig. 2b and 2a). The short and long arms (Fig. 2c) condense at similar rates, except for C13, C15 and C16, which exhibit more variable condensation in the short arm in successive stages of prophase. Overall, the ratio of the long arm to the short arm decreases in most chromosomes (table 1), simply because the long arm condenses more than the short arm during successive stages of prophase. The decrease is seen for all chromosomes except 1 and 10, although the variation is sufficiently high that the change is significant only for chromosomes 2, 3, 4 and 16. The exceptional chromosomes, 1 and 10, are metacentric, and both arms condense at similar rates agree with the arm ratio approximately 1 throughout (Fig. 2a).

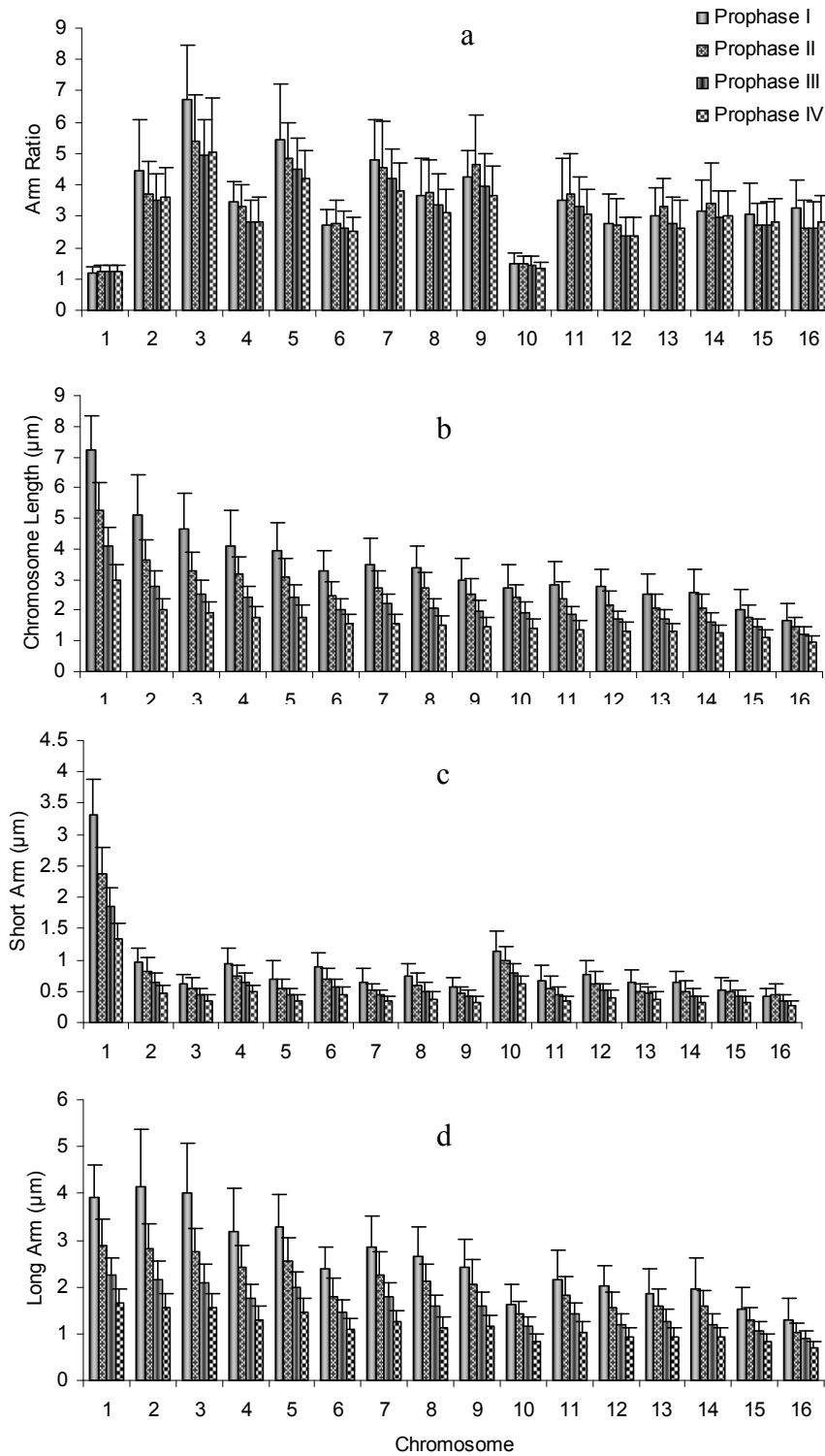


**Fig. 2.** Means of (a) Arm ratio, (b) chromosome, (c) short and (d) long arm length of individual chromosome at four stages of prophase, and stained with DAPI.

The chromosomes can be classified either statistically using the means of the length and arm ratio or the Levan's (1964) nomenclature. Using the last mentioned, the chromosomes can be classified in three groups: two metacentrics, six submetacentrics, and eight subtelocentric chromosomes (Table 3). Using the arm ratio, the chromosomes can be ranked from most consistently metacentric to most telocentric, with the chromosomes assigned into 10 groups: chromosomes 1 and 10 (Group 1), 12 and 6 (Group 2), 15 and 16 (Group 3), 4 and 13 (Group 4), 14, 8 and 11 (Group 5), 14, 8, 11, and 2 (Group 6), 8, 11 and 2 (Group 7), 9 and 7 (Group 8), 5 (Groups 9) and 3 (Group 10). Using this grouping and Levan's classification, an empirical grouping can be generated as is shown in the Table 3 and Fig. 3. Combining the two methods, a subsequent empirical grouping eliminates the confusing overlapping of the Tukey's grouping and the chromosome heterogeneity of the Levan's (1964) classification. Thus chromosomes 1 and 10 are not significantly different and according to the Levan et al. (1964) are classified as metacentric. C6 and C12 are also not significantly different and are grouped as submetacentric (Sub-Metacentric-A). Chromosomes 4, 13, 15 and 16 are sub-metacentric (Sub-Metacentric-B). In the same way the sub-telocentric chromosomes, 14, 8, 11, 2, 9, 7, 5, and 3 were separated into two groups based on arm ratio. Perhaps this grouping has no meaning, but it is important to mention that the Sub-Metacentric-A group contains the chromosomes with the ribosomal signal, C6 and C12. The Sub-Metacentric-B grouping contains the highly heterochromatic chromosomes; the Sub-Telocentric-A groups contain the most euchromatic C2, C8, C11, and C14. The last group contains the chromosomes that can be considered acrocentric. If a telocentric chromosome exists, it should be C3 - in the early stages of prophase, the arm ratio is very close to the threshold value (arm ratio = 7) given by Levan et al. (1964). Although C9 seems to be less telomeric than C3, a visual inspection suggests that the C9 could be also telomeric. Thus, C9 and C3 could be considered the most acrocentric chromosome of the honey bee karyotype. A number of the chromosomes are categorized into different groupings as prophase progresses (Fig. 3). As can be observed in the Fig. 3, the

chromosome classification is influenced by the stages of the prophase, however in the late prophase and pro-metaphase, the chromosome classification stabilizes.

**Table 3.** Chromosome classification based on arm ratio. Shown are means and standard deviations of arm ratio, Tukey's means comparison ( $\alpha = 0.05$ ) with different letters assigned to significantly different means, Levan et al. (1964) chromosome classification and empirical groupings shown as different colors.

Chromosome	Standard Deviation	Chromosome Groups and Classification					Chromosome Classification (Levan et al., 1965)
		Metacentric	Sub-Metacentric-A	Sub-Metacentric-B	Sub-Telocentric-A	Sub-Telocentric-B	
1	0.1930	1.241a					Metacentric
10	0.2369	1.430a					Metacentric
12	0.7358		2.559b				Sub-Metacentric
6	0.6404		2.651bc				Sub-Metacentric
16	0.9194			2.809bcd			Sub-Metacentric
15	0.8047			2.862cd			Sub-Metacentric
4	0.7403			2.919cde			Sub-Metacentric
13	0.8856			2.974de			Sub-Metacentric
14	1.0235				3.189ef		Sub-Telocentric
8	0.9767				3.412fg		Sub-Telocentric
11	1.0473				3.447fg		Sub-Telocentric
2	1.1222				3.697g		Sub-Telocentric
9	1.1187					4.047h	Sub-Telocentric
7	1.1130					4.234h	Sub-Telocentric
5	1.1125					4.539i	Sub-Telocentric
3	1.5657					5.207j	Sub-Telocentric

### Chromosome banding

The chromosomes stained by with the different band techniques show no significant differences in relative chromosome size and arm ratio (Table 4). The variation in arm ratio observed among four of the six treatments and during prophase are due to unbalanced number of observations for the different treatments and stages of prophase; however the relative length were homogeneous through the groups (Fig. 4a),

and the final chromosome classification based on length and arm ratio was not affected because of that variation (Fig. 4b).

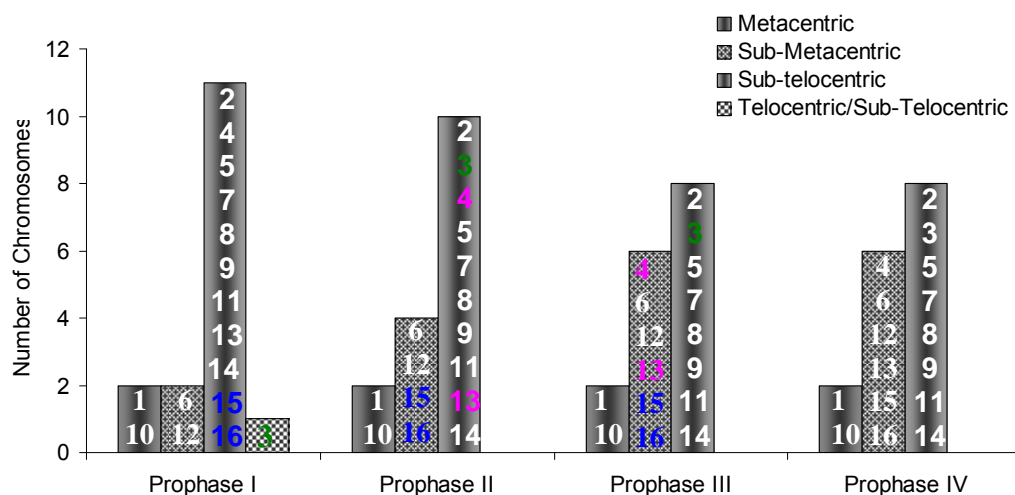


**Fig. 3.** Chromosome classification at different stages of prophase. The number inside the bars represent the chromosome number, the colored numbers represent chromosomes that change its classification during prophase.

**Table 4.** Average length and arm ratio of honey bee chromosomes. Means comparison for two independent source of variation, methods of staining and stages of prophase based on Tukey' significance ( $\alpha = 0.05$ ).

Band Method	Absolute Length	Standard Deviation	Relative Length	Standard Deviation	Arm Ratio	Standard Deviation	N
Banding Methods							
AgNO <sub>3</sub> -	3.128a	1.064	6.25 a	2.32	3.40 b	1.67	192
Giemsa	3.656b	1.298	6.25 a	2.05	3.10 a	1.20	160
R-Banding	2.209bc	1.508	6.25 a	2.31	3.32 b	1.41	112
C-Banding	2.645cd	1.041	6.25 a	2.27	3.41 b	1.35	208
Trypsin	3.391e	1.140	6.25 a	2.33	3.37 b	1.33	192
DAPI	2.397f	0.352	6.24 a	2.06	3.16 ab	1.37	2658
Stages of prophase							
Prophase I	3.163a	0.444	6.276a	0.764	3.572a	0.968	833
Prophase II	2.481b	0.367	6.229a	0.631	3.364a	0.799	1488
Prophase III	1.968c	0.283	6.240a	0.488	3.118b	0.618	865
Prophase IV	1.570d	0.603	6.242a	1.040	3.030c	1.316	336
Tukey's test: Means for groups in homogeneous subsets are displayed. These are based on Type III Sum of Squares. The group sizes are unequal and the harmonic mean of the group sizes is used. Type I error levels are not guaranteed to equal $\alpha = 0.05$ .							

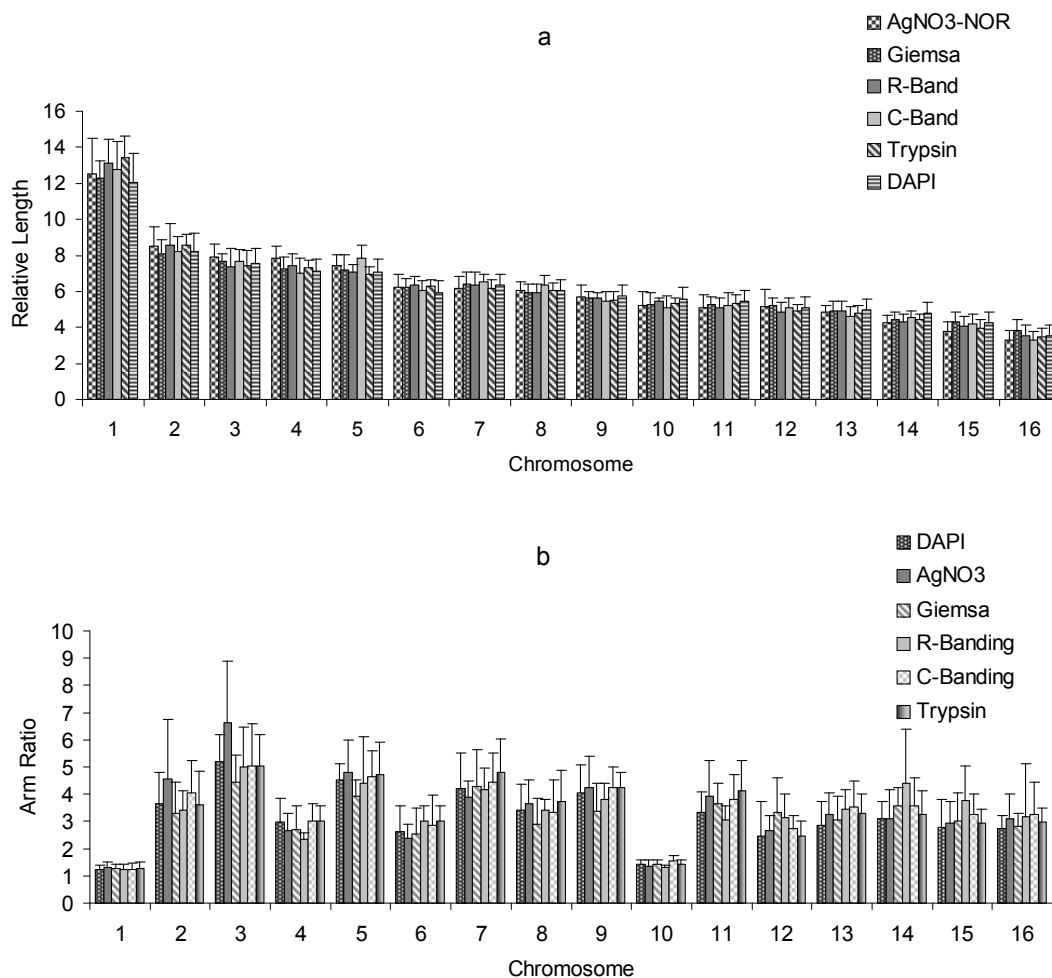


**Fig. 4.** Means of (a) Relative length and (b) arm ratio of chromosomes of honey bee stained with six methods. The lines above the bars represent the standard deviations.

Band data was obtained and organized only after the objective of classifying the chromosome as nearly correctly as possible was met. As the number of the band was vary variable among staining methods as well as within and between the stages of the prophase, the number of bands read was not representative to determinate the banding number in honey bee chromosomes. Therefore, cells were sorted by phase, to see if bands are consistent through the phases as explained in materials and methods. The sample size for the DAPI band technique was large enough to detail the analysis and to

construct an ideogram for each stage of prophase. For the rest of the banding techniques an ideogram was constructed using the relative length means of the bands.

The fewest bands were observed in R-banding, while the largest number of band was observed with giemsa-banding and DAPI-banding (Table 5). The number of giemsa and DAPI bands was not significantly different from the number of band shown by trypsin-banding. Although the number of bands produced with C-banding is low (zero, one, or two total), additional and differentially stained C-bands were obtained with the Ba(OH)<sub>2</sub> method, which later will be considered as C-facultative heterochromatin bands. In early prophase, the number of readable bands in DAPI method was larger than in later stages of prophase, except for C6, C7, C12, and C13 (Fig. 5a), where the number of bands read was similar in PII to PIV. As earlier explained, the banding data from all DAPI stained chromosomes was used to order the bands. When the bands were sorted, the total number of the bands increased and this total was similar through the different phases, which highlights the importance of sorting the bands (Fig. 5b).

**Table 5.** Means of number of bands read per staining method and stage of prophase for DAPI method

Band Method	Num. of Bands	Phase	Num. of DAPI - Bands
R-band (RHG)*	2.20 a	Prophase I	3.20 d
DAPI	2.27 a	Prophase II	2.62 c
C-band (CBG)	2.69 b	Prophase III	2.42 b
AgNO <sub>3</sub> -NOR	3.12 c	Prophae IV	2.026a
Trypsin (GTG)	3.33 cd	Turkey's Means comparison, a) Based on Type III Sum of Squares, b) The group sizes are unequal. $\alpha = .05$ .	
Giemsa (G)	3.43 d		
* Abbreviation nomenclature recommended by ISCN (2005): RHG			

Grouping the banding techniques by affinity for euchromatin or heterochromatin (Sumner, 1994), the results of banding number; read and sorted, per chromosomes are plotted in two groups (Fig. 6). Euchromatin detecting methods, R-banding, AgNO<sub>3</sub>, and trypsin (sometimes used for euchromatin reference) are plotted against DAPI (Fig. 6a). In a second grouping, C-Banding, G-Banding is plotted against DAPI banding (Fig. 6c).

The plot of number of bands read in three of the methods (C-, G- and DAPI) gives a consistent pattern in most chromosomes, although C-band show more bands than giemsa; while giemsa shows more bands than DAPI (Fig. 6c). Exceptions are C3 and C4, where the numbers of DAPI bands were a little more than for giemsa but significantly less than for C-banding. In C7, more bands were read in giemsa (Fig. 6c).

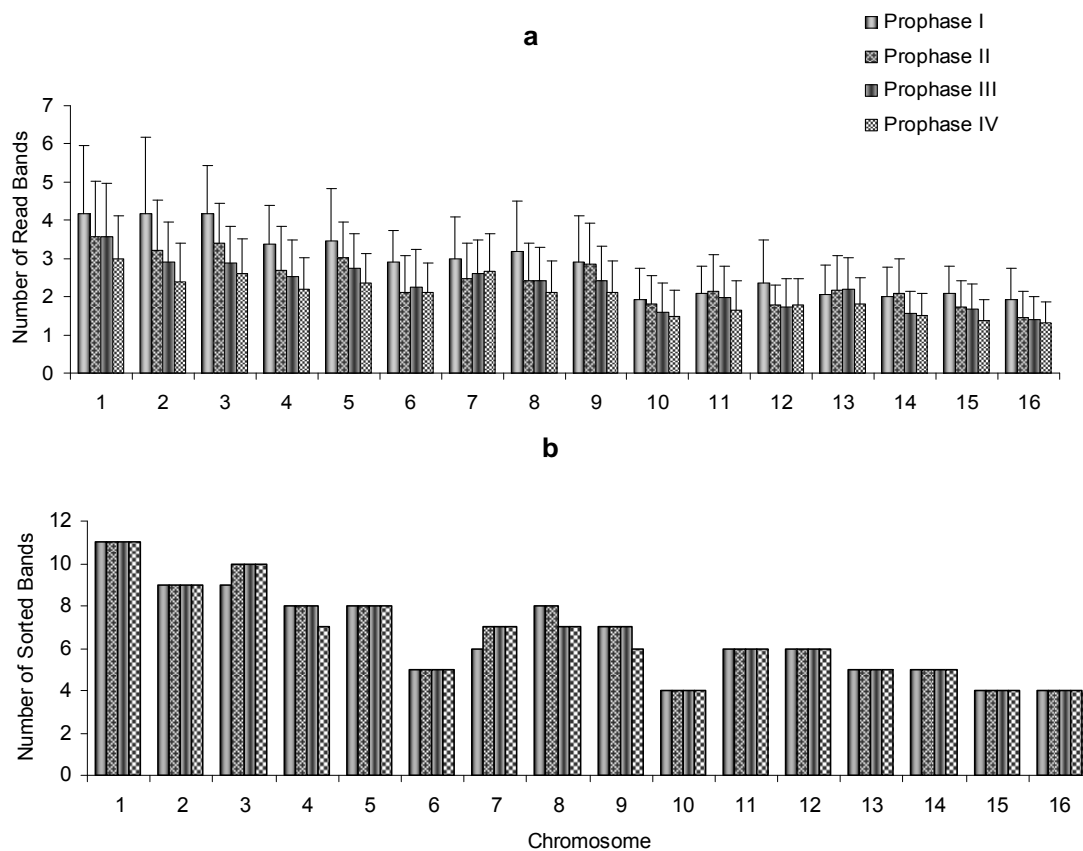


**Fig. 5.** Number of bands detected in honey bee chromosomes using DAPI staining method at four stages of prophase. (a) Number of bands read and (b) number of sorted bands.



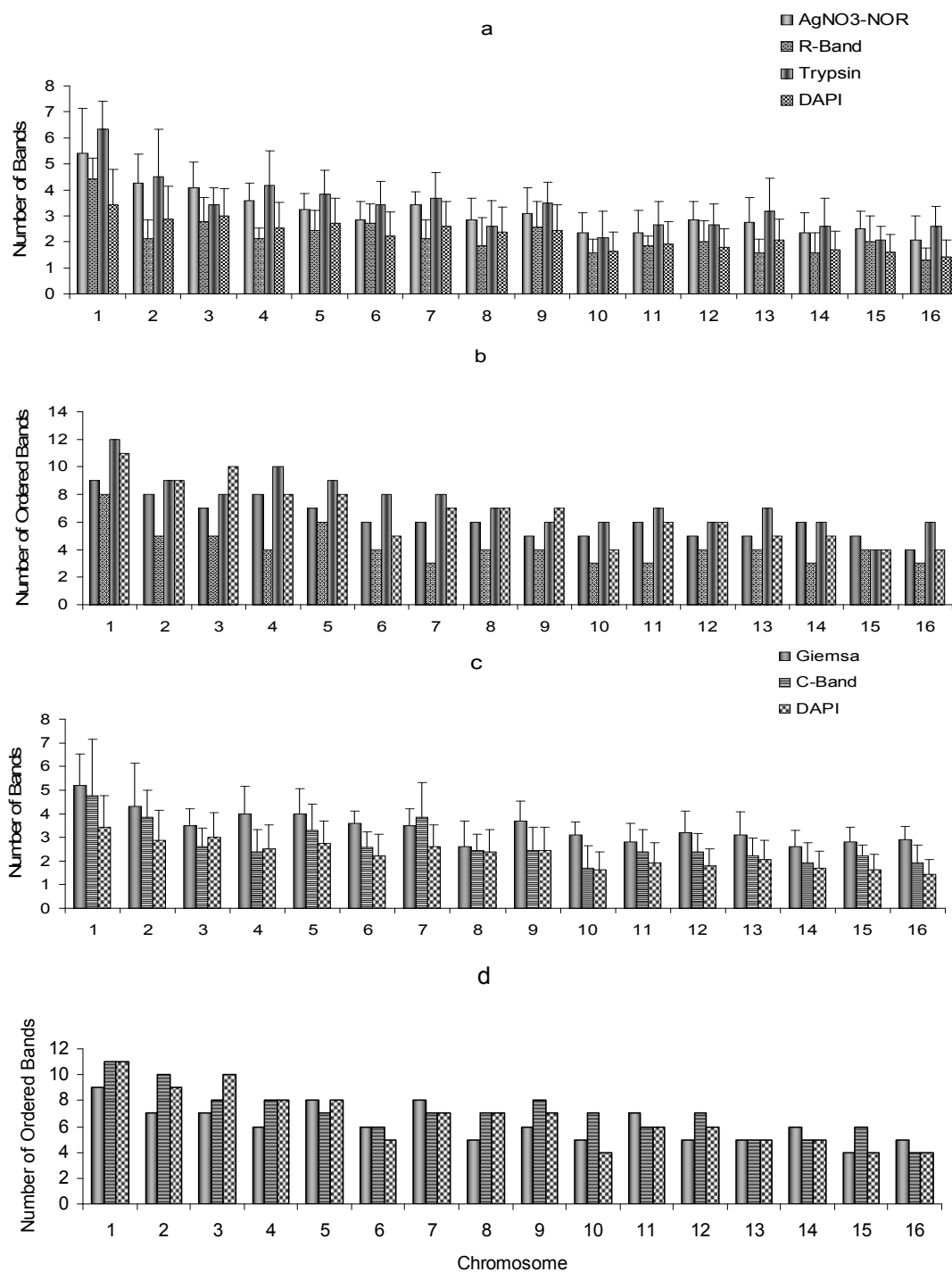


**Fig. 6.** Number of bands detected in honey bee chromosomes. (a and c) number of bands read, (b and d) number of bands detected (sorted) stained with different methods.

Comparing the banding of AgNO<sub>3</sub>-NOR, R-banding and trypsin-banding (Fig. 6a and 6b), it was noticed that the number of bands read were less variable among those three methods than when they were sorted. Consistently fewer R-bands and DAPI-bands were read, which remained true when they were sorted. Trypsin-banding resulted in the largest number of read and ordered bands. Even though AgNO<sub>3</sub>-banding produced a large number of read bands; AgNO<sub>3</sub> banding resulted in fewer sorted bands than any other method except R-Bands. Chromosomes 4, 7, 10, 11, and 14 produced proportionally less R-bands, with the fewest observed in C7.

When the bands were sorted, 9 chromosomes, 1-4, 8-9, 12 and 15, show consistently less bands with C-banding than with giemsa and DAPI, while C7, C11, C14 and C16 show more C-bands than giemsa and DAPI. C6 showed equal number of C-bands and giemsa bands, while chromosome 5 presented equal numbers of C- and DAPI bands but more than with giemsa (Fig. 6c and 6d). C3 was the only chromosome with equal numbers of C-, giemsa and DAPI bands - a result that was initially expected for all chromosomes.

### **Heterochromatin content**

In the following, C-bands and constitutive heterochromatin will be considered equivalent. When constitutive heterochromatin was detected by DAPI, we will refer to that as a DAPI-C band or DAPI constitutive heterochromatin. However, in later stages the heterochromatin detected by DAPI is significantly larger than earlier stages; the difference was further considered as DAPI facultative heterochromatin. The most approximate content of that heterochromatin will be based on the difference with Ba(OH)<sub>2</sub> method. In general, the C-banding technique produced a banding pattern that was similar to G- and DAPI-banding. C-banding based on Ba(OH)<sub>2</sub>.8H<sub>2</sub>O is specific for constitutive heterochromatin, which were mostly detected in the pericentromeric region, but also produced additional bands that were considered as C-facultative heterochromatin bands. Almost all chromosomes show evidence of pericentromeric constitutive heterochromatin bands. However, C8, C11, C14 show very low frequency of

this band suggesting that pericentromeric heterochromatin might be absent in these chromosomes (Fig. 7a). Except for C1 and C10, all chromosomes show evidence of pericentromeric heterochromatin in the first bands. C1 and C10 show evidence of pericentromeric heterochromatin at bands 5 and 3 respectively (Fig. 7a). Additional constitutive heterochromatin bands were located in C1, C2, C7, C10, C13 and C15 (Fig. 7b). Except in C1, these non-pericentromeric bands were observed less frequently than the pericentromeric bands. The very low frequency of C-band or constitutive heterochromatin in C8, C11 and C14 explain the high frequent euchromatic appearance of these chromosomes, consequently they showed the lowest content of constitutive heterochromatin, but with relatively more facultative heterochromatin (Fig. 8a).

Facultative heterochromatin in this study is scored as the difference between total heterochromatin (total bands produced by  $\text{Ba}(\text{OH})_2$  method) and C-Bands. The two kinds of heterochromatin can also be detected if the DAPI stained heterochromatin is considered (Fig. 8 b and 8c). DAPI- heterochromatin seems to be a more reliable way to detect the facultative heterochromatin than  $\text{Ba}(\text{OH})_2$ . This assumption is based on the observation that, in early prophase, DAPI detects approximately the same C-banding pattern as  $\text{Ba}(\text{OH})_2$ , in later stages (PII and PIV), DAPI stains additional bands, classified as facultative heterochromatin, mainly because they show high variability and dynamics during the stages of prophase. Thus, DAPI banding information was used to estimate facultative heterochromatin, called DAPI-facultative heterochromatin. To differentiate it from the facultative heterochromatin stained by  $\text{Ba}(\text{OH})_2$ . Although, most of the unspecific C-bands match with the DAPI bands, we separate the two kind of heterochromatin because the difference shows additional facultative heterochromatin bands that were important to help characterize some of the chromosomes (Table 6). DAPI-facultative heterochromatin was obtained by subtracting the total heterochromatin stained by DAPI from the constitutive heterochromatin stained by Barium hydroxide. DAPI-specific facultative heterochromatin was estimated subtracting the DAPI-facultative heterochromatin to the  $\text{Ba}(\text{OH})_2$ -facultative heterochromatin.

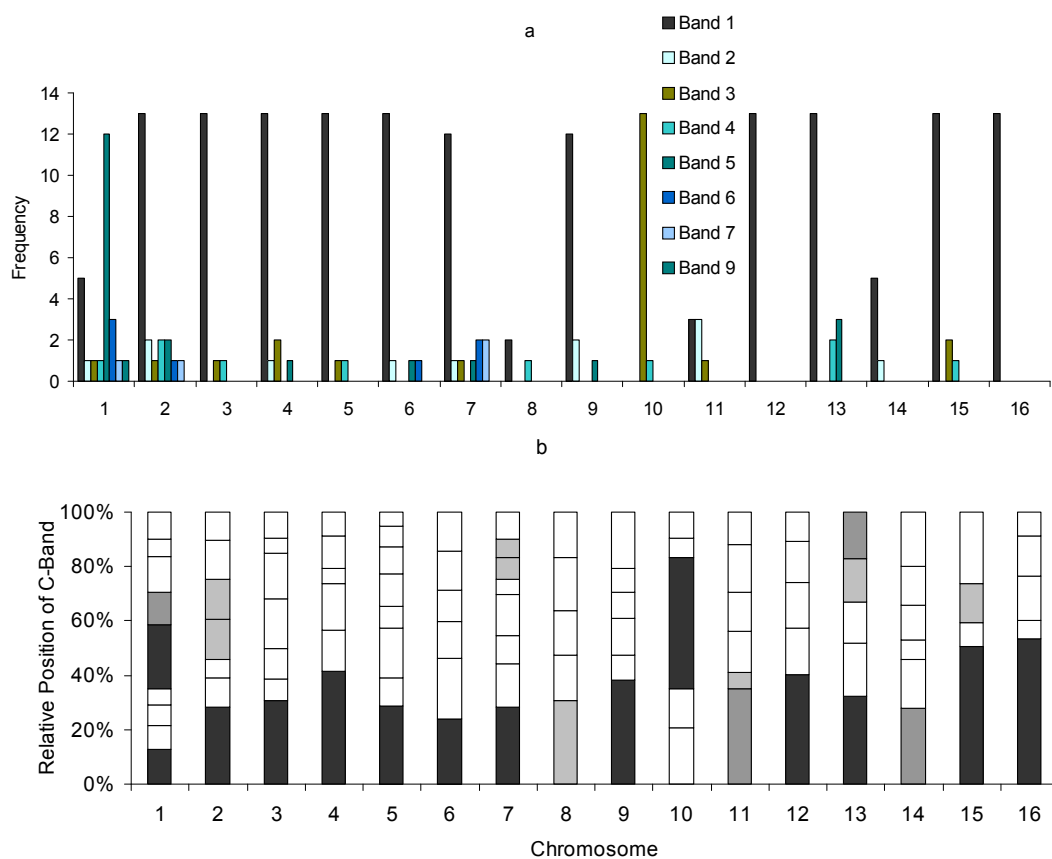


**Fig. 7.** Banding pattern of honey bee chromosomes based on  $\text{Ba}(\text{OH})_2$ . (a) frequency and (b) interval for relative position.

Chromosomes C3, C8, C11 and C14 have the highest content of DAPI-Facultative heterochromatin (Fig. 8a and 8c). Chromosomes C1, C6 and C7 do not contain DAPI-specific facultative heterochromatin (arrows in the Fig. 8c), while C8, C11, and C14 contain significant amounts (Fig. 8c). All the same chromosomes contain the largest amount of facultative heterochromatin as estimated by both barium hydroxide and DAPI methods, while C4 and C10 contains the least amount of these kinds of heterochromatin (Fig. 8a and 8c). Additional information comparing heterochromatin using DAPI data is presented in the Table 6. Chromosomes C8, C11 and C14 are consistently grouped as having less content of DAPI-C heterochromatin but higher DAPI-facultative and DAPI specific heterochromatin; C10, C9, C13, C15, and C16 are

characterized as very heterochromatic and are grouped together by total DAPI heterochromatin and DAPI-C heterochromatin

**Table 6.** Heterochromatin content in honey bee chromosomes based on Ba(OH)<sub>2</sub> and DAPI staining methods. Means comparisons (Tukey's test;  $\alpha = 0.05$ ) for relative heterochromatin content.

Chromosome	Total of DAPI-Heterochromatin	Chromosome	Total DAPI Facultative Heterochromatin	Chromosome	DAPI-C-Band	Chromosome	DAPI-Specific Heterochromatin
1	0.333 a	1	0.095 A	11	0.024 a	1	-0.057 a
11	0.417 b	10	0.137 Ab	8	0.036 b	6	-0.010 ab
3	0.427 b	6	0.157 Bc	14	0.111 c	7	-0.002 ab
2	0.428 b	13	0.163 Bc	3	0.190 d	2	0.017 bc
5	0.434 bc	4	0.174 Bcd	5	0.224 e	13	0.032 bcd
8	0.436 bc	2	0.178 Bcd	1	0.238 f	12	0.037 bcd
4	0.454 bcd	7	0.186 Bcd	2	0.250 g	10	0.061 cdef
6	0.458 bcd	15	0.190 Bcd	4	0.280 h	5	0.069 cdef
14	0.461 bcd	12	0.195 Cde	7	0.283 h	15	0.076 def
7	0.469 bcd	5	0.210 Cde	12	0.294 i	3	0.093 ef
12	0.489 cde	9	0.224 Def	6	0.301 j	16	0.093 ef
10	0.506 de	3	0.237 Efg	9	0.315 k	9	0.096 f
9	0.533 ef	16	0.250 G	16	0.339 l	4	0.106 f
13	0.542 ef	14	0.350 H	10	0.369 n	14	0.117 fg
15	0.566 f	11	0.392 H	15	0.376 o	8	0.170 gh
16	0.589 f	8	0.401 H	13	0.378 o	11	0.181 h
Mean	0.4714		0.2213		0.2505		0.0674
Tukey's test: Means for groups in homogeneous subsets are displayed. These are based on Type III Sum of Squares. The group sizes are unequal and the harmonic mean of the group sizes is used. Type I error levels are not guaranteed to equal $\alpha = 0.05$ .							

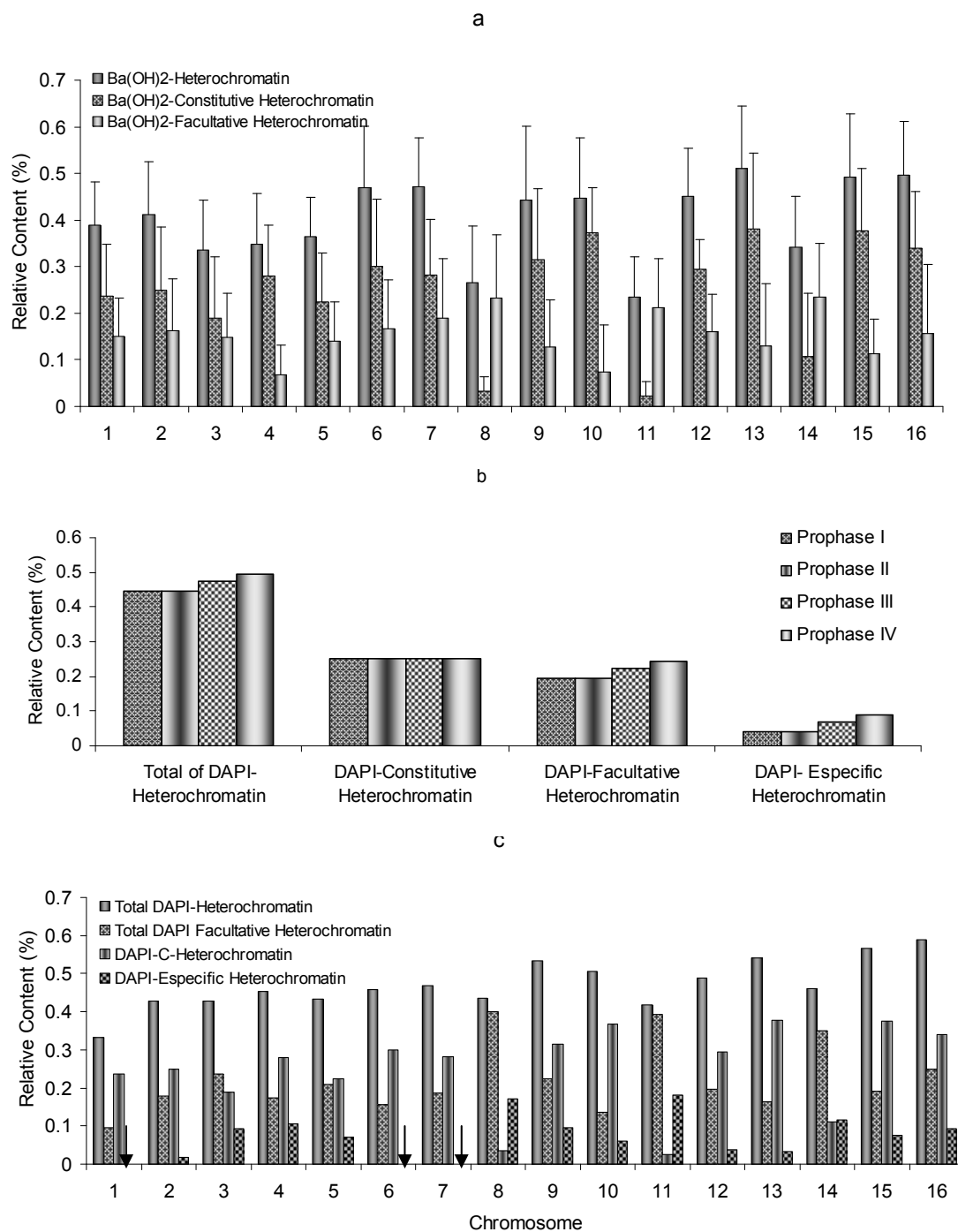


**Fig. 8.** Relative content of heterochromatin in honey bee chromosomes. (a) estimated using the  $\text{Ba}(\text{OH})_2$  method for C-Band detection, (b) estimated in different stages of prophase using DAPI data and (c) heterochromatin content based on DAPI data.

### **Description of the chromosomes**

The information from DAPI stained preparations was classified in four phases according to length and configuration of spermatogonial mitotic chromosomes. Length, arm ratio, and the range (the point where the band start and the point where the band ends) of the bands were measured. With that information the ideograms were constructed. Individual chromosome ideograms were compared through the four phases in DAPI experiments to verify consistency in the banding pattern. The bands were classified following the general rules of ISCN (2005) for human chromosomes. Bands that appeared in very close proximity that overlapped in the later stages were considered as members of a single band or as sub-bands. In the case of pericentromeric heterochromatin, decimal numbers were used to separate overlapped bands. Because the limits of most of the bands are not very well defined and the euchromatin is consequently diffuse, band classification focused on the heterochromatin banding of DAPI and was compared with C-banding. This banding classification was subsequently compared with the rest of the banding techniques ideograms. In the Fig. 9, PI, PII, PIII and PIV stand for the stages of prophase, the letters D, C, G, T, nr, and R refers to DAPI- (Fig. A.1), C-Ba(OH)<sub>2</sub>- (Fig. A.2), giemsa- (Fig. A.3), AgNO<sub>3</sub>-NOR- (Fig. A.4), R- (Fig A.5), and trypsin- (Fig. A.6) banding methods respectively. The added number represents the chromosome number. Complete ideograms, karyograms and karyotypes are presented in the appendix Figs. A.1-A.6, comparative ideograms are found in the Fig. 9.

The position of the centromere and bands vary a little among phases. This was in part due to the unbalanced number of preparations from different stages of prophase in the experiments and the condensation pattern of the chromosomes. With the exception of C2, C4 and C15, for giemsa and AgNO<sub>3</sub>-NOR banding, none of these differences are statistically significant and the positions of the chromosomes in the karyotype were not affected.

The results for Ba(OH)<sub>2</sub> are presented with two kind of bands, the properly called C-band, which is the strongest stained band observed, and the unspecific C-bands, which are lightly stained. In the Fig. 9, the C-bands are colored deep blue while the unspecific C-bands are colored light blue. The degree of transparency is used in all cases to indicate the frequency at which the bands occurred. To facilitate the chromosome description, DAPI, C-, G- and T- banding will be treated as heterochromatin-related banding techniques and AgNO<sub>3</sub>-NOR and R-Banding will be considered as euchromatin-related banding techniques. Because the ideogram is based on frequency of the bands and not intensity of staining, the resultant ideograms could appear more heterochromatic when the chromosome carries many low frequency bands. This is potentially a problem with C8, C11 and C14. The gradient of colors is utilized to correct this problem. Because of the variation and dynamics in the chromosome condensation and heterochromatinization (as mentioned above and more detailed discussed in A-3), bands often could not be matched among stages of prophase or methods of staining. Wherever possible, a very light line is drawn to show banding correspondence.

Chromosome 1 (C1). This is the largest chromosomes of the honey bee karyotype, and together with C10, belongs to the metacentric group. C1 consistently presented 11 bands in all heterochromatin banding techniques. The heterochromatic banding techniques resulted in similar banding patterns, except for the pericentromeric band that is not consistently stained by giemsa and trypsin. Consistently, a pair of bands was observed in DAPI, trypsin and giemsa, giving bands that in later stages of prophase are usually observed as a single band in the DAPI technique (Fig. 9a). This result has a particular meaning in terms of the chromosome organization, because it suggests that some special genetic information could be present between these facultative heterochromatin bands. AgNO<sub>3</sub>-NOR and R-Banding (with some variation) match the most euchromatic regions between bands; particularly the inter-bands between q42 and q41, q41 and q31, q31 and q22, p31 and p41. With some frequency, AgNO<sub>3</sub>-NOR, R-banding and the rDNA marker all detect a NOR region in the euchromatic region of the short arm, which NOR region corresponds approximately to inter-band between p31 and



p21 bands. A gold-green circle marks the euchromatic band delimited by the end of band q13 and the start of the band q21. This region (referred to as A.2) is one of the points where condensation forces meet, making this band alternately variable in size.

Chromosome 2 (C2). This chromosome is the least heterochromatic of the heterochromatic chromosomes; R-banding confirms the relatively euchromatic condition of this chromosome. In the early stage of prophase using the DAPI method, C2 shows a double band in the short arm, which doublet is quickly lost in later stages of prophase (Fig. 9). A distinctive characteristic, this chromosome presents two additional centromere-like constrictions, one at telomeric, 0.35 of the p arm and another at 0.8 in the q arm. Variation associated with these constrictions make C2 characterization difficult. Size and the pericentromeric heterochromatin are the most reliable characteristic for correct identification. In general, DAPI, C-Banding, giemsa, and trypsin show great similarity in banding patterns. DAPI and giemsa show that bands p4 and p5 are double bands like those described in C1, but fail to stain the pericentromeric q arm heterochromatin identified by DAPI and C-Banding, although it could be possible that the last result is a consequence of variation in the measurements. R-Banding matches euchromatic bands at q5 and the inter-band between q3 and q4, and q31 and q21. Contrasting the R-banding against the heterochromatin banding techniques, C-, DAPI- and G- banding, it seems that chromosome 2 is highly banded but euchromatic in appearance as in R-banding. This pattern fits with what is seen in C8, C11 and C14, with the exception that, at pre-metaphase and sometimes late prophase, C2 can be visualized as heterochromatic.

Chromosome 3 (C3). C3 is one of the most acrocentric chromosomes. In the early stages, its arm ratio is closet to the telocentric classification value (observed arm ratio 6.4, expected telomeric arm ratio 7.0) given by Levan et al. (1964). C3 frequently is confounded with C5 because both carry a large constriction after the pericentromeric heterochromatin in the long arm. However, C5 consistently carries this constriction immediately after pericentromeric band; while C3 carries this constriction after the q12 band. Chromosome 7 carries a similar constriction but it is less frequently observed. One

distinctive characteristic of chromosome 3, which is shared with chromosomes 8 and 11, is the large infrequently observed heterochromatic region between q12 and q31 bands (Fig. A.1.3, circle in the karyogram). DAPI consistently stained 10 bands; C-, G- and trypsin- stained 8 bands. The banding pattern among the different techniques was a little different. DAPI band q22 is apparently not present in G-banding and band q53 apparently is not detected in C-banding. One telomeric band in the long arm in G- and trypsin-band methods was not recorded in DAPI banding. A match with R-Bands was found in the inter-band between q23 and q31, with another match between the bands q31 and q41 and one more that matched between the low frequency bands q51 and q52.

Chromosome 4 (C4). C4 is sub-metacentric and considered in the group of heterochromatic chromosomes due to the low frequency large band q31 that together with bands q32 and q21 gives the heterochromatic appearance when all bands were present. In some cases this chromosome was observed to be completely heterochromatic - even in the early stages of the prophase. Trypsin and giemsa show similar banding patterns. DAPI and giemsa show consistently 8 bands. C- stained 6 bands, and trypsin 10 bands. The large DAPI band q31 seems to be composed of two bands; this is confirmed by C- and trypsin band techniques, and by giemsa, which only stained the distal band. One short band between the inter-band of q21 and q12.2 is stained only by G-banding and detected as a euchromatic region by R-Banding. Ba(OH)<sub>2</sub> does not stain the DAPI and G-band positive telomeric band. R-Banding detects the low frequency DAPI band q31 and the subtelomeric euchromatic band of q41 as euchromatic. The circles show one of the variations in the position of band q22, which suggest that the region between q21 and these q22 is the point of separation between the condensation forces coming from pericentromeric and q3 region (Fig. 9).

Chromosome 5 (C5). DAPI-, C-, G- and trypsin banding showed similar numbers of bands for chromosome 5, and there is general concordance for DAPI-Bands through the different stages of prophase. However, some bands become more distal at pre-metaphase possibly due to the irregular condensation of this chromosome or some imprecision on the measurements. As in C3, C5 shows a large overlapped region (q3)

composed of three bands at the distal end of the long arm. As heretofore described for heterochromatinization and condensation, circles show bands that are variable in the position (q21 and q22). Arrows show the possible movements of band q31 and the pericentromeric region (Fig. 9). Band q33 is observed in DAPI-, G- and trypsin banding but is absent in C-banding. Bands q22 and q21 appear more distal in C-, G- and trypsin, than in DAPI, and seem to be pulled toward q31. An additional band was found in trypsin between q12.2 and q21. There are two R-bands that match regions of q31 and q22; q31 is a low frequency DAPI band and the euchromatic region of q22 is below the heterochromatic band and circled in the DAPI maps. One R-band matches the euchromatic region (below q21) that in C- and G- appears as low frequency heterochromatic bands. G- and R-Banding confirm that band p12 is composed of two bands, which stained by C- and DAPI- would be p12.1 and p12.2. AgNO<sub>3</sub>-NOR and R-banding show similar results.

Chromosome 6 (C6). This chromosome carries a NOR region on the distal region of the short arm, and is most similar in size to chromosome 8, but morphologically is similar to chromosome 4. C6 was frequently confounded with 4 when the rDNA marker was omitted. C6 and C12 are highly variable in size and morphology through the different stages of prophase, thus the use of rDNA as marker was required to identify these two chromosomes. Except for a telomeric band q32, the DAPI banding pattern through the different stages is in good agreement with C-Banding (Fig. 9f). Bands q21 and q31 appear as low frequencies C-bands; R-Banding confirms that assignment. R-Banding shows short euchromatic regions in the inter-bands between q21 and q31, and q12.2 and q21. AgNO<sub>3</sub>-NOR show better fit with the euchromatic band shown by C-banding technique than with any DAPI-Band. C-banding detected that the constitutive heterochromatin of the short arm is composed of two bands, one of which, p12 (p12.2), is detected by G-band; but this last technique fails to detect the pericentromeric heterochromatin (p12.1). In general, G- and trypsin banding look different, but detect approximately the same pattern as DAPI- and C-Banding. The circles and ovals mark the observed variation in the DAPI euchromatic regions. Relatively low variation in the

position of the heterochromatic bands suggests that the three heterochromatic bands detected play similar roles in the condensation of this chromosome (Fig. 9f).

Chromosome 7 (C7). C7 is the second sub-telocentric, very heterochromatic and relative easily to band. DAPI at prophase II-IV and C-banding heavily stains the long arm of this chromosome. C-banding stains three additional constitutive stain heterochromatin bands at positions q32, q31 and a small unspecific low frequency band at q21. With some little variation, G- and trypsin stain the same pattern. The region between q31 and q33 was stained and scored as heterochromatin by DAPI, as euchromatic with one short C-band by Ba(OH)<sub>2</sub>, and as euchromatic by R-banding. That region includes the heterochromatic specific facultative DAPI band, q32. The euchromatic region between q21 and q31 matches an R-band. The circles, ovals and arrows suggest the pattern of condensation and heterochromatinization of this chromosome.

Chromosome 8 (C8). This is a euchromatic chromosome, which when the central heterochromatin band is early-condensed, can be confounded with C9 and C6. Otherwise it could be confounded with chromosome 11, which shares many characteristics. In general, C- and DAPI- banding show a similar pattern except for the pericentromeric region and a band q32 which are not clearly detected by Ba(OH)<sub>2</sub>. DAPI showed this chromosome as very euchromatic. Most of DAPI bands were low frequency, which means that in most of the cases they were not deeply stained or not stained at all. C-banding only detected, at very low frequency, the pericentromeric band of the short arm and an additional band that seems to be close to the q41. G-banding detected pericentromeric banding as did DAPI, but showed an additional band at a more distal position, which according to DAPI nomenclature, is part of the p12 band. This latter was also detected with trypsin, which in general matched DAPI and C-banding on the long arm. R-banding showed a low frequency euchromatic band on the short arm where C- banding failed to stain. R-Banding also stained 75% of the long arm as euchromatic at different levels, just as DAPI did for low frequency heterochromatin, which makes this chromosome look euchromatic. AgNO<sub>3</sub>-NOR match the euchromatic

regions presented by C-Banding, except in the short arm. In general, AgNO<sub>3</sub>-NOR and R-Banding also suggest that C8 is very euchromatic. The circles and band q21 show some evidence of the condensation pattern of this chromosome. Little effect is observed from the centromeric region.

Chromosome 9 (C9). Chromosome 9 is the third most acrocentric of the karyotype of honey bee. It is very heterochromatic, as R-banding and C-Banding confirm. Its configuration is similar to that of C7 allowing confusion between these two chromosomes. The data for DAPI-banding produced 7 bands but the centromere split the pericentromeric region to give 8 bands. Except for band q32, the agreement in banding pattern is good between C-Banding and trypsin, both of which produced 6 bands. Band q32 was detected by trypsin but not by Ba(OH)<sub>2</sub>, while q33 was detected by DAPI-, C-Ba(OH)<sub>2</sub>, and G-Banding but not by trypsin. Bands q31 and q21, which are a little skewed toward a distal position compared to the position displayed by other methods, are stained as three very short bands by giemsa. In DAPI and C-banding, q21 is a large band, but giemsa stained it in two short bands. DAPI also stained the q12.2 band, which is not stained by G-, C- and trypsin- banding; the last technique stained only part of q12.1. AgNO<sub>3</sub>-NOR showed a similar pattern to trypsin, and different from the R-banding pattern, which detected as euchromatin the region of band q33. The q31-q41 region consists of very large overlapping bands that include q32 and q33 bands. The euchromatic region between q21 and q31 matches perfectly with the R-band. The circles and ovals suggest that q31 and q21 positions are affected by the condensation in both direction, q21 was consistently pulled toward the centromere except in PIV, q31 and q32 were pulled toward centromere in PII but then toward the telomere in PIII and PIV.

Chromosome 10 (C10). C10 is the second metacentric chromosome, and frequently appeared as the most heterochromatic chromosome. Whenever the central heterochromatin was deeply stained, C10 was easily confounded with C8 and 11. When the low frequency heterochromatic band p21 was deeply stained, the metacentric configuration was lost; thus a sub-metacentric or sub-telocentric chromosome configuration was initially assumed. In those cases, chromosome 10 was classified by

elimination, after chromosomes 7, 8, 9, 11 and 12 were identified. Sometimes the p12 band is lost and the appearance of the chromosome could be that of chromosome 15. DAPI-banding of C10 is in very good agreement with C-banding and (for the large arm) trypsin banding (Fig 9j), although for the short arm, the pericentromeric band was not trypsin stained. G-Banding showed that bands q21 and q12.2 are composed of two bands. In the short arm, G-banding detected correctly the band p21, but showed an additional band that matches with the euchromatic band between p12 and p21. AgNO<sub>3</sub>-NOR and R-Banding stained the short arm of C10 as very euchromatic, leaving as heterochromatin just the q21 band and a very short fragment of pericentromeric heterochromatin (p12) that C-banding detected as low and high frequency C-bands, respectively. The euchromatic region between q12.2 and q21 matches only the R-band in the large arm - a result that is not in agreement with the pattern shown in AgNO<sub>3</sub>-NOR banding.

Chromosome 11 (C11). C11 is the second most euchromatic chromosome, and is morphologically similar to C8 and C14. Occasionally, DAPI stained deeply the pericentromeric region and the short arm. In those cases, the appearance can be confounded with C12 or C10. As was true for C8 and C14, the usual configuration of C11 is a "V", which suggests an acrocentric morphology. As in C8 and C14, this chromosome, carries a euchromatic fragment at a distal position on the short arm which, when completely unstained, is difficult to detect. When the same fragment is deeply stained, the configuration changes and chromosome identification become complicated; in those cases the intensity of the staining can be used as a reference. DAPI and giemsa detected 6 bands; C-Banding and trypsin detected 7 (Fig. 9k). The pericentromeric band is infrequently stained as a C-band. More frequently stained is a C-band that is a very short distance from the pericentromeric band, the latter seems to be the only specific C-band in chromosome 11. A second short and low frequency C-band was detected by Ba(OH)<sub>2</sub> in the euchromatic DAPI-region of q13 band. This infrequently observed band was produced by condensation in late prophase and pre-metaphase. A region of overlapping bands q21 to q31 agreed with the four separated unspecific C-bands, and

frequently were G-banding and trypsin stained. Thus, the pattern shown by trypsin- was in very good agreement with DAPI and C-banding. Surprisingly, R-banding stained all the overlapping regions including the low frequency C-band. Even so, we can say that R-banding showed a very euchromatic chromosome. It is possible that the result for this chromosome comes from difficulties with the staining procedure, and that chromosome 11 requires a stronger treatment to detect the correct R-banding pattern. However, an In Situ Nick translation banding (chapter III) shows a similar pattern. The DAPI euchromatic region is only partially labeled by prolonged incubation, indicating that this region is hardly accessed by nick translation. The ovals suggest the condensation pattern for this chromosome.

Chromosome 12 (C12). C12 carries the nucleolus organizer at the telomeric region of the short arm. This chromosome was heavily stained and similar in size to C11, C13 and C14, and can be confounded with any of the latter. A total of 6 bands were detected by DAPI, trypsin, G- and C-banding. The pattern, although a little offset in C-banding, basically was the same (Fig. 9I). C- and G-banding detected one additional band in the DAPI euchromatic region between q12.3 and q21; however, band 12.2 was absent with both staining methods, which suggest that q21 could be shifted to a distal position in G- and trypsin banding methods. R-banding stained the inter-bands between q21 and q22 as well as between q21 and q12.3. Another low frequency R-band was detected between the region of q12.2 and q12.3, which was classified as a low frequency DAPI band and unspecific C-band. The region stained by AgNO<sub>3</sub> as the NOR-region was stained by R-banding as a large euchromatin band; that same region was frequently stained by giemsa in a series of short bands.

Chromosome 13 (13). Chromosome 13 is very heterochromatic and almost submetacentric according to Levan et al. (1967) nomenclature. A distinctive characteristic that C13 shared with C14 and C15 is the high frequency telomeric heterochromatic band in the long arm, which can be used to identify this chromosome. Trypsin stained 7 bands; all other heterochromatin-detection techniques stained 5 bands. The banding patterns of DAPI, trypsin and C-Banding are in good agreement, although G-banding did

not detect the q22 and q12.1 bands (Fig. 9m). In addition, G-banding detected a very infrequently stained band close to the centromere, and a high frequency band a more distal region, both in the short arm. Ba(OH)<sub>2</sub> detected C-heterochromatic bands q31 and q22, although less frequently than the C-pericentromeric band. R-banding detected the euchromatic region between q12.2 and q22, which matched approximately the euchromatic region of C-banding. This euchromatic region included two unspecific C-bands that correspond to bands q21 and q12.2. Band q31, and a euchromatic region below that, were infrequently detected. The same low frequency C-banding was obtained for the short arm and pericentromeric region, and show chromosome 13 as euchromatic. This was unexpected. Technical problems could be involved because DAPI, trypsin and C-banding show C13 as very heterochromatic.

Chromosome 14 (C14). Chromosome 14 was the third-most euchromatic chromosome. Except for giemsa that detected 5 bands, all banding techniques for heterochromatin detected 6 bands. This chromosome, like C8 and C11, showed many low frequency bands that could be confused as heterochromatic. DAPI, C-banding and with some little deviation, trypsin banding are in good agreement. According to the Ba(OH)<sub>2</sub> result, the pericentromeric heterochromatin was very short, and shorter in the short arm (Fig. 13). DAPI-, C- and trypsin- detected a large euchromatic band in the distal position of the short arm. R-banding detected most of this same region as euchromatic. R-banding stained a large euchromatic region in the long arm which includes q12.1 and most of q21. Band q22 was stained as a low frequency euchromatin region by R-banding, in agreement with early results that showed heterochromatin bands in the large arm of C14 are low frequency. The result obtained with R-banding is considered good because the chromosome is confirmed as euchromatic.

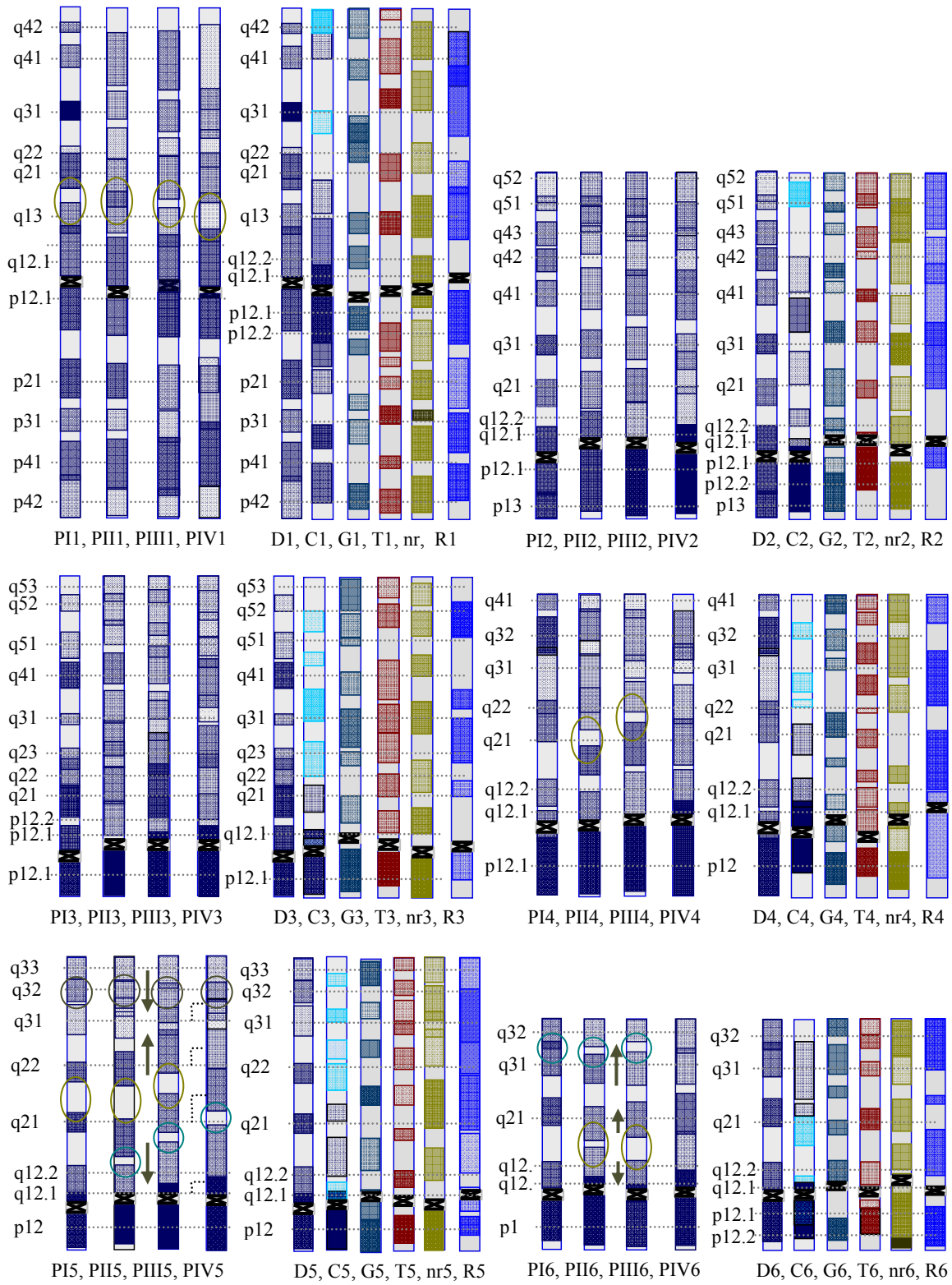
Chromosome 15. C15 belongs among heterochromatic chromosomes. Its distinctive characteristic is the distal low frequency C-band. Except for giemsa that detected 6 bands, all heterochromatin banding techniques detected four bands. C15 is the only chromosome whose classification, as sub-telocentric or metacentric remains problematic. One explanation is that the short arm was frequently lost, whereupon the



chromosome assumes the appearance of a metacentric chromosome. In those cases, because of configuration, chromosome 15 can be misclassified as chromosome 10. DAPI and C-banding patterns were approximately similar. G- and trypsin-banding failed to detect the pericentromeric band q12.1 in the long arm; however, the centromere's position was a little shifted compared to the position obtained by DAPI and C-banding (Fig 9o). The distal half of band q21 and band q31 were detected as low frequency C-bands by Ba(OH)<sub>2</sub>, and detected as euchromatic bands by R-banding; the infrequent band q12.2 was detected as euchromatic by R- and C-banding techniques.

Chromosome 16. C16 is the smallest chromosome and classified as very heterochromatic in all stages of prophase. Apparently most of its heterochromatin is DAPI specific stained. The trypsin method supports this observation, while Ba(OH)<sub>2</sub> and giemsa show a very unstained chromosome (Fig. 9q). Except for trypsin that shows 6 bands, most techniques stain only four bands. DAPI- and C-banding are in good agreement. Giemsa presented the best banding pattern of this chromosome, showing the three bands in the long arm, but fails to stain the p-pericentromeric heterochromatin. However, the large euchromatic band matches with the large central euchromatic region of DAPI-banding. This last characteristic makes this chromosome more euchromatic than C13 and C15. However, given the unspecific C-bands in the Ba(OH)<sub>2</sub> method, the heterochromatic condition of this chromosome detected by DAPI is supported. Fortunately the low frequency and light staining differentiate this region from the euchromatic one, which consistently is the most strongly stained.

**Fig. 9.** Comparative ideograms and banding classification of chromosomes of honey bee stained with DAPI (D), Ba(OH)<sub>2</sub> (C), giemsa (G), trypsin (T), AgNO<sub>3</sub> (nr), and R-banding (R) at different stages of prophase: prophase I (PI), prophase II (PII), prophase (PIII), and prophase IV (PIV). The numbers after the letters indicate the chromosome number. The bands are classified based on nomenclature of human chromosomes ISCN (2005), however because of the irregularities in the boundaries and overlapping bandings, the classification was focused on heterochromatic bands only. The pericentromeric region was differentially classified using decimal numbering, for the short arms of the chromosomes 4 – 16, as only one band was read for pericentromeric region the decimal numbering was omitted but they should be referred as decimal identification. In chromosome 12, an overlapped band, q13.1 was left unlabeled. The ovals and circles on some ideograms indicate the variation in the length of the euchromatin bands because of the effect of the condensation and heterochromatinization of the chromosome. These bands suggest some forces (indicated by arrows) are modifying its size and their position and affecting the position of some bands as in chromosome 5, 7, and 9. This phenomenon was described earlier. The circles and arrows indicate only examples since the phenomena can be observed in almost all chromosomes but less evident.



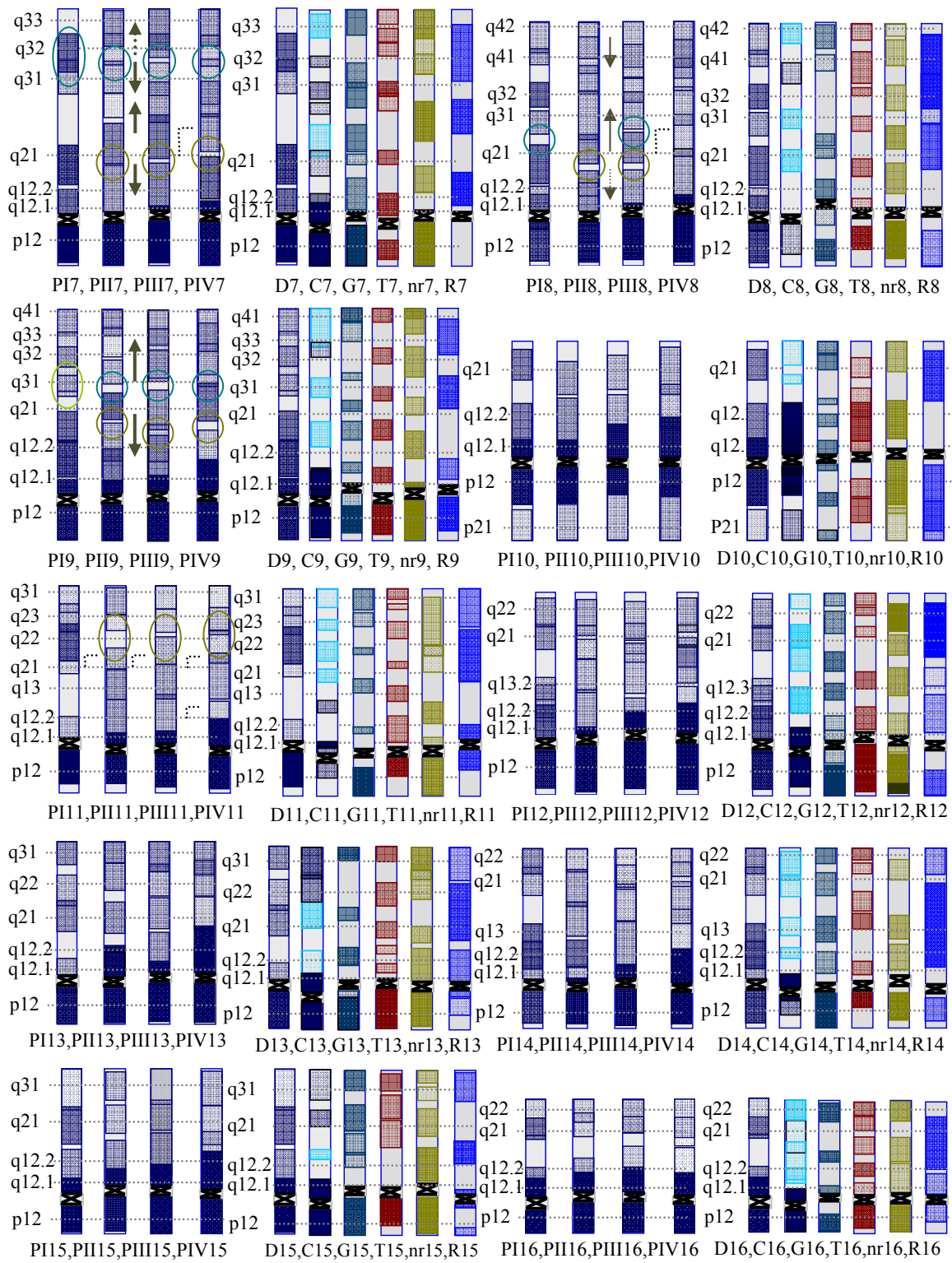


Fig. 9. Continued

## Discussion

The data suggests that chromosome condensation takes place in individual chromosome fashion, influenced by the banding pattern that affects the length of chromosomes and arm ratio. Observed variation in condensation could be due to the variable chromatin domains, proteins, and nucleotide composition in these domains. Although chromosome length reveals a definite pattern of reduction of chromosome size, that reduction is nonlinear throughout all prophase, but linear during the period studied, similar result has been found in Kireeva et al. (2004) and Maddox et al. (2006); the arm ratio reveals chromosome specific variation as previously determined in mammals (Hiraoka et al., 1989; Li et al., 1998). For example C5, C7 and C12 show a gradual decrease in the arm ratio from PI to PIV, which means that the arms shorten similarly throughout; while chromosomes 6, 8, 9, 11, 13 and 14 showed a gradual reduction beginning with PII, but with the arm ratio consistently lower in PI than in PII (Fig. 2a). The banding patterns also show chromosome specific patterns of condensation. For example, heterochromatinization progresses from preexisted heterochromatin in some cases. In other cases preexisting heterochromatin can work as a barrier to the heterochromatinization process, as happened with the pericentromeric heterochromatin of the short arm of the C1.

Some bands show variation in size that implies a differential nucleotide composition that may influence condensation through the prophase. Thus, in this process the different kinds of heterochromatin play different roles. Constitutive heterochromatin usually has been assigned a protective role and are responsible for genes silencing and cell differentiation (Claussen, 2005; Lakhota, 2004), with facultative heterochromatin controlling gene expression and cell differentiation (Chadwick and Willard, 2004) through epigenetic control by methylation and acetylation (H3 and H4) of some histones and HP1 protein distribution (Maison et al., 2002; Spector, 2003; Grewal and Moazed, 2003; Lakhota, 2004; Grewal and Rice 2004; Lamb et al., 2007). Euchromatin houses

middle expressed genes and house-keeping genes (Holmquist, 1992; Claussen, 2005, Lamb et al., 2007). Based on this general frame regarding heterochromatin function, distribution of nucleotide domains and heterochromatin content is an important characteristic for architectural of the chromosomes, gene distribution and genes expression (Millot et al., 1996; Festenstein et al., 1996; Cuvier et al., 2002; Maizon and Almouzni, 2004).

Based on DAPI and C-Banding staining, the genome of honey bee contains  $47 \pm 11.5$  % heterochromatin, of which  $25 \pm 11.12$  % is constitutive and  $22 \pm 10.4$  % is facultative; 7% of facultative heterochromatin is DAPI specific stained and 15 % of that is C- and DAPI stained. Only 3.5 % of the constitutive heterochromatin occurs in low frequency C-bands, which means that the (A/T) rich regions should be lower than 21.5 % in the remaining mostly pericentromeric heterochromatin. Assuming that constitutive heterochromatin is mostly repetitive sequence, the estimated A/T content of the heterochromatin is considerable higher than the 8% to 10% estimated by Cot-1 and Cot-2 analysis (Crain et al., 1976). The heterochromatin content estimated in this experiment is similar to the 36% reported in the section “Genetic and Physical Maps and Chromosome Organization” (HBSCP, 2006), but is different from the percentage in the sequenced genome, which is reported to be 67% (A/T) rich, however this latter value is for the sequenced portion of the genome and not specific for heterochromatin as we estimated. As in the plant, *Arabidopsis thaliana* (Stack et al., 1974; Freanz et al., 2000) and mammals (Berríos et al., 1999), the heterochromatin in honey bee chromosomes is distributed mainly in pericentromeric heterochromatin and knobs, and located in the peripheral nucleus, where multiple overlapping bands suggest its systematic regulatory function though epigenetic regulation. With the exception of the short arms of C1, C6, C12, these overlapping bands were detected in pericentromeric heterochromatin of all chromosomes; and all chromosomes presented a second region of overlapped bands in a subtelomeric position. In most of these chromosome some low frequency of constitutive heterochromatin was detected.

Heterochromatin may also function as a barrier for further heterochromatinisation, as happens in the short arm of C1, C6 and C12. Grewal and Jia (2007) and Maison and Almouzni (2004) mention that the boundaries of constitutive heterochromatin can be delimited by inverted repeats (IR). Some sequences recruit a specific protein system that prevents heterochromatin propagation (Thon et al., 2002). Heterochromatin boundaries are sometimes related to the positive interaction of heterochromatin with polymerase III (Pol III) and transcription factors that facilitate the transcription of the genes are located in these boundaries (Noma et al., 2006). The heterochromatin boundaries of *Saccharomyces pombe*, for example, usually are occupied by tRNA clusters (Grewal and Jia, 2007) and micro RNAs (Maison and Almouzni, 2004), which possibly function to demarcate the limits of heterochromatin domains under the model of “Loops Domains” of genome organization (Ostashevski, 1998; Labrador et al., 2002; Grewal and Jia, 2007). Pericentromeric heterochromatin is observed in the short arm of chromosomes with a sub-telomeric unstained band, such as in C2, C4, C6, C8, C10, C11, C12, and C14. The latter showed size stability through prophase as has been observed in prophase chromosomes of yeast. There is evidence that the ribosomal cluster in chromosomes 6 and 12 might be a heterochromatin barrier in the honey bee genome. A similar pattern of distribution and function of pericentromeric heterochromatin is observed in *Arabidopsis thaliana* (Luo et al., 2004). Pericentromeric heterochromatin of the short arm of C1 can also be considered in the same model, although the presumed NOR region is not at the heterochromatin boundary. It will, therefore, be important to identify the content, and study the structure and organization of, the pericentromeric boundaries of C1.

Location of pericentromeric heterochromatin also determines the chromosome distribution in the nucleus (Berríos et al., 1999; Carvalho et al., 2001). When pericentromeric heterochromatin is present, chromosomes are located in the nuclear periphery; when pericentromeric heterochromatin is diffuse or absent, the chromosomes tend to be located in the central region of the nucleus. This difference has a particular significance for C8, C11, C14 and maybe C4 as it was characterized in this study.

Regulation related to heterochromatin may be particularly important in the case of C11, in which the large cluster of major royal jelly family proteins (MRJP) and the yellow family genes (gene related to the pigmentation in *Drosophila* and many flies) are located (Drupeau et al., 2006). According to NCBI, these clusters are located at distal regions that match a short overlapping region between q21 and q31. This suggests the most probable position of the major royal jelly family proteins is band q23, a low frequency band (C- and DAPI facultative heterochromatin) that matches with an AgNO<sub>3</sub>-NOR band and the large R- euchromatic band of C11. The position of the MRJP cluster in a consistently facultative heterochromatin band is important because Royal Jelly genes are temporally expressed and restricted to some organs like mushroom bodies of the honey bee brain of workers in the first week after emergence (Kurcharski and Maleszka, 1998). MRJP are highly but temporally expressed genes that are essential for castes differentiation in the honey bee society (Drupeau et al., 2006). Therefore, the location fits exactly with the model that the location of the genes and the distribution of the facultative and constitutive heterochromatin is not random (Berríos et al., 1999), and supports the idea that heterochromatin has an important function in gene expression and cell differentiation (Grewal and Jia., 2007; Yasuhara and Wakimoto et al., 2006). Corradini et al. (2007) published a list of 450 predicted genes whose function and expression is associated with heterochromatin. Most of these genes are classified as non-essential or required in specific steps of cell division, DNA repair, chromosome segregation, chromosome condensation, metabolism and cell interaction. Some highly expressed ribosomal protein-coding genes are located between constitutive heterochromatin (Marygold et al., 2005), and these genes characteristically have short overall size and short introns. Konev et al. (2003) mention that heterochromatin harbors important genes for viability and fertility as well as important genes for kinetochore formation, sister-chromatid cohesion, and disjunction of achiasmate chromosomes.

Heterochromatin is also an important target of mobile elements (transposon and retrotransposons) which implies a protective function in *Drosophila*. Large essential genes are also located in those regions; the explanation of this is heterochromatin



protects regions differentially targeted by transposable elements (Corradini et al., 2007). That the MRJP is in the facultative heterochromatin of C4, the NORs are in the boundaries of pericentromeric heterochromatin of C6 and C12, and the apparent static pericentromeric heterochromatin is in the short arm of chromosomes all suggest the important role of heterochromatin in the honey bee genome. Therefore it is important to study and clarify the importance of heterochromatin and its role in gene regulation and expression in the honey bee. The irregular banding pattern of the honey bee offers an advantage in the study of the role of gene organization in the genome. It is particularly tempting to propose to use honey bee chromosomes to study the CpG methylation system and imprinting mechanism that underlie castes differentiation. It has been proposed that the imprinting mechanism in honey bees is different and does not involve repetitive DNA (Wang et al., 2006). However, in our study, the facultative heterochromatin seems to be important in gene regulation and differentiation, as shown by its plasticity.

The karyotype of honey bee analyzed in this study is characterized by two metacentric chromosomes (C1 and C10), two sub-metacentric and ribosomal organizer carrier chromosomes (C6 and C12), four sub-metacentric and heterochromatic chromosomes (C16, C15, C4 and C13), four euchromatic and sub-telocentric chromosomes (C2, C8, C11 and C14) and four acrocentric chromosomes (C3, C5, C7 and C9). This above grouping is different from that previously published by Hoshiba and Okada (1986), who classified the honey bee karyotype in four metacentric and 12th submetacentric chromosomes. It is also different from the karyotype described by Beye and Moritz (1995) who classified the chromosomes as one metacentric, with the rest classified based on the size; and with eleven chromosomes which are about 0.5 times larger than the fourth group of remaining chromosomes. Beye and Moritz assigned the rDNA region to chromosomes 4 and 11, but recognized that chromosome 12 carries a weak signal, which is in agreement with our results. The difference was that the signal on chromosome 11 was rarely observed. However, the different clones used for NOR-

detection can explain the difference, although it should be taken into account that our results were verified with  $\text{AgNO}_3$  staining.

Baudry et al. (2004) estimated the centromere location using half tetrad analysis for three linkage groups (I, II, and IV) and determined that linkage group I is metacentric and corresponds to C1. Linkage group II was estimated to be telocentric but was not assigned to any particular chromosome. The result of Baudry et al. (2004) could be correct if Linkage group II refers to C2. In C2 blocks heterochromatin are not restricted to pericentromeric heterochromatin. There are two blocks of heterochromatin, detectable in early prophase (Fig. A.1.1) and mapped as a single band in this study. If we assume that these blocks are pericentromeric, this suggests that Baudry et al. (2004) could be correct and C2 could be telocentric. However, the occurrence of relic constriction between these blocks of heterochromatin suggests the occurrence of a pseudo-centromere or neocentromere. Some observations suggest that the constriction is not the centromere since the blocks are distinguishable only in early prophase and always appear as a tightly packed block. Additionally the constriction is always stained rather than unstained as expected of a functional centromere. Rather than marking a telomeric centromere, the heterochromatin appears as expected of the pericentromeric heterochromatin of the short arm of C2. Mitotic and meiotic anaphase analysis is required to verify the centromere position and clarify the kind of constrictions located in C2. It could be also be that Baudry's linkage group II refers to C3. In linkage group IV the centromere was estimated to be telomeric; Beye et al. (1996) assigned that linkage group to C8. However, it is difficult to confirm this result in their paper, thus we cannot determinate the chromosome equivalence in our maps.

## CHAPTER III

### MAPPING 35 CLONES FROM SOLIGNAC'S BAC LIBRARY ON THE KARYOTYPE OF HONEY BEE

#### Introduction

Historically, the honey bee (*Apis mellifera*) has been economically important in agriculture because of honey, wax, pollination (Michener, 2000) and many derivatives (Mizrahi and Lensky, 1997). The consequences and behavioral implications of the social condition of this insect (eusociality) have been intensively studied to obtain strategies for control and management of diseases, and parasites, and for possible strategic applications in human societies (Seeley, 1989; Kaufman et al., 2002; Seeley and Visscher; 2004, Robinson et al., 2005). Evolutionarily significance genetic change in the eusocial, haplo/diploid honey bee has been determined based on genomic similarities; thus 60% of the genes involved in the immune system are orthologues to other sequenced insects, such as *Drosophila* and *Anopheles*; the other 40% could be related to the demands of eusociality (Evans et al., 2006; Gregory et al., 2005). Some of the genes that are unique to the bee could be related to social behavior and haplodiploidy, and these could provide the foundation for understanding the role of genome structure and function in haplodiploidy and social evolution (Evans et al., 2006). With the publication of honey bee genome sequence, all these areas have been strongly supported (HBGSP, 2006).

A number of studies provided genetic information important for the honey bee genome sequencing project. Genetic linkage groups were established in the honey bee based on randomly amplified polymorphic DNA (RAPD) scored for haploid males. The map covered 3110 cM distributed in 26 linkage groups, and showed for the first time, a very high recombination rate 52 kb/cM in honey bee (Hunt and Page, 1995). A second map, based on simple sequence repeats (SSr's or microsatellites) isolated from genomic

DNA or from bacterial artificial chromosomes (BACs) was developed (Solignac et al., 2003); this map resulted in twenty-four linkage groups spanning 4061 cM in total (Solignac et al., 2004). A genetic and physical relationship of 44kb/cM was estimated, which estimate was 15% shorter than that estimated by Hunt and Page (1995). Additional mitochondrial and microsatellite data (Franck et al., 2001) and expressed sequence tag data (EST) from a honey bee cerebral library were available (Whitfield et al., 2002) along with a BAC library in which quality of reads was tested with sequence tagged sites (STS) (Tomkins et al., 2002), and gave results similar to those from the cerebral (honey bee brain) cDNA library generated by Whitfield et al. (2002). Finally a relatively small honey bee genome size of 270 Mb was estimated. With this information, the complete sequencing of the honey bee genome was initially proposed and the Honey Bee Genome Sequencing Project (HBGSP) subsequently conducted by a consortium lead by the Human Genome Sequencing Center at Baylor College of Medicine (BCM-HGSC). The sequence project was authorized based on the small genome and the impact of the honey bee on human activities (Evans and Gundersen-Rindal, 2003).

In the present genomic sequence release version 4 (Amel\_4.0), the genome of the honey bee is arranged in 16 chromosomes plus a mitochondrial chromosome (HBGSPC, 2006) that includes 626 scaffolds of which 81.6% are oriented (Solignac et al., 2007). Release version 4 includes information from 2,032 mapped genetic markers and 3,136 STS covering 231 Mb of the 236 Mb estimated sequencable genome. Given the 264 Mb total genome size estimated by cytometry (HBGSPC, 2006), 79% (186 Mb) of the genome is assembled and currently placed on the 16 chromosomes. The physical sequence assembly was aided by the STS information from the two available genetic maps, but mostly by the Solignac et al. (2004) map whose markers were isolated from their own BAC libraries. The genome sequence in Amel\_4.0 was primarily based on whole genome shotgun (WGS) reads, because the physical map based on BACs libraries (CHORI-224 constructed by Baylor's College of Medicine) failed to co-assemble correctly with WGS (HBGSPC, 2006, Supplementary Notes and Methods). Given the failure of agreement between the WGS assembly and the map based on complete BAC

sequencing and BAC end sequencing, it became problematic to FISH the CHORI-224 BACS to chromosomes of the sequenced honey bee strain. The decision was made, therefore, by members of the honey bee sequencing consortium, that the better option for verifying the physical sequence map using fluorescence *in situ* hybridization was the Solignac BAC library.

Fluorescence In Situ Hybridization (FISH) has become one of the most reliable techniques for physical mapping. However its resolution is limited by the size of the probes and detection of these probes, which detection even with use of antibodies is difficult for fragments smaller than 5 kb. Detection of smaller probes, even when possible, is limited by a consequent annoying background (Bentley, 1990; Liehr and Claussen 2002). Probes of 1-3 kb (and in some cases < 1 kb) have been detected, but the frequency of detection and reproducibility is very low (Jiang and Gill, 2006). FISH further cannot resolve signals separated by less than 130 kb (0.2-3  $\mu\text{m}$ ) in the interphase nucleus (G2) and 1Mb (0.4 $\mu\text{m}$ ) in metaphase chromosomes (Bentley, 1990, Cheng et al., 2002). With two or several-color FISH, the resolution cannot be increased beyond signals separated by 750 kb or less on metaphase chromosome (Bentley, 1990), while signals with 3.21 kb/ $\mu\text{m}$  of separation can be resolved with Fiber-FISH (Cheng et al., 2002). In pachytene chromosomes of plants the resolution is on the order of 2-5 Mbp - 10 times higher than in metaphase chromosomes (Kim et al., 2003). Detection and correct location can be affected not only by the size of probes and phase of the chromosomes, but also by the occurrence of repetitive DNA in the probes and genomes (Levsky and Singer, 2003). Probes containing repetitive DNA require high levels of assessment (Cheng et al., 2002; Jiang and Gill, 2006). Even with these limitations, FISH is currently a powerful tool for chromosomal identification, especially for small chromosomes (Jiang and Gill, 2006). Because of its versatility in combinatorial experiments using multicolor FISH or multi-probes cocktails, FISH is invaluable for genome mapping verification and extremely useful in genomic disease diagnostics in mammals (Davison et al., 2002; Kearney, 2006). Citing a few examples, in sorghum FISH has successfully been used for integrated karyotyping of landed BACs (Kim et al.,

2002), chromosome morphology (Kim et al., 2005a), molecular cytogenetic map (Kim et al., 2005b) and chromosome identification and nomenclature (Kim et al., 2005c). In parasites such as *Ciona intestinalis* with very small chromosomes and genome, the sequencing maps and scaffold alignments has been supported by FISHing landed BACs (Shoguchi et al., 2005, 2007). That same procedure is routinely used to verify the genome sequence maps in human and *Drosophila* (The International Human Genome Mapping Consortium 2001), to characterize the genes of *Drosophila* that resides in heterochromatin regions (Rossi et al., 2007), to map genome heterochromatin sequencing (Hosking et al., 2002), and to study the structural chromosome organization based on mobile elements (Yan et al., 2002). In *Aedes aegypti*, FISH is used to integrate the genetic linkage groups and the physical maps (Brown et al., 2001, Sallam et al., 2005, Severson et al., 2004). In *Bombyx mori* FISH is applied to assign the small and holocentric chromosomes to linkages groups (Yoshido et al., 2005) and for comparative analyses (Yasucochi et al., 2006). In honey bee, FISH of repetitive sequence have been used to characterize the ribosomal organizer (Beye and Moritz, 1993) and centromere (Beye and Moritz, 1994). FISH has also been used to characterize the honey bee chromosomes (Beye and Moritz, 1995) and telomeric region (Sahara et al., 1999 and Frydrychová et al., 2004). Here, FISH was used to confirm the identity of the sixteen chromosomes of honey bee DH4 drones and karyotype based on 35 BACs provided by Michel Solignac and his colleagues (The Laboratory of Evolution, Genomes and Speciation, CNRS, Gif sur Yvette cedex F 91198, France).

## **Material and Methods**

### **Biological materials**

Drones for chromosome preparation from the DH4 strain queen were kindly provided by Danny Weaver of BeeWeaver Apiaries. Workers bees and drone pupae for genomic DNA extraction were obtained from Dr. Tania Pankiw, Department of Entomology, TAMU. BACs were selected and provided by Michel Solignac and his

colleagues [The Laboratory Evolution, Genomes and Speciation, CNRS, Gif sur Yvette cedex F 91198, France (Table 1)]. Ribosomal DNA (rDNA) inserted in the Plasmid p3629 carrying *S. cerevisiae* 1750pb of 18S rDNA and cloned in DH5 $\alpha$  *E. coli* strain was kindly provided by Dr. P. Klein, Institute for Plant Genomics and Biotechnology, TAMU, and used as rDNA marker.

### **Chromosome preparation**

Chromosome slides were prepared according to the procedure of Mandrioli and Manicardi (2003) with a modification consisting of dissection and incubation of testes in physiological solution (Sahara et al., 1999) and distilled water as hypotonic solution. After dissection and incubation, follicles were disaggregated, and the cell suspension centrifuged at 1000g for 3 min. After discarding the supernatant, 200 mL of Carnoy's fixative solution (Methanol: Acetic acid 3:1) was added and the mixture incubated at room temperature for 30 min, then re-centrifuged at 100g for 3 min. The procedure was repeated several times until the sample slides prepared with material remaining in the pellet were clean, without significant loss of chromosomes and cells. A pair of testes from one drone was enough to obtain 40 to 60 slides, which were stored at -80°C until further use. For slide preparation, a light microscope, Zeiss (Model 039539-47 16 90-0000/09) equipped with phase contrast (47 3356-9901) and objectives Plan apo 25/0.65 and Apo 40/0.95 was used.

When slides were older than a year, a re-hydration in TC-100 (Sigma, Cat# T3160) culture media complemented with 5% of fetal bovine serum (FBS, Sigma, Cat# F-6178) for 35 min at 36°C was applied then re-fixed in Carnoy's solution. The slides in Carnoy's solution were kept on a hotplate at 52°C overnight, and formaldehyde pretreated according to Anamthawat-Jónsson (2001).

### **DNA extraction and labeling**

Genomic DNA was extracted from ground thorax and legs of honey bee workers following the procedure of Aljanabi and Martinez (1997), followed by phenol purification (Phenol:Chloroform:Isoamyl Alcohol 25:24:1 saturated with 10mM Tris adjusted to pH 8.0 and 1 mM of EDTA). Cot-1 DNA was prepared following the Zwick et al. (1997) protocol. As needed for probe preparation (below), genomic DNA was autoclaved for 7 min to obtain 50 to 100 bp fragments. BAC-DNA was extracted by alkaline lysis and purified with DNeasy spin columns (Qiagen, Valencia, Calif.) following the vendor directions. BAC-DNA was labeled by standard procedure using a Biotin- and Dig-Nick Translation Mix kit (Roche Diagnostic GmbH, Indianapolis, Ind., U.S.A., Cat# 11 745 824 910 and Cat# 11 745 816 910). Once the labeling reaction was completed and blocked, QIAquick nucleotide removal kit (Qiagen, Cat# 28306) was used for further purification, and ethanol precipitation for probe drying, were carried out. Before final drying of the BAC-DNA, 300x of Salmon testes DNA (Sigma D-7656) and 150x of honey bee Cot-1 or autoclaved genomic honey bee DNA were added. The dried labeled probes were dissolved in TE solution, adjusting the concentration to 10 ng of labeled probes per  $\mu\text{L}$  of solution. DNA labeled probes was stored at  $-80^{\circ}\text{C}$ .

### **In situ hybridization**

The general procedure followed was as described in Kim et al. (2003) with some modification based on Pinkel et al. (1986), Beye and Moritz (1995) and Sahara et al. (1999). Modifications to the Kim et al. (2003) procedure consisted of RNase incubation reduced from 45 min to 30 min with the temperature for denaturation increased to  $75^{\circ}\text{C}$  for 3 min, and hybridization incubation time increased to 36 hours. After incubation, the slides were rinsed twice at  $40^{\circ}\text{C}$  for 3min in 2xSCC, once at  $36^{\circ}\text{C}$  in 50% formamide (Sigma, St Louis Mo, USA, Cat# F7503) for 10 min, twice at  $36^{\circ}\text{C}$  2xSCC, and once with 4xSCC plus 0.2% Tween 20 (Sigma, P9415) at  $37^{\circ}\text{C}$ , and held at room temperature in 4xSCC plus 0.2% Tween-20, for 5 min. The slides were blocked for 30 min with 250 $\mu\text{L}$  of 5% non fat milk dissolved in 4xSCC plus 2% Tween-20. The signals were



detected with a solution containing 7 -15  $\mu\text{g}$  of both Cy<sup>TM</sup>3-conjugate Streptavidin (Jackson ImmunoResearch, Cat# 016-160-084) and Fluorescein (FITC)-conjugated IgG fraction monoclonal mouse anti-digoxigenin (Jackson ImmunoResearch, Cat# 200-092-156) diluted in 100-150  $\mu\text{L}$  of TNT buffer (100mM Tris-HCl pH7.5, 150mM NaCl, 0.5% BSA). Following incubation for 30 min at 37°C, the slides were rinsed three times at 37°C in 4xSCC plus 0.2% Tween-20 for 3 min each. After blocking with 250 mL of TNB buffer containing 0.5% (v/v) of NGS and 0.5% BSA for 10 min at 36°C, the signals were enhanced with a mix containing 10  $\mu\text{g}$  of FITC-conjugated affinity pure goat antimouse IgG (H+L) (Jackson ImmunoResearch, Cat# 115-095-003), and 10 $\mu\text{g}$  of Biotinylated antistreptavidin (Ambion, Cat# BA-0500) or Cy3 conjugated antistreptavidin (Ambion, Cat# BA-0500) diluted in 100-150 $\mu\text{L}$  of TNB for 30 min at 37°C. After the slides were rinsed in TNB three times for 3 min each at the same temperature with gently shaking, 250 mL of TNB buffer containing 0.05% BSA was added to the slides, incubated for 10 min at 37°C, following which 100-150  $\mu\text{L}$  containing 10 $\mu\text{g}$  of Cy<sup>TM</sup>3-conjugate Streptavidin and 10 $\mu\text{g}$  of FITC antimouse was added. After incubating at 37°C for 30 min, the slides were washed four times, 3 min each, with TNB in a shaking water bath at the same temperature. Following an alcohol series (70%, 85%, and 100%) and air-drying, the slides was kept at room temperature in a dark dried chamber for *c.a.* 30 min before counterstaining. After the slides were briefly equilibrated in 4xSCC plus 0.2% Tween-20, 250 $\mu\text{L}$  of 5 $\mu\text{g}/\text{mL}$  of 4' 6-diamidino-2 phenylindole (DAPI, Sigma, Cat# D-9542) in McIlvaine's (9 mM citric acid, 80 mM Na<sub>2</sub>HPO<sub>4</sub>·H<sub>2</sub>O, 2.5 mM MgCl<sub>2</sub>, pH 7.0) was applied and incubated for 30 min at room temperature. After a brief wash in 4X SCC plus 0.2% Tween-20, 25  $\mu\text{L}$  of home-prepared antifade solution was applied to each slide following the Trask (1980) recommendations.

### **Slide observation**

The slides were analyzed under an epi-florescence microscope AX-70 and a Peltier-cooled 1.3 M pixel Sensys camera (Roper Scientific) and MacPro v. 4.2.3 digital

image system (Applied Imaging Corp., Santa Clara, Cal., USA) equipped with 4',6-diamidino-2-phenylindole (DAPI), fluorescein isothiocyanate (FITC), and Cy3 filter sets located at New Beasley Laboratory on Agronomy Road, College Station, TX, which also serves as TAES Laboratory for Plant Molecular Cytogenetics.

As the identity of the different honey bee chromosomes is not available and the location of the BACs in the current physical and genetics map is not consistent, the images were processed to obtain black and white pictures to identify *a priori* the chromosomes. Signals were mapped on the previously constructed ideograms of the honey bee karyotype.

## Results

### Strength and frequency of the signals

Most of BACs hybridized on several sites on different chromosomes, which was expected since the physical maps displayed on Map Viewer also gave several locations and position of BACs in the different versions of AmelMap3 (NCBI: [http://www.ncbi.nlm.nih.gov/mapview/map\\_search.cgi?taxid=7460&query=AJ509637&qchr=&advsrch=off&neighb=off](http://www.ncbi.nlm.nih.gov/mapview/map_search.cgi?taxid=7460&query=AJ509637&qchr=&advsrch=off&neighb=off)). Many secondary signals were not discarded because they consistently co-hybridized with other BACs on several chromosomes, indicating some synteny between these BACs. When considerable data were available, histograms for each BAC was constructed to identify the chromosomes with the most frequent signal or signals (Fig. 10a, 10c); for those chromosomes that had signals at high frequency, a histogram was constructed to identify the position of the signals (Fig. 10b, 10d). When double or triple signals were detected, confirmatory checks back to the original pictures was carried out; if the multiple signals were confirmed in several pictures, the signals were considered as multiples. If not, the more frequent signal was mapped; the others signals appear on the list of table A.1. The location and position of BACs were cross tested by individual, triple or combinatorial experiments (Table 7, last column). For example, to confirm the position of 6F1, 2D1 was utilized; for 36H10 and 5G9, 8H7 was included;

they also were tested in a triple cocktail mix. In the examples shown in Fig. 11, where the location and frequency of BACs expected on C1 and C10 were plotted, the experiment consisted of all mapped BACs, except 6H3 and 56F6, which were tested in a separated experiment where 8H8 and 4E8 were included as markers. The experiments consisted of three treatments in three replicates. Each treatment consisted of a different label for every BAC in the mix, thus in one treatment BAC “X” was labeled with digoxigenin and detected with FITC (green), in the second treatment the same BAC was labeled with biotin and detected with Cy3 (red), in the third treatment a mix of Digoxigenin and Biotin labeled probes of the same BAC was added. In the Fig. 11b, a triple cocktail combination experiment that included 6B9, 8H7, and 6G8 was mapped to verify the position of these BACs on C10 and C11. Most of the triple experiments were designed based on the location displayed on Map Viewer (MVV). For example, MVV1 set the position for 8H7, 5G9 and 36H10 on C13, MVV2 and MVV3 mapped them on C10. A previous experiment confirmed the location of 8H7 on C10, thus the chromosome to be tested was C10 and the definitive test marker was 8H7. One triple experiment was designed for each chromosome.

The position and locations here reported can be affected by several factors: (a) when probe hybridization was in constitutive heterochromatin, the signal usually was very weak, (b) when probe hybridization occurred in facultative heterochromatin the strength and the position were affected by the level of the condensation and heterochromatinization, (c) when the probe hybridization occurred in a euchromatic region, usually the strength and frequency of the signal was high and very consistent, but the position were variable according to the condensation and proximity of a heterochromatin band. Therefore, metaphase chromosomes seem to be the most reliable phase to determine the position of the markers; however, very few hybridizations can be obtained from metaphase chromosomes. Due to the condensation of the metaphase chromosome, metaphase provides very limited resolution for chromosome identification. In fact, the most of the useful signals were obtained in early stages of mitotic chromosomes (Fig. 12a to 12d and Fig. 13). However, considerable hybridization was

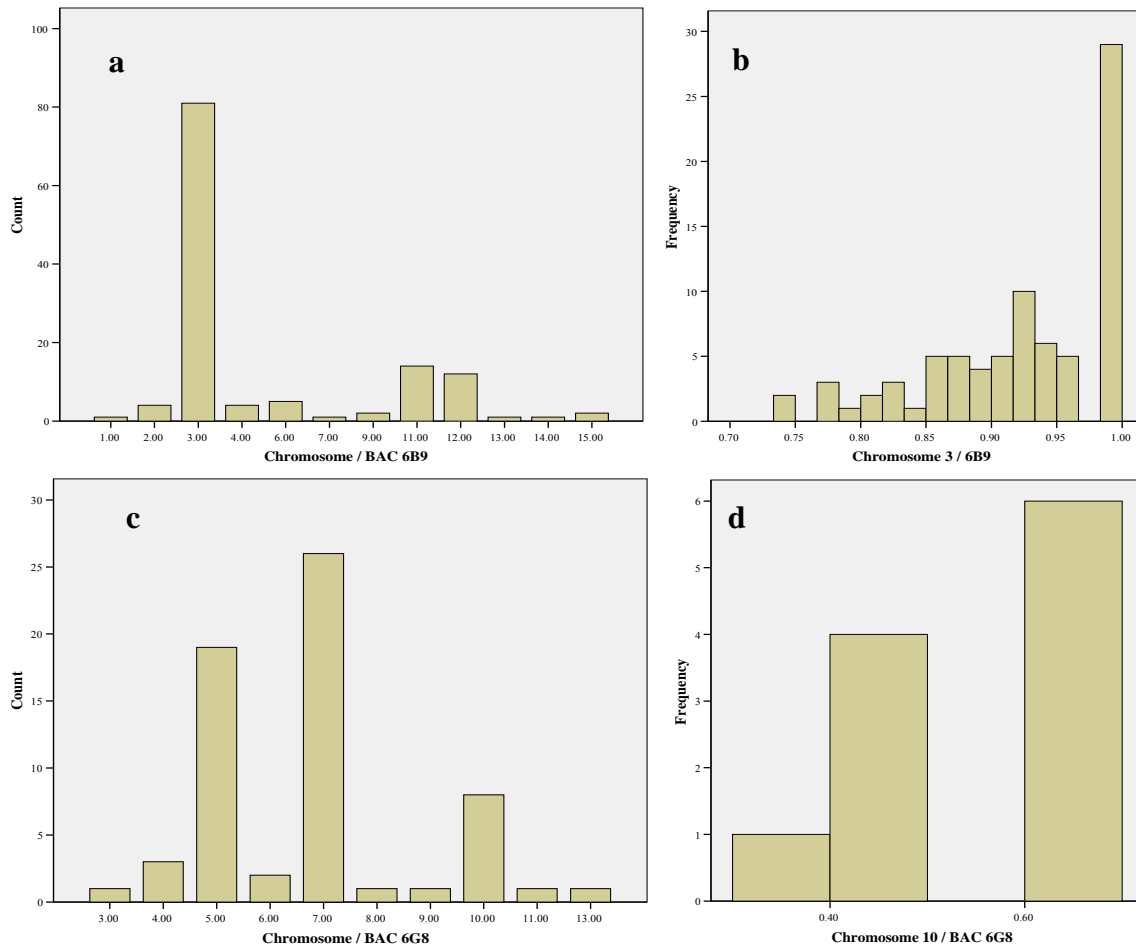
also observed on prophase meiotic chromosomes (Fig. 12e and 12f). Usually meiotic chromosomes were clearly differentiated because of their smaller size, being very condensed and heterochromatic. In contrast, mitotic chromosomes were considerably larger and morphologically better defined, allowing better characterization and identification and better location of signals. Evidence relating the most important and frequent signals are shown on individual mitotic chromosome figures accompanied with a black and white version alongside the Ba<sub>2</sub>OH (C-banding) and DAPI ideogram in Fig. 14. The final map is also accompanied by the C-banding ideograms where all the important signals of the worked BACs are represented (Fig. 15).

**Table 7.** List of the Solignac BACs worked with Fluorescence In Situ Hybridization (FISH). The column Experiment type indicates: I-individual experiment, T- cocktail containing three BACs, M-cocktail containing more than 3 BACs

ID References				MAP VIEWER (NCBI V2) V1		MAP VIEWER (NCBI V3) V2/V3				MAP VIEWER (NCBI) V4		Experiment type
Locus	Am	Accession number	Clones	Relative Position	Chromosome	Relative Position	Chromosome	Relative Position	Chromosome	Relative Position	Chromosome	
A113	059	AJ509290	1A8,	0.1969	2	0.572	6	No match	NM	0.210, NP	16, NP	T
Ap225	223	AJ509454	97B3	0.5006	10	0.5	5	0.5312	5	0.4526	5.0	ITM
Ac005	403	AJ509634	1F2	0.1980	NP	0.8676	1	0.757, 0.8676	1	0.755, 0.865	1	M
Ac011	406	AJ509637	1F6	0.1105	8	Tel	9	Tel	9	0.024, NP	9 and Np	TM
Ac012	407	AJ509638	1C6	0.4836	2	0.5714	6	0.4167	6	0.4757	6	T
Ac033	411	AJ509642	2D1	0.3720	2	0.772	2	0.772	2	0.1860	2	TM
Ac062	417	AJ509648	2B11	0.9159	3	0.1136	2	0.1136	2	NP	NP	T
Ac092	430	AJ509661	3F5	0.4447	2	0.7045	2	0.7045	2	0.2683	2	T
Ac101	435	AJ509666	3H8	0.3289	11	0.642, NP	7 and NP	0.7142	7	0.025, NP	9 and NP	T
Ac127	444	AJ509675	4E8	0.0075	1	1tel	1	1tel	1	0.995	1	M
Ac129	445	AJ509676	4G8 or 5E2	0.7174	13	0.36667	13	0.3666	13	3 NP	NP	TM
Ac139	450	AJ509681	5E2	0.0082	12	tel	4	tel	4	Tel, NP	4 and NP	TM
Ac140	451	AJ509682	5E2	0.316	15	0.5	15	0.5	15	0.3509	15	TM
Ac141	452	AJ509683	5E2	0.316	15	0.55	15	0.55	15	0.3509	15.0	TM
Ac149	455	AJ509686	5B10	0.37612	6	0.6364	3	0.6364	3	0.3542	3	T
Ac157	458	AJ509689	5G9	0.13398	13	0.846	10	0.8518	10	0.1333	10	T
Ac158	459	AJ509690	6F1	0.2693	6	0.7667	13	0.7667	13	0.7731	13	T
Ac159	460	AJ509691	5B10	0.18583	8	0.8518	9	0.8518	9	0.125	9	T
Ac172	464	AJ509695	6B8	0.9627	12	tel	4	tel	4	0.8579	4	ITM

**Table 7. (Continued)**

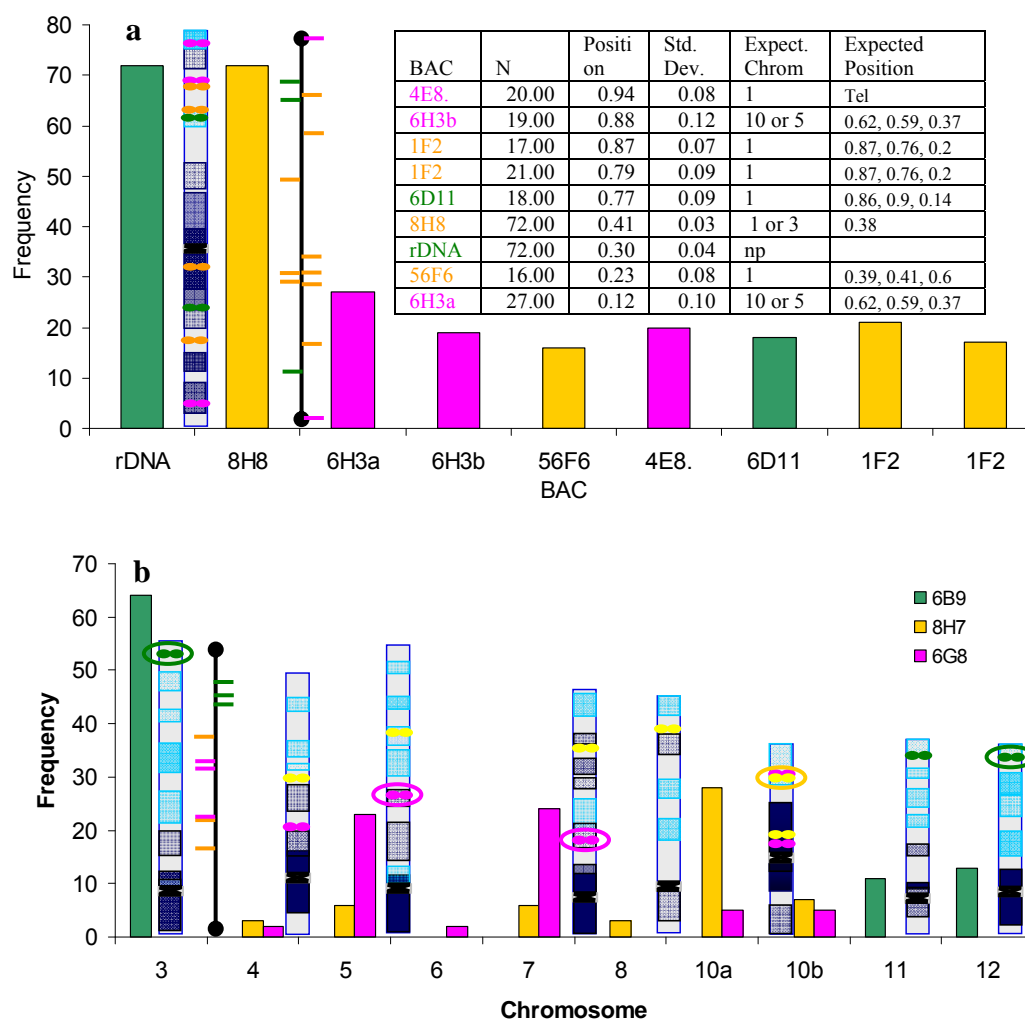
ID References				MAP VIEWER (NCBI V2) V1		MAP VIEWER (NCBI V3) V2/V3				MAP VIEWER (NCBI) V4		Experiment type
Locus	Am	Accession number	Clone	Relative Position	Chromosome	Relative Position	Chromosome	Relative Position	Chromosome	Relative Position	Chromosome	
Ac179	467	AJ509698	6B9	0.8822	11	0.8387	11	0.80645	11	0.191	11	ITM
Ac184	469	AJ509700	6G8	0.4402	6	0.5758	3	0.6061	3	0.3958	3	ITM
Ac191	470	AJ509701	6D11	0.14587	1	0.86765	1	0.8971	1	0.8911	1	M
Ac193	471	AJ509702	7B4	0.7877	1	0.2353	1	0.2206 0.9559	1	0.205 and 0.945	1	T
Ac203	474	AJ509705	7B4	0.2166	8	0.7586	9	0.7586	9	0.175	1	T
Ac216	480	AJ509711	8H7	0.6892	13	0.3333	10	0.4074	10	0.5	10	ITM
Ac217	481	AJ509712	8H8	NP	1	0.3864	2	0.3864	NP	0.5742	2	ITM
Ac303	488	AJ509719	49H2	0.9421	9 or 6	No Match	NM	No Match	NP	0.375 and NP	7 and NP	TM
Ac306	490	AJ509721	26F7	0.6936	3	0.2954	2	0.2727 0.4773	2	0.4733 and 0.7176	2	I
Ag005a	491	AJ509722	56F6	0.60407	1	0.3971	1	0.4117	1	0.37	1	IM
Ag005d	493	AJ509724	35D9	0.4529	14	No Match	NM	0.8064	4	0.2111	4	T
Ag016	496	AJ509727	44B2	0.023	8	No Match	NM	0.9643 0.9643	9	Tel	9	T
Al007	500	AJ509731	11A3	0.3301	3	0.7954	2	0.7954	2	0.1846 and NP	2 and NP	IT
Al082	506	AJ509737	82B7	0.640	2	0.2286	6	0.2286	6	0.3204	6	T
Av006	507	AJ509738	6H3	0.3721	10	0.625	5	0.59375	5	0.5914	5	M
ANTP	550	AJ276511	22F1	0.4669	14	0.4187	16	0.4187	NP	0.5333	16	ITM
RJP57-1	552	Z26318	57E10	0.1869	16	0.1333	11	0.1833	11	0.8111	11	T
Ac051(d)	415	AJ509646	2G7	0.3007	15	0.6542	15	0.62 and 0.8	15.0	0.1754 and 2807	15	I
Av036D	510	AJ509741	36H10	0.3662	13	0.5926	10	0.62963/ C10	10	0.2987	10	T
Ag011	495	AJ509726	37D2	0.60245	11	NM	NM	0.3571/ C7	7	0.4878	7	T
Al011	502	AJ509737	11G6	0.228	6	0.228	6	0.3721	10	0.314	6	I
-	-	-	8A2	NP	NP	NP	NP	NP	NP	NP	NP	M
-	-	-	rDNA	NP	NP	NP	NP	NP	NP			ITM



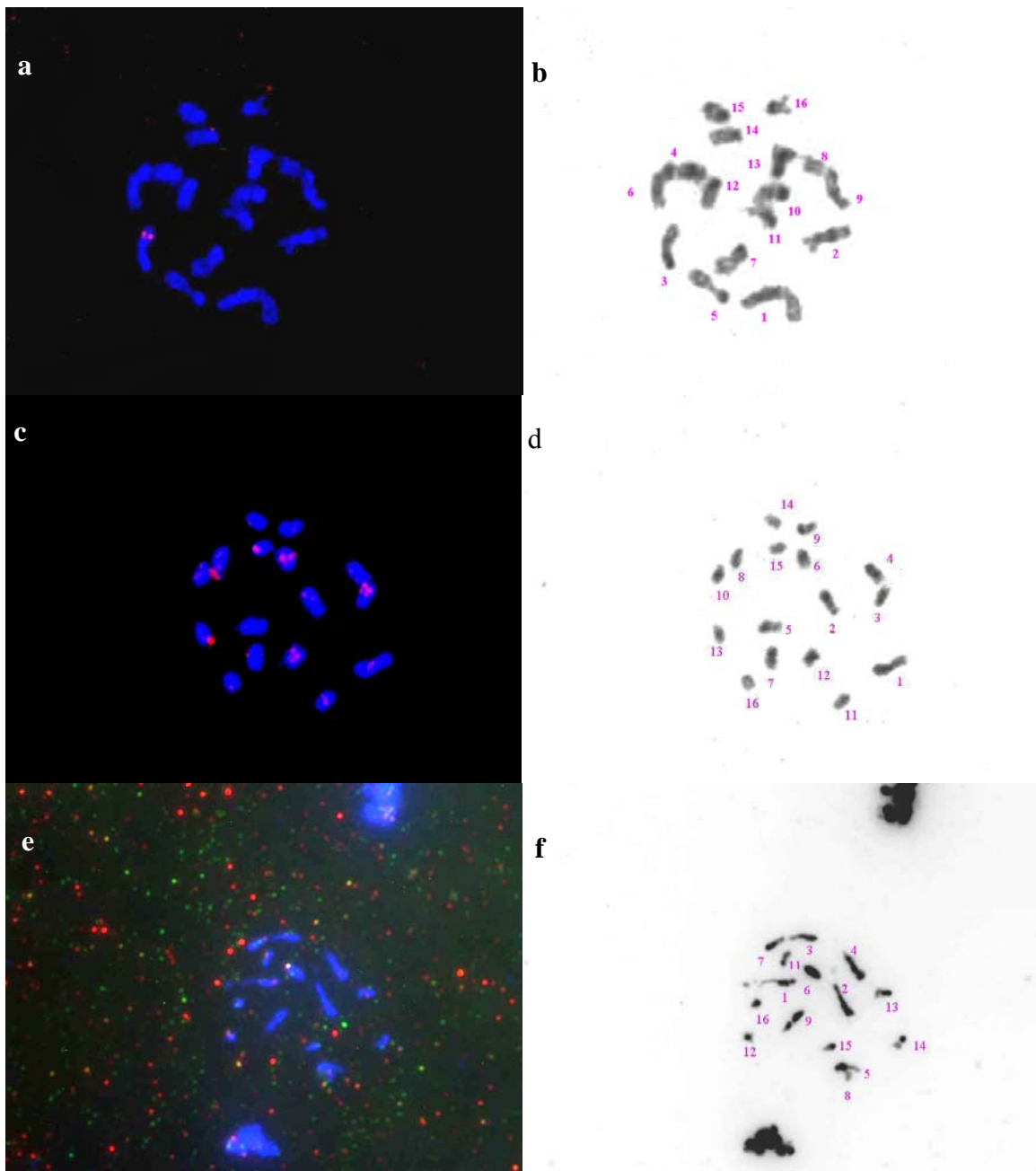
**Fig. 10.** Examples of count plots and histograms for detecting location and position of the BACs on the chromosomes of honey bee. The chromosome location was determined with count plots (a and c) and the position on the chromosome was determined with the histogram (b and d). (a-b) 6B9, (c-d) 6G8

Table 6 lists the 35 BACs worked, with all information about their identification (locus, *Am*, and accession number), location (chromosomal) and position (place in the chromosome) through the different versions of genome assembly (Amel). In Table 8 and Table A.1, the information obtained for the listed 35 BACs, which includes chromosomal location and position on the chromosome, is compared with those positions given in Table 7. There have been four version of the Map viewer (MVV1 to MVV4); each of these positions and chromosome locations were compared against the

position and location obtained using FISH. To compare the position of BACs using FISH with that shown in map viewer, a one sample *T-test* for significance (\*) or non-significance (NS) was used. When no significant difference (NS) was obtained the position of the BAC was marked with a  $\sqrt{\quad}$  symbol indicating a match with NCBI Map Viewer. The same check mark was used to indicate the match with a chromosome. The obtained score was not used to confirm or suggest the location and position of the signals; it was used as reference in some cases when that information was insufficient, as was the case with 36H10 and 5G9.



**Fig. 11.** Examples of plots to map the BACs in chromosomes of honey bee. (a) BACs hitting on chromosome 1, and (b) 6B9, 8H7 and 6G8 on chromosome 11 and 10.



**Fig. 12.** Examples of FISH experiments for mapping 35 BACs of Soliganc library. (a) FISH of 11A3 in individual experiment and (b) black and white (BW) of same picture with numbered chromosomes, (c) FISH of 6B8 showing 6 of the hybridization sites (d) BW of the same picture, (e) hybridization of meiotic chromosomes, rDNA (C1, C6 and C12), 8H8 (C1), 6H3 (C3, C7), 49H2 (C11), 5E2 (C6, C7, C14, C15, 6G8 (C7) and (f) BW of the same picture.



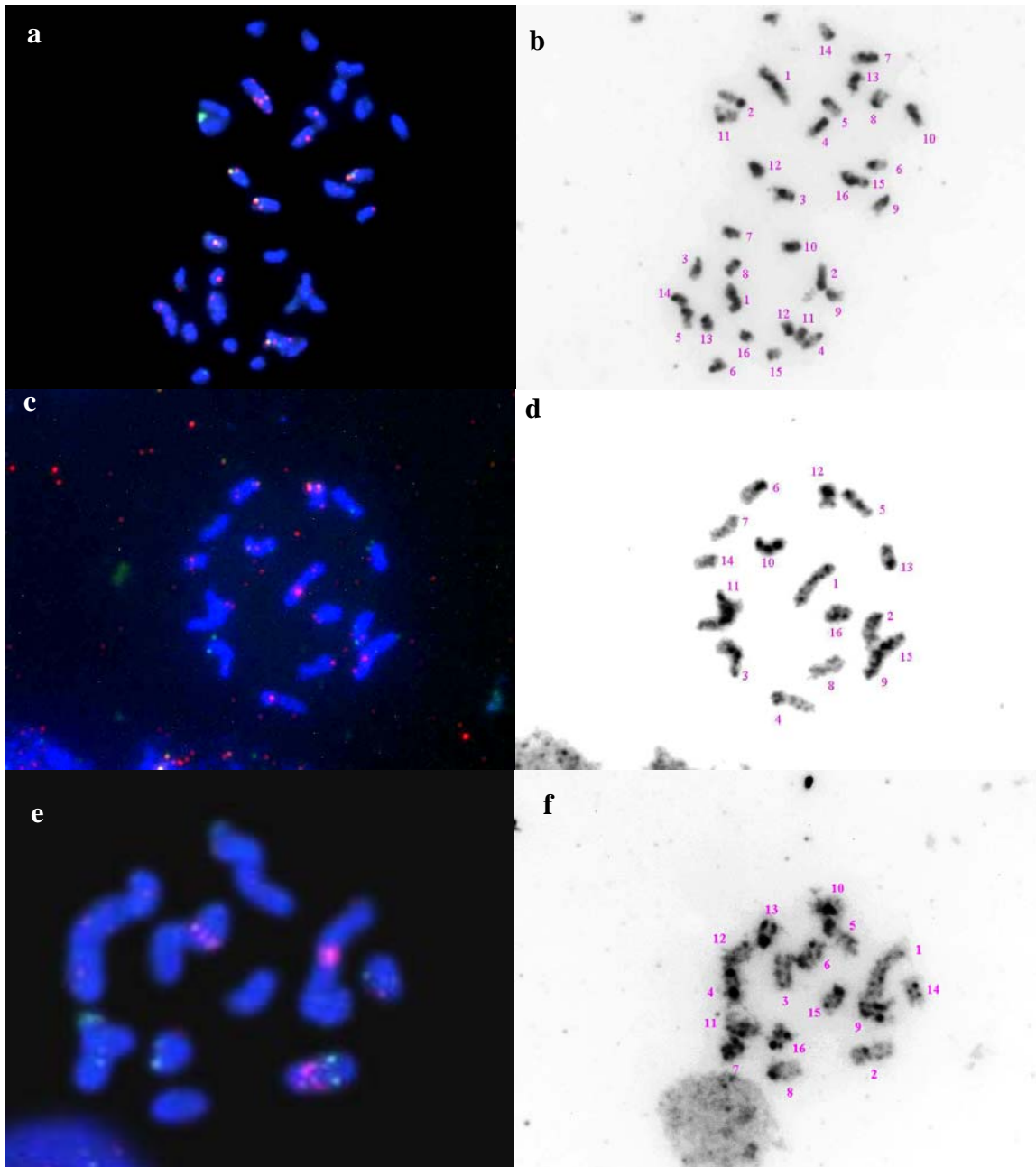


**Fig. 13.** Examples of FISH experiments for mapping 35 BACs of Soliganc library for multiple experiments. (a) Prophase III (Late prophase), 6D11 (C1), 6B9 (C3, C11), 8A2 (C4, C8), 6B8 (C3, C5, C11, C14), (b) BW of the same picture, (c) Prophase III, 6B8 (C4, C6, C12, C14), 6B9 (C3, C13), 2D1 (C2, C9), (d) BW of the same picture, (e) Hybridization of 1C6 (green), 1A8 (Greenish red), and 82B7 (red) in prophase II chromosomes, (f) BW of the same picture.

### Mapped signals

146 signals were recorded from the 35 FISHed BACs in individual, triple and multiple experiments. On average 4 signals per BAC was obtained; 21 of the signals hit in doublets and two triplets (49H2 on C11 and 6H3 in C1). C11 showed the highest rate of doublets, in which 1F6, 3H8, 49H2, 6B8, 6B9 and 5E2 hybridized in two or three places. Hybridization with 8H7 and 6G8 resulted in double signals in C10, with 6H3, 97B3, and 5E2 on C7 and 3H8 and 1F6 on C8. Thus, the BACs 1F6, 3H8, 6B8, 6H3, 97B3, and 5E2 hybridized in several places on the same chromosomes (Table A.1). The rDNA markers on chromosomes 6 and 12 were confirmed. Less frequently observed, but also consistent, was an rDNA marker on C1, which was scored together with six BACs places - two for 1F2 and one for 56F6, 6D11, 7B4 and 4E8. The number of places hit, the BACs whose places were confirmed, and those places that are suggested as the most probable hybridization sites are listed in Table 8, and the maps are shown in Fig. 14.

The next set of information obtained is summarized in the Table 8 and Figs. 14 - 16, where the chromosomes and position is displayed by BAC and by group depending on the coincidence with the MVV information. Seven BACs, 4E8, 56F6, 7B4, 6D11 (C1), 11G6 (C5), 11A3 (C3), 26F7 (C4), hybridized on a single place. Of the four BACs that hit on C1, BAC 56F6 showed the most consistent and strongest signal. The other three along with 1F2 showed very weak signal, the exception being the most distal signal of 1F2. The heterochromatic (facultative) state of the bands where the hybridization occurred could explain the weak signals observed (Fig. 14a). BACs 1F2 (C1), 37D2 (C7 and C11), 44B2 (C8 and C11), 6F1 (C6 and C11), and 8A2 (C4 and C8) all hybridized on two places. With the exception of 8A2 that showed very high frequency on C4, the rest of the BACs resulted in a similar frequency between signals. BACs 2B11 (C1, C2 and C9), 5B10 (C2, C6 and C14), 5G9 (C4, C6 and C10), and 57E10 (C4, C12 and C16) all hybridized on three chromosomes. Only 5B10 can be placed on C6 using the frequency of the signal (16/33). BACs with 4 signals were 1F6, 35D9, 36H10, 3F5, and

8H8. Using the frequency of the signal, C8 is the most probable carrier of 1F6. In the same way, with 72 hits in 93 cells analyzed, we can say that 8H8 is on C1. BACs with 5 signals are 22F1 and 49H2, which are located on C16 and C11; while among BACs with six signals, 1A8 and 1C6 occur on C2, 6B8 on C14, and 6G8 on C5 and C7. BAC 3H8, cannot be clearly placed because the frequency of 3H8 hits are not different between 5 different chromosomes, and the positions obtained are significantly different from those places given in MVV versions. BACs with 7 signals are 2D1, 6B9, 82B7, 8H7 and 97B3, which are located on C2, C3, C2, and C10 respectively; only 97B3 cannot be place clearly by frequency, although C7 have the highest frequency with two hybridization sites on that chromosome. BACs 6B8, 6H3, and 5E2 hit on more than 7 chromosomes when no DNA blocker was added, and under some combinations, these BACs hit on almost all chromosomes. Even so, using the frequency between signals, 6H3 can be placed on C7, 5E2 on C14 and C15; 6B8 cannot be clearly placed, but the most probable position seems to be C14. However, when 6B8 is combined with 6B9, the most frequent hit is to C11, and as in C14, the hits are on a euchromatic region. Therefore 6B8 can be mapped in both chromosomes. In Fig. 12c six chromosomes are marked for the 6B8 BAC. Many of the placed BACs that are assigned by frequency are not in agreement with the MVV maps. In those cases the golden green color on the maps indicates that it is a suggested place.

**Table 8.** Mapped signals, places confirmed, places suggested, and places for secondary signals for 35 FISHed BACs

Chromo Some	Num BACs places confirmed	Num of BACs places suggested	Secondary signals	Total number of signals mapped	BACs places confirmed	BACs places suggested
1	5	1	0	7	56F6, 6D11, 1F2, 7B4, 4E8	8H8, rDNA
2	4	3	1	8	2D1, 82B7, 8H8, 3F5	1A8, 1C6, 2B11
3	0	2	2	4		6B9, 11A3
4	2	3	3	8	5E2, 6B8	8A2, 26F7, 49H2
5	1	2	1	4	6H3	6G8, 11G6
6	2	2	5	9	87B2, 1C6, rDNA	5B10, 1A8
7	2	2	3	8	3H8, 37D2	6H3, 97B3
8	0	2	6	8		1F6, 44B2
9	0	0	3	3		
10	3	0	2	5	5G9, 36H10, 8H7	
11	1	2	10	13	6B9	6F1, 49H2
12	0	0	5	5	rDNA	
13	0	0	2	2		
14	0	2	1	3		6B8, 5E2
15	1	0	1	2	5E2	
16	1	2	1	4	22F1	57E10, 35D9
Total	22	23	47	91	22 BACs plus rDNA	23 BACs plus rDNA

In summary, 22 BACs can be placed by frequency of their signal and match with the last version of MVV (Red color), 10 BACs (1F2, 22F1, 2D1, 4E8, 56F6, 6D11, 7B4, 82B7, 8H7, and 5E2 on C15) can be placed as confirmed, and 12 BACs can be placed as suggested (golden green) (11A3, 1A8, 1C6, 1F6, 26F7, 5B10, 6B8, 6B9, 6G8, 6H3, 8H8, and 5E2 on C14). Most of the BACs of this last group (suggested) presented a second and less frequent signal that coincides with the last version of MVV; they have been grouped separately and mapped as confirmed as well. BACs 11A3 and 6B9 hit no matches with the mapped location in MVV. BAC 1A8 has no MVV identity, and two BACs, 1F2 and 5E2, have two places and more than two places in MVV. Of these 22 BACs, 1A8, 1C6, 26F7, 6B8, 6H3, and 5E2 on C14 were poorly qualified with low

agreement score with the MVV maps. That means that 16 of 35 BACs were unambiguously placed by the FISH experiments, they are: 1F2, 22F1, 2D1, 4E8, 56F6, 6D11, 7B4, 82B7, 8H7, 11A3, 1F6, 5B10, 6B9, 6G8, 8H8, and 5E2 on C15 (Table 8 and Fig. 15). However, 1A8 and 1C6 are clearly in synteny with 87B2 (Fig. 18a), which matches with MVV with a high score and high frequency. BAC 2D1 also was unambiguously mapped in the first group of 10 BACs. This BAC (2D1) was used as a marker to determine the position of 3F5 and 2B11, which were found in synteny in C2 and C6 (Fig 18b). In the same way using 6B9 as marker, BACs 3H8 and 37D2 were placed on C7 and C11 (Fig 18c); however only the signals on C7 were mapped because the signals on this chromosome are clearer and stronger. Thus 1C6, 1A8, 3F5, 2B11, 3H8 and 37D2 can be considered as unambiguously mapped. These last six BACs will be further re-examined following other grouping, which will confirm this result. If these BACs can be considered as unambiguously mapped, adding these BACs to the 16 previously mentioned, brings to 22 the number of BACs unambiguously mapped.

Considering matches with the last version of MVV and moderate frequency or secondary signals (Table 8); several other BACs can be placed, such as 1C6, 1A8, 36H10, 37D2, 3F5, 3H8, 5G9, 6B8, 6B9, 6H3, 82B7, 8H8, 5E2, and 97B3. Of this group, the BACs 1A8, 1C6, 6B8, 6B9, 6H3, 8H8, 5E2 were mapped in other chromosomes as suggested because of the high frequency of the signals on those chromosomes. In each case, the mapped position of BACs in this group is found as a secondary signal. The most important characteristic of these BACs is that their hit frequency cannot define clearly their position, but the chromosomes match with the last versions of MVV. Because of that match, these BACs are mapped as confirmed and listed in the Table 8. Of these same BACs, only 1A8 and 97B3 were mapped as suggested because even if one ignores the low hybridization rate, the highest frequency hit was on a different chromosome than in MVV4. The main disadvantage of this second group of BACs is the similar hybridization rate on the different chromosomes where they hit. For example, 36H10 occurs on C4 (0.604), 7 (0.874), 8 (0.574) and 10 (0.521) at frequencies of 7/20, 5/20, 2/20, and 4/20 respectively. Even though C4 is hit

at the highest frequency, it is not significantly different from the frequency of the signals on C7 and C10. MVV2, MVV3 and MVV4 placed this BAC on C10 at 0.592, 0.629, and 0.2987 relative units respectively. Therefore with matches for places on MVV2 and MVV3 and chromosome matches for MVV2, MVV3 and MVV4, the most probable position of 36H10 is C10 at 0.584. On the other hand, the position in C4 is on a very low frequency facultative band while in C10 it is on constitutive heterochromatin, which suggests that the correct place is C4, and this position was mapped as a suggested place. In several cases, such as 6B8 and 6B9, the signal was very weak or very low in frequency (C4, 18/93 and C11, 14/93 respectively) compared with the first signal mapped (C14, 28/93 and C3, 80/93 respectively). BAC 97B3 was expected on C10 (MVV1) and C5 (MVV2-MVV4) at a position between 0.45 (MVV4) to 0.53 (MVV1). Compared with the rest of the locations where this BAC hybridized, the position 0.525 on C7 resulted in the highest frequency. The match to the MVV position was a compelling reason to map this BAC on C7 as a confirmed. Using this procedure the BACs of this group was mapped as confirmed (red mark) or suggested (Table 8 and Fig. 16).

**Fig. 14.** Map references of 35 BACs of Soliganc library by chromosomes. (a) C1, (b) C2, (c) C3, (d) C4, (e) C5, (f) C6, (g) C7, (h), C8, (i) C9, (j) C10, (k) C11, (l) C12, (m) C13, (n) C14, (o) C15, and (p) C16. The green color in the pictures comes from digoxigenin / FITC system, red from biotin/Cy3 system and yellow, greenish red, reddish green colors come from probes combination labeled with dig/FITC and biotin/Cy3. In the last column are the map ideogram of the chromosomes holding the signals detected, the red color indicates that the signal has some coincidence with some version of the NCBI Map Viewer (MVV), golden green color indicates that there is not complete agreement with the MVVs maps but high frequency of hybridization suggest that place is correct, the green color indicates secondary signals and signals with no agreement with MVV. Beside the color scheme, the ideogram of BaOH<sub>2</sub>-C-band and DAPI-band are shown to indicate the characteristic of the region where the BAC was placed. The positions indicated in the figures are approximate because they represent a mean with a standard deviation as shown in the table A.1, in addition to this variation, the natural variation of position caused by the band dynamics in the chromosomes through prophase may affect the position of the BACs on the chromosomes. The position related to the bands of reference, may have some variation because the DAPI ideogram used as reference is of prophase I, therefore, the BACs location in later stages can be slightly different. To reduce this potential problem, a black and white version of the picture of the chromosome is presented beside the colored. Additional information about the FISHed BACs is provided. In the first columns of the table are the identification references of each BAC, in the fourth column the number of cell recorded with the signal and in the last row of each table the chromosome and position are given.

( a ) ID References			Freq	56f6	rDNA/8H8/1F2/4E8	8H8	6H3/rDNA/8H8/6H3	Chromosome 1	rDNA/6B8/6D11/1F2	
Ac217	8H8	AJ509712	72 (93)							
Ag005a	56F6	AJ509722	16 (20)							
Ac005	1F2	AJ509634	38(58)							
				rDNA/8H8/6D11		56F6/7B4/4E8	6H3/8H8/49H2		rDNA/6B8/6D11	
Ac127	4E8	AJ509675	20(58)							
Ac193	7B4	AJ509702	7(10)							
Av006	6H3	AJ509738	27(93)							
Ac191	6D11	AJ509701	18(34)							
NCBI Location: Chrom. Num (Locations)										

( b ) ID References			Freq	2D1	2B11	2D1	3F5	1F6	2D1	2D1	6B8	Chromosome 2
Ac033	2D1	AJ509642	44/69									
Ac062	2B11	AJ509648	6(22)									
Ac092	3F5	AJ509661	8(22)									
Ac011	1F6	AJ509637	4(34)									
Ac172	6B8	AJ509695	12(34)									
Ac217	8H8	AJ509712	15(93)				6B8/1F6					
NCBI Location: Chrom. Num . (Locations)				2 (0.37, 0.18)	3/ np (0.91, np); 2 (0.44, 0.7, 0.26)			8/9 (0.11, np)		12/14 (0.96, 0.85)		



(c) ID References			Freq	11A3	6B9	35D9	97B3	97B3	Chromosome 3
AI007	11A3	AJ509731	10(15)						
Ac179	6B9	AJ509698	80(93)						
Ag005d	35D9	AJ509724	4(17)						
Ap225	97B3	AJ509454	14(93)						
NCBI Location: Chrom. Num . (Locations)				3/2(np(0.33,0.18 and np)	11(0.88, 0.19)	14/4(0.45, 0.21)	10/5(0.5, 0.45)	10/5(0.5, 0.45)	

(d) ID References			Freq	49H2	8H7/36H10	36H10	57E10	26F7	8A2	6B8	Chromosome 4
Ac172	6B8	AJ509695	18(93)								
RJP57-1	57E10	Z26318	9(12)								
Av036D	36H10	AJ509741	7(18)								
Ac303	49H2	AJ509719	13(93)								
-	8A2	-	29(64)								
Ac306	26F7	AJ509721	8(12)								
				Np(0.375)	13/10(0.69,0.5)	13/10(0.62, 0.3)	16/11(0.19,0.81)	3/2(0.69,0.47 and 0.71)	?	12/4(0.96,0.85)	

Fig. 14. (Continued)

( e ) ID References				Freq	6G8	6H3	6G8/49H2/5E2	49H2	11G6	Chromosome 5
Ac172	6B8	AJ509695	nd							
Ac184	6G8	AJ509700	32(64)							
Av006	6H3	AJ509738	42(74)							
Ac303	49H2	AJ509719	13(93)							
Al011	11G6	AJ509733	nd							
NCBI Location: Chrom. Num . (Locations)					6/3	10/5	6/3, 9/6, 4/12/15	9/6/no placed	5/8	

( f ) ID References				Freq	rDNA/2D1	5B10	rDNA/97B3	6B8	1A8	3F5/2D1	5G9	Chromosome 6
Ac159	5B10	AJ509691	16(26)									
Ap225	97B3	AJ509454	nd									
Ac172	6B8	AJ509695	3(12)									
Ac033	2D1	AJ509642	7(69)									
Ac092	3F5	AJ509661	6(18)									
NCBI Location: Chrom. Num . (Locations)					2	6/3	10/5	12/4	2/6/nm	2/2, 2/2	13/10	

**Fig. 14. (Continued)**

(g) ID references			Freq	6G8	8H7	6H3	22F1/97B3	22F1/97B3	22F1/97B3/6H3	Chromosome 7
Av006	6H3	AJ509738	48(148)							
Ac184	6G8	AJ509700	27(64)							
Ap225	97B3	AJ509454	31(93)							
ANTP	22F1	AJ276511	31(102)							
Ac216	8H7	AJ509711	6(64)							
NCBI Location: Chrom. Num (Locations)				6/3	13/10	10/5	14/16; 10/5	14/16; 10/5	14/16; 10/5; 10/5	

(k) ID References			Freq	6G8/1F6	11G6	6F1	1F6/49H2	6B8	5E2	6B9	Chromosome 11
Ac184	6G8	AJ509700	Nd								
Al011	11G6	AJ509733	nd								
Ac158	6F1	AJ509690	4(8)								
Ac011	1F6	AJ509637	8(32)								
Ac303	49H2	AJ509719	15(30)								
Ac172	6B8	AJ509695	55(148)								
Ac179	6B9	AJ509698	14(124)								
Ac139	5E2	AJ509681	11(85)								
				6/3 (0.61/0.39); 8/9 (0.1, Tel)	5/8 (0.14, 0.86)	6/13 (0.81)	8/9 (0.1, Tel); 9/6 (0.375)	12/4 (tel)	132/4 (tel)	11 (.838, 0.191)	

Fig. 14. (Continued)

(h) ID Reference				Freq	1F6	8A2	44B2	2D1/1F6	Chromosome 8
Ac011	1F6	AJ509637	16(64)						
-	8A2	-	nd						
Ag016	44B2	AJ509727	6(9)						
Ac193	7B4	AJ509702	7(10)						
Ac033	2D1	AJ509642	8(93)						
Ap225	97B3	AJ509454	nd						
NCBI Location: Chrom. Num . (Locations)				8/9 (0.02, np)	?	8/9(0.02, tel)	2 (0.18, 0.77); 8/9 (0.02, np)		

(i) ID References				Freq	5E2	49H2	Chromosome 9
Ac129	4G8 or 5E2	AJ509676	nd				
Ac303	49H2	AJ509719	15(64)				
NCBI Location: Chrom. Num . (Locations)				12/4(0.008)	9/6/nm (0.9421)		

(j) ID References				Freq	8H7/6G8	36H10/8H7	5G9	Chromosome 10	8H7
Ac184	6G8	AJ509700	10(77)						
Ac216	8H7	AJ509711	34(74)						
Ac157	5G9	AJ509689	4(10)						
Av036 D	36H10	AJ509741	4(18)						
NCBI Location: Chrom. Num . (Locations)				13/10 (0.4); 6/3 (0.57,0.39)	13/10 (0.62, 0.29)	13/10(0.846) 13/10 (0.84,0.13)			13/10 (0.62,0.29)

(l) ID References				Freq	rDNA/5E2	rDNA/6H3	rDNA/6B8/6B9	Chromosome 12
Ac172	6B8	AJ509695	17(148)					
Ac179	6B9	AJ509698	22(124)					
Av006	6H3*	AJ509738	15(220)					
NCBI Location: Chrom. Num . (Locations)				12/4(0.0082,tel)	10/5(0.37,0.59)	12/4(0.96,0.85)11/ 11(0.83,0.19)		

Fig. 14. (Continued)

( m ) ID References				Freq	8H7	97B3	Chromosome 13
Ac216	8H7	AJ509711	nd				
Ap225	97B3	AJ509454	16(96)				
NCBI Location: Chrom. Num . (Locations)					13/10(0.33,0.69)	10/5(0.45,0.53)	

( n ) ID References				Freq	22F1	5E2/22F1	6B8	Chromosome 14
ANTP	22F1	AJ276511	37(102)					
Ac140	5E2	AJ509682	17(85)					
Ac172	6B8	AJ509695	46(148)					
NCBI Location: Chrom. Num . (Locations)					14/16(0.41,0.53)	12/15(0.008,0.5)	12/4(0.85,tel)	

( o ) ID References				Freq	5E2	Chromosome 15
Ac140	5E2	AJ509682	36(85)			
Ac141	5E2	AJ509683				
NCBI Location: Chrom. Num . (Locations)					12/4/15(0.0082,0.35)	

( q ) ID References				Freq	22F1	35D9/22F1/57E10	Chromosome 16
ANTP	22F1	AJ276511	32(102)				
NCBI Location: Chrom. Num . (Locations)					14/16 (0.46,0.53)		

**Fig. 14.** (Continued)

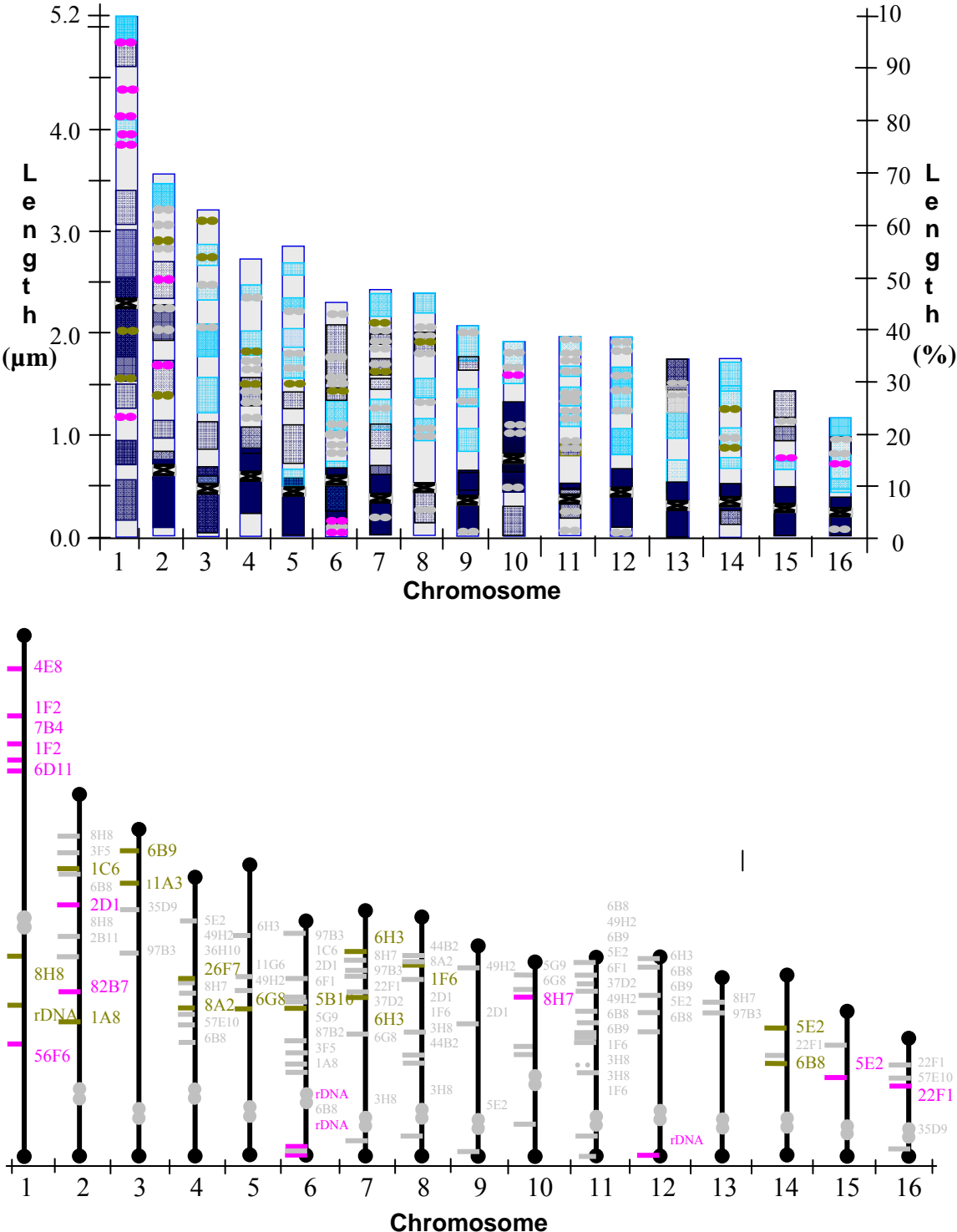


**Fig. 15.** Position of the signals on the chromosomes represented by the Ba<sub>2</sub>OH-C-banding ideogram (up), and map location with BAC names (down), Group 1. Frequency and match with last version of MVV, the scales of ideograms are for prophase I.

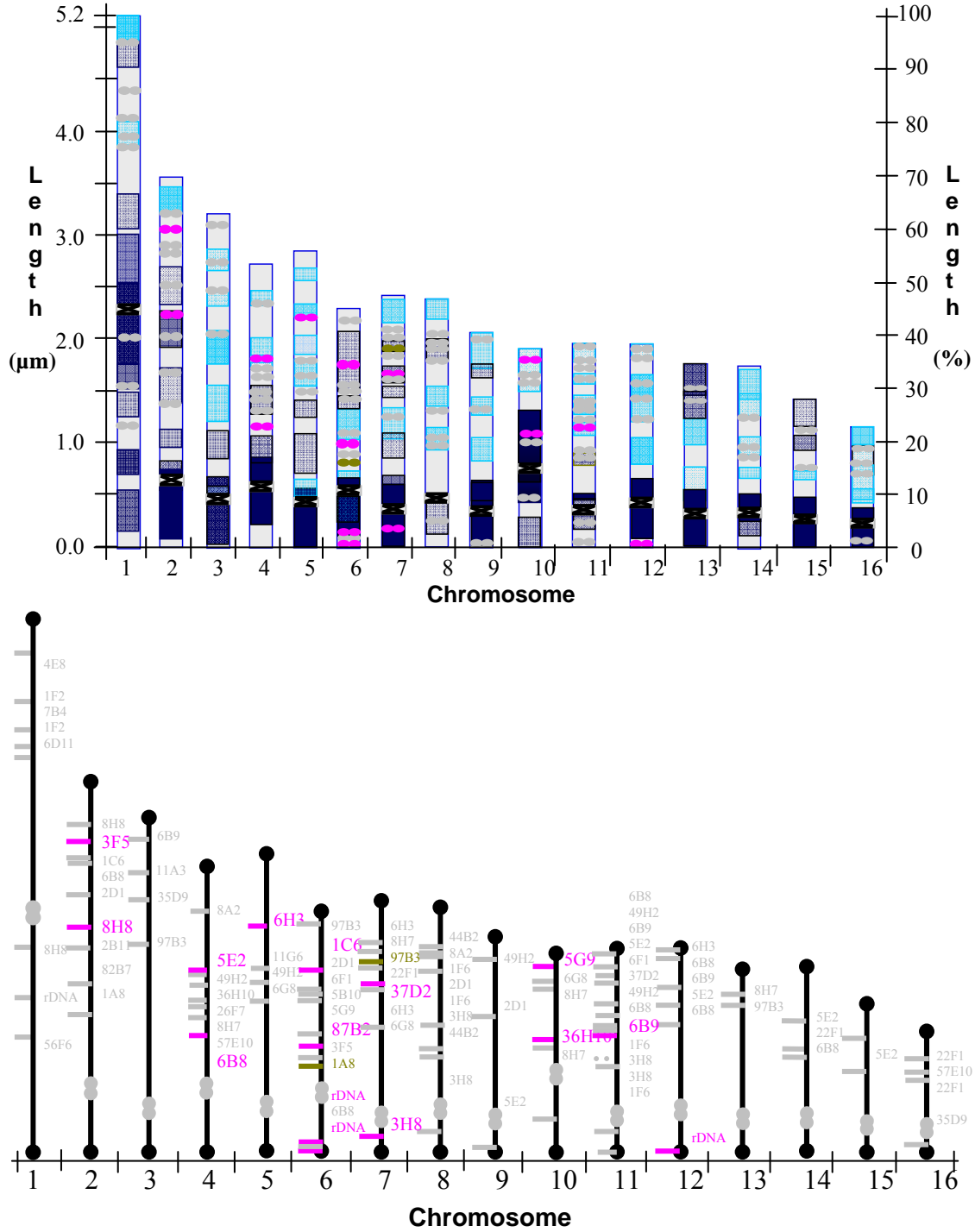


**Fig. 16.** Position of the signals on the chromosomes represented by the Ba<sub>2</sub>OH-C-banding ideogram (up), and map location with BAC names (down). Group 2. Only matches with last version of MVV, the scales of ideograms are for phase I.

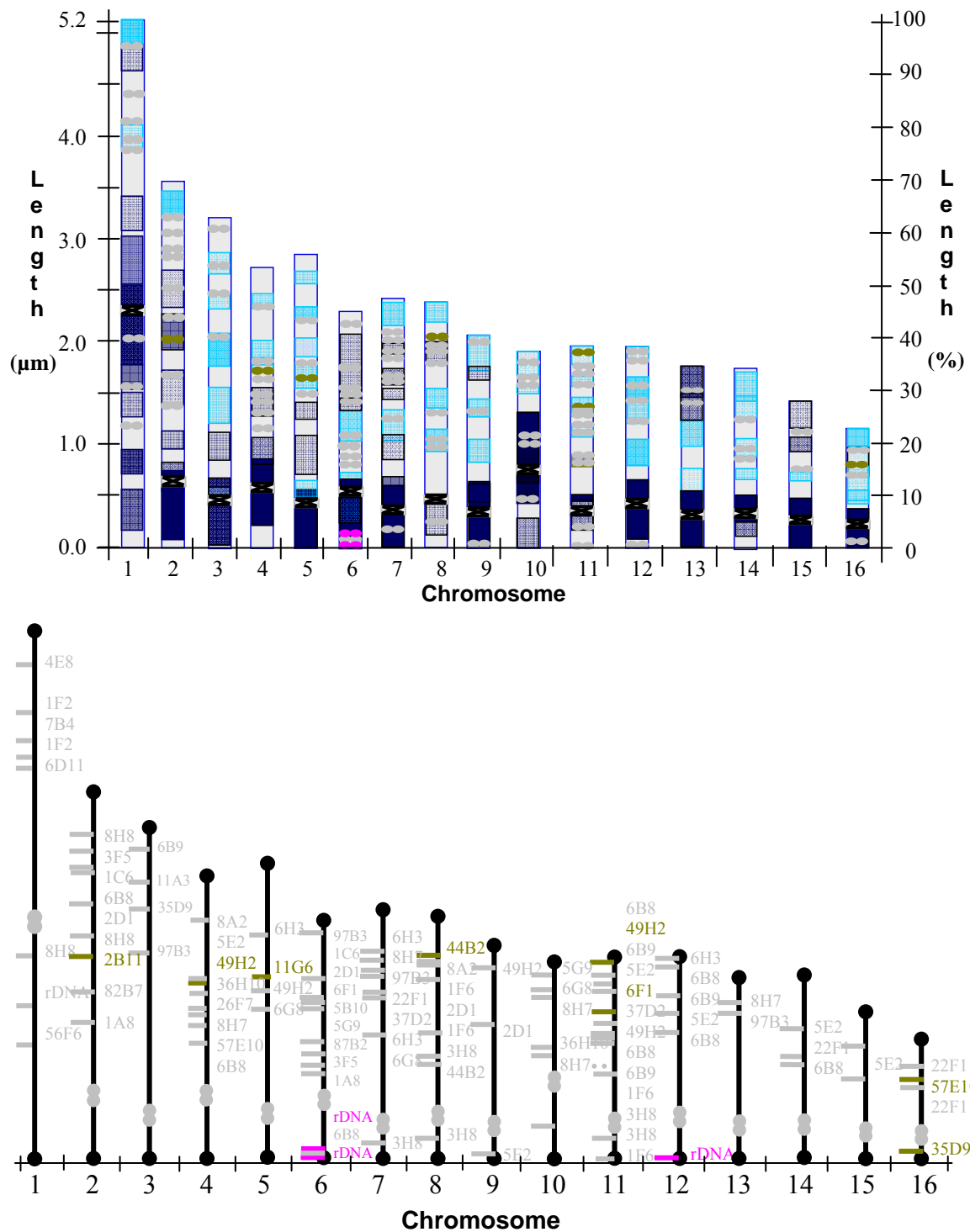


**Fig. 17.** Position of the signals on the chromosomes represented by the Ba<sub>2</sub>OH-C-banding ideogram (up), and map location with BAC names (down), Group 3. Matches with earlier MVV or no matches, the scales of ideograms are for prophase I.



BACs 35D9, 44B2, 49H2, 6F1, 57E10, 11G6, and 2B11 could not be placed by either of the last two ways because of the low frequency of hybridization and lack of match or very low score obtained. When a match with some location or position was obtained, it was only with an earlier version of MVV. With this information, 35D9 can be placed on C16 (0.254) using only the frequency (8/20), 44B2 was placed on C8 (0.843) using frequency (6/20) and position match with MVV3, and chromosome number match with MVV1. 49H2 could be placed on C4 (0.58) and C11 (0.912) using only frequency (15/64). For the signal on C11, the position match (0.9421) with MVV1 was considered even though no chromosome match was observed. BAC 6F1 that hit on chromosome 6 (0.639) and 11 (0.674), was expected on C6 (MVV1) or 13 (MVV2 to MVV4) at position 0.269, 0.766, 0.773 respectively. A clearer signal was recorded on C11 at 0.639, which could be the correct location, thus, 6F1 could be located on C11 (Fig. 14k). 57E10, BAC containing the Major Royal Jelly Protein (MRJP) cluster, was expected on C16 (MVV1) or C11 (MVV2-MVV4) at position 0.452 (MVV1), 0.183 and 0.8064 (MVV3) or 0.811 and 0.211 (MVV4); the most frequent signal for this BAC was obtained on C4 and C16 at 0.477 and 0.697 with frequency of 9/20 and 8/20 respectively. Some matches for position was obtained for C16 with MVV1, however the strongest signal was located on C4 (Fig 18d); thus 57E10 could not be clearly placed but can be mapped on both C4 and C16. BAC 11G6 was tested in a single individual experiment, and a single hybridization site was obtained on C5 at position 0.663. The 11G6 BAC was not cross tested with the position of other BACs and the hybridization was on a metaphasic chromosome only; this BAC was expected on C10 (MVV3), or C6 (MVV1, MVV2, MVV4) at 0.228 (MVV1 and MVV2), 0.314 (MVV4) and 0.372 (MVV3). Therefore, we cannot determine accurately the location and position of this BAC. 2B11 was expected on C3 (MVV1), C2 (MVV2 and MVV3) and was not placed in MVV4. With very few hybridizations obtained (only 6 cells in 3 slides) this BAC hits on C1, C2 and C9; at position 0.189, 0.465 and 0.527 respectively, which are very different to the expected positions (0.9159 or 0.1136). However, this BAC was tested

with 2D1 and 3F5, which hybridize on their expected chromosomes and locations, giving very good definition of the location of this BAC on C2 at 0.465. In summary, in this last group, only BACs 35D9, 44B2, and 2B11 can be placed with some accuracy; they can be observed in the Table 9 and Fig. 17.

**Table 9.** Number of BAC signals observed in the FISH experiments, location and position on the chromosome grouped by coincidences with the different versions of NCBI Map Viewer. Group 1 (Frequency and match with last version of MVV), Group 2 (Moderate frequency and matches with last version of MVV), and Group 3 (Matches with earlier MVV or no Matches). Bold letter indicates confirmed positions, the rest are suggested positions

BAC	Num of Signals	Double signals	Triple signals	Single signal	Chrom. with double signal	Frequency and Match with last version of MVV		Matches with last version of MVV		Matches with earlier MVV or no Matches	
						Chromosome	BAC Position	Chromosome	BAC Position	Chromosome	BAC Position
1A8	6			6		2	0.374	6	0.319		
11A3**	1			1		3	0.824				
1C6	6			6		2	0.789	<b>6</b>	<b>0.758</b>		
<b>1F2*</b>	<b>2</b>	<b>1</b>		<b>1</b>	<b>1</b>	<b>1</b>	<b>0.795, 0.869</b>				
1F6**	4	2		2	11, 8	8	0.769, 0.508				
<b>22F1*</b>	<b>5</b>	<b>1</b>		<b>4</b>	<b>16</b>	<b>16</b>	<b>0.651</b>				
26F7	1			1		4	0.534				
2B11	3			3						2	0.465
<b>2D1*</b>	<b>7</b>	<b>1</b>		<b>6</b>	<b>2</b>	<b>2</b>	<b>0.661</b>				
35D9	4			4						16	0.254
36H10	4			4				<b>10</b>	<b>0.584</b>		
37D2	2			2				<b>7</b>	<b>0.658</b>		
3F5	4			4				<b>2</b>	<b>0.844</b>		
3H8	6	2		4	11, 8			<b>7</b>	<b>0.21</b>		
44B2	2			2	11					8	0.843
49H2	5	1		4	11					4 and 11	0.58 and 0.912
<b>4E8*</b>	<b>1</b>			<b>1</b>		<b>1</b>	<b>0.943</b>				
<b>56F6*</b>	<b>1</b>			<b>1</b>		<b>1</b>	<b>0.228</b>				
5B10**	3			3		6	0.652				

**Table 9.** (continued)

BAC	Num of Signals	Double signals	Triple signals	Single signal	Chrom. with double signal	Frequency and Match with last version of MVV		Matches with last version of MVV		Matches with earlier MVV or no Matches	
						Chromosome	BAC Position	Chromosome	BAC Position	Chromosome	BAC Position
5G9	3			3				<b>10</b>	<b>0.285</b>		
6B8	8	3		5	11, 12, 14	14	0.54, 0.852	<b>4</b>	<b>0.425</b>		
6B9**	7	1		6	11	3	0.921	<b>11</b>	<b>0.905</b>		
<b>6D11*</b>	<b>1</b>			<b>1</b>		<b>1</b>	<b>0.774</b>				
6F1	2			2						11	0.639
6G8**	6	1		5	10	5	0.469, 0.429				
6H3	10	1	1	8	7, 1	7	0.572, 0.779	<b>5</b>	<b>0.543</b>		
<b>7B4*</b>	<b>2</b>			<b>2</b>		<b>1</b>	<b>0.21 or 0.799</b>				
<b>82B7*</b>	<b>7</b>			<b>7</b>		<b>2</b>	<b>0.476</b>	6	0.45		
8A2	2			2		4	0.456				
<b>8H7*</b>	<b>7</b>	<b>1</b>		<b>6</b>	<b>10</b>	<b>10</b>	<b>0.49, 0.808</b>				
8H8**	4	1		3	4	1	0.404	<b>2</b>	<b>0.596</b>		
97B3	7	2		5	3, 7			7	0.525		
57E10.	3			3						11 and 16	.477 and 0.697
<b>5E2*</b>	<b>10</b>	<b>3</b>		<b>7</b>	<b>11, 7, 9</b>	<b>15</b>	<b>0.559</b>	<b>4</b>	<b>0.618</b>		
5E2	10	3		7	11, 7, 9	14	0.893				
11G6	1			1						5	0.663
Average	4.294	1.5	1	3.647							
35 BACs	147	21	1	125		23					

### Synteny and chromosome morphology

Several problems were faced with the provided BACs, (a) some of them, such as 8A2 do not have a recognizable identification or accession number and locus number, (b) others, as 49H2, are still not correctly placed in the MVV, or (c) were placed in the early version but these places have been changed through the different version of MVV,

as is the case of the majority of the BACs. In the last version, many major changes were made. For example, 1A8, 1C6 and 87B2 (BACs that occur in synteny) were placed on C2 in map MVV1, and on C6 in MVV2 and MVV 3. In the last version (MVV4) 1A8 and 1C6 appear on C16 while 87B2 remains in C6. We observed these three BACs in C2 and C6 in the same order on each chromosome, but no signal that calls our attention was observed on C16. Another earlier mentioned problem was the multiple signals, especially in 6H3, 6B8, 6B9, 8H8, 5E2, 97B3, 8H7, 6G8, 3H8, 1A8 and 1C6. The most dramatic situation is 5E2 that appears in almost all chromosomes, but with almost all signals very weak and low in frequency except for that in C15. MVV also shows several accession numbers placed in several chromosomes including C4, C12, C13, C15 and additional places still not mapped (Tables 7 and A.1). The 8H8 BAC mapped on C1 (MVV1) and C2 (MVV2-MVV4) at 0.386 (MVV1-MVV3) and 0.574 (MVV4) and 6B9 mapped invariably on chromosome 11 between 0.806 (MVV3) and 0.882 (MVV1) and 0.191 (MVV4) and hybridized consistently on C1 (8H8) and C3 (6B9) at 0.404 and 0.921 respectively. These places are supported by 72 and 80 cells of the 93 observed respectively. However, 8H8 also shows a weak signal on C2 (0.596) and C4 (0.528 and 0.814) in 9 and 16 cells respectively of 93 analyzed. 6B9 appears in low frequency on C11 and C12 apparently in synteny with 6B8 (Figs. 14k and 14l). 6B8 hits on several chromosomes, particularly on C2, C4, C11, C12 and C14, (Fig. 12b, 13a and Fig. 14). The last three chromosomes show double signals (not all mapped) - one characteristic of these signals is that the most frequent signal occurs on a low frequency band and the less frequent signal occurs on more heterochromatic band.

When 8H8 and 6H3 are FISHed without sheared genomic DNA or with Cot-1, multiple signals are observed in almost all chromosomes, hybridizing preferably on constitutive heterochromatin. Most of the signals of 6H3 hybridize at telomeric regions of almost all chromosomes; particularly consistent are the telomeric regions of C1, C3, C6 and C12 (Fig. 14a, 14c, 14f, 14l). However, these locations were not consistently observed when the 6H3 BAC was FISHed alone; in that a case, 6H3 hybridizes to C3 (0.488), C5 (0.542) and C7 (0.572 and 0.779) (Fig 14e and 14g). The distal position on

C7 falls on a low frequent constitutive band (q31), which is a variable position band. As the double signal was not clearly confirmed in the pictures, we assume that the distal position is correct and the proximal is one of the places influenced by the band position. It is important to add that C3, C5 and C7 are very similar in morphology and usually the BACs that hit on one of these chromosomes hit also at least in one of the other two, as is the case of 6G8 and 97B3 (Fig 14c, 14e, and 14g).

22F1 has been placed on C14 (MVV1) and C16 (MVV2 and MVV4) between 0.418 (MVV2 and MVV3) and 0.533 (MVV4), the signal was frequent (31/102) and strong in C7 but weak on C14 (37/102) and C16 (32/102) (Figs 14g, 14n, 14p). In both C14 and C16, the signal occurred close to a euchromatic band but near a heterochromatic band; while the signal on C7 occurred on a constitutive heterochromatin. BACs 22F1 and 5E2 apparently hybridize in two locations on C14, both in overlapping bands. BAC 6B8, however, although at a low hybridization frequency, produces a signal that is strong and double; the proximal is much more frequent (28/93) and apparently occurs on a euchromatic band of C14. Curiously, double hybridization sites and strong secondary signals were also observed for some of the BACs that hit on C11 (BACs 1F6, 6B8, 6B9, 3H8, and 49H2) and C8 (1F6, 44B2, and 3H8). Clearly, 6B8 hybridizes on C11 and C14 and 1F6 and 3H8 hybridize on C11 and C8. In fact, these three chromosomes have been grouped together using the arm ratio and heterochromatin content (Fig. 18).

Earlier it was mentioned that 1C6, 1A8, and 82B7 occur in synteny on C2 and C6. 2D1, 3F5 and 2B11 also occur on both chromosomes. On C2, they occur in the order p|Cen|q:2B11:2D1:3F5 while in C6 they occur p:rDNA:6B8:2D1:rDNA|Cen|q:3F5:3F5:2D1 (Fig. 22a), although the signals of 6B8 and 2D1 on C6 were neither easily observed nor frequently analyzed, they show strong signals in those position when rDNA was not present in the cocktail. Close analysis of the hybridization pattern of rDNA on C6 (Fig. 14f, 14l) reveals at least three rows of spots. The distal two are very much closer to each other than the more proximal. It is within this region that the signal for 6B8 and 2D1 hits. In chapter I, it was pointed out that giemsa and trypsin differentially stained this region while C- and

DAPI show this region as heterochromatic (Fig. 18f). On the other hand, R-banding suggests a large euchromatic region in that area.

The BACs 37D2, 3H8 and 6B9 were also combined in one experiment with weak and irregular but consistent signals. 3H8 presented a single couplet signal on C7 (0.21) and two on C11 (0.174 and 0.512), 37D2 hybridized in a single couplet signal on C7 (0.737) and C11 (0.822). 6B9 was consistent in position on C3, C11, and C12. However, 3H8 clearly hybridized at two positions on C8 (0.166 and 0.389 respectively) (Fig. 18b). The signals for 3H8 on C8 are seen in each arm. The signal in the long arm was mapped close to 1F6 in C11. Significant portions of the sequence in BAC 3H8 and BAC 1F6 on C8 appear duplicated in inverted directions around the centromere on C11 (Fig. 22c). Unfortunately, we did not run an experiment that includes 1F6 and 3H8 to verify this result. Apparently 3H8 is consistently located on pericentromeric heterochromatin of the short arm of the three chromosomes, but it is strongest on C7, on a band that is consistently stained as constitutive heterochromatin, contrary to C8 and C11 where the band DAPI stains as constitutive heterochromatin, while Ba<sub>2</sub>OH stained the bands on C8 and C11 as low frequency C-bands (Fig. 18h and 18k). This result suggests that BAC 3H8 carries some repetitive sequence common between those three chromosomes and the repeat sequence occurs more frequently interspersed in C7 than in C8 and C11.

ID References				Chromosome 2	Chromosome 6	Chromosome 2	Chromosome 6	Chromosome 2	Chromosome 6	C2 and C6	
<b>(a) Experiment for Chromosome 2</b>											
Ac012	407	AJ509638	1C6								
A113	059	AJ509290	1A8								
A1082	506	AJ509737	82B7								
<b>(b) Experiment for Chromosome 6</b>											
Ac033	411	AJ509642	2D1								
Ac092	430	AJ509661	3F5								
Ac062	417	AJ509648	2B11								
Ac172	464	AJ509695	6B8								
				1C6/1A8/82B7				2D1/3F5/2B11			

(c) ID References			Position	Chromosomes 3 and 7	Chromosomes 8 and 11	Chromosomes 11	Chromosome 8/Chromosome 7/Chromosome 11
Ag011	37D2	AJ509726	C7 = 0.658 C11 = 0.727				
Ac101	3H8	AJ509666	C7 = 0.21 C11 = 0.64 C8 = 0.17, 0.38				
Ac179	6B9	AJ509698	C11 = 0.536				
11/7 (0.602, 0.48), 11/7/np (0.32, 0.714, 0.025, np)							

**Fig. 18.** Cases of BACs synteny on the chromosomes of honey bee. Result comes from cocktails containing three BACs. (a) C2 testing 1C6, 1A8, and 82B7, (b) C6 using 2D1, 3F5, and 2B11, and (c) C7 using 37D2, 3H8, and 6B9. The colors in the pictures are under the same indication as Fig. 3.

49H2 is another BAC showing scattered hybridization; especially significant signals were on C11 (0.32, 0.635, and 0.912), C4 (0.58), C8 (0.505), and C9 (0.957). Because of low frequency of the first signal on C11 and the single signal on C8, they were not mapped. The two remaining signals on C11 together with the signals of 6B8 and 6B9 apparently show a reversal of the order (Fig. 19a) that suggests a chromosome re-arrangement within C11 and between C11 and C12 (Fig. 19b). Additionally, 6B9 and 6B8 at distal positions on C11 are apparently linked with 5E2, which appeared in the most proximal position - an order that seems to be syntenic to the arrangement observed in C12 (Fig. 19b).

BACs 6G8, 97B3 and 8H7 were expected to hybridize on C6 and C3 (between 0.444 and 0.606), on C10 and C5 (between 0.5 and 0.53), and on 13 and 10 (between 0.333 and 0.689) according to MVV1 and MVV2-MVV4 respectively. BACs 97B3 and 8H7 were confirmed on C7 and C10 respectively, and 6G8 was located on C5. Secondary signals were also consistently found on C4, C5, C7, and C10. Because of low frequency of 97B3 and 6G8 on C4 (6/93 and 2/64 respectively) they were not mapped. Even so, the positions of these signals show some relationship between C4, C7, C10, and C13. BACs C10, 8H7 and 6G8 showed double signals and 97B3 did the same on C7. 6G8 and 8H7 in C10 occur in the order 6G8:8H7 in the proximal position and 97B3:8H7:6G8 in the distal region. These two blocks are separated by 0.295 relative units. In C7 the order 97B3:8H7 is detected in the distal signal while the order 6G8:97B3 was proximally detected. These two blocks are separated by 0.199 relative units (Table 10). The pair 97B3:8H7 appeared at similar distances on C4, C7, C10 and C13. The block 6G8:8H7 on C10 suggest some kind of duplication and inversion, which apparently involved the pair 97B3:8H7 of C7. On C4 the three BACs are also detected, although the order is not the same probably due to imprecision in the measurements. Something interesting is that the size of the fragment occupied by these three BACs in C7 is approximately double of that in C4, while in C10 the fragment occupied is double that in C7 (Table 10 and Fig. 19c). A progressive increase of separation between 6G8 and 97B3 is also apparently observed between C4, C7 and C10. Except for the proximal



position in C7 and distal position in C10, all sites where these blocks occur, are constitutive heterochromatic, and the chromosomes are themselves classified as heterochromatic (Fig. 14d, 14g, 14j and 14m).

In summary, the tested Solignac's selected BACs using FISH show a significant level of chimerics which explains not only the variation in the different versions of MapViewer, but also the multiple FISH signals and interaction between BACs when they are used in cocktail. The source of this chimerics may not be only from defective BACs, but also the natural occurrence of repeat sequences - especially in the heterochromatin of the genome of honey bee. The discussion addresses this possibility.

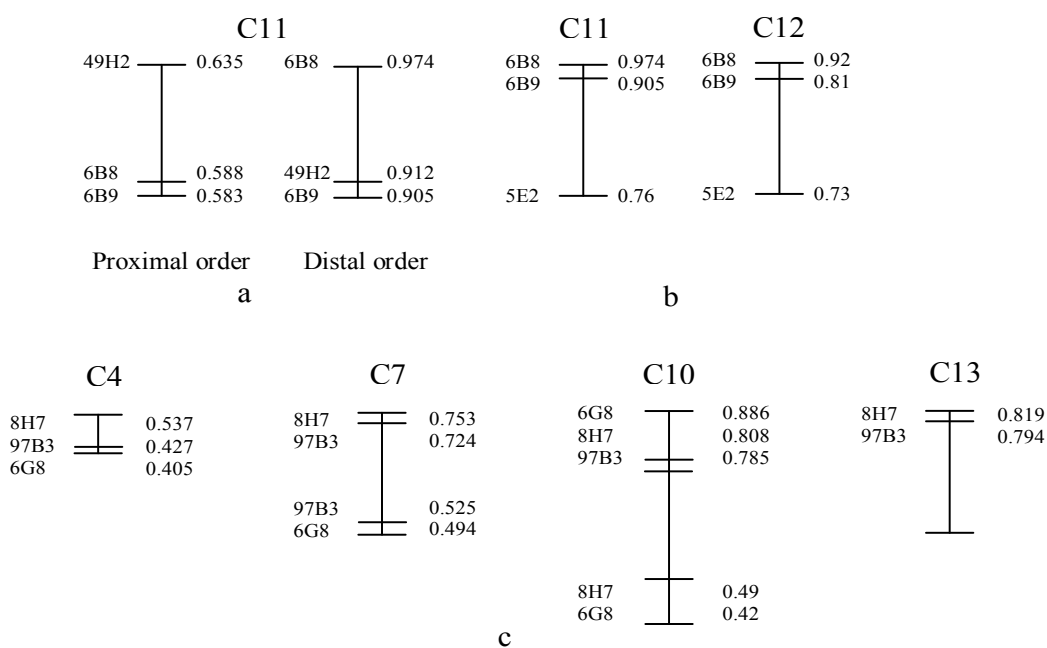


**Fig. 19.** Cases of synteny of the Solignac BACs in honey bee chromosomes. Map illustration showing the order of (a) 49H2, 6B8 and 6B9 on C11, (b) 5E2 and 6B8 and 6B9 in C11 and C12, (c) order in proportional scale of the BACs 8H7, 97B3 and 6G8 on C4, C7, C10, and C13.

**Table 10.** Approximate relative distances between pairs of BACs in four chromosomes of honey bee

Separation between	C4	C7	C10	C13
97B3-8H7	0.11	0.029	0.023	0.025
6G8-97B3	0.022 (x)	0.031 (2x)	0.078 (3x)	-
6G8-8H7	0.132 (2x)	0.259 (3x)	0.073/0.07 (x)	-
Proximal-Distal	-	0.199	0.295	-

## Discussion

The genome assembly Amel 4.0 released by Baylor College of Medicine on March 10, 2006, was qualified as being pure whole genome shotgun (WGS) (HBGSC, 2006 Sup), because the BAC library (CHORI-224; [bacpac.chori.org/bee1224.htm](http://bacpac.chori.org/bee1224.htm)) had little positive effect on the WGS. According to HBGSC (2006 Sup) CHORI-224 showed significant deletions and instability that tended to produce smaller inserts and novel rearrangements that were detrimental to the assembly. The worked Solignac BACFISH experiments suggest similar problems. This problem has been previously found in BAC clones based on *E. coli* of organism with high frequency of tandem repeats, and small genomes, BACs from these kinds of genomes, with some frequency, experience instability and rearrangements (Song et al., 2001). Some information is available showing that chromosomal regions with long inverted repeats and AT-rich regions produce the same problem in large insert libraries, which are more stable in yeast (YACs), as demonstrated with DNA from different mammals species (Kouprina and Larionov, 1999; Kouprina et al., 2003) and plants (Song et al., 2003). Perhaps, the instability of the honey bee BACs, which are based on *E. coli*, comes from similar characteristics of the genome. Characteristics of the honey bee genome including A/T rich genome [67% according to HBGSC (2006)], presence of large blocks of heterochromatin and large content of facultative heterochromatin could explain the BAC problem. The large content of facultative heterochromatin, which agrees with the observation that the honey bee genome is organized in different arrangements of

interspersed repeats (Crain et al., 1976), could be affecting the stability of the inserts in the BACs.

The FISH results show that only 5 (15%) of 35 BACs hybridize in a single site. Six (17 %) of the BACs hybridize on two sites, which means that no more than one third of the tested BACs produce reliable signal for mapping. A high percentage of the BACs (20%, 7 BACs) hybridize on more than 7 hybridization sites. Many of these signals occur in synteny on some chromosomes, which suggest a very high degree of chimerism, deletions or rearrangements in those clones. The site where the signals occur affects hybridization and visualization of the signals. Thus, most of the signals mapped (22 of 35) to euchromatic or facultative heterochromatic bands. These mapped signals were considered as the primary and most important signal. Secondary signals usually occurred on constitutive or highly frequent facultative heterochromatin, which suggest that these hybridizations come from repetitive sequences. These results also suggest that the genome of honey bee is rich in repetitive sequence that is widely distributed along the genome. However, the karyotype of early stages of prophase suggests that the honey bee genome is not highly heterochromatic from a cytogenetics point of view. This apparent contradiction can be explained by the possibility that the repetitive sequences are variable in amount and concentrated not only in the constitutive heterochromatin bands but also interspersed or distributed as scrambled repeats in the facultative heterochromatin (CSHL/WUGSC/PEB Arabidopsis Sequencing Consortium, 2000; Gilbert et al., 2003). Unlike constitutive heterochromatin, facultative heterochromatin is not characterized by repetitive sequences but shares with the first many characteristics which make possible the temporal and spacial flexibility in condensation that finally terminates in the epigenetic control of gene expression (Grewal and Moazed, 2003; Gilbert et al., 2003). Scramble repeats are characteristic of mobile elements (CSHL/WUGSC/PEB Arabidopsis Sequencing Consortium, 2000). Interspersion and scrambling of DNA sequence binding factors (Grewal and Rice, 2004) are characteristic of facultative heterochromatin euchromatin bands - characteristics that are important in the heterochromatinisation spreading process during gene silencing, epigenetic

expression and condensation (Millot et al., 1996; Grewal and Moazed, 2003). The FISH experiments of the worked BACs demonstrate that some DNA fragments are represented in several BACs sequences, and occur in several chromosomes at similar separation or at proportional multiples of that separation distance (Fig. 19). One interpretation of this result is that mobile elements have been modeling the organization of the genome of honey bee. The occurrence of these secondary hybridizations on heterochromatin, support this possibility.

Many mechanisms can alter genome size - including polyploidy, fixation of accessory chromosomes or large duplications (John and Miklos, 1988), expansions of satellite DNA or transposable elements (TE) (San Miguel et al., 1998), and “spontaneous” loss of nonessential DNA (Petrov 1996, Petrov et al., 2000). These changes can act to model the genome to produce the most advantageous structural arrangements in each species. The interaction between satellite DNA (heterochromatin) and transposable elements has a deep impact on the genome organization (Biémont and Vieira, 2005). Some of these changes include induction of mutations, disruption of regulatory gene functions and triggering of chromosomal rearrangements (Biémont and Vieira, 2006). Although their harmful effect is very well documented, some of the TEs are used as vector elements and as regulators of genes in genetics improvements (Biémont and Vieira, 2006). In humans it has been documented that TEs may have reshaped the genome by ectopic rearrangements, creating new genes, and modifying and shuffling existing genes (Lander et al., 2001). The role of TEs, that is in some way regulated via hypermethylation (O’Donnell and Boeke, 2007), suggests, "Recombination between LTRs is an efficient way to counteract retrotransposon expansion, at least among certain grasses” (Moffat, 2000) and insects (Burnette et al., 2005). Recently Lowe et al. (2007) suggested that mobile elements may have played a larger role than previously recognized in shaping the landscape of gene regulation during mammalian evolution; since mobile elements exist, they are constantly selected to become adapted to the genome, especially when they occur close to regulatory genes. Thus, cytogenetics characteristics of honey bee chromosomes (plasticity of the heterochromatin, banding

size variation) and frequency and distribution of the hybridization sites, suggest that deletions, duplications and transposition of repetitive elements has played an important role in modeling of honey bee genome. In small genomes, this fact has a particular importance because apparently the interactive mechanism of TE, satellites and regulatory genes, can drive the organism to an increase of recombination rate and faster replication (Moffat, 2000; Schön and Martens, 2002). However, TEs usually insert in areas of lower recombination rate, heterochromatic regions; and their presence by itself negatively recombination (Rizzon *et al.*, 2002) because they disrupt colinearity and may occur as inverted sequences (Charlesworth, 1994). In *Caenorhabditis elegans* accumulation of TEs (DNA-based elements) correlated positively with the recombination rate but not with the amount of LTR and non-LTR retrotransposons (RNA-based elements) (Duret *et al.*, 2000; Rizzon *et al.*, 2002). The role of TEs on recombination rate is, therefore unclear, since they correlate negatively with recombination rate in most of the genomes analyzed (Gorelick, 2003), including *Arabidopsis thaliana* (Wright *et al.*, 2003) and maize (Fu *et al.*, 2002). The contradictory effect of TEs on genomes in different species may relate to distribution, density and effect of TEs on regulatory genes and may not be directly related with other factors that are associated with recombination rate (Rizzon *et al.*, 2002; Wright *et al.*, 2003). Some studies report that crossing over is significantly correlated with the density of single repeats and the CpG ratio, but not with genes, pseudogenes, transposable elements, or dispersed repeats (Drouaud *et al.*, 2006). Dimitri (1997) reported gene-containing heterochromatin regions harbor several retro-element clusters with no repetitive satellites, which suggests their function is regulatory gene expression (Mendstrand *et al.*, 2005; Nishihara *et al.*, 2006). Besides, many of the transposon-like elements, such as helitron rolling-circle elements in maize, are responsible for copying various genes segments into new location in the genome of maize (Messing and Dooner, 2006), results that support the role of TEs in genome remodeling. The honey bee is an organism with little diversity of TEs, and it is not clear what role mariner transposition plays in this relatively small genome with its very high recombination rate (Beye *et al.*, 2006). Much

of the repetitive DNA of the honey bee remains unsequenced and 3 % of the clonable sequence is still waiting for screening (HBGSC, 2006). Transposable elements (TEs) are widely distributed in organisms in which they have been scored. Gains and losses of TE copies associated with small and large genomes, and the formation of solo-LTRs as a result of unequal homologous recombination are the main events that are continuously shaping the genomes, and can explain the difference in genome size between some organisms such as *Drosophila* and *Anopheles* (Biemont and Vieira 2005). Evidently, although the number of different types of TE elements is restricted in the honey bee, they have had a major role in the relatively small genome of the honey bee.

Thus the proposed chimerism in the mapped BACs, can also be considered as evidence of transpositions that have lead to deletions, inversion and translocations, mutations and other chromosomal rearrangements in honey bee, as has been mentioned for yeast (Kim et al., 1998) and *Drosophila* (Biemont and Vieira 2005). The occurrence of rearrangements of the FISHed BACs, such as the duplications and inverted order seen for 49H2, 6B8, 6B9 and 5E2 on chromosomes 11 and 12, as well as for 8H7, 97B3 and 6G8 in chromosomes 4, 7, 10 and 13, might be explained by the TE modeling hypothesis. In both cases the pair 6B8/6B9 on C11 and C12 are frequently observed with 8H7/97B3 - not only in the chromosomes mentioned, but also on other chromosomes (Fig. 17a). As additional information, we can add that, in the first case mentioned, one euchromatic and one heterochromatic chromosome is involved, with clear participation of their constitutive heterochromatin regions; in the second example, four heterochromatic chromosomes and their heterochromatic regions are involved.

It may be a weakness of this transposition hypothesis that, in the last version of the genome map of the honey bee, almost no diversity of transposable elements has been detected. Only the Mariner family transposon has been confirmed as present. Further, little evidence of active retrotransposable elements were detected. Little cytological evidence of structural rearrangement polymorphisms among honey bee chromosomes has been detected because of the haploid nature of the material analyzed. However, frequent chromosome breakage, especially in C1, C2, C5, C11, C10 and C15 (all in the

most heterochromatic arm) and apparently non homologous pairing between chromosomes has been observed, and suggests the possibility of chromosome rearrangements that need to be studied in the queen meiosis. Breakage and rearrangements can be also related to TEs. Fragile chromosomes sites, are related to genomic disorders in humans and other mammals because they are related to chromosomal rearrangements through nonallelic homologous recombination (NAHR) and to non homologous end-joining (NHEJ) that are responsible for recurrent and nonrecurrent rearrangements, respectively (Lupski and Stankiewicz, 2005). These TE and fragile regions usually are located in constitutive heterochromatin, which in case of *Drosophila* heterochromatin, harbor several regulatory genes that are frequently surrounded by a cluster of retroelements. Although, it is not clear that the honey bee genome harbors active retrotransposable elements, there is evidence for active non-LTR retroelements and for a high number of eroded LTR and non-LTR retroelements in the genome of honey bee, suggesting that some times in the past, the honeybee genome harbored many retrotransposons (HBGSC, 2006).

Using FISH, Liehr et al. (2001) mapped in humans chromosomes. 10 mariner transposon-like ESTs and demonstrated that their location correlates with chromosomal fragile sites. Notable is the similarity between the result of that study and that observed in this work. Four EST mariner markers gave multiple signals; some chromosomes such as HS17q12 showed four signals. In some chromosomes the signal was weak and in others strong, with cross hybridization to others chromosomes such as HS5q13. The high hybridization sites and variation in the strength of the signals can be explained by the promiscuous behavior of members of the mariner family. Its transposase can mobilize complete or defective copies of mariner elements (Lampe et al., 2003). Mariner TE also is related to (T/A) nucleotide duplication which are typical of mariner elements, and which are not typically tightly clustered (Ebert et al., 1995) - a characteristic observed in the honey bee genome. However, in some species such as *Ceratitidis capitata*, mariner TEs can invade new sites and may accumulate in high density in T/A rich regions (Torti et al., 2000). There is evidence that mariner TEs induce chromosome rearrangement,

gene duplication and chimerism (Gueiros-Filho and Beverley, 1997). Thus, mariner transposon seems to be a very good candidate responsible for multiple hits and synteny of the signals of the worked BACs. Also, they explain at least in part the behavior of the BAC 6H3, whose hybridization is altered by the presence of other BACs in the hybridization cocktail. Therefore, it is suggested that Mariner fragments have been causing instability honey bee genome and in the BAC libraries, complicating thereby the BAC-FISH mapping and the assembly of the honey bee genome. Recently mariner has been associated with high rate of interchange of nuclear and mitochondrial genomes in honey bee (Pamilo et al., 2007).

The major royal jelly protein (MRJP) cluster was expected on chromosome 11, where NCBI-MVV has it mapped. However, 57E10, that carries the marker that identifies this cluster, was BAC-mapped onto C4 and C16. A very infrequent signal, which was not mapped, is present in the subteleomeric euchromatic region of the short arm of C14. It is clear that the signal on C4 is located in a large euchromatic region while in C16 it is in a region that is heterochromatic. The signal on C14 is very infrequent but, when present, was on the subtelomeric p arm of C14. This region was frequently de-attached and observed as a minichromosome. Nevertheless, it is clear that the MRJP cluster is mainly mapped on chromosome 4 and chromosome 14 but not in C11.



## CHAPTER IV

### ***IN SITU* NICK-TRANSLATION BANDING IN DH4 HONEY BEE DRONES CHROMOSOMES**

#### **Introduction**

Although banding techniques based on aceto-carmin dye were earlier used by Barbara McClintock to study the heritability of constitutive heterochromatin (nodes) in maize in 1931, it was in the 1960s that Torbjörn Oskar Caspersson began studies showing the use of chromosome banding as valuable tool in chromosome characterization in human diseases (Caspersson, 1989). However, it was not until the 1970s that the formal introduction of chromosome banding techniques provided not only a very powerful tool for chromosome identification (de la Torre and Sumner, 1994), structure and organization, but also as means to improved our knowledge about evolution and, more recently, genome mapping (Yang et al., 2000; Gartler, 2006). In that decade, there were also experiments with high resolution banding. Early prophase chromosomes, or chemicals that keep the metaphasic chromosomes relaxed (Yunis 1981), were used along with nuclease and restriction endonuclease to produce nick banding (Sahasrabudde et al., 1978). It was only after molecular techniques improved during the 1980s that restriction endonuclease (REs) banding for chromosome characterization was extended to plants (Olszewska et al., 1999), insects (Bianchi et al., 1985), fish (Abuin et al., 2007; Leitão et al., 2004, 2006) amphibians and reptiles. In general, REs such as *AluI*, *RsaI*, *MboI*, *HaeIII*, *AcoRII*, produce C-like patterns. When *in situ* nick translation and biotinylated label is incorporated into DNase I treated chromosomes, R-banding pattern is obtained (Bickmore and Craig, 1997).

DNase I hypersensitivity and nick banding associated with that hypersensitivity has been used to map active genes on fixed chromosomes, and study imprinting differences between active or inactive X chromosome in mammals (Gait et al., 1982;

Karen et al., 1983,1984), although often with contradictory results (Murer-Orlando and Peterson, 1985). While Nick banding can be applied with other endonucleases, such as *Eco* R1 and *Pvu* II for example, the nick translation system ordinarily uses DNase I to characterize human chromosomes (Bullerdiek et al., 1985, 1986), C-banding in mammals (Adolph, 1988), G- or R- banding (Adolph and Hameister, 1985), chromosome mapping (Karem et al., 1984), and to differentiate facultative and constitutive heterochromatin (Sperling et al., 1985). DNase I is also used to measure methylation level on chromosomes (Jablonka et al., 1985; Loebel and Johnston, 1993; Olszewska et al., 1999), show regionalization of sex chromosomes (Richler et al., 1987), and for gene detection (Kamissago et al., 1999). Because of the difficulty controlling the enzyme (temperature and time) activity, the consistency and reproducibility of this method were quickly seriously questioned (Bickmore and Craig, 1997). It was shown that the banding pattern produced by restriction enzymes is not exactly related to the distribution of the enzyme's recognition sequence on the chromosome, because the banding is affected by several factors, such as the distribution of recognition sites, accessibility (de la Torre and Sumner, 1994, Bickmore and Craig, 1997), and enzyme concentration (Adolph and Hameister, 1985). Even so, based on agreement of RE banding with FISH experiments (Chaves et al., 2002) the technique is still used in karyotypes with chromosomes that are difficult to identify, as in Ostreidae (Leitão et al., 2006). Endonuclease chromosome banding using *Eco* RI, *Hae*III, and *Tru*9I, by Lorite et al. (1999a), and nick translation banding based on DNAase I sensitivity in *Tapinoma nigerrimum* (Hymenoptera, Formicidae) by Lorite et al. (1999b) have been reported. In the aphid *Megoura viciae*, the sensitivity of DNase I (Manicardi et al., 1998) as well as imprinting of the paternal chromosome set in holocentric chromosomes of *Planococcus citri* (Bongiorni et al., 1998) has been tested. Non-uniform DNase I sensitivity in different chromosome domains has been found, and in consequence, no correlation with the traditional banding pattern was observed. Instead, a preference of DNase I for heterochromatic regions was described (Lorite et al., 1999b). A more sophisticated technology, so-called FISH banding (Liehr et al., 2006) or IPM-FISH [IRS-PCR

multiplex FISH based on interspersed polymerase chain reaction (Aurich-Costa et al., 2001 cited by Jiang and Katz, 2002)] has been created to characterize the R-banding-like pattern for diagnostic uses in humans (Jiang and Katz, 2002). In an attempt to reproduce GTG-like banding, Spectral Color Banding (SCAN) has been developed (Senger et al., 1998) based on microdissection libraries. In the present study we applied two-color nick translation banding to support the different banding patterns generated previously in honey bee chromosomes. In order to reduce ambiguous results, we collected data from different cells, at different stages of prophase, and constructed an ideogram with early, middle and late-digested bands and compare that with C- and R- banding. Chromosome spreads on slides were treated with Roche nick translation kit at two different incubation times using two detection systems, Digoxigenin-FITC and Biotin-Cy3. The resultant nick bands were then compared to bands produced by other methods.

## **Materials and Methods**

### **Chromosome preparation**

Drones from DH4 strain queen were kindly provided for chromosome preparations by Danny Weaver of BeeWeaver Apiaries. Chromosome slides were prepared according to the procedure of Mandrioli and Manicardi (2003) with modifications consisting of dissection and incubation of testes in physiological solution (Sahara et al., 1999) and distilled water as hypotonic solution. Follicles were disaggregated, and the cell suspension centrifuged at 1000g for 3 min. After discarding the supernatant, 200 mL of Carnoy's fixative solution (Methanol: Acetic acid 3:1) was added, and the resultant mixture incubated at room temperature for 30 min and re-centrifuged at 100g for 3 min. The procedure was repeated until the sample slides were clean, without significant lost of chromosomes and cells. The slides were scanned with a Zeiss binocular stereoscopy, and for slide preparation, a light microscope, Zeiss (Model 039539-47 16 90-0000/09) equipped with phase contrast (47 3356-9901) and Plan apo 25/0.65 and Apo 40/0.95 objectives. When slides were more than a year old, a re-

hydration in TC-100 (Sigma, Cat# T3160) culture media complemented with 5 to 7% of fetal bovine serum (FBS, Sigma, Cat# F-6178) for 35 min at 36°C was applied, then the material on the slide was re-fixed in Carnoy's solution.

### **Digestion and labeling**

In a preliminary experiment, several incubation times were tested, 30, 45, 60, 90 and 120 min. To support the period of times selected (45 and 90 min) for the formal experiment, the effect of those incubation times is described first.

The slides were equilibrated in a diluted TE solution pH 7.5 (0.5 ddH<sub>2</sub>O: 0.5 TE), then treated with 40 µL of nick translation mix dilution containing 4 µL of DIG-Nick (Cat# 1 745 816) or Biotin-Nick Translation Mix (Cat# 1 745 824, Roche Diagnostic GmbH, Penzberg, Germany). The volume was determined for an area of 24x24mm. The slides were covered with a plastic cover slides, and incubated at 15°C in a humidity chamber for 45 min. The slides were briefly washed with diluted TE solution and drained before applying a new nick translation mix dilution with a different label, and incubated at the same time and temperature. Two series of slides were prepared; one starting with DIG-Nick mix and the other with Biotin-Nick mix. After the first period of 45 min, those slides treated with Biotin-Nick mix were treated with DIG-Nick mix and visa versa. After the second incubation, the slides were placed in a slide jar containing 50 mL of 0.5M EDTA (Ethylenediaminetetraacetic acid) pH 8.0 at 52°C for 5 min and allowed to cool 10 min, after which they were washed three times in 2xSCC at 36°C followed by an alcohol series dehydration. After several hours of air-drying at room temperature, the slides were processed for signal detection following the procedure used for Fluorescence In Situ Hybridization (FISH), as described in the chapter II. Briefly, after incubation, the slides were rinsed twice at 40°C for 3min in 2xSCC, once at 36°C in 50% formamide (Sigma, St Louis Mo, USA, Cat# F7503) for 10 min, twice at 36°C 2xSCC, and once with 4xSCC plus 0.2% Tween® 20 (Sigma, P9416) at 37°C, and cool at room temperature in 4xSCC plus 0.2% Tween 20 for 5 min. The slides were blocked for 30 min with 250µL of 5% nonfat milk dissolved in 4xSCC plus 0.2% Tween 20. The

signals were detected with a mix solution containing 7 -15  $\mu\text{g}$  of both Cy<sup>TM</sup>3-conjugate Streptavidin (Jackson ImmunoResearch, Cat# 016-160-084) and Fluorescein (FITC)-conjugated IgG fraction monoclonal mouse anti-digoxigenin (Jackson ImmunoResearch, Cat# 200-092-156) diluted in 100-150  $\mu\text{L}$  of TNT buffer (100mM Tris-HCl pH7.5, 150mM NaCl, 0.5% BSA). Following incubation for 30 min at 37°C, the slides were rinsed three times at 37°C in 4xSCC plus 0.2% Tween 20 for 3 min each. The slides were next briefly equilibrated in 4xSCC plus 0.2% Tween 20. Subsequently, 250 $\mu\text{L}$  of 5 $\mu\text{g}/\text{mL}$  of 4' 6-diamidino-2-phenylindole (DAPI, Sigma, Cat# D-9542) in McIlvaine's buffer (9 mM citric acid, 80 mM Na<sub>2</sub>HPO<sub>4</sub>·H<sub>2</sub>O, 2.5 mM MgCl<sub>2</sub>, pH 7.0) was applied to the slides and incubated for 30 min at room temperature. After a brief wash in 4xSCC plus 0.2% Tween 20, 25  $\mu\text{L}$  of home-prepared antifade solution was applied to slides following Trask (1980) recommendations.

### **Slide observation**

Slides were analyzed under an epi-florescence microscope AX-70 with a Peltier-cooled 1.3 M pixel Sensys camera (Roper Scientific) and a MacPro v. 4.2.3 digital image system (Applied Imaging Corp., Santa Clara, Cal., USA) equipped with 4',6-diamidino-2-phenylindole (DAPI), fluorescein isothiocyanate (FITC), and Cy3 filter sets located at New Beasley Laboratory on Agronomy Rd y Laboratory, which also serves as the TAES Laboratory for Plant Molecular Cytogenetics.

## **Results**

All chromosomes showed very good labeling. Clear and strong signals were obtained in pre-metaphase and metaphase chromosome; however banding was produced only in earlier prophase chromosomes. In metaphase chromosomes, a significant result was the even nick translation activity that digested and labeled heterochromatin and euchromatin equally (Fig 20a). Frequently, the nick translation activity starts in the center and spreads evenly to the outside of the cell, suggesting that remaining

cytoplasmic components initiate the nick translation system from that point. It was frequently observed, in interphase nuclei and metaphase chromosomes, which nick translation labeled evenly and preferentially, the periphery of nuclei or chromosomes (Fig. 20b and 20c). Prophase chromosomes were differential banded. When overly digested (120 min), the heterochromatin was deeply stained than euchromatin (Fig 20d). Reducing the digestion time (45 and 90 min) improved the differential banding between heterochromatin and euchromatin (Fig 20e and 20f).

Based on the preliminary results, 90 min of incubation was chosen for *in situ* nick translation banding. The slides that began with biotin-Cy3 label develop the first band (red) (Fig. 21a-21d) better than the second band (green) labeled with the DIG-FITC system applied 45 min after the biotin. The positions of green bands were confirmed in complementary experiments when Biotin-Cy3 was applied after 45 min of incubation in DIG-FITC (Fig. 21e and 21f). Bands labeled in the middle of the experimental period were usually labeled with the two haptens, biotin-Cy3 and Dig-FITC giving a yellow, greenish-red or reddish-green color (Fig. 21a-21f). The banding staining was not homogenous, mainly because the digestion seems to depend on the prophase stage. Therefore, data were recorded from a sample of 12 cells and the ideogram was constructed with the average frequency of the bands. For this the pictures were converted to black and white, to enhance the DAPI banding pattern, and facilitate chromosome identification based on the previously constructed DAPI and C-banding ideograms.

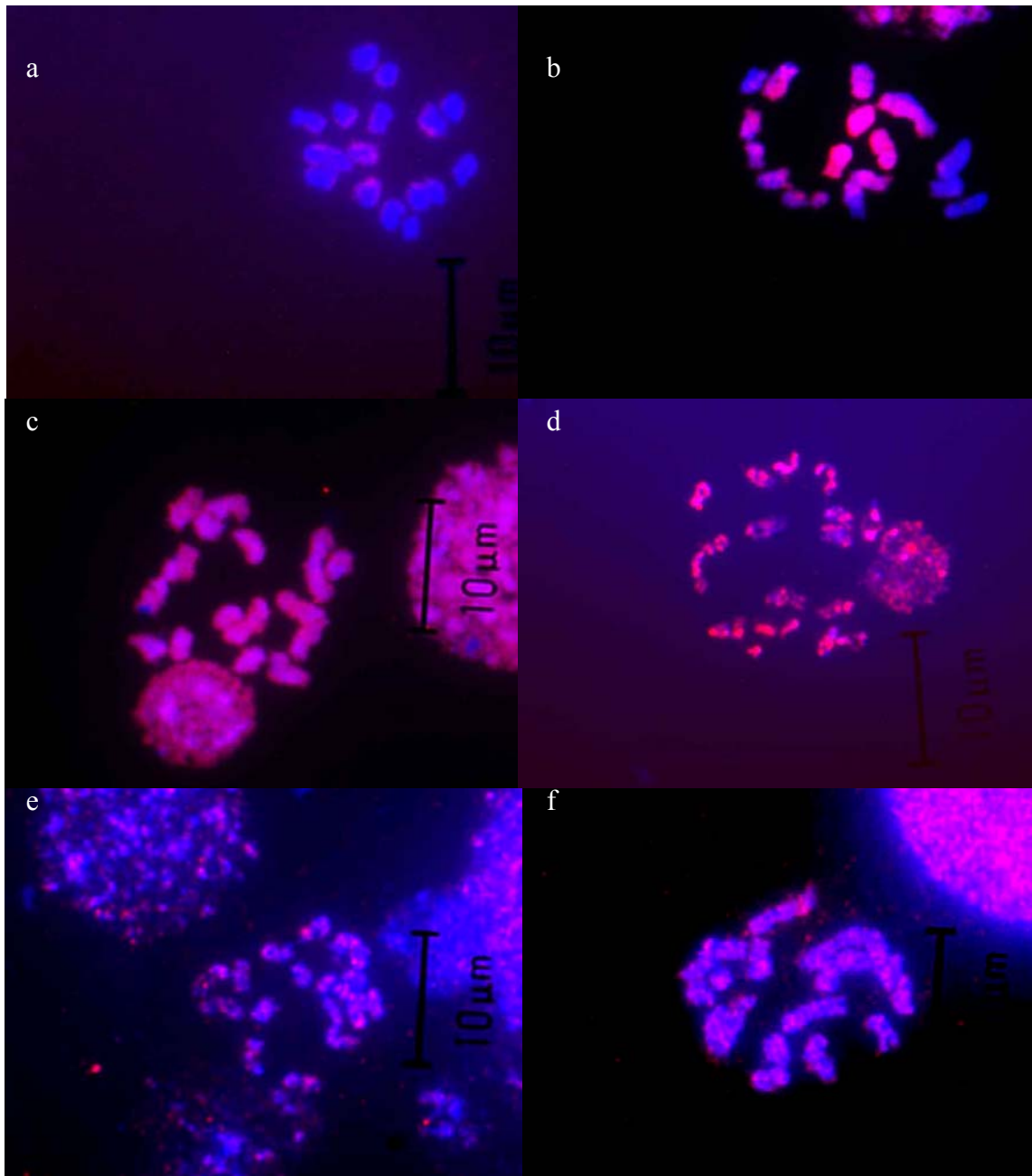


**Fig. 20.** Preliminary test with in situ biotin-nick translation mix kit (Roche Applied Science) on honey bee chromosomes at 15°C and developed with streptavidin-Cy3 conjugate. Incubation times were: (a) 30 min, (b) 60 min, and (c) 120 min on metaphase chromosomes; (e) 120 min, (f) 45 min, and (g) 90 min on prophase chromosomes.

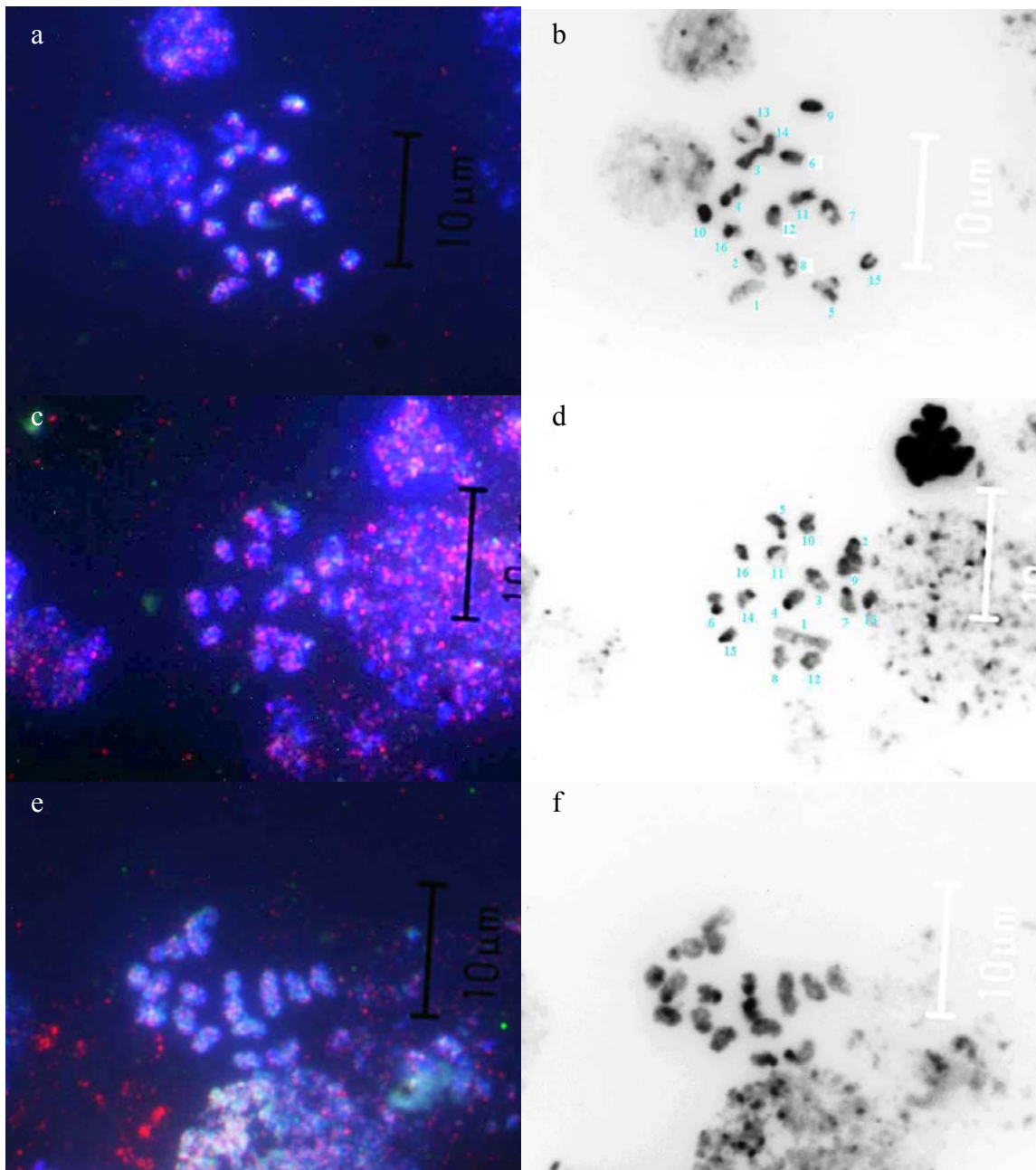


**Fig. 21.** Banding evidence obtained from use of the biotin and digoxigenin nick translation mix (Roche Applied Science) on prophase chromosomes of honey bee. (a-d) first period treated with biotin nick translation mix and the second period with digoxigenin nick translation mix, (e-f) first period treated with digoxigenin nick translation mix and the second period with biotin nick translation mix. The experiment was carried out at 15°C, and 45 min in each period. The signals were developed with streptavidin-Cy3 conjugate and anti-Dig-FITC conjugate.



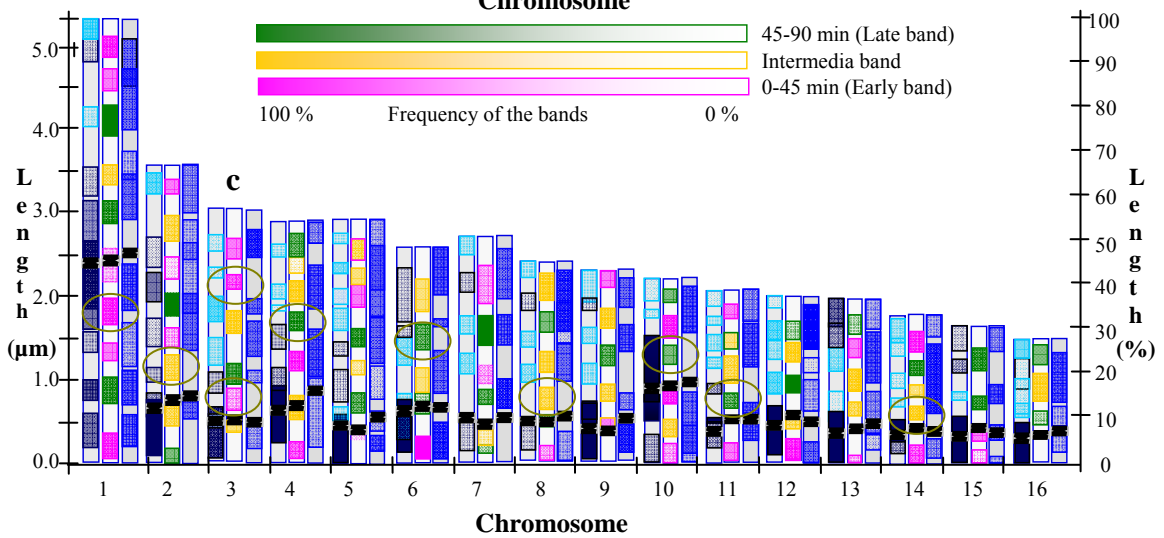
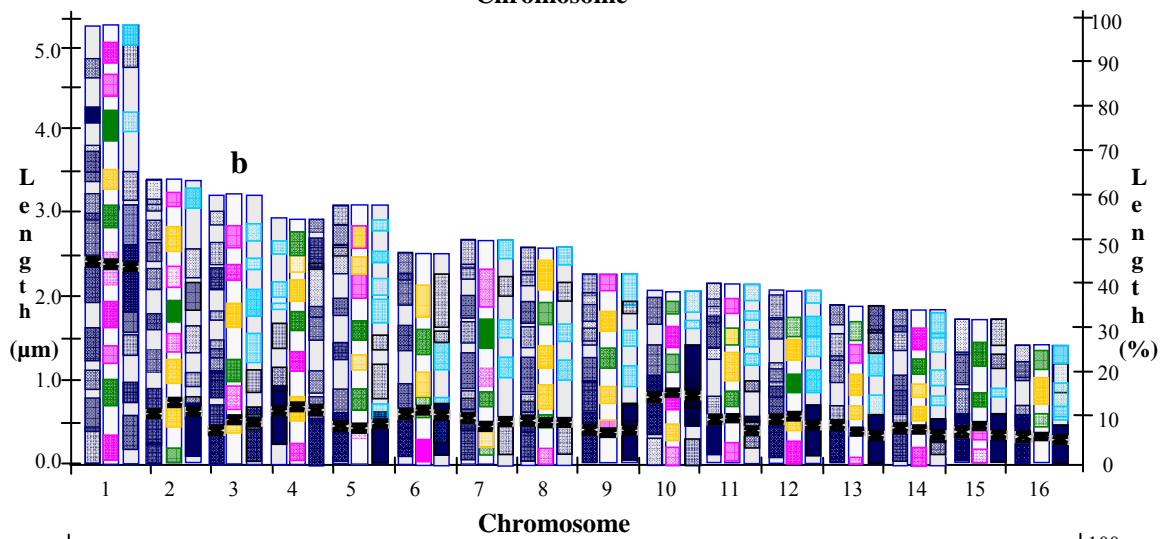
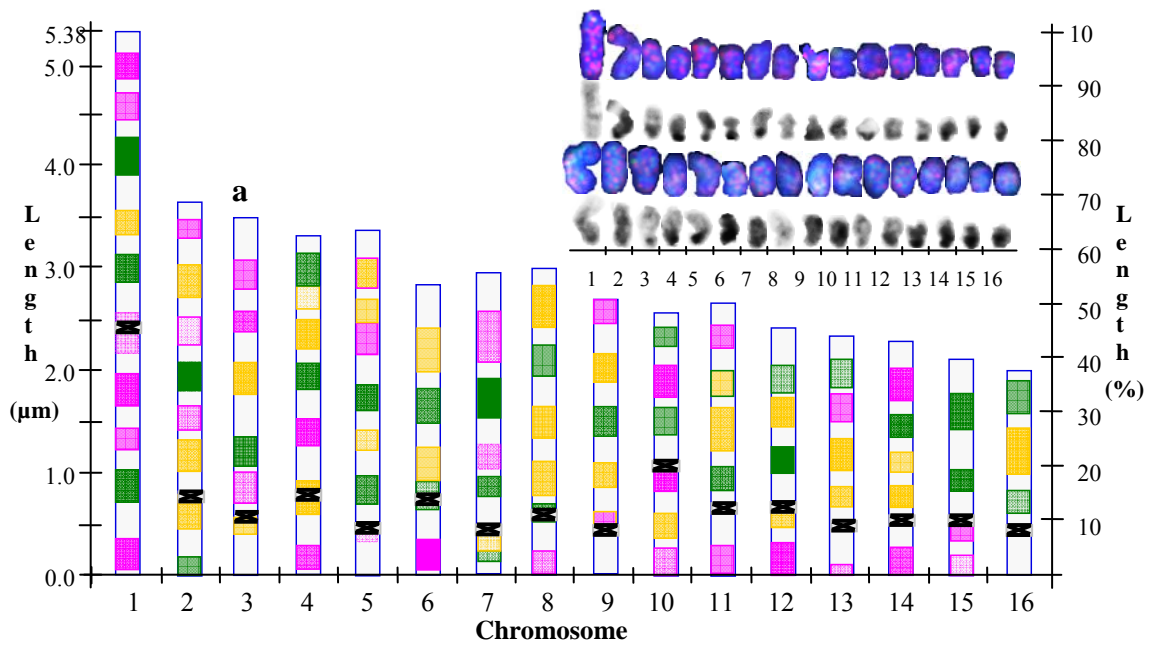
### **Ideogram description**

The color bars in the nick-banding ideogram represent the type of band, which were semi-qualitatively classified as early digested (red), intermediate digested (yellow) and late digested (green) (Fig. 22a). The early nick-bands refer to bands that were completely digested in the first 45 min of incubation and develop just one color. The yellow or intermediate bars represent intermediate bands whose color comes from the combination of the red from Cy3 and the green from FITC. The green bars represent the late bands, which were labeled in the second period of incubation only. The color of the late band is green if the last incubation was performed with Dig-FITC, or red if the last incubation was carried out with Biotin-Cy3. Each type of band is represented based on its frequency. Thus the most frequently observed bands are deeply colored, and the low frequency bands are lightly colored. Chromosome 1 (C1), for example, showed 10 nick bands, six of them (red) are early nick-bands, one is an intermediate nick band (yellow) and three are later nick bands (green). The most distal (p42) and the most proximal (interband between p12.2 and p21) red bands in the p arm, as well as the last distal band in the q arm (inter-band between q41 and q42) are high frequency bands - the red bar is darker than the rest of the red bars - an indication that those bands are prone to attack by the nick translation system, while the centromeric band of C1 is the lightest red colored band, indicating that band was a less prone to attack by the nick translation system.

When the nick-ideogram is compared with DAPI and C-band ideograms, some variation in the position of the centromere is observed, which suggests an effect on the measurements, mainly due to variation in the stage of prophase and dynamics of the heterochromatization and condensation of the chromosomes. Even so, some interesting results can be highlighted from ideogram comparisons. Except for the centromeric bands, most of the nick bands match inter-bands of the DAPI- and C-bands (Fig. 22b). Except in C10, C11, C13, and C14, the nick translation mix labelled all pericentromeric heterochromatin. However, the frequency at which they were labeled was low. The C-band ideogram was used to determine the kind of heterochromatin in the bands. Dark

blue represents the C-band (constitutive heterochromatin). These differ in the frequency observed as indicated by the level of the blue; the brighter blue represents secondary bands that in most of the cases match with a lower frequent DAPI band; thus those secondary bands, together with DAPI-bands that do not match with C-bands, are considered facultative heterochromatic bands. Based on that simple classification, most of the earlier nick-bands match with inters- or euchromatic bands and most of the intermediate and later nick-band coincides with facultative heterochromatin bands. Some low frequency C-bands, such as those in C7 and C13 coincide with an early and low frequency nick-band, as in C7 (q32) and C13 (q22), or with a late nick band, as in C13 (q31) and C10 (q12.2) (Fig. 22b) – a result that is in agreement with the assumption that constitutive heterochromatin is strongly but evenly attacked by DNase I throughout the cell division. C3, C7 and C10 are three chromosomes that, according to the karyotype characterization (Chapter I) and BAC-FISH experiment (Chapter II), are closely related. It is important to mention that C15 and C16 did not show intermediate and early bands; all bands were late bands, as expected of chromosomes with constitutive heterochromatin, but no facultative heterochromatin. Nick translation consistently and incorporated biotin or digoxigenin early on the distal region of q arms of 10 chromosomes and late in C2.

**Fig. 22.** Comparative nick translation banding pattern with Ba(OH)<sub>2</sub>-C- and DAPI- banding. (a) Nick-Banding ideogram and an example of two karyograms from which the data was collected and upon which the construction was based. The colored bar at the top of the graphic indicates the type of band, while the level of the color within the bar indicates the frequency at which the bands were observed. The red color represent the first band digested (early band), the yellow color represents the bands that were being digested when the new hapten was added, producing a band that was either green / red or yellow. These bands were classified as intermediate. The green color represents bands that were labeled only in the second period of incubation. (b) A comparison between the nick-banding ideogram (middle), DAPI- (left), and C-banding (right), (c) A comparison between the nick-banding ideogram (middle), C-banding (left), and R-banding (right). C-banding was based on Ba<sub>2</sub>OH (Sumner, 1972) and R-banding following the procedure of Sumner (1994).



An overall comparison between the nick-banding and R-banding ideogram, shows that most of the bands are R-banding regions (Fig. 22c). However, in 9 chromosomes (C1-C4, C6, C8, C10, C11, and C14) at least one nick-band matched unstained R-bands (circled in golden green ovals), and in most of the cases matched facultative heterochromatin bands. It is important to mention that these same nick-bands are low frequency and usually late-digested. Thus it seems that nick translation may digest the facultative heterochromatin late (Fig 23). It is of note that the nick bands located immediately after the centromeric band on C8, C11 and C14 are similar, late digested, low frequency bands on chromosomes that are morphologically and euchromatically similar. Therefore, it seems that the DAPI and C- banding inter-bands (euchromatic) are first attacked, followed by the facultative heterochromatin, which usually increased in frequency as the incubation time was progressing. Constitutive heterochromatin did not show a very clear tendency, but in general increased in the intermediate period of incubation (Fig. 23).

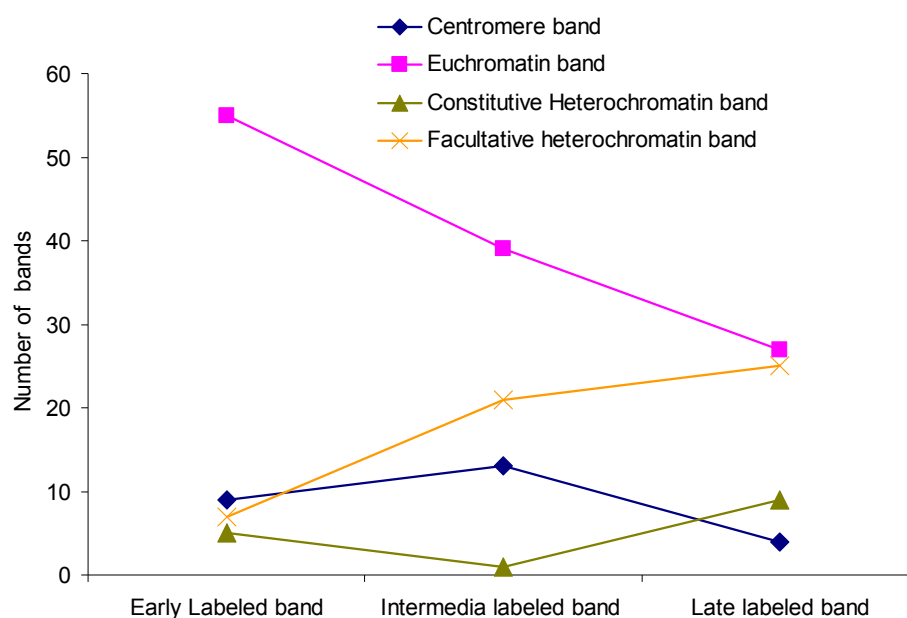


**Fig. 23.** Number of bands of honey bee chromosomes digested by the nick translation mix (Roche Diagnostic GmbH, Penzberg, Germany) system. Centromere bands (blue line), constitutive heterochromatin bands (golden green line), facultative heterochromatin bands (yellow line) and inter-bands or euchromatic bands of honey bee chromosomes.

### Discussion

It was clear that metaphase chromosomes are of limited use for nick-banding characterization of honey bee karyotype, leaving the prophase chromosomes which, even given the variability, are a very good alternative, since early, mid and late prophase have different sensitivities to DNase I. A similar result was reported by Raman et al. (1988) for meiotic chromosomes of mouse. As pointed out here in chapters II and III, the chromosomes of honey bee can be grouped by similar morphology, size and banding pattern as well as by molecular markers (Chapter III). Some of these groups also show similarities in nick-banding pattern. This similarity was seen for euchromatic chromosomes (C8, C11 and C14), nucleolus organizer carriers (C6 and C12), acrocentric

and heterochromatic chromosomes (C3, C5, C7, and C9), and sub-metacentric and heterochromatic chromosomes (C16, C15, C13), which confirm the *bona fide* of the karyotype of honey characterization given in previous chapters. Nick-banding also confirms the chromatic nature of the bands detected; and suggest, to a very good approximation, the structure and organization in cytogenetic terms, of the honey bee genome. The nick banding technique, as carried out in this work, clarifies many of the inconsistencies and contradictory results reported earlier, and demonstrates the usefulness of this procedure to characterize the honey bee karyotype. One inconsistency was the incorporation of haptens in heterochromatin when incorporation was expected only in euchromatin and transcriptionally active regions such as rDNA - a result earlier reported by Adolph and Hameister (1985). Here we show that euchromatin, facultative heterochromatin and constitutive heterochromatin are differentially attacked by DNase I under the nick translation system. The activity is dependant on the stage of the chromosomes, which agrees with the result reported by Sentis et al. (1990) in *Baetica ustalata*. Thus, Gross and Garrard (1988) mention that a variety of functional sequences are associated with DNase I hypersensitive sites, such as the centromere, silencers, recombination sequences, replication origins, upstream activation sequences (UASs), promoter elements and transcription terminators. However, trans-acting factors and epigenetic determinants, such as DNA methylation, looping sequence composition, alternative conformation, and protein composition (Gross and Garrard, 1988) modify the detection of these sites (Foster and Bridger, 2005). These properties can be utilized in chromosome characterization, especially in karyotypes with small chromosomes and irregular banding, whose metaphase chromosomes are poorly known.

Pericentromeric heterochromatin was attacked differentially among chromosomes - especially in the intermediate period. A similar pattern of incorporation of biotinylated dUTP in C- bands was produced after increasing the concentration of DNase I from 50ng/mL to 100 ng/mL in *Megoura viciae* (Manicardi et al., 1998) and *Tapinoia nigerrimun* (Lorite, et al., 1999). Incorporation of labeled nucleotides in constitutive heterochromatin is a general characteristic of DNase I at high concentration

or with a long time of digestion (de la Torre et al., 1992, de la Torre and Sumner, 1994). Many that have examined the DNase I activity in a nick translation system in metaphase chromosomes explain the apparently random DNase I activity in terms of patterns of replication and pachytene chomomeres distribution on chromosomes (Manicardi et al., 1998; Lorite et al., 1999). However, Paul (1987) mention that active genes are more prone to DNase I digestion because they are less protected over the entire region; hypersensitive sites are more frequently observed 5' to the start of a transcription sequence. In some genes the hypersensitive sites can be determined by non histone proteins such as  $\beta^A$ -globin (Emerson et al., 1985; Elgin, 1984), and by altered conformation of the DNA strand (Elgin, 1984) in genes other than  $\beta$ -interferon (Zinn and Maniatis, 1986). Hypersensitive sites and transcriptional regulation have been successfully correlated with active proteins in the *Drosophila* glue protein gene (Shermoen and Beckendorf, 1982), mouse (Senear and Palmiter, 1983) and chicken (Kaye et al., 1986), but not in others (Murray and Kenard 1984). Hypersensitive sites also correlate with recombination hot spots in some genes, such as the HIS4 locus in *Saccharomices cereviceae* (Fan and Petes, 1996) and in meiotic chromosomes of mouse (Raman et al., 1988). Hypersensitive sites can also be induced by external factors, as in maize, in which the induced sites include TATAA and CAAT sequences (Paul et al., 1987). Tuan and London (1984) found that hypersensitive DNase sites correlate with  $(Ts)_{28}$ ,  $(C-A)_{15}(T-A)_6$  sequences. Taken together, these observations suggest that DNase I has a preference for regions rich in T/A nucleotides, although not to specific sequences, which would explain the tendency of DNase I to induce nicks in the DNA located in constitutive heterochromatin, allowing thereby polymerase I incorporation of labeled nucleotide during the repair process. The low frequency of C-labeled bands and the consistency of attack with the different incubation times at the concentration analyzed (*c. a.* 1 ng of DNase I per 10 $\mu$ L of nick translation mix; Roche Applied Science, 2006, Nonradioactive In Situ Hybridization Application Manual) suggest that high A/T sequence attracts DNase I action, while the highly protected chromatin slows the activity relative to less protected regions. Sentis et al. (1990) found this result for constitutive



heterochromatin and facultative heterochromatin. Thus, the strong signal of restriction bands at higher concentration, higher time of incubation and higher working temperature suggest that the accessibility of the DNA in constitutive heterochromatin can be enhanced by reducing the resistance provided by protein protection and tightly packaged chromatin (Gross and Garrard, 1988; Sumner et al., 1994). Interesting and comparative results are described by Crawford et al. (2006) and Sabo et al. (2006) in two very elegant experiments for DNase I mapping. The authors show that the lowest number of DNase I hypersensitive sites was located on gene poor regions with highest level of conservation. Those gene poor regions could be facultative and constitutive heterochromatin regions. In the test of this hypothesis on the honey bee, Figs. 20a-20d shows that the nick system did not distinguished between bands in metaphase chromosome regions and interphase nuclei; both evenly incorporate the hapten, dUTP-biotin or dUTP-digoxigenin. The relatively external location of the signals in both structures could be explained by the hypothesis that repetitive sequence or A/T rich sequences can usually located in the bend of loops (SAR: scaffold associated region) and external bends (Ostashevsky 1998) of DNA in metaphase chromosomes (Saitoh and Laemmli, 1994; Ostashevsky 1998) and that heterochromatin usually is located in the periphery of the nucleus (Ferreira et al., 1997; Carvalho et al., 2001; Cremer and Cremer, 2001; Foster and Bridger, 2005; Meaburn and Mistelli, 2007). This would explain our result about the peripheral location of the signals in the nucleus and metaphase chromosome. It would also explain the differential incorporation of labeled dUTP in prophase chromosomes. An interaction between time, temperature and concentration of DNase I in optimization of the banding pattern and improvement of banding resolution is expected. That interaction would be desirable to define in future experiments.

## CHAPTER V

### CONCLUSIONS AND FUTURE WORK

The karyotype of the honey bee is analyzed in this study. The karyotype is characterized by two metacentric chromosomes (1 and 10), two submetacentric, ribosomal organizer carrier chromosomes (6 and 12), four submetacentric, heterochromatic chromosomes (16, 15, 4 and 13), four euchromatic, subtelocentric chromosomes (2, 8, 11 and 14) and four acrocentric chromosomes (3, 5, 7 and 9). The above 5 groups are based on arm ratio and are statistically supported.

The reduction in size of chromosomes during prophase results from condensation in several specific spots on the chromosomes. These usually are pericentromeric and subtelomeric regions -particularly in overlapping bands close to subtelomeric regions, although other bands sometimes play an important role in this process. Condensation can take place at the same or at different time, and can be synchronized or not. Analyzing the condensation pattern in general terms, it seems there exists a unique condensation and heterochromatization program for each chromosome. Part of the variation in the chromosome size, arm ratio and band position is explained by this phenomenon. This can be seen in fig. 26 (a and b) where alternation of periods of high variability and low variability in length of the chromosomes and arms is observed.

Chromosomes 1, 6 and 7 do not contain DAPI specific facultative heterochromatin, while chromosomes 8, 11, and 14 contain a significant proportion of this kind of heterochromatin. The latter, chromosomes 8, 11 and 14, are consistently grouped as chromosomes with less DAPI-C heterochromatin but higher DAPI-facultative and DAPI specific heterochromatin; chromosomes 10, 9, 13, 15, and 16 are characterized as very heterochromatic chromosomes and are grouped together by total DAPI heterochromatin and DAPI-C heterochromatin. Based on DAPI and C-Banding staining, the genome of honey bee contains  $47 \pm 11.5$  % heterochromatin, of which  $25 \pm$

11.12 % is constitutive and  $22 \pm 10.4$  % is facultative; 7% of facultative heterochromatin is DAPI-specific stained and 15 % of that is C- and DAPI stained. Only 3.5 % of the constitutive heterochromatin occurs in low frequency C-bands, which means that A+T richness should be lower than 21.5 % in the remaining, mostly pericentromeric heterochromatin.

As the BACs hybridized to multiple sites, assignment of the signal to the cytomolecular map was based on strength and frequency of the signals. The location and position of the BACs was compared with those published in the different version of Map Viewer at the NCBI and BeeBase web sites. The cytomolecular position of 22 BACs was well supported by data: 10 were confirmed with the last version of Map Viewer V4, with the chromosome number and position on the chromosome perfect matches to the cytomolecular map, 12 BACs were mapped using the high frequency of a signal and coincidence of chromosome or position with some of the early versions of Map Viewer, 11 BACs were mapped as suggested places based on a low frequency of the signal and coincidence with chromosome or position in earlier versions of Map Viewer, 2 BACs were placed with no coincidence with Map Viewer. Only seven BACs, 4E8, 56F6, 7B4, 6D11 (C1), 11G6 (C5), 11A3 (C3), 26F7 (C4), hybridized at a single place. The secondary signals usually hit constitutive heterochromatin, and in some cases, occurred on facultative heterochromatin. Many of the primary and secondary signals show some degree of synteny in different chromosomes, including 6B8/6B9 on chromosomes 3, 11, and 12, and 8H7/97B3 on chromosomes C4, C7, C10, and C13. The interphase nucleus, prophase and metaphase chromosomes were differentially labeled by nick banding. Prophase chromosomes show a consistent and useful banding pattern that agrees with the banding pattern generated by C-, DAPI- and R- banding. C- and DAPI inter-bands were more frequently early digested than were facultative and constitutive heterochromatin. Constitutive heterochromatin was accessible to DNase I activity throughout the time of incubation tested. However, the low frequency of these bands suggests that the DNA is less accessible than that it is in facultative and euchromatin bands.

Important advances in the karyotype characterization, chromosome identification, and FISH mapping of the honey bee have been carried out in the present study. However, additional studies are necessary not only to confirm the results and improve the maps but also to extend these studies into new areas. For this, there is a need to generate additional molecular resources for molecular mapping. It is important to identify additional cloned DNA markers specific for each honey bee chromosome and especially to identify unique sequence clones detectable by FISH techniques. Primers developed from sequence information, BACs and cosmid libraries, EST and STS from the Solignac (2004) and Hunt and Page (1995) publications can be used to generate a small library whose function will be chromosome identification and mapping reference points. Given the problems with known BACs libraries, an alternative of interest would be to generate this resource using individual chromosome microdissection and FISH-banding technology.

FISH-banding technology also can be used to generate and characterize the described heterochromatin classification and confirm the mapping location, based on the hypothesis that highly repetitive DNA equates to constitutive heterochromatin and middle repetitive heterochromatin equates to facultative heterochromatin. For highly repetitive sequences, Beye and Moritz (1994) is a very good reference, however libraries for this kind of marker can also be generated by re-association kinetics (Vogel et al., 1990; Bishop et al., 1994; Araya et al., 1997; Fisher et al., 1998); chromatin immunoprecipitation with antibodies against several histones modifications followed by ChIP-PCR kit (Biocompare Cat# IP-PCR-NFkb) is also a good alternative to quick and more specific heterochromatin amplification (Yang et al., 2005). The main goal would be to obtain at least two specific late prophase and metaphase FISHable markers for each chromosome of the honey bee, with additional markers that can be used as references for mapping and positional cloning protocols. Interspersed markers based on LTR and mariner-like elements could support the mapping and positional cloning, since these elements appear widely distributed, and are most of the time, in synteny. Especially

important is the ribosomal organizer (NOR), since accumulated evidences suggest that the ribosomal genes are not only localized in the traditionally described NOR but also scattered throughout the genome - a distribution that is shaped by transposable elements (Datson and Murray 2006). In summary, I propose for future work, to use molecular resources and available FISH technology to: (a) generate or prescreen existing BAC-library for markers useful for specific chromosome identification, (b) generate a highly and middle repetitive sequence clone library for chromosome FISH that serves as a reference for future gene mapping and positional cloning, and (c) generate for the same purpose sequences for FISH of mobile elements. Reaching these three goals would complete the foundation upon which the genome resources and sequence map of honey bee could rest and be fruitful exploited.

In order to confirm and accumulate evidences about the role of Mariner transposon-like elements in the organization of the genome of honey bee, it is important to map extensively and systematically these elements using specific TE probes (Reiter et al., 1999). Several techniques have been used in mammals (Reiter et al., 1999; Wilson et al., 2007), plants (Jacobs et al., 2004) and insects (Russel and Shukle, 1997) to reach this objectives, for example, PCR assisted by terminal inverted repeats as primers (Reiter et al., 1999; Datson and Murray, 2006), STS and EST (Liehr et al., 2001; Wilson et al., 2007) and PRINS (Reiter et al., 1999). It is now known that mariner elements are extensively represented in the honey bee genome with low divergence from the consensus sequence (HBGPC,2006). Thus, PRINS and the conserved sequence of the mariner transposase gene can be a good reference to generate the necessary probes. Specific kits for large fragment amplification with low levels of replication error are now available; therefore, clones based on PCR amplification could be a good choice for producing mariner probes.

Another chromosome characteristic that needs to taken into account is the multiple constrictions, probably inactive centromeres or neocentromeres located in chromosome 2. Apparently, these centromere-like constrictions also are present in chromosome 4, 10, 13 and 15. It would be desirable to specifically map those structures,

since they apparently are correlated with secondary signals of the BACs mapped here. Confirmation of those chromosomes structures would explain difficulties with identification of chromosomes 2, 4 and 10, and would support karyological studies about honey bee phylogeny and dynamics of africanization of European honey bees.

Banding patterns, transposon-like markers, and chromosome structures have been used in many organisms to study genetic profiles, and have been used for genetic improvement and characterization of the dynamics of the evolution of the organisms. Documentation of changes in the chromosome structure and morphology, which are based on chromosome molecular markers, have still not been used in the africanization problem of the honey bee; this field could be well supported by improved honey bee karyotype characterization and enriched cyto-molecular maps. Such changes, if demonstrated would be key to understanding widespread expression array differences between European and Afrinized bees.

## REFERENCES

- Abuin A, Hansen GM, Zambrowicz B: Gene trap mutagenesis, in Feil R, Metzger D (eds): *Conditional Mutagenesis: An Approach to Disease Models*, Handbook of Experimental Pharmacology V178, pp 129-147 (GmbH & Co. K, Springer-Verlag Berlin, Heidelberg 2007).
- Adam GV, Csondes A, Fondrk MK, Page-Jr RE: Complex social behavior derived from maternal reproductive traits. *Nature* 439:76-78 (2006).
- Adams MD, Celniker SE, Holt RA, et al.: The genome sequence of *Drosophila melanogaster*. *Science* 287:2185-2195 (2000).
- Adolph S, Hameister H: In situ nick translation of metaphase chromosomes with biotin-labeled d-UTP. *Hum Genet* 69:117-121 (1985).
- Adolph S: In situ nick translation distinguishes between C-band positive regions on mouse chromosomes. *Chromosoma* 96:102-106 (1988).
- Aljanabi M, Martinez I: Universal and rapid salt-extraction of high quality genomic DNA for PCR-based techniques. *Nucleic Acids Res* 25:4692-4693 (1997).
- Anamthawat-Jónsson K: Genetic and genomic relationships in *Leymus* Hochst. *Hereditas* 135:247-253 (2001).
- Araya J, Cano MI, Gomes HBM, Novak EM, Requena JM, Alonso C, Levin MJ, Guevara P, Ramirez JL, Franco Da Silveira J: Characterization of and interspersed repetitive DNA element in the genome of *trypanosoma cruzi*. *Parasitology* 115:563-570 (1997).
- Aurich-Costa J, Vannier A, Gregoire E, Nowak F, Cherif D: IPM-FISH, a new M-FISH approach using IRS-PCR painting probes: Application to the analysis of seven human prostate cell line. *Genes Chromosomes Cancer* 30:143-160 (2001).
- Baroux C, Spillane C, Grossniklaus U: Genomic imprinting during seed development. *Adv Genet.* 46:165-214 (2002).
- Baudry E, Kryger P, Allsop M, Koenigr N, Vauntrin D, Mougel F, Cornuet J-M, Solignac M: Whole-genome scan in thelytokous-laying workers of the Cape Honeybee (*Apis mellifera capensis*): Central fusion, reduced recombination rates and centromere mapping using half-tetrad analysis. *Genetics* 167: 243-252 (2004).

- Belmont AS: Mitotic chromosome scaffold structure: New approaches to an old controversy. *Proc Nat Acad Sci* 99:15855-15857 (2002).
- Belmont AS: Mitotic chromosome structure and condensation. *Curr. Opin in Cell Biol* 18:632-638 (2006).
- Belmont AS, Braunfeld MB, Sedat JW, Agard DA: Large-scale chromatin structural domains within mitotic and interphase chromosomes in vivo and in vitro. *Chromosoma* 98:129-143 (1989).
- Belmont AS, Dietzel S, Nye AC, Strukov YG, Tumbar T: Large-scale chromatin structure and function. *Curr Opin Cell Biol.* 11:307-311 (1999).
- Bentley JL: A fluorescence in situ hybridization approach for gene mapping and the study of nuclear organization, in: Davies KE, Tilghman SM (eds.) *Genome Analysis Vol. I: Genetic and Physical Mapping*, pp. 1-38 (Cold Spring Harbor Laboratory Press, New York, 1990).
- Berríos S, Ayarza E, Moreno M, Paulos A, Fernández-Donoso R: Non-random distribution of pericentromeric heterochromatin in meiotic prophase nuclei of mammalian spermatocytes. *Genetica* 106:187-195 (1999).
- Beye M, Gattermeier I, Hasselmann M, Gempe T, Schioett M, Baines JF, Schlipalius D, Mougél F, Emore C, Rueppell O, Sirviö A, Guzman-Novoa E, Hunt G, Solignac M, Page Jr E: Exceptionally high levels of recombination across the honey bee genome. *Genome Res* 16:1339-1344 (2006).
- Beye M, Moritz RFA: A centromere-specific probe for fluorescence in situ hybridization on chromosomes of *Apis mellifera* L. *Apidology* 25: 322-326 (1994).
- Beye M, Moritz RFA: Characterization of honeybee (*Apis mellifera* L.) chromosomes using repetitive DNA probes and fluorescence in situ hybridization. *Heredity* 86:145-150 (1995).
- Beye M, Moritz RFA: In situ hybridization of rDNA on chromosomes of the honeybee, *Apis mellifera* L. *Experientia* 49:337-338 (1993).
- Beye M, Moritz, RFA: Mapping the sex locus of the honeybee (*Apis mellifera*) *Naturwissenschaften* 83:424-426 (1996).
- Bianchi D, Bianchi NO, Pantelias GE, Wolff S: The mechanism and pattern of banding induced by restriction endonucleases in human chromosomes. *Chromosoma* 91:131-136 (1985).



- Bickmore WA, Craig JM: Chromosome Bands: Patterns in the Genome. (Landes Bioscience, New York : Chapman & Hall, Austin, Tex, 1997).
- Biémont C, Vieira C: Junk DNA as an evolutionary force. *Nature* 443:521-524 (2006)
- Biémont C, Vieira C: What transposable elements tell us about genome organization and evolution: The case of *Drosophila*. *Cytogenet Genome Res* 110:25-34 (2005).
- Biliński SM, Bilińska B: A new version of the Ag-NOR technique. A combination with DAPI staining. *Histochem J* 28:651-656 (1996).
- Bishop RP, Sohanpal BK, Morzaria SP: Cloning and characterisation of a repetitive DNA sequence from *Theileria mutans*: Application as a species-specific probe. *Parasitol Res.* 80:33-41 (1994).
- Boggs BA, Chinault AC: Analysis of DNA replication by fluorescence in situ hybridization. *Methods: A companion to Methods in Enzymology* 13:259-270 (1997).
- Bongiorni S, Cintio O, Prantera G: The relationship between DNA methylation and chromosome imprinting in the coccid *Planococcus citri*. *Genetics* 151:1471-1478 (1998).
- Bongiorni S, Pasqualini B, Taranta M, Singh PB, Prantera G: Epigenetic regulation of facultative heterochromatinisation in *Planococcus citri* via the Me(3)KH3-HP1-Me(3)K20H4 pathway. *J Cell Sci* 120:1072-1080 (2007).
- Bottari B, Ercolini D, Gatti M, Neviani E: Application of FISH technology for microbiological analysis: Current state and prospects. *Appl Microbiol Biotechnol* 73:485-494 (2006).
- Brown SE, Severson DW, Smith LA, Knudson DL: Integration of the *Aedes aegypti* mosquito genetic linkage and physical maps. *Genetics* 157:1299-1305 (2001).
- Bullerdiek J, Dittmer J, Faehre A, Bartnicktzke S: An improved method for in situ nick translation of human chromosomes with biotin 11-labelled dUTP detected by biotinylated alkaline phosphatase. *Cytobios* 45:35-43 (1986).
- Bullerdiek J, Dittmer J, Faehre A, Bartnicktzke S: Mechanism of in situ nick translation of chromosomes using restriction endonucleases. *Cytobios* 47:33-44 (1985).

- Burnette JM, Miyamoto-Sato E, Schaub MA, Conklin J, Lopez AJ. Subdivision of large introns in *Drosophila* by recursive splicing at nonexonic elements. *Genetics* 170:661-674 (2005).
- Carvalho C, Pereira HM, Ferreira J, Pina C, Mendonça D, Rosa AC, Carmo-Fonseca M: Chromosomal G-dark bands determine the spatial organization of centromeric heterochromatin in the nucleus. *Mol Biol Cell* 12:3563-3572 (2001).
- Caspersson TO: The William Allan Memorial Award address: The background for the development of the chromosome banding techniques. *Am. J. Hum Genet* 44:441-451 (1989).
- Chadwick BP, Willard HF: Multiple spatial distinct types of facultative heterochromatin on the human inactive X chromosomes. *Proc Nat Acad Sci* 101:17450-17455 (2004).
- Chan QWT, Howes CG, Foster LG: Quantitative comparison of caste differences in honeybee hemolymph. *Mol Cell Proteomics* 5.12:2252-2262 (2006).
- Chandra HS, Brown SW: Chromosome imprinting and the mammalian X chromosome. *Nature* 253:165-168 (1975).
- Charlesworth B: Patterns in the genome. *Curr Biol* 4:182-184 (1994).
- Chaves R, Adegas F, Santos S, Heslop-Harrison JS, Guedes-Pinto H: In situ hybridization and chromosome banding in mammalian species. *Cytogenet Genome Res* 96:113-116 (2002).
- Cheng Z, Buell CR, Wing RA, Jiang J: Resolution of fluorescence *in-situ* hybridization mapping on rice mitotic prometaphase chromosomes, meiotic pachytene chromosomes and extended DNA fibers. *Chromosome Res* 10:379-387 (2002).
- Chuang ChH, Belmont AS: Close encounters between active genes in the nucleus. *Genome Biol* 6:237 (2005).
- Claussen U: Chromosomics. *Cytogenet genome Res* 111:101-106 (2005).
- Cook PR: A chromomeric model for nuclear and chromosome structure. *J. Cell Sci.* 108:2927-2935 (1995).
- Corona M, Estrada E, Zurita M: Differential expression in mitochondrial genes between queens and workers during caste determination in honeybee *Apis mellifera*. *J. Exp Biol* 202:929-938 (1999).

- Corradini N, Rossi F, Giordano E, Caizzi R, Verní F, Dimitri P: *Drosophila melanogaster* as a model for studying protein-encoding genes that are resident in constitutive heterochromatin. *Heredity* 98:3-12 (2007).
- Craig JM, Bickmore WA: Chromosome bands – flavours to savour. *Bioessay* 15:349-354 (1993).
- Crain WR, Davidson EH, Britten RJ: Contrasting patterns of DNA sequence arrangement in *Apis mellifera* (Honeybee) and *Musca domestica* (housefly). *Chromosoma* 59:1-12 (1976).
- Crawford GE, Davis S, Scacheri PC, Renaud G, Halawi MJ, Erdos MR, Green R, Meltzer PS, Wolfsberg TG, Collins FS: DNase-chip: A high-resolution method to identify DNase I hypersensitive sites using tiled microarrays. *Nat Methods* 3:503-509 (2006).
- Cremer T, Cremer C: Chromosomes territories, nuclear architecture and gene regulation in mammal cells. *Nat Rev Genet* 2:292-301 (2001).
- CSHL/WUGSC/PEB Arabidopsis Sequencing Consortium: The complete sequence of a heterochromatic island from a higher eukaryote. *Cell* 100:377-386 (2000).
- Cuvier O, Hart CM, Käs E, Laemmli UK: Identification of multicopy chromatin boundary element at the borders of silenced chromosomal domains. *Chromosoma* 110:519-531 (2002).
- Datson PM, Murray BG: Ribosomal DNA locus evolution in *Nemesis*: Transposition rather than structural rearrangement as the key mechanism? *Chrom Res* 14:845-857 (2006).
- Davison EH, Rast JP, Oliveri P, Ransik A, Calestani C, Yuh C-H, Minokawa T, Amore G, Hinman V, Arenas-Mena C, Otim O, Brown CT, Livi CB, Lee PY, Revilla R, Rust AG, Pan ZJ, Schilstra MJ, Clarke PJC, Arnone MI, Rowen L, Cameron RA, McClay DR, Hood L, Bolouri H: A genomic regulatory network for development. *Science* 295:1669-1678 (2002).
- de la Casa-Esperon E, Sapienza C: Natural selection and the evolution of genome imprinting. *Ann Rev Genet* 37:349-370 (2003).
- de la Torre J, Sumner AT : Analysis of chromosomes with restriction endonucleases and Dnase hypersensitivity, in: Gosden JR (ed): *Chromosome Analysis Protocols. Methods in Molecular Biology V 29*, pp 123-139 (Humana Press, Totowa, NJ, 1994).

- de la Torre J, Sumner AT, Gosalvez J, Stuppia L: The distribution of genes on human chromosomes as studied by in situ nick translation. *Genome*, 35:890-894 (1992).
- Dietzel S, Belmont A: Reproducible but dynamic positioning of DNA in chromosomes during mitosis. *Nature Cell Biology* 3:767-771 (2001).
- Dimitri P: Constitutive heterochromatin and transposable elements in *Drosophila melanogaster*. *Genetica* 10:85-93 (1997).
- Dimitri PHM, Berloco M, Wakimoto BT: Cis-effects of heterochromatin on heterochromatic and euchromatic gene activity in *Drosophila melanogaster*. *Genetics* 140(3):1033-45 (1995).
- Dong F, McGrath JM, Helgeson JP, Jiang J: The genetic identity of alien chromosomes in potato breeding lines revealed by sequential GISH and FISH analysis using chromosome-specific cytogenetic DNA markers. *Genome* 44:729-734 (2001).
- Drapeau MD, Albert S, Kucharski R, Prusko C, Maleszka R: Evolution of the yellow/major royal jelly protein family and the emergence of social behavior in honeybees. *Genome Res* 16: 1385-1394 (2006).
- Drouaud J, Camilleri C, Bouguignon P-Y, Canaguier A, Bérard A, Vezon D, Giancola S, Brunel D, Colot V, Prum B, Quensneville H, Mézard C: Variation in crossing-over rates across chromosome 4 of *Arabidopsis thaliana* reveals the presence of meiotic recombination 'hot spots'. *Genome Res.* 16:106-114 (2006).
- Duret L., Marais G., and Biémont C: Transposons but not retrotransposons are located preferentially in regions of high recombination rate in *Caenorhabditis elegans*. *Genetics* 156: 1661-1669 (2000).
- Eastmond DA, Schuler M, Rupa DS: Advantages and limitations of using fluorescence in situ hybridization for the detection of aneuploidy in interphase human cells. *Mutation Res* 348:153-162 (1995).
- Ebert PR, Hileman JP, and Nguyen UT: Primary sequence, copy number, and distribution of mariner transposons in the honey bee. *Insect Mol Biol* 4:69-78 (1995).
- Elgin CR: Anatomy of hypersensitivity sites. *Nature* 309:213-214 (1984).
- Emerson BM, Lewis CD, Felsenfeld G: Interaction of specific nuclear factors with the nuclease-hypersensitive region of the chicken adult beta-globin gene: Nature of the binding domain. *Cell* 41:21-30 (1985).

- Evans JD, Aronstein K, Chen YP, Hetru C, Imler J-L, Jiang H, Kanost M, Thompson G, Zhou Z, Hultmark D: Immune pathways and defense mechanisms in honey bees, *Apis mellifera*. *Insect Mol Biol* 15:645–656 (2006).
- Evans JD, Gundersen-Rindal DG: Beenomes to *Bombyx*: Future directions in applied insect genomics. *Genome Biol.* 4:107 (2003).
- Evans JD, Wheeler DE: Differential gene expression between developing queens and workers in the honey bee, *Apis mellifera*. *Proc Nat Acad Sci USA* 96:5575-5580 (1999).
- Evans JD, Wheeler DE: Expression profiles during honey bee caste determination. *Genome Biol* 2:1-6 (2000).
- Fahrenhorst H: Nachweis übereinstimmender chromosomen-Zahlen (n=16) bei allen 4 *Apis*-Arten. *Apidiologie* 8:89-100 (1977).
- Fan QQ, Petes TD: Relationship between nuclease-hypersensitive sites and meiotic recombination hot spot activity at the HIS4 locus of *Saccharomyces cerevisiae*. *Mol Cell Biol* 16:2037-2043 (1996).
- Ferreira J, Paoletta G, Ramos C, Lamond A: Spatial organization of large-scale chromatin domains in the nucleus: A magnified view of single chromosome territories. *J Cell Biol* 139:1597-1610 (1997).
- Festenstein R, Tolaini M, Corbella P, Mamalaki C, Parrington J, Fox M, Miliou A, Jones M, Kioussis D: Locus control region function and heterochromatin-induced position effect variegation. *Science* 271:1123-1125 (1996).
- Field LM, Lykot F, Mandrioli M, Prantera G: DNA methylation in insects. *Insect Mol Biol* 13:109-115 (2004).
- Foster HA, Bridger JM: The genome and the nucleus: A marriage made by evolution genome organization and nuclear architecture. *Chromosoma* 114:212-229 (2005).
- Franck P, Garney L, Loiseau A, Oldroyd BP, Hepburn HR, Solignac M, Corneut JM: Genetic diversity of the honeybee in Africa: Microsatellite and mitochondrial data. *Heredity* 86:420-430 (2001).
- Freanz PF, Armstrong S, de Jong JH, Parnell LD, van Drunen C, Dean C, Zabel P, Bisseling T, Jones GH: Integrated cytogenetic map of chromosome arm 4S of *A. thaliana*: Structural organization of heterochromatic knob and centromere region. *Cell* 100:367-376 (2000).

- Frydrychová R, Grossman P, Trubac P, Vitková M, and Marec F: Phylogenetic distribution of TTAGG telomeric repeats in insects. *Genome* 47:163-178 (2004).
- Fu H, Zheng Z, Dooner HK: Recombination rates between adjacent genic and retrotransposon regions in maize vary by 2 orders of magnitude. *Proc Natl Acad Sci USA* 99:1082-1087 (2002).
- Gartler SM: The chromosome number in humans: A brief history. *Nat Rev Genet* 7:655-600 (2006).
- Gazit B, Cedar H, Lerer J, Voss R: Active genes are sensitive to deoxy-ribonuclease I during metaphase. *Science* 217:648-650 (1982).
- Geigl JB, Uhrig S, Speicher MR: Multiplex-fluorescence *in situ* hybridization for chromosome karyotyping. *Nat Protocols* 1:1172-1184 (2006).
- Gilbert N, Boyle S, Sutherland H, de las Heras J, Allan J, Jenuwein T, Bickmore WA: Formation of facultative heterochromatin in the absence of HP1. *EMBO J* 22:5540-5550 (2003).
- Gorelick R: Transposable elements suppress recombination in all meiotic eukaryotes, including automitotic ancient asexual: A reply to Schön and Martens. *J Nat Hist* 37:903-909 (2003).
- Granau C, Buard J, Brun M-E, De Sario A: Mapping of the juxtacentromeric heterochromatin-euchromatin frontier of human chromosome 21. *Genome Res* 16:1198-1207 (2006).
- Gregory PG, Evans JD, Rinderer T, and Guzman L: Conditional immune-gene suppression of honeybees parasitized by *Varroa* mites. *J Insect Sci* 5:1-7 (2005).
- Grewal SI, Moazed D: Heterochromatin and epigenetic control of gene expression. *Science* 301:798-902 (2003).
- Grewal SI, Rice JC: Regulation of heterochromatin by histone methylation and small RNAs. *Curr Opin Cell Biol* 16:230-238 (2004).
- Grewal SI, Jia S: Heterochromatin revisited. *Nat Rev Genet* 8:35-45 (2007).
- Gross DS, Garrard WT: Nuclease hypersensitive sites in chromatin. *Ann Rev Biochem* 57:159-197 (1988).

- Gueiros-Filho FJ, Beverley SM: Trans-kingdom transposition of the *Drosophila* element *mariner* within the protozoan *Leishmania*. *Science* 276:1716-1719 (1997).
- Guzzo F, Campagnari E, Levi M: A new FISH protocol with increased sensitivity for physical mapping with short probes in plants. *J Exp Bot* 51: 965-970 (2000).
- Gvozdev VA, Alatortsev VE, Aravin AA, Kalmykova AI, Kogan GL, Lavrov SA, Naumova NM, Nurminskii DI, Rasheva VI, Tolchikov EV: Heterochromatin: Molecular evolution and effects of gene location in *Drosophila melanogaster*. *Mol Biol (Mosk)* 33:14-25 (1999).
- Hart CM, Laemmli UK: Facilitation of chromatin dynamics by SARs. *Curr Opin Genet & Dev.* 8:519-525 (1998).
- Harper LC, Cande WZ: Mapping a new frontier: Development of integrated cytogenetic maps in plants. *Funct Integr Genomics* 1:89-98 (2000).
- Herrick G, Seger J: Imprinting and paternal genome elimination in insects, in Ohlsson R (Ed): *Genomic Imprinting: An Interdisciplinary Approach*, pp. 41–71 (Springer-Verlag, Berlin/Heidelberg, Germany, 1999)
- Hiraoka Y, Minden JS, Swedlow JR, Sedat JW, Agard DA: Focal points for chromosome condensation and decondensation revealed by three-dimensional *in vivo* time-lapse microscopy. *Nature* 342:293-296 (1989).
- Holmquist GP: Chromosome bands, their chromatin flavors and their functional features. *Am J Hum Genet* 51:17-37 (1992).
- Hoshiba H, Duchateau MJ, Velthuis HHW: Diploid males in the Bumble bee *Bombus terrestris* (Hymenoptera) karyotype analysis of diploid females, diploid males and haploid males. *Jpn J Ent* 63:203-207 (1995)
- Hoshiba H, Imai HT: Chromosome evolution of bees and wasps (Hymenoptera: Apocrita) on the basis of C-banding pattern analysis. *Jpn J Ent* 61:465-492 (1993).
- Hoshiba H, Kusanagi A: Karyological study of honey bee. *J Apic Res.* 17:105-109 (1978).
- Hoshiba H, Okada I, Kusanagi A: The diploid drone of *Apis cerana japonica* and its chromosomes. *J Apic Res* 20:143-147 (1981).
- Hoshiba H, Okada I: G-banding analyses of male chromosomes in *Apis cerana* and *Apis mellifera linguistica*. *Apidiologie* 17:101-106 (1986).

- Hoshiba H: The C-banding analysis of the diploid male and female honeybee (*Apis mellifera*). Proc Japan Acad 60(B):238-240 (1984a).
- Hoshiba H: Karyotype and banding analyses of haploid males of the honey bee (*Apis mellifera*). Proc Japan Acad 60(B):122-124 (1984b).
- Hosking RA, Nelson CR, Berman BP, Lavery TR, George RA, Ciesiolka L, Naeemuddin M, Arenson AD, Durbin J, David RG, Tabor PE, Bailey MR, DeShazo R, Catanese J, Mammoser A, Osoegawa K, de Jong PJ, Celniker SE, Gibbs RA, Rubin GM, Scherer SE: A BAC-based physical map of the major autosomes of *Drosophila melanogaster*. Science 287:2271-2274 (2000).
- Hosking RA, Smith CD, Carlson JW, Carvalho AB, Halpern A, Kaminker JS, Kennedy C, Mungall CJ, Sullivan BA, Sutton GG, Yasuhara JC, Wakimoto BT, Myers EW, Celniker SE, Rubin GM, Kerpen GH: Heterochromatic sequences in a *Drosophila* whole-genome shotgun assembly. Genome Biol 3: 1-16 (2002).
- Houben A, Wako T, Furushima-Shimogawara R, Presting G, Künzel G, Schubert I, Fukui K: The cell cycle dependant phosphorylation of hystone H3 is correlated with the condensation of plant mitotic chromosomes. Plant Journal 18:675-679 (1999).
- Howell WM, Black DA: Controlled silver staining of nucleolus organizer regions with a protective colloidal developer: A 1 step method. Experientia 36:1014-1015 (1980).
- Hunt GJ, Page EJr: Linkage map of the honey bee, *Apis mellifera*, based on RAPD markers. Genetics 139:1371-1382 (1995).
- ISCN: An international system for human cytogenetics nomenclature: High resolution banding: Birth defects. Cytogenet Cell Genet 31:1-23 (1981).
- ISCN: An international system for human cytogenetics nomenclature, in: Shaffer LG, Tommerup N, (eds) ISCN 2005: The long-awaited new edition, 130p (S. Karger, Cytogenetic and Genome Research, Copenhagen 2005).
- Ito T: Role of histone modification in chromatin dynamics. J Biochem 141:609-614 (2007).
- Jablonka E, Goiten R, Marcus M, Cedar H: DNA hypomethylation causes an increase in DNase I sensitivity and an advance in the time of replication of the entire inactive X chromosome. Chromosome 93:152-156 (1985).
- Jacobs G, Dechyeva D, Menzel G, Dombrowski C, Schmidt T: Molecular characterization of *Vulmar1*, a complete *mariner* transposon of sugar beet and



diversity of *mariner*- and *En/Spm*-like sequences in the genus *Beta*. *Genome* 47:1192-1201 (2004)

Jiang F, Katz RL: Use of interphase fluorescence in situ hybridization as a powerful diagnostic tool in cytology. *Diagnostic Mol. Pathol* 11:47-57 (2002).

Jiang J, Gill BS: Current status and the future of fluorescence in situ hybridization (FISH) in plant genome research. *Genome* 49:1057-1068 (2006).

Jinno Y, Yun K, Nishiwaki K, Kubota T, Ogawa O, Reeve AE, Niikawa N: Mosaic and polymorphic imprinting of the WT1 gene in humans. *Nat Genet* 6:305-309 (1994).

John B, and Miklos GLG: *The Eukaryotic genome in development and evolution*. 420p (Allen & Unwin Hyman, London, 1988).

Kamissago M, Kimura M, Furutani Y, Furutani M, Takao A, Momma K, Matsuoka R: Assignment of human desert hedgehog gene (DHH) to chromosome band 12q13.1 by in situ hybridization. *Cytogenet Genome Res* 87:117-118 (1999).

Karem BS, Goiten R, Daimond G, Cedar H, Marcus M: Mapping of DNase I sensitive regions on mitotic chromosomes. *Cell* 38:493-499 (1984).

Karem BS, Goiten R, Richler C, Marcus M, Cedar H: In situ nick translation distinguishes between active and inactive X chromosomes. *Nature* 304:88-90 (1983).

Kaufman TC, Severson DW, Robinson GE: The *Anopheles* genome and comparative insect genomics. *Science* 298:97-98 (2002).

Kaye JS, Pratt-Kaye S, Bellard M, Dretzen G, Bellard F, Chambon P: Steroid hormone dependence of four DNase I-hypersensitive regions located within the 7000-bp 5'-flanking segment of the ovalbumin gene. *EMBO J.* 5:277-285 (1986).

Kearney L: Multiplex-FISH (M-FISH): Technique, development and applications. *Cytogenet. Genome Res.* 114:189-198 (2006).

Killian JK, Nolan CM, Wyle AA, Li T, Vu TH : Divergent evolution in M9P/IGF2R imprinting from the Jurassic to the Quaternary. *Hum. Mol. Biol.* 10:1721-1728 (2001).

Kim JM, Vanguri S, Boeke JD, Gariel A, Voytas DF: Transposable elements and genome organization: A comprehensive survey of retrotransposons revealed by the

complete *Saccharomyces cerevisiae* genome sequence. *Genome Res* 8:464-478 (1998).

Kim J-S, Childs KL, Islam-Faridi N, Menz MA, Klein RR, Klein PE, Price HJ, Mullet JE, Stelly DM: Integrated karyotyping of sorghum by in situ hybridization of landed BACs. *Genome* 45:402-412 (2003).

Kim J-S, Klein PE, Klein RR, Price HJ, Mullet JE, Stelly DM: Molecular cytogenetic maps of sorghum linkage groups 2 and 8. *Genetics* 169:955-965(2005a).

Kim J-S, Islam-Faridi MN, Klein PE, Stelly DM, Price HJ, Klein RR, Mullet JE: Comprehensive molecular cytogenetic analysis of sorghum genome architecture: Distribution of euchromatin, heterochromatin genes and recombination in comparison to rice. *Genetics* 171:1963-1976 (2005b).

Kim J-S, Klein PE, Klein RR, Price HJ, Mullet JE, Stelly DM: Chromosome identification and nomenclature of *Sorghum bicolor*. *Genetics* 169:1169-1173 (2005c).

Kireeva N, Lakonishok M, Kireev T, Hirano T, Belmont AS: Visualization of early chromosome condensation: A hierarchical folding, axial glue model of chromosome structure. *J Cell Biol* 166:775-785 (2004).

Konev AY, Yan CM, Acevedo D, Kennedy K, Ward E, Lim A, Tickoo S, Karpen GH: Genetics of P-elements transposition into *Drosophila melanogaster* centric heterochromatin. *Genetics* 165:2039-2053 (2003).

Kouprina N, Larionov V: Selective isolation of mammalian genes by TAR cloning, in Boyle, A.L. (ed.): *Current Protocols in Human Genetics*, pp. 5.17.1–5.17.21 (John Wiley and Sons, Inc, New York 1999)

Kouprina N, Leem S-H, Solomon G, Ly A, Koriabine M, Otstot J, Pak E, Dutra A, Zhao S, Barret JC, Larionov V: Segments missing from the draft human genome sequence can be isolated by transformation-associated recombination cloning in yeast. *EMBO Reports* 4:257-262 (2003).

Krustaleva LI, Kik C: Localization of single-copy T-DNA insertion in transgenic shallots (*Allium cepa*) by using ultra-sensitive FISH with tyramide signal amplification. *Plant J.* 25:699-707 (2001).

Kucharski R, Maleszka R: A royal jelly protein is expressed in a subset of Kenyon cells in the mushroom bodies of the honey bee brain. *Naturwissenschaften* 85:343-346 (1998).

- Labrador M, Corces VG: Setting the boundaries of chromatin domains and nuclear organization. *Cell* 111:151-154 (2002).
- Lakhotia SC: Epigenetics of heterochromatin. *J Biosci* 29:219-224 (2004).
- Lalande M: Parental imprinting and human disease. *Annu Rev Genet* 30:173-195 (1997).
- Lamb JC, Yu W, Han F, Birchler JA: Plant chromosomes from end to end: Telomeres, heterochromatin and centromeres. *Curr Opin Plant Biol* 10:116-122 (2007).
- Lampe DJ, Witherspoon DJ, Soto-Adames F, Robertson HM: Recent horizontal transfer of *Mellifera* subfamily *Mariner* transposon into insect lineages representing four different orders show that selection acts only during horizontal transfer. *Mol Biol Evol* 20:554-562 (2003).
- Lander EA, Linton LM, Birren B, et al. (256 co-authors): Initial sequencing and analysis of the human genome. *Nature* 409:860–921 (2001).
- Leitão A, Chaves R, Matias D, Joaquim S, Ruano F, Guedes-Pinto H: Restriction enzyme digestion chromosome banding on two commercially important venerid bivalve species: *Ruditapes decussates* and *Cerastoderma edule*. *J Shellfisheries Res* 25:857-863 (2006).
- Leitão A, Chaves R, Santos S, Guedes-Pinto H, Boudry P: Restriction enzyme digestion chromosome banding in *Crassostrea* and *Ostrea* species: Comparative karyological analysis within Ostreidae. *Genome* 37:781-788 (2004).
- Levan A, Fredga K, and Sandberg AA: Nomenclature for centromeric position on chromosomes. *Hereditas* 52:201-220 (1964).
- Levsky JM, Singer RH: Gene expression and the myth of the average cell. *Trends Cell Biol.* 13:4 -6 (2003).
- Li G, Sudlow G, Belmont AS: Interphase cell cycle dynamics of a late-replicating, heterochromatic homogenously staining region: Precise choreography of condensation/decondensation and nuclear positioning. *J Cell Biol* 140:975-989 (1998).
- Liehr T, Heller A, Starke H, Claussen U: Fluorescence in situ hybridization (FISH) banding methods - applications in research and diagnostic. *Expert Review of Molecular Diagnostics* 2:217-225 (2002).

- Liehr T, Reiter LT, Lupski JR, Murakami T, Claussen U, Rautenstrauss B: Regional localization of 10 mariner transposon-like ESTs by means of FISH-evidence for a correlation with fragile sites. *Mammalian Genome* 12:326-328 (2001).
- Liehr T, Starke H, Heller A, Kosyakova N, Mrasek K, Gross M, Karst C, Steinhäuser U, Hunstig F, Fickelscher I, Kuechler A, Trifonov V, Romanenko SA, Weise A: Multicolor fluorescence in situ hybridization (FISH) applied to FISH-banding. *Cytogenet Genome Res* 114: 240-244 (2006).
- Liehr T, Claussen U: Multicolor FISH approaches for the characterization of human chromosomes in clinical genetics and tumor cytogenetics. *Curr Genom* 3:213-235 (2002).
- Lloyd V: Parental imprinting in *Drosophila*. *Genetica* 109:35-44 (2002).
- Loebel DA, Johnston PG: Analysis of DNase I sensitivity and methylation of active and inactive X chromosomes of kangaroos (*Macropus robustus*) by in situ nick translation. *Chromosoma* 102:81-87 (1993).
- Lorite P, García MF, Carrillo JA, Palomeque T: Restriction endonuclease chromosome banding in *Tapinoma nigerrimum* (Hymenoptera, Formicidae). *Hereditas* 131:197-2001 (1999a).
- Lorite P, García MF: Patterns of DNase I sensitivity in the chromosomes of the ant *Tapinoma nigerrimum* (Hymenoptera, Formicidae). *Genetica* 106:247-250 (1999b).
- Lowe CB, Bejarano G, Haussler D: Thousands of human mobile element fragments undergo strong purifying selection near developmental genes. *Proc Natl Acad Sci USA* 104:8005-8010 (2007).
- Luo S, Hall AE, Hall SE, Preuss D: Whole-genome fractionation rapidly purifies DNA from centromeric regions. *Nature Methods* 1:67-71 (2004).
- Lupski JR, Stankiewicz P: Genomic disorders: Molecular mechanisms for rearrangements and conveyed phenotypes. *PLOS Genet.* 1:627-633 (2005).
- Maddox PS, Portier N, Desai A, Oegema K: Molecular analysis of mitotic chromosome condensation using a quantitative time-resolved fluorescence microscopy assay. *Proc Natl Acad Sci USA* 103:15097-15102 (2006).
- Maison C, Almouzni G: HP1 and the dynamics of heterochromatin maintenance. *Nat Rev Mol Cell Biol* 5:296-304 (2004).

- Maisson C, Bailly D, Peters AHFM, Quivy J-P, Roche D, Taddei A, Lachner M, Jenuwein T, Almouzni G: Higher-order structure in pericentromeric heterochromatin involves distinct pattern of histone modification and an RNA component. *Nat Genet* 30:329-334 (2002).
- Malik HS, Henikoff S: Phylogenomics of the nucleosome. *Nat Struct Biol* 10:882-891 (2003).
- Mandrioli M, Manicardi GC: Analysis of insect holocentric chromosomes by atomic force microscopy. *Hereditas* 138:129-132 (2003).
- Manicardi GC, Mandrioli M, Bizzarro D, Bianchi U: Patterns of DNase I sensitivity in the holocentric chromosomes of the Aphid *Megoura viciae*. *Genome* 41:169-172 (1998).
- Marko JF, Poirier MG: Micromechanics of chromatin and chromosomes. *Biochem. Cell Biol.* 8:209-220 (2003).
- Marygold SJ, Cohelo CM, Leever SJ: Genetic analysis of RpL38 and RpL5, two minute genes located in the centric heterochromatin of chromosome 2 of *Drosophila melanogaster*. *Genetics* 169:683-695 (2005).
- McClintock, B: The order of the genes C, Sh, and Wx in *Zea mays* with reference to a cytologically known point in the chromosome. *Proc Nat Acad Sci USA.* 17:485-91 (1931).
- Meaburn KJ, Mistelli T: Chromosome territories. *Nature* 445:379-381 (2007).
- Mendstrand P, van de Lagemaat LN, Dunn CA, Landry J-R, Svenback D, Mager DL: Impact of transposable elements on the evolution of mammalian gene regulation. *Cytogenet Genome Res* 110:342-352 (2005).
- Messing J, Dooner HK: Organization and variability of the maize genome. *Current Opin Plant Biol* 9:157-163 (2006).
- Michener ChD: The importance of Bees, in Michener ChD (ed): *The Bees of the World*, pp 3 (The John Hopkins University Press, Baltimore, Maryland, 2000).
- Millot E, Strouboulis J, Trimborn T, Wigerde M, de Boer E, Langeveld A, Tan-Un K, Vergeer W, Yannoutsos N, Grosveld F, Fraser N: Heterochromatin effects on the frequency and duration of LCR-mediated gene transcription. *Cell* 87:105-114 (1996).

- Mizrahi A, Lensky Y: Bee products: Properties, applications and apitherapy, 288p (Plenum Press, New York 1997).
- Moffat AS: Transposons help sculpture a dynamic genome. *Science* 289:1455-1457 (2000).
- Moter A, Göbel UB: Fluorescence in situ hybridization (FISH) for direct visualization of microorganisms. *J. Microbiol. Methods* 41:85-112 (2000).
- Murer-Orlando ML, Peterson AC: In situ nick translation of human and mouse chromosomes, detected with biotinylated nucleotide. *Exp. Cell Res.* 157:322-334 (1985).
- Murray MG, Kenard WC: Altered chromatin conformation of the higher plant gene phaseolin. *Biochemistry* 23:4225-4232 (1984).
- Natarajan AT, Boei JJWA: Formation of chromosome aberrations: Insights from FISH. *Mutation Res* 544:299-304(2003).
- Nezer C, Moreaus L, Brouwers B, Coppieeters W, Detilleux J: An imprinted QTL with major effect on muscle mass and fat deposition maps to the IGF2 locus in pigs. *Nat Genet.* 21:155-156 (1999).
- Nishihara H, Smit AAF, Okada N: Functional noncoding sequences derived from SINEs in the mammalian genome. *Genome Res* 16:864-874 (2006).
- Noma K, Cam HP, Maraja RJ, Grewal SI: A role for TFIIC transcription factor complex in genome organization. *Cell* 125:859-872 (2006).
- Nowak SJ, Corces VG: Phosphorilation of histones H3: A balancing act between chromosome condensation and transcriptional activation. *Trends in Genetics* 20:214-220 (2004).
- Nur U: Evolution of unusual chromosome systems in scale insects (Coccoidea: Homoptera), in: RL Blackman, GM Hewitt, M Ashburner (eds.): *Insect Cytogenetics*, 10:97-117 (Symposia of the Royal Entomological Society of London: number ten, Royal Entomological Society, Blackwell Scientific Publications, Oxford 1980).
- O'Donnell KA, Boeke KD: Mighty Piwis defend the germline against genome intruders. *Cell* 129:37-44 (2007).

- O'Neil MJ, Ingram RS, Vrana PB, Tilghman SM: Allelic expression of IGF2 in marsupials and birds. *Dev Genes Evol* 210:18-20 (2000).
- Oleszczuk S, Zimny J, Bednarek PT: The application of AFLP method to determine the purity of homozygous lines of barley (*Hordeum vulgare* L.). *Cellular & Mol Biol Letters* 7:777-783 (2002).
- Olszewska MJ, Gernand D, Sakowicz T: Methylation-sensitive restriction endonuclease digestion patterns revealed in *Vicia faba* L. chromosomes by in situ nick-translation. *Folia Histochem Cytobiol.* 37(4):267-74 (1999).
- Ostashevsky JA: Polymer model for the structural organization of chromatin loops and minibands in interphase chromosomes. *Mol Biol Cell* 9:3031–3040 (1998).
- Pamilo P, Viljakainen L, Vihavainen A: Exceptionally high density of NUMTs in the honey bee genome. *Mol Biol Evol* 24:1340-1346 (2007).
- Paul AL, Vasil V, Vasil IK, Ferl RJ: Constitutive and anaerobically induced DNase-I-hypersensitivity sites in the 5' region of the maize *Adh1* gene. *Proc Natl Acad Sci USA* 84:799-803 (1987).
- Petrov DA, Lozovskaya ER, Hartl DL: High intrinsic rate of DNA loss in *Drosophila*. *Nature* 384:346-346 (1996).
- Petrov DA, Sangster TA, Johnston JS, Hartl DL, Shaw KL: Evidence for DNA loss as a determinant of genome size. *Science* 287:1060-1062 (2000).
- Pinkel DT, Straume T, Gray JU: Cytogenetic analysis using quantitative, high sensitivity, fluorescence hybridization. *Proc Natl Acad Sci USA* 85:2934-2938 (1986).
- Queller DC: Theory of genomic imprinting conflict in social insects. *BMC Evol Biol* 3:15 (2003).
- Raman R, Singh AP, Nanda I: DNase I nick translation in situ on meiotic chromosomes of the mouse *Mus musculus*. *J Cell Sci* 90:629-634 (1988).
- Ravenel JD, Broman KW, Perlman EJ, Niemitz EL, Jayawardena TM, Bell DW, Heber DA, Uejima H, Feinberg AP: Loss of imprinting of Insulin-Like Growth Factor-II (IGF2) gene in distinguishing specific biologic subtypes of Wilms Tumor. *J Natl Cancer Institute* 93:1698-1703 (2001).

- Reiter LT, Liehr T, Rautenstrauss B, Robertson HM, Lupski R: Localization of mariner DNA transposons in the human genome by PRINS. *Genome Res.* 9:839-843 (1999).
- Richer CL, Droulin R, Murer-Orlando M, Jean P: High-resolution ideogram of giemsa R-banded human prophase chromosomes. *Can J Genet Cytol* 25:642-650 (1983).
- Richler C, Uliel E, Kerem B-S, Wahrman J: Regions of active heterochromatin conformation in 'inactive' male meiotic sex chromosomes of the mouse. *Chromosoma* 95:167-170 (1987).
- Rizzon C, Marais G, Gouy M, Biémont C: Recombination rate and the distribution of transposable elements in the *Drosophila melanogaster* genome. *Genome Res* 12:400-407 (2002).
- Robinson GE, Ben-Shahar Y: Social behavior and comparative genomics: New genes or new gene regulation? *Genes, Brain and Behavior* 1:197-203 (2002).
- Robinson GE, Grozinger CM, Whitfield CW: Sociogenomics: Social life in molecular terms. *Nat Rev Genet* 6:257-270 (2005).
- Rocha MP, Cruz MP, Fernandes A, Waldschmidt AM, Silva-Junior JC, Pompolo SG: Longitudinal differentiation in *Melipona mandacaia* (Hymenoptera, Meliponini) chromosomes. *Hereditas* 138:133-137 (2003).
- Rocha MP, Pompolo SG, Abdala J, Fernandes A, De Oliveira LAC: DNA characterization and karyotypic evolution in the bee genus *Melipona* (Hymenoptera, Meliponini). *Hereditas* 136:19-27 (2002).
- Rocha MP, Pompolo SG: Karyotypes and heterochromatin variation (C-bands) in *Melipona* species (Hymenoptera, Apidae, Meliponinae). *Genet Mol Biol* 21:1415-4757 (1998).
- Roche Applied Science: Nonradioactive In Situ Hybridization Application Manual. 2nd ed (Roche Diagnostics, Mannheim, Germany 2005).
- Roshchina MP, Naumova NM, Devin AB, Gvozdev VA: Heterochromatic stellate repeats of *Drosophila* and the reporter gene silencing in the yeast *Saccharomyces cerevisiae*. *Dokl Biochem Biophys* 401:122-124 (2005).
- Rossi F, Moschetti R, Caizzi R, Corradini N, Dimitri P: Cytogenetic and molecular characterization of heterochromatin gene models in *Drosophila melanogaster*. *Genetics* 175:595-607(2007).



- Russel VW, Shukle RH: Molecular and cytological analysis of *mariner* transposon from Hessian fly. *J. Heredity* 88:72-76 (1997).
- Sabo PJ, Kuehn MS, Thurman R, Johnson BE, Johnson E, Cao H, Yu M, Rosenzweig E, Goldy J, Haydock A, Weaver M, Shafer A, Lee K, Neri F, Humbert R, Singer MA, Richmond TA, Dorschner MO, McArthur M, Hawrylycz M, Green RD, Navas PA, Noble WS, Stamatoyannopoulos JA: Genome-scale mapping of DNase I sensitivity in vivo using tiling DNA microarrays. *Nat Methods* 3:511-518 (2006).
- Sahara K, Marec F, Traut W: TTAGG telomeric repeats in chromosomes of some insects and other arthropods. *Chromosome Res* 7:449-460 (1999).
- Sahasrabudde CG, Pathak, Hsu TC: Responses of the mammalian metaphase chromosomes to endonuclease digestion. *Chromosoma* 69:331-338 (1978).
- Saitoh Y, Laemmli UK: Metaphase chromosome structure: Bands arise from a differential folding path of the high AT-rich scaffold. *Cell* 76:609-622 (1994).
- Sallam FAE, El Ela RGA: Cytogenetics analysis of metaphase chromosomes from pupal testes of four mosquito species using fluorescence in situ hybridization technique (FISH). *World J. Microbiol & Biotechnol* 21:515-518 (2005).
- SanMiguel P, Gaut BS, Tikhonov A, Nakajima Y, Bennetzen JL: The paleontology of intergene retrotransposons of maize. *Nat. Genet.* 20: 43-45 (1998).
- Schön I, Martens K: Are ancient asexuals less burdened? Selfish DNA, transposons and reproductive mode. *J Nat History* 36:379-390 (2002).
- Schotta G, Ebert A, Reuter G: SU(VAR)3-9 is a conserved key function in heterochromatic gene silencing. *Genetica.* 117:149-158 (2003).
- Schubert I, Franz PF, Fuchs J, De Jong JH: Chromosome painting in plants. *Methods Cell Sci* 23: 57-69 (2001).
- Schulze SR, McAllister BF, Sinclair DAR, Fitzpatrick KA, Marchetti M, Pimpinelli S, Honda BM: Heterochromatic genes in drosophila: A comparative analysis of two genes. *Genetics* 173:1433-1445 (2006).
- Seabright M: A rapid banding technique for human chromosomes. *Lancet* 2:971-971 (1971).
- Seeley TD, Visscher PK: Group decision making in nest-site selection by honey bees. *Apidologie* 35:101-116 (2004).

- Seeley TD: The honey bee colony as a super organism. *American Scientist* 77:546-553 (1989).
- Sen P, Sharma T: Characterization of G-banded chromosomes of the Indian muntjac and progression of banding pattern through different stages of condensation. *Cytogenet. Cell Genet.* 39:145-149 (1985).
- Seneer AW, Palmiter RD: Expression of the mouse metallothionein I gene alters the nuclease hypersensitivity of its 5' regulatory region. *Cold Spring Harb Symp Quant Biol* 47:539-547 (1983).
- Senger G, Weimer J, Claussen U, Chudoba I: Reverse chromosome painting, in Wegner RD (ed): *Diagnostic Cytogenetic: Spring Verlag Lab Manual*, pp 357-375 (Spring-Verlag, Berlin 1998).
- Sentis C, Santos J, Robledo M, Fernández-Piqueras J: Differential sensitivity of constitutive heterochromatin and facultative heterochromatin in Orthopteran chromosomes to digestion by DNase I. *Genetica* 81:229-235 (1990).
- Severson DW, Knudson DL, Soares MB, Loftus BJ: *Aedes aegypti* genomics. *Insect Biochem Mol Biol.* 34:715-721 (2004).
- Shermoen AW, Beckendorf SK: A complex of interacting DNase I-hypersensitive sites near the *Drosophila* glue protein, Sgs4. *Cell* 29:601-607 (1982).
- Shi S, Calhoun HC, Xia F, Li J, Le L, Li WX: JAK signaling globally counteracts heterochromatic gene silencing. *Nat Genet* 38:1071 – 1076 (2006).
- Shoguchi E, Ikuta T, Yashizaki F, Satou Y, Satoh N, Asano K, Saiga H, Nishikata T: Fluorescent *in situ* hybridization to ascidian chromosomes. *Zool. Sci* 21:153-157 (2004).
- Shoguchi E, Kawashima T, Nishida-Umehara C, Matsuda Y, Satoh N: Molecular cytogenetic characterization of *Ciona intestinalis* chromosomes. *Zool Sci* 22:511-516 (2005).
- Shoguchi E, Kawashima T, Satou Y, Hamaguchi M, Sin-I T, Kohara Y, Putnam N, Rokhsar DS, Satoh N: Chromosomal mapping of 170 BAC clones in the ascidian *Ciona intestinalis*. *Genome Res* 16:297-303 (2007).
- Sloter ED, Lowe X, Moore DH, Nath J, Wyrobek AJ: Multicolor FISH analysis of chromosomal breaks, duplications, deletions, and numerical abnormalities in the sperm of healthy men. *Am J Gent* 67:862-872 (2000).

- Smith JS, Costello JF: A broad band of silence. *Nat Genet* 38:504-506 (2006).
- Solignac M, Vautrin D, Baudry E, Mougél F, Loiseau A, Cornuet JM: A microsatellite-based linkage map of the honey bee, *Apis mellifera* L. *Genetics* 167:253-262 (2004).
- Solignac M, Vautrin E, Loiseau A, Cornuet J-MD., Baudry E: Five hundred and fifty microsatellite markers for the study of the honey bee genome (*Apis mellifera* L.). *Mol Ecol Notes* 3:307-311 (2003).
- Solignac M, Zhang L, Mougél F, Li B, Vautrin D, Monnerot M, Cornuet J-M, Worley KC, Weinstock GM, Gibbs RA: The genome of *Apis mellifera*: Dialog between linkage mapping and sequence assembly. *Genome Biol.* 8:403 (2007).
- Song J, Bradeen JM, Naess SK, Helgeson JP, Jiannng J: BIBAC and TAC clones containing potato genomic DNA fragments larger than 100 kb are not stable in *Agrobacterium*. *Theor Appl Genet* 107:958-964 (2003).
- Song J, Dong F, Lilly JW, Stupar RM, Jiang J: Instability of bacterial artificial chromosome (BAC) clones containing tandemly repeated DNA sequence. *Genome* 44:463-469 (2001).
- Spector DL: The dynamics of chromosome organization and gene regulation. *Annu Rev Biol* 72:573-608 (2003).
- Sperling K, Kerem BS, Goiten R, Kottush V, Cedar H, Marcus M: DNase I sensitivity in facultative and constitutive heterochromatin. *Chromosoma*, 93:38-42 (1985).
- Stack SM, Clark CR: Chromosome polarization and nuclear rotation in *Allium cepa* roots. *Cytologia* 39:553-560 (1974).
- Stanimirovic Z, Stevanovic J, Andjelkovic M: Chromosomal diversity in *Apis mellifera carnica* from Serbia. *Apidology* 36:31-42 (2005).
- Straub T, Becker PB: Dosage compensation: The beginning and end of generalization. *Nat Rev Genet* 8:47-57 (2007).
- Sullivan BA, Blower MD, Karpen GH: Determining centromere identity: Cyclical stories and forking paths. *Nat Rev Genet* 2:584-596 (2001).
- Sumner AT: A simple technique for demonstrating centromeric heterochromatin. *Exptl Cell Res* 75:304-306 (1972).

- Sumner AT: Chromosome banding and identification absorption staining, in Gosden JR (ed): Chromosome Analysis Protocols: Methods in Molecular Biology V 29, pp. 59-81 (Humana Press Inc, Totowa, NJ 1994).
- Sumner AT: Chromosomes: Organization and Function. (Blackwell Scientific, Oxford 2003).
- Takehisa S: Negative heterochromatin, positive heterochromatin, and chromosome condensation in *Vicia faba*. *Experientia* 32:303-304 (1976).
- Tares S, Cornuet J-M, Abad P: Characterization of unusual conserved *Alu I* highly reiterated DNA sequence family from the honey bee, *Apis mellifera*. *Genetics* 134:1149-1174 (1993).
- Taucher S, Kurtaran A, Leimer M, Angelberger P, Pangerl T, Beck M, Gnant M, Jakesz R, Virgolini I: Validation of VIP and somatostatin receptor scanning in primary breast cancer. *Eur J Nucl Med* 23:1094A (1996).
- Tautz D, Hancock JM, Webb DA, Tautz C, Dover GA: Complete sequences of rRNA genes of *Drosophila melanogaster*. *Mol Biol Evol* 5:585-589 (1989).
- The Honeybee Genome Sequencing Consortium (HGSC): Insights into social insects from the genome of the honeybee *Apis mellifera*. *Nature* 443: 931-949 (2006).
- The Honeybee Genome Sequencing Consortium (HGSC): Insights into social insects from the genome of the honeybee *Apis mellifera*. *Nature* 443: 931-949 (2006).  
Supplementary Information.
- The International Human Genome Mapping Consortium: Initial sequencing and analysis of the human genome. *Nature* 409:860-922 (2001).
- The National Cancer Institute Breast and Prostate Cancer Cohort Consortium: A candidate gene approach to searching for low-penetrance breast and prostate cancer genes. *Nat Rev Cancer* 5:977-985 (2005).
- Thon G, Bjerling P, Bunner CM, Verhein-Hansen J: Expression –state boundaries in the mating-type region of fission yeast. *Genetics* 161:611-622 (2002).
- Tomkins JP, Luo M, Fang GC, Main D, Goicochea JL, Atkins M, Frish DA, Page RE, Guzman-Novoa E, Yu Y, Hunt G, and Wing A: New genomic resources for the honey bee (*Apis mellifera* L.): Development of a deep-coverage BAC library and a preliminary STC database. *Genet Mol Res* 1:306-316 (2002).

- Tönnies H, Stumm M, Wegner R-D, Chudoba I, Kalscheuer V, Neitzel H: Comparative genomic hybridization for the analysis of different chromosome imbalances detected in conventional cytogenetic diagnostics. *Cytogenet Cell Genet* 93:188-194 (2001).
- Topp CN, Dawe RK: Reinterpreting pericentromeric heterochromatin. *Curr Opin Plant Biol* 9:647-653 (2006).
- Torti C, Gomulski M, Moralli D, Raimondi E, Robertson HM, Capy P, Gasperi G, Malacrida AR: Evolution of different subfamilies of mariner elements within the medfly genome inferred from abundance and chromosomal distribution. *Chromosoma* 108:523-532 (2000).
- Trask B: Fluorescence in situ hybridization, in: Birren B, Eric D, Hieter P, Klapholz S, Myers RM, Riethman H, Roskams J (eds): *Genome Analysis: A Laboratory Manual V4: Mapping Genomes*, pp 303-406 (Cold Spring Harbor Laboratory Press, Cold Spring Harbor, NY 1980).
- Traut W, Sahara K, Otto TD, Marec F: Molecular differentiation of sex chromosomes probed by comparative genomic hybridization. *Chromosoma* 108:173-180 (1999).
- Tuan D, London IM: Mapping of DNase I-hypersensitive sites in the upstream DNA of human embryonic  $\epsilon$ -globin gene in K562 leukemia cells. *Proc Natl Acad Sci USA* 81:2718-2722 (1984).
- Tulin AV, Naumova NM, Aravin AA, Gvozdev VA: Repeated, protein-encoding heterochromatic genes cause inactivation of a juxtaposed euchromatic gene. *FEBS Letters* 425:513-6 (1998).
- Tulin T, Stewart D, Spradling AC: The *Drosophila* heterochromatic gene encoding poly(ADP-ribose) polymerase (PARP) is required to modulate chromatin structure during development. *Genes Dev.* 16:2108-2119 (2002).
- Vogel M, Muller N, Gottstein B, Flury K, Eckert J, Seebeck T: *Echinococcus multilocularis*: Characterization of a DNA probe. *Acta Trop.* 48:109-116 (1990).
- Wang Y, Jordan M, Jones PL, Maleszka R, Ling X, Robertson HM, Mizzen CA, Peinado MA, and Robinson GE: Functional CpG Methylation system in a social insect. *Science* 314:645-647 (2006).
- Whitfield CW, Band MR, Bonaldo MF, Kumar CG, Liu L, Pardinas JR, Robertson HM, Soares MB, Robinson GE: Annotated expressed sequence tags and cDNA

- microarrays for studies of brain and behavior in the honey bee. *Genome Res* 12:555-566 (2002).
- Wienberg J: Fluorescence in situ hybridization to chromosomes as a tool to understand human and primate genome evolution. *Cytogenet Genome Res* 108:139-160 (2005).
- Wilson MH, Coates CJ, George Jr AL: *PiggyBac* transposon-mediated gene transfer in human cells. *Mol. Therapy* 15:139-145 (2007).
- Wright SI, Agrawal N, Bureau TE: Effects of recombination rate and gene density on transposable element distributions in *Arabidopsis thaliana*. *Genome Res* 13:1897-1903 (2003).
- Yan CM, Dobie KW, Le HD, Konev AY, Karpen GH: Efficient recovery of centric heterochromatin P-element insertion in *Drosophila melanogaster*. *Genetics* 161:217-229 (2002).
- Yang F, Graphodatsky AS, O'Brien CM, Colabella A, Solanky N, Squire M, Sargan DR, Ferguson-Smith MA: Reciprocal chromosome painting illuminates the history of genome evolution of the domestic cat, dog and human. *Chromosome Res* 8:393-404 (2000).
- Yang H, Jin W, Nagaki K, Tian S, Ouyang S, Buell CR, Talbert PB, Henikoff S, Jiang J: Transcription and histone modifications in the recombination-free region spanning a rice centromere. *Plant Cell* 17:3227-3238 (2005).
- Yasuochi Y, Ashakumary LA, Baba K, Yoshido A, Sahara K: A second-generation integrated map of the silkworm reveals synteny and conserved gene order between Lepidopteran insects. *Genetics* 173:1319-1328 (2006).
- Yasuhara J C, Wakimoto BT: Oxymoron no more: The expanding world of heterochromatin genes. *Trends Genet* 22:330-338 (2006).
- Yasuhara JC, Marchetti M, Fanti L, Pimpinelli S, Wakimoto BT: A strategy for mapping the heterochromatin of chromosome 2 of *Drosophila melanogaster*. *Genetica* 117:217-226 (2003).
- Yoshido A, Bando H, Yasukochi Y, Sahara K: The *Bombix mori* karyotype and the assignment of linkage groups. *Genetics* 170:675-685 (2005).
- Yunis JJ: Mid-prophase human chromosome. The attainment of 2000 bands. *Hum Genet* 56:293-298 (1981).

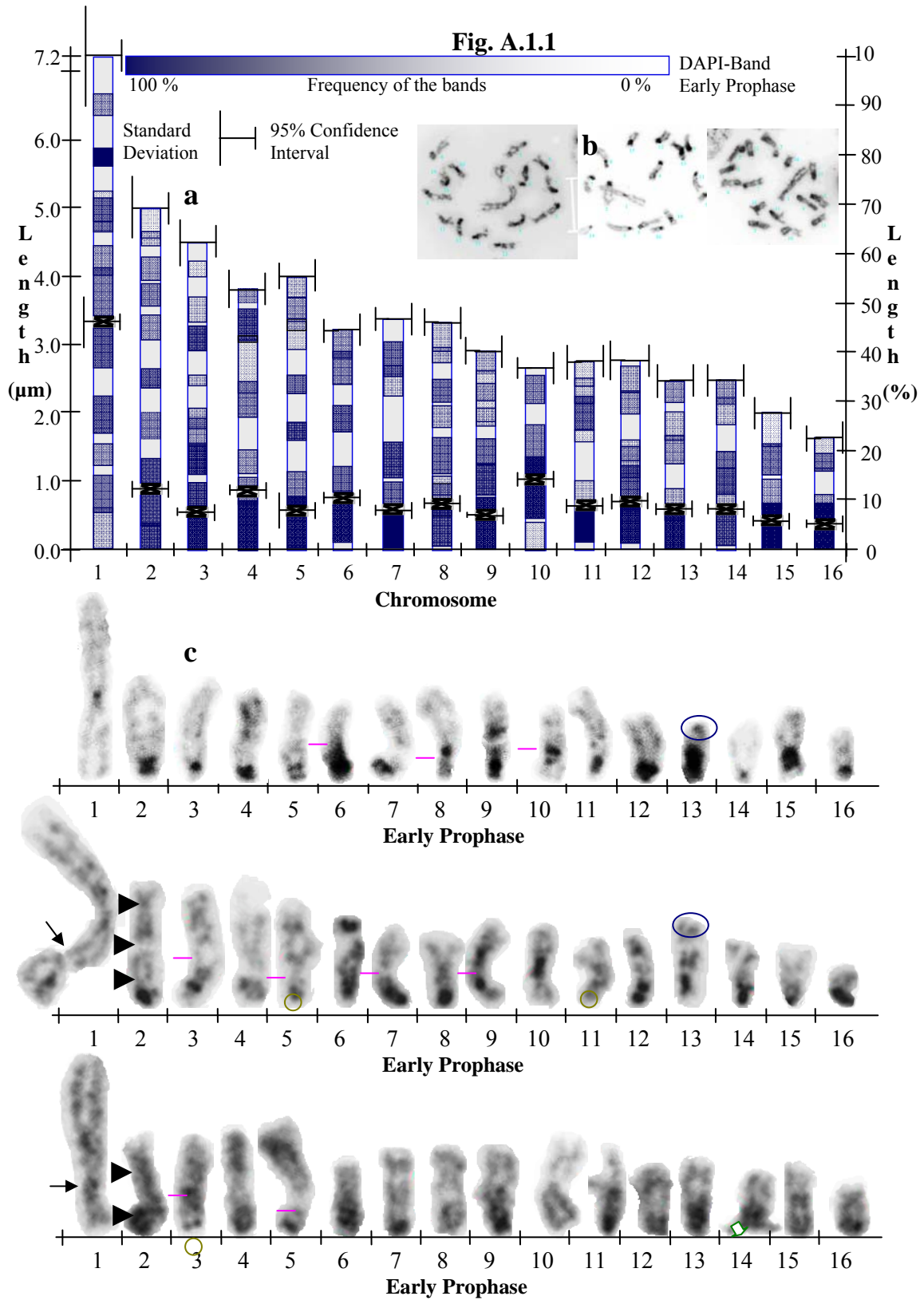
Zinn K, Maniatis T: Detection of factors that interact with the human  $\beta$ -interferon regulatory region in vivo by DNase I footprinting. *Cell* 45:611-618 (1986).

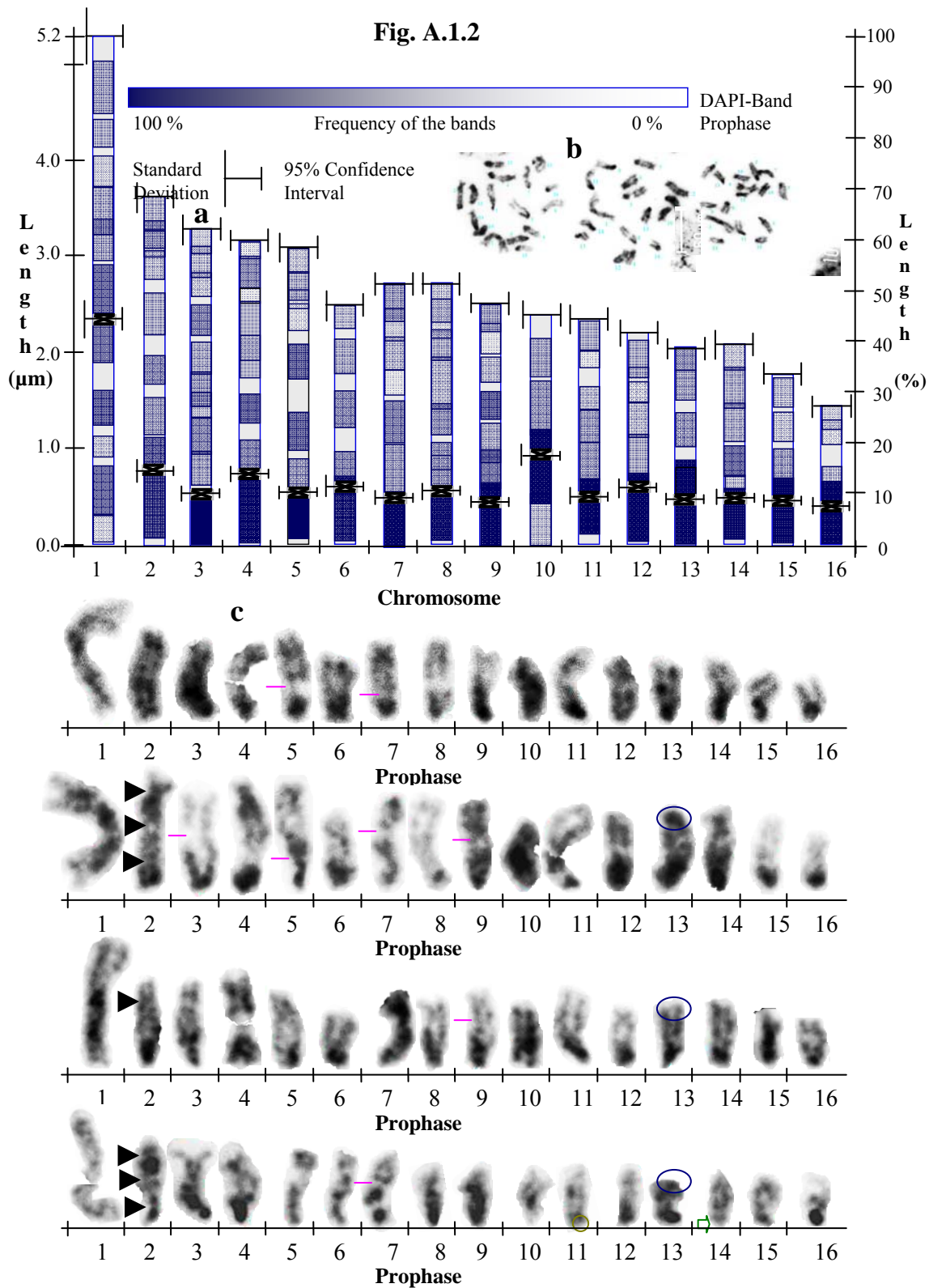
Zwick, MS, Hanson RE, McKnight TD, Islam-Faridi MH, Stelly DM, Wing RA, Price HJ: A rapid procedure for the isolation of Cot-1 DNA from plants. *Genome* 40:138-142 (1997).

**APPENDIX**

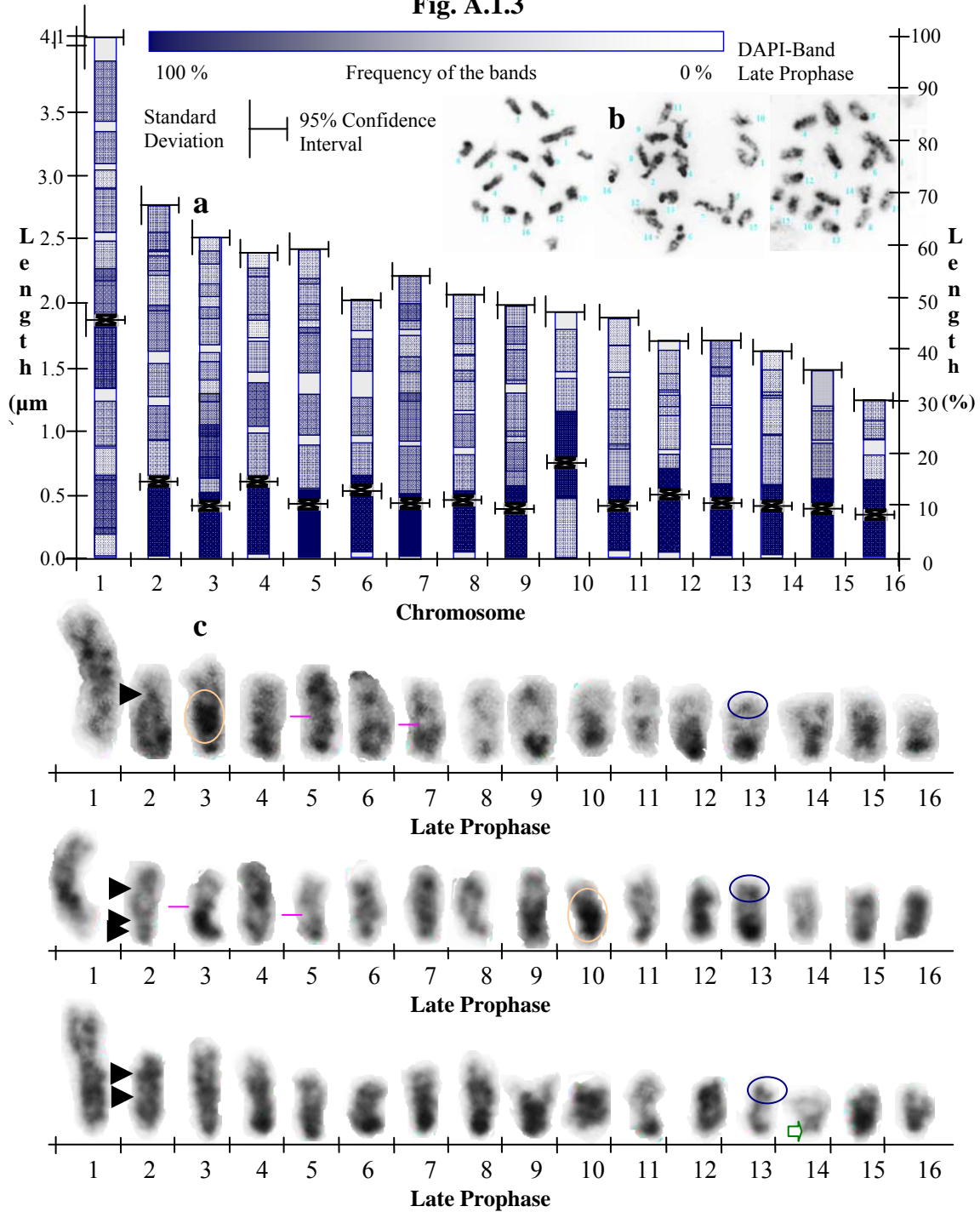


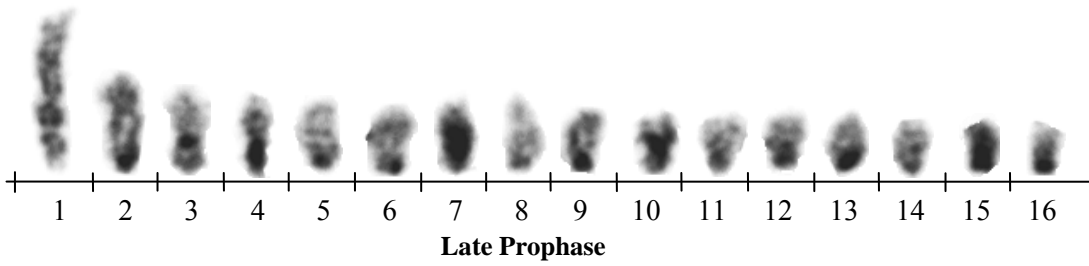
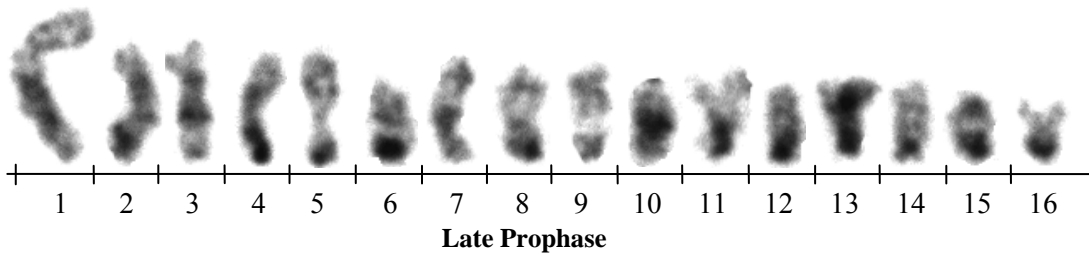
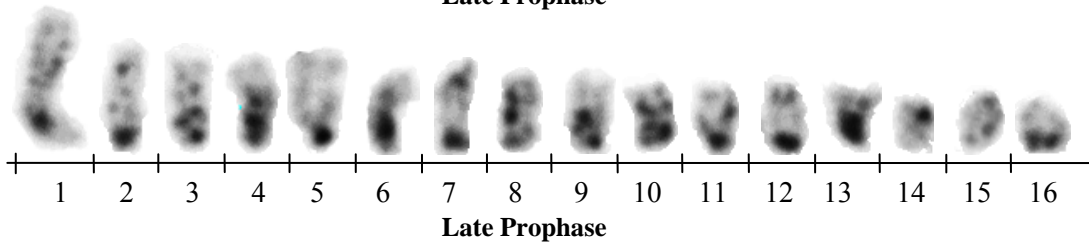
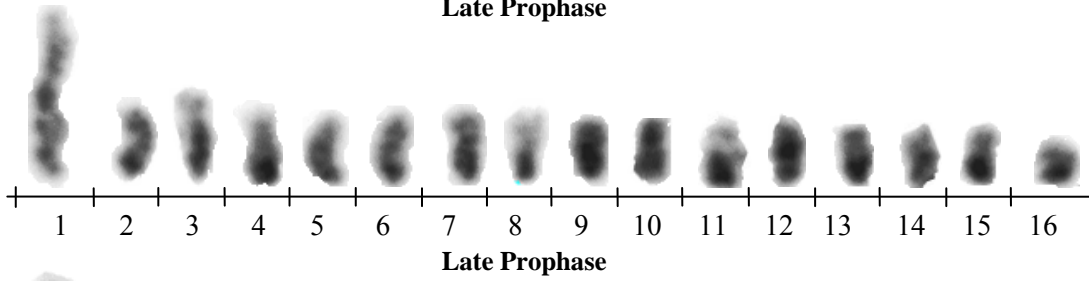
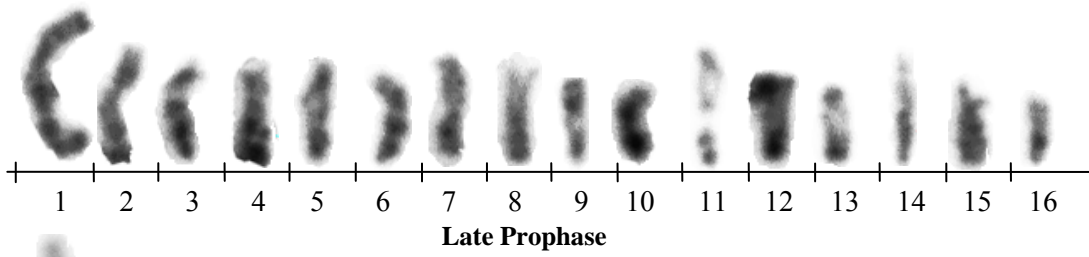
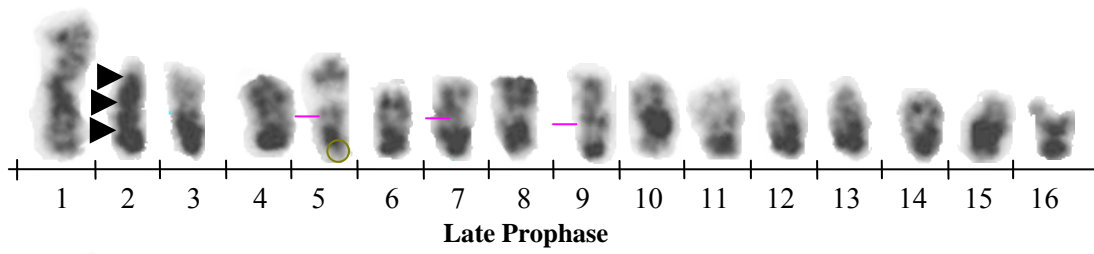
**Fig. A.1.** Ideogram (a), chromosome spread (b), and karyogram (c) of honey bee karyotype stained with 4' 6-diamidino-2phenylindole (DAPI). (A.1.1) Prophase I (PI) with landmarks: the break point in C1 (arrow), C2 shows three constrictions - the distal and proximal ones are the possible neocentromeres (arrow head), C3, C5 and C11 each show a satellite band that is frequently lost (circle), C14 shows the large p-euchromatic band where a FISH signal of 57E10 (Royal Jelly marker) was frequently observed, which frequently de-attached and was lost or observed as a mini-chromosome, arrows on cC3, C5, C7 and C9 show the large constrictions in these chromosomes, and the oval on C13 shows the distal C-band. (A.1.2) Prophase II (PII). The same characteristics are highlighted on the chromosomes but the frequency at which they were observed was lower, although the banding provides added contrast, the increased number of bands makes the correct identification of each chromosome difficult, the most heterochromatic chromosomes at this stage were C9, C10 and C13; in the ideograms C8, C11 and C14 seem to be very heterochromatic because of the relatively large number of the bands, but the light blue color indicates that those bands are infrequently observed. (A.1.3) Prophase III or late prophase (PIII). Most of the chromosomes have a reduced number of bands, but the bands are larger: C1, C2, C3, C7 are better banded at this stage. The smallest chromosomes (13-15) are poorly banded at this stage but the patterns more contrasting. Additional karyograms are added to show the variability in the chromosomes at this stage. (A.1.4) Prophase IV or Pre-Metaphase (PIV), the banding at this stage is poorly represented: In most of the cases the bands are few because the small bands have overlapped and provide few contrasting patterns. The banding pattern observed at this stage are the probable banding pattern at metaphase, however, the high condensation of the metaphase chromosomes reduces the frequency of bands observed at metaphase, even so, some chromosomes can be identified with some frequency as C1, C3, C5, C7, the rest of chromosomes are very difficult to identify, the most difficult are C6, C10 and C12; notice the configuration of C10, which is like a sub-acrocentric chromosome. In a very few cases, the sizes of the chromosomes are useful for chromosome identification at PIV. These ideograms were constructed with 11 prophase I, 37 prophase II, 68 prophase III and 50 pre-metaphase spreads

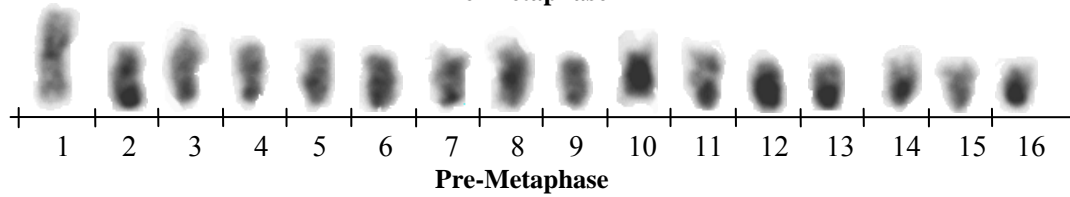
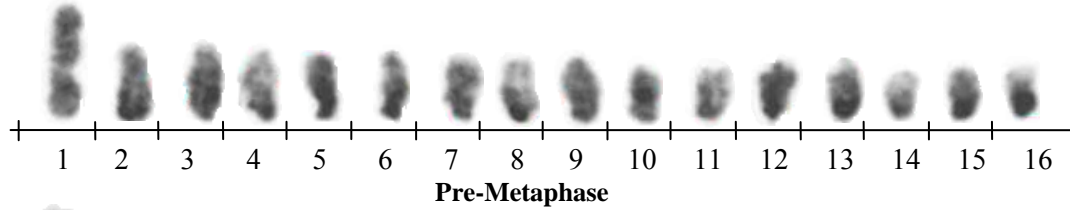
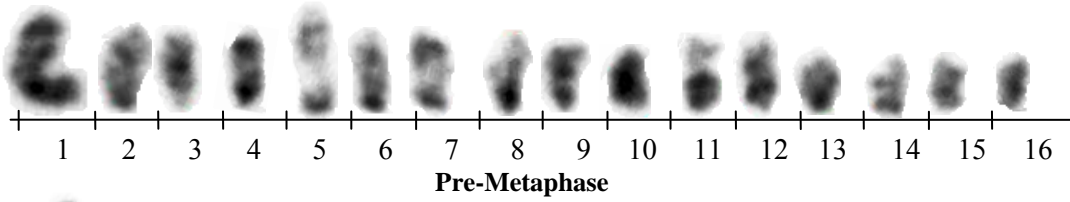
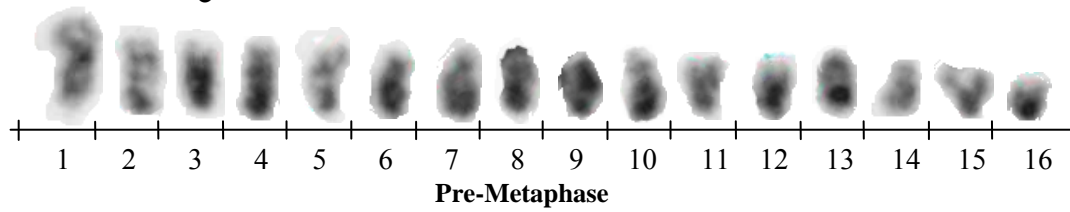
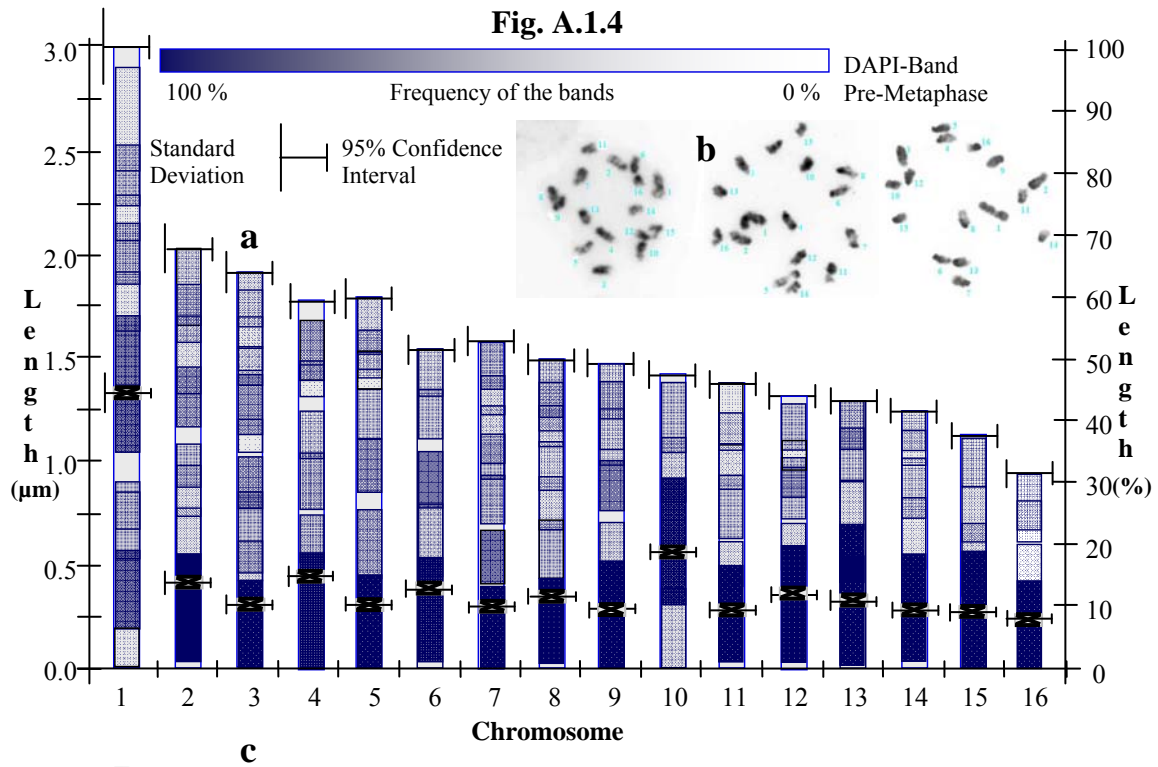




**Fig. A.1.3**









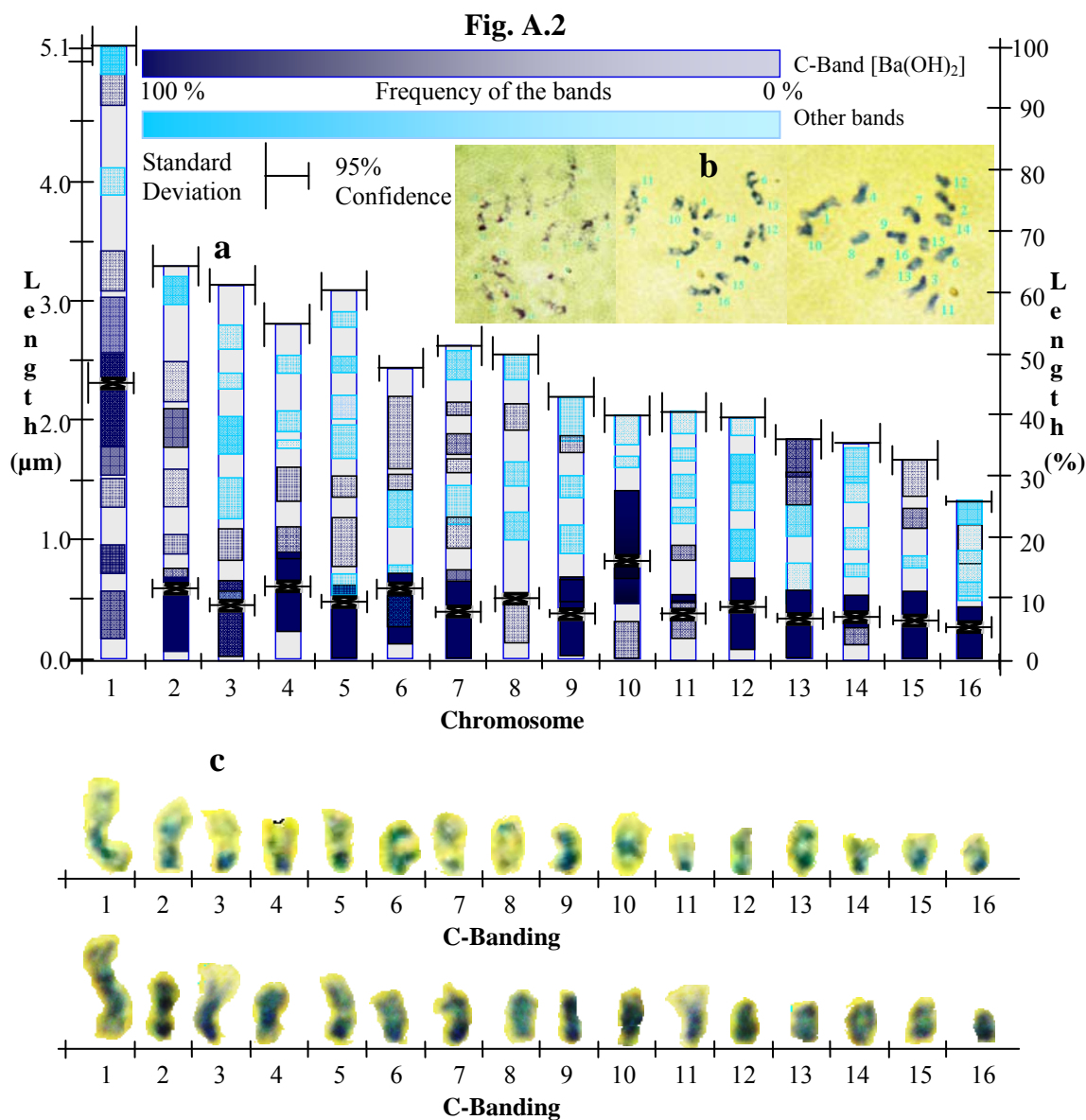


**Fig. A.2.** Ideogram (a), chromosome spread (b), and karyogram (c) of the honey bee karyotype stained with Ba(OH)<sub>2</sub> after the method of Sumner (1972). Notice the variation in the chromosome staining, which is dependant on the chromosome stage - the earlier the prophase the better contrast in the band staining. Notice that C8, C11 and C14 are the most euchromatic chromosomes because of the shorter and lower frequency pericentromeric heterochromatin band. Chromosomes 1, 2, 7, 10 and 13 seem to be the most heterochromatic. They usually show no pericentromeric constitutive heterochromatin. As in DAPI-banding, notice the p-euchromatic band on C4, C6, C8, C11, C12 and C14. This ideogram was constructed based on 3 prophase I, 4 prophase II, 4 prophase III, and 2 pre-metaphase spreads.

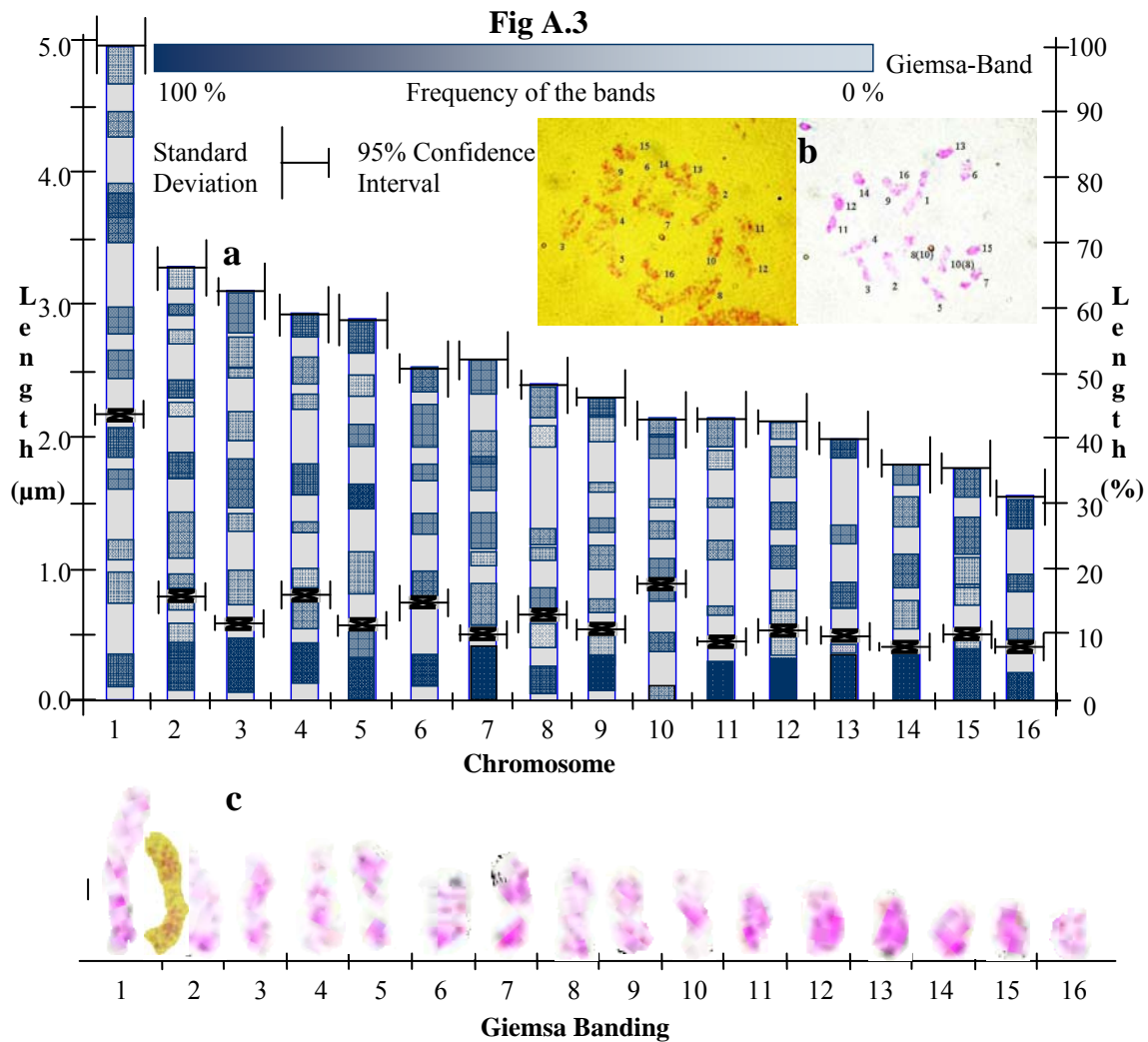


**Fig. A.3.** Ideogram (a), chromosome spread (b), and karyogram (c) of the honey bee karyotype stained with giemsa. The banding generated by giemsa was not clear enough to construct a highly detailed map. The banding seems to be similar to that generated by  $\text{Ba}(\text{OH})_2$  and DAPI. One distinctive characteristic was that most of the bands are doublets. In some cases, as in C1, C3, C6, C11, and C16, the pericentromeric bands were not clearly stained. In this experiment, pre-metaphase and metaphase chromosomes were not clearly banded. This ideogram was constructed based on 2 prophase I, 2 prophase II, 6 prophase III, and 0 pre-metaphase.



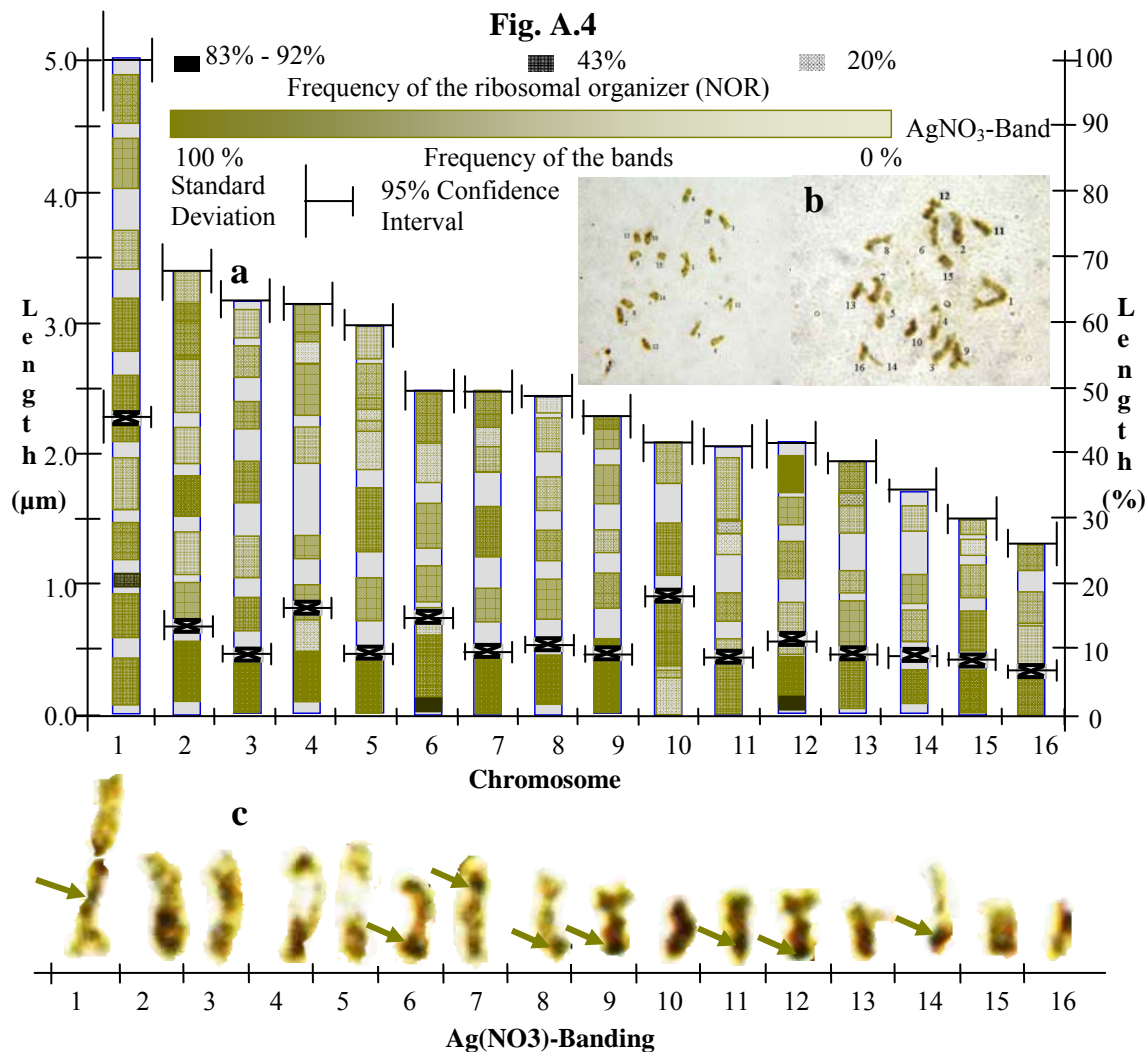


**Fig. A.4.** Ideogram (a), chromosome spread (b), and karyogram (c) of the honey bee karyotype stained with AgNO<sub>3</sub> after the method of Howell and Black (1980). The main purpose of this method is to detect the nucleolus organizer (NOR). As in the FISH method, sometimes many places are observed as in this case on chromosomes 1, 6, 7, 8, 9, 11, 12 and 14. However, the strong and consistent signals are only on C1, C6, and C12. The banding pattern, although characteristic for this method, does not have complete correspondence with other methods. This ideogram was constructed with 5 prophase I, 6 prophase II, 2 prophase III, and 0 prophase IV

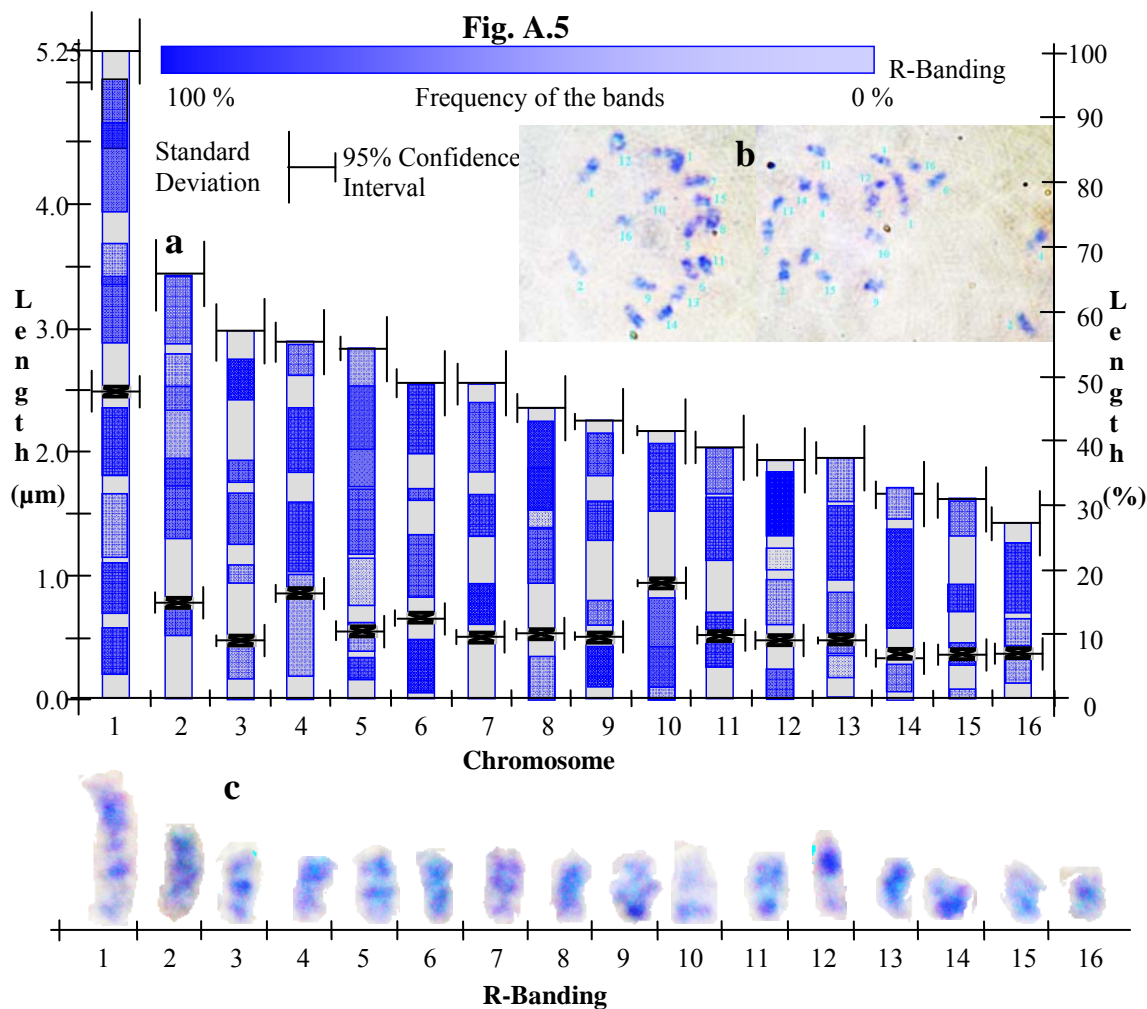


**Fig. A.5.** Ideogram (a), chromosome spread (b), and karyogram (c) of the honey bee karyotype stained with giemsa after the method of Sumner (1993) to detect the R-banding. The banding produced by this method is very good, the problem is the chromosome classification, because the bands generated are not completely correspondent to the DAPI and  $\text{BaOH}_2$  inter-bands. The reason was that, contrary to other methods, the metaphase and pre-metaphase chromosomes were better banded because they tolerate better the conditions of the procedure. However, sometimes the C-band was not completely digested and was also differentially stained as in C3, and C9. This ideogram was constructed based on 0 prophase I, 2 prophase II, 5 prophase III, and 0 pre-metaphase spreads.

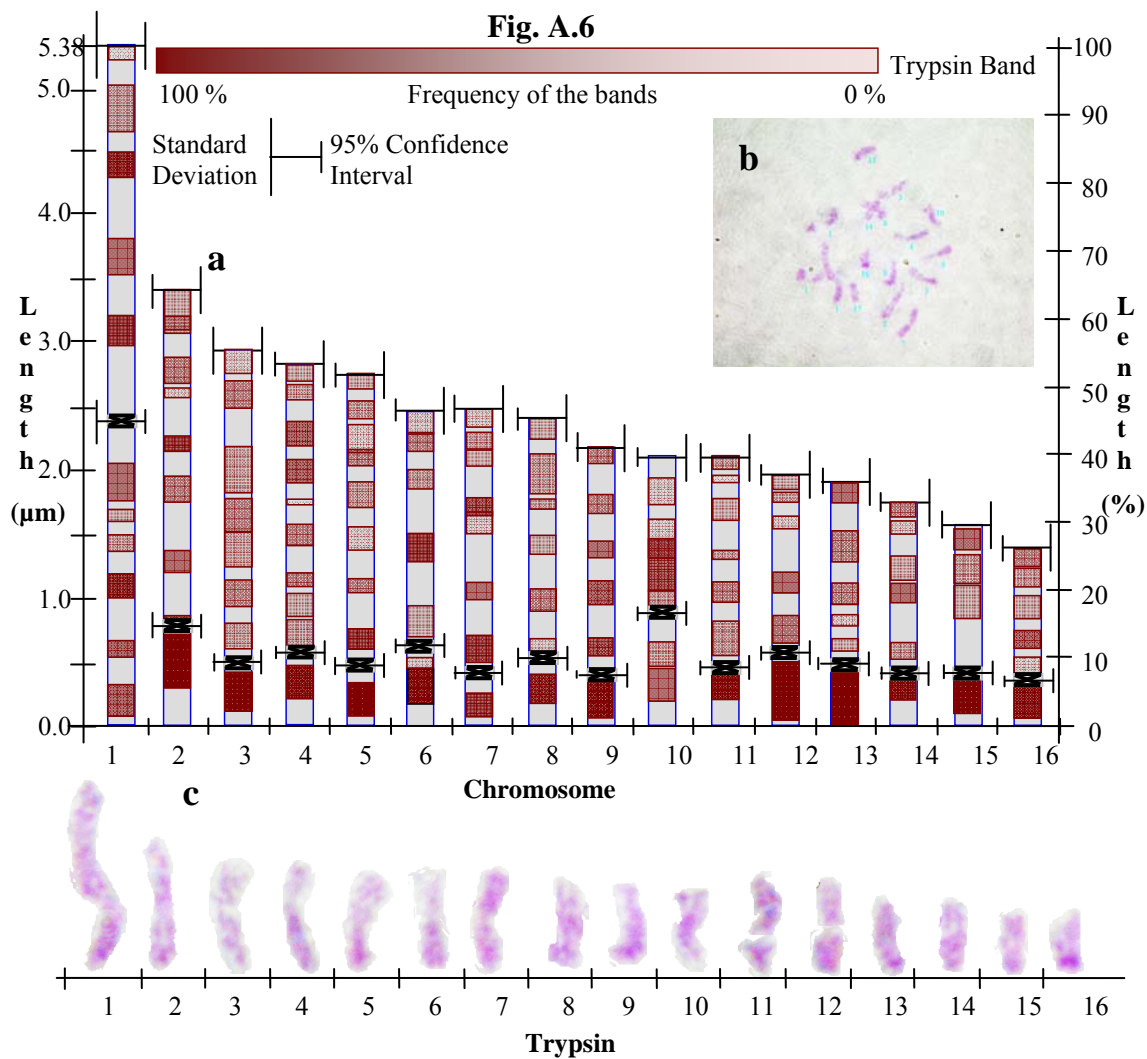


**Fig A.6.** . Ideogram (a), chromosome spread (b), and karyogram (c) of the honey bee karyotype stained with giemsa after the method of Seabright (1971) for trypsin-banding method. As the giemsa staining, this method did not produce a clear banding pattern in all chromosomes, the banding was dependant on the stages of prophase and highly variable. In consequence, the number of bands detected was higher than with any other method. Better banding was obtained in early prophase (PI and PII). Notice that pericentromeric band is not clearly contrasted. This banding pattern seems to be characteristic for each chromosome, but it is difficult to compare it with other methods because of their very low correspondence. Since the bands are very variable and numerous, it requires a very high number of spread to provide confidence in this banding pattern. The ideogram was constructed based on 2 prophase I, 5 Prophase 2, 5 prophase III, and 0 prophase IV.

## A.2

### **GENERATION OF AN INTEGRATED KARYOTYPE OF THE HONEY BEE (*Apis mellifera* L.) BY BANDING PATTERN AND FLUORESCENT *IN SITU* HYBRIDIZATION: ADDITIONAL OBSERVATION ABOUT CHROMOSOME CONDENSATION DURING PROPHASE**

#### **Introduction**

Chromosomes are visible rod-like structures consisting of tightly coiled DNA and supporting proteins called chromatin. Found in the cell nucleus of plants and animals, chromosomes condense to maximum levels during cell division in order to facilitate reproduction and cell division. The chromosomes differentiate in characteristic domains in the form of chromosome bands. These bands reflect nucleotide composition and condensation can be enhanced in cytogenetic preparations with staining techniques (Craig and Bickmore, 1993). Thus staining can differentiate chromosome domains. Called nodes in the early literature (McClintock, 1931), these domains were renamed as positive heterochromatin (chromosome regions stained) or negative heterochromatin (chromosome region not stained) (Takehisa, 1976). And, although the term heterochromatin (positive) and euchromatin (negative) was recognized by Heitz in 1928 (Sumner, 2003), it was in the 1960s that banding techniques and the banding concept was developed by T. Caspersson (Caspersson, 1989). Since chromosome banding demonstrated consistency, it was confidently used for chromosome classification and identification - especially for clinical uses (Caspersson, 1989). Given the clinical and other uses of banding, a common banding nomenclature was necessary. Several nomenclatures and definitions were used before the one agreed upon as the International Standard Chromosome Nomenclature (ISCN) in 1981 (ISCN, 1981).

Since its creation in 1976, the ISCN recognized difficulties in the chromosome and banding classification due to the variability in the resolution and dynamics of banding during prophase (ISCN, 2005). These problems were also detected by the

different banding techniques, making it necessary to periodically review and update the chromosome and banding classification (ISCN, 2005). Coincidentally, in the decade of 1970s, the variation and dynamics of chromosome banding were intensively studied, especially in mammals (Sen and Sharma, 1985; ISCN, 2005) and sporadically in insects (Belmont et al., 1989) and plants (Takehisa, 1976).

Chromosome banding during the progression of prophase is seen not only as a reduction of the number of bands and growth of heterochromatin bands, but also as variation and reorganization during condensation, and specially in R-bands (Craig and Bickmore, 1993). In *Vicia faba*, heterochromatin bands become euchromatic twice during mitotic prophase, but the number of bands remain unchanged or reduce gradually in number (Takehisa, (1976). Human chromosomes, show the appearance and disappearance of bands reported in *V. faba* also show variation in the size of the bands. The relative positions of bands were in agreement with the ISCN nomenclature, but the size of bands differed during the different stages of prophase. Something interesting was an intercalated euchromatic band that was present within an otherwise heterochromatic region. Observed at different prophase stages, band dynamics was considered important for detection of abnormalities (Richer et al., 1983). Thus there are bands that fuse during prophase and become thicker and darker; there are inter-bands or heterochromatic bands that retain their size during prophase and throughout condensation (Sen and Sharma 1985).

The appearance and disappearance of bands is a common phenomenon during condensation stages of prophase and is part of the dynamics of the chromosome. R-bands are the most dynamics in this process (Craig and Bickmore, 1997). Condensation and decondensation of the chromosomes are not random events. They start on discrete sites, which depend on the kind of chromatin and the original location of the chromosome in the nucleus. Elongation can be bidirectional or not (Hiraoka et al., 1989; Li et al., 1998). The total number of bands depends on the degree of resolution. The maximum band number depends on visualization of the chromosomes during the early stages of prophase; the number at any given stage, however, depends on the dynamics in

band evolution in R-banding regions, methods of staining, and differentiation of the cells. Thus “although homologous chromosomes are similarly shaped, they rarely have exactly the same banding patterns or lengths” and this dynamic has important implications in gene expression and DNA replication and is described by as the foci factories model (Cook, 1995; Chuang and Belmont, 2005).

The primary function of the chromosome condensation is to reduce the size of the chromosomes to facilitate the proper separation and segregation of sister chromatids (Belmont, 2006). However, facilitating the genome reprogramming at certain development stages is seen as an additional function of heterochromatin banding in eukaryotic cells (Belmont, 2006). Condensation of the chromosome in mitotic prophase is mostly linear (Belmont, 2006); but condensation is not a continuous event (Kireeva et al., 2004). Several pauses, separated by plateau phases, can be observed during this process, and the relative position of the chromosomal markers can be modified (Kireeva et al., 2004; Maddox et al., 2006). Prophase of human chromosomes can be divided in four stages separated by three specific structural transitions represented by pauses (Kireeva et al., 2004). The second transition separates the early prophase and the middle prophase, the third separates the late prophase and metaphase (Kireeva et al., 2004).

Based on micromechanics of chromatin, and chromosomes studies (Marko and Poirier, 2003), Belmont (2002) developed a hierarchical folding model for chromosome structure. The model assumes that condensation of mitotic chromosomes is not a continuous event, but rather depends on a large number of local interactions. There are dynamics in the protein assembly distribution, where histone modification (Ito, 2007) and specific DNA sequences called scaffold associated regions (SAR), related to bands or chromosome domains (Hart and Laemmli, 1998), play an important role in chromosome condensation and chromosome morphology during cell division (Belmont, 2002). Given the emerging evidence that the micromechanics of chromosomes is important in gene expression (Hart and Laemmli, 1998; Belmont et al., 1999; Belmont, 2002, Nowak and Corces, 2004; Ito, 2007) and epigenetically regulated (Nowak and

Corces, 2004), even in insects (Bongiorni et al., 2007), we compare here the banding patterns in different prophase stages in the fully sequenced strain of the honey bee.

## **Materials and Methods**

The method for preparing chromosomes spreads and DAPI staining has been described in previous chapters. The basic staining technique was DAPI and the stages of prophases were determined following the general observation of Kireeva et al. (2004). Adjustments from absolute to relative length were and confidence intervals for the mean of the chromosome bands were determined as described in chapter I. The data file was that used in the final karyotype description.

### **Ordering of bands**

The bands of the prophase I (early prophase) and prophase II (middle prophase) were ordered by similar size and position, using the middle point of each band. Each band was first quantified by taking the distance from the telomere of the short arm to the start point of the band. The end point of the band was similarly measured and the midpoint and range determined. Once sorted into bands with similar midpoint and range, the number of band was generated. Prophase III (Late prophase) and prophase IV (pre-metaphase) bands were ordered following the band dimensions obtained from Prophase I and II. As bilateral and unilateral growing of some bands in the later stages of prophase were detected, some adjustments were necessary. When unilateral growth, one side of the band was generally approximately constant and that value was used as reference to place the band. When several bands were fused or bilateral growing was observed, the measure of the first and last band matched with the end and start of external band, these values were used to place the block. When the block terminates into euchromatic bands, the blocks were placed using the most proximal bands as reference.

In order to validate the criteria used to sort the bands, more than five chromosomes from five different spreads must present evidence of the number of bands

determined for early prophase. To validate a new band, the band must be detected in more than three chromosomes, in a new location, with no evidence of overlap when first detected, although in the subsequent stages they may appear fused or engulfed a proximal band. The sorting procedure used usually accommodates automatically the new bands, therefore, the criteria mentioned was used as a reference to verify a chromosome band once mapped on the ideogram. When a band forms by fusion of one or more bands, it usually shows slight constrictions that delimiting the edges., Once the bands are sorted and assigned, means, standard deviation and confidence of intervals for the start and end point of each bands was calculated and these statistics used to map the bands and obtain the ideogram. Addition of the start and end point of each band completed their characterization..

Analysis of the band of two randomly selected chromosomes shows the dynamic position of bands and the condensation pattern in the selected chromosomes. Since all chromosomes show that characteristic, the result for the two chromosomes used as example can be extended to the rest of the chromosomes. To further support the banding dynamics hypothesis, the map location of the Solignac BAC 1F2 (Acc # AJ509634) (Solignac et al., 2004) on chromosome 1 is described in detail.

## **Result and Discussion**

Plots of the sorted data by phase and cell, shows three different patterns of condensation, the exponential pattern best fits early prophase (Prophase I) and the end of the pre-metaphase (Prophase IV), with a linear fit from prophase II to the first half of pre-metaphase (Fig. A.2.1). These patterns suggest that the chromosomes condense exponentially in early prophase and again immediately before metaphase. During the majority of the time, between early prophase and metaphase, condensation takes place in a linear fashion with several pauses indicated by several plateau throughout that period.

This temporal change in the banding pattern is very important because it describes, in some detail, the dynamics of chromosome condensation and



heterochromatinization. The banding pattern dynamics during prophase best fit a cubic model ( $y = \alpha + \beta_1x + \beta_2x^2 + \beta_3x^3 + e$ ) (Table A.2.1). Short arms consistently fit less well to any model because of their relatively high variability. However, the larger the short arm, the better the fit as is seen for chromosomes 1, 2, 4, 6, 10, and 12. The least squares estimates for the all tested model ( $\alpha, \beta_i$ ) are specific for each arm and chromosome (Fig. A.2.1).

**Table A.2.1.** Parameter estimates and fit (R-square) for different descriptive models of honey bee chromosome size reduction through the prophase.

Model	Variable	$\alpha$	$\beta_1$	$\beta_2$	$\beta_3$	R	R-Square
Linear	Length	3.290	-0.936			0.936	0.876
	Long Arm	2.435	-0.930			0.930	0.864
	Short Arm	0.856	-0.938			0.938	0.878
Logarithmic	Length	5.153	-0.983			0.983	0.966
	Long Arm	3.867	-0.985			0.985	0.969
	Short Arm	1.288	-0.958			0.958	0.917
Cubic	Length	4.013	-3.786	6.159	-3.398	0.982	0.964
	Long Arm	3.006	-3.834	6.189	-3.370	0.980	0.960
	Short Arm	1.008	-3.548	5.919	-3.405	0.973	0.946

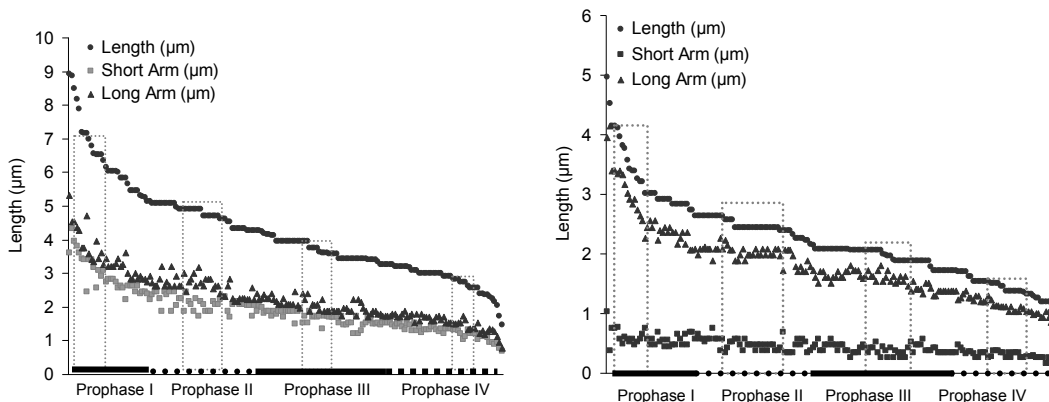


**Fig. A.1.1.** Trend lines for total length (●), long arm (▲) and short arm (■) for (a) chromosome 1 and (b) chromosome 7. The dotted bars in the graphs represents confidence intervals at that stage of prophase for each variable.

The absolute and relative length of chromosomes and their arms at all stages were negatively correlated with total heterochromatin content ( $r = -0.329, -0.248, -0.321$ ;  $p < 0.000$  respectively) and with the amount of pericentromeric heterochromatin ( $r = -0.530, \text{ and } -0.521$ ;  $p < 0.000$  respectively). However, the same variables (length of chromosomes and arms) were positively correlated with number of bands ( $r = 0.437, 0.246, \text{ and } 0.446$ ,  $p < 0.0001$  respectively). More heterochromatin equates to shorter chromosomes and arms, and yet shorter chromosomes have smaller numbers of discrete bands of heterochromatin. This seeming contradiction reflects the different effect of constitutive and facultative heterochromatin. Long and short arm lengths were negatively correlated with constitutive heterochromatin amount ( $r = -0.514 \text{ and } -0.271$ ,  $p = 0.000$  respectively), and positively correlated with facultative heterochromatin amount ( $r = 0.084, \text{ and } 0.293$ ;  $p < 0.000$  respectively). Thus chromosome condensation is significantly and inversely influenced by facultative and constitutive heterochromatin during prophase. Most of the constitutive heterochromatin in honey bee chromosomes is located in the pericentromeric region, which showed little growth during prophase. However the location of the bands reveal that the reduction of chromosome length is influenced by this region and by sub-telomeric regions.

To explain the condensation pattern observed, honey bee chromosomes, C1 and C7 will be used as examples. In Figs A.2.2 and A.2.3, the start and the end of bands in C1 and C7 are graphed by phase in two directions; from the distal band (telomeric) to the centromere in the short arm and from the centromere to the distal band (telomeric) in the long arm. The first band (p42, Fig. A.2.2a), in the sub-telomeric region of the short arm of C1, grew in both directions throughout the stages of prophase. The next band (p41, Fig. 4b) also grew in both directions. Band p31 grew in both directions, but at a very low rate (Fig. A.2.2c). Bands, p41 and p31, apparently change position toward the telomere; while band p21 is pulled toward the centromere (Fig. A.2.2d and e). The pericentromeric band p12.1 does not show visible change, and even seems to be pulled a little toward the adjacent q12.1 band that shows a very low growth rate in both

directions. Thus the euchromatic region next to p12.1 seems to experience condensation without significant heterochromatinization.

The forces that act between centromeric and telomeric regions can be observed even more clearly in the long arm of the C1, where the end of the pericentromeric band q13 and the start of the band q21 (Fig. A.2.2f) show evidence of opposite forces acting between them, with consequent expansion of the band toward the centromere and toward the telomere, an effect also observed for bands q41 and q42 (Fig. A.2.2h) and q22 and q31 (Fig. A.2.2g). In chromosome 7, a highly banded chromosome, band q31 experiences the action of opposite forces – one that comes from the pericentromeric band (Fig. A.2.3a and b) and bands q21 (Fig. A.2.3c), and the other from the telomeric and sub-telomeric band q31. An adjacent band q32 grew a little in both directions but narrows in the first three stages of prophase and finally increases in relative width in PIV (Fig. A.2.3d). The next band, q33b, is consistently pulled toward the telomeric region (Fig. A.2.3e). As in C1, the pericentromeric and telomeric regions of chromosome 7 do not show significant growth through prophase but seem to pull bands toward them. These results suggest that very strong condensation is taking place in those regions but is not accompanied by heterochromatinization, which explains the low growth and even reduction in size of some bands.

The results further suggest that condensation and heterochromatinization are two different characteristics of the chromosomes that interact to reduce chromosome size during prophase. Condensation occurs in specific spots on the chromosomes - usually the pericentromeric and sub-telomeric regions and the overlapping bands close to subtelomeric regions, although other bands may play an important role in this process. At least a portion of the variation in the chromosome size, arm ratio and band position in prophase chromosomes is explained by this phenomenon, as shown in Fig. A.2.2, where alternating periods of high and low variability in chromosomal arm lengths are observed.

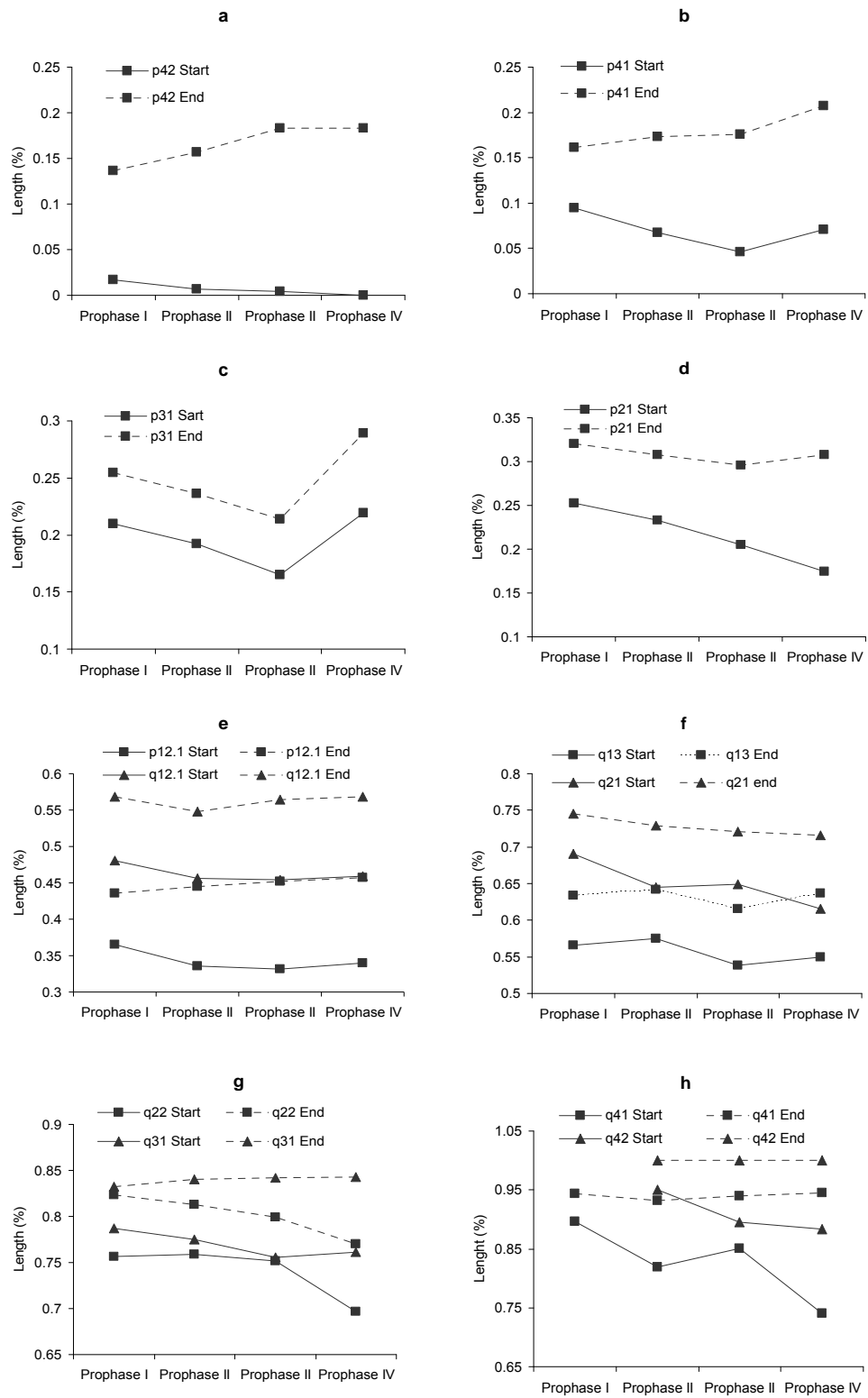


**Fig. A.2.2.** Start and end (range) of bands of chromosome 1 at fourth stages of prophase.

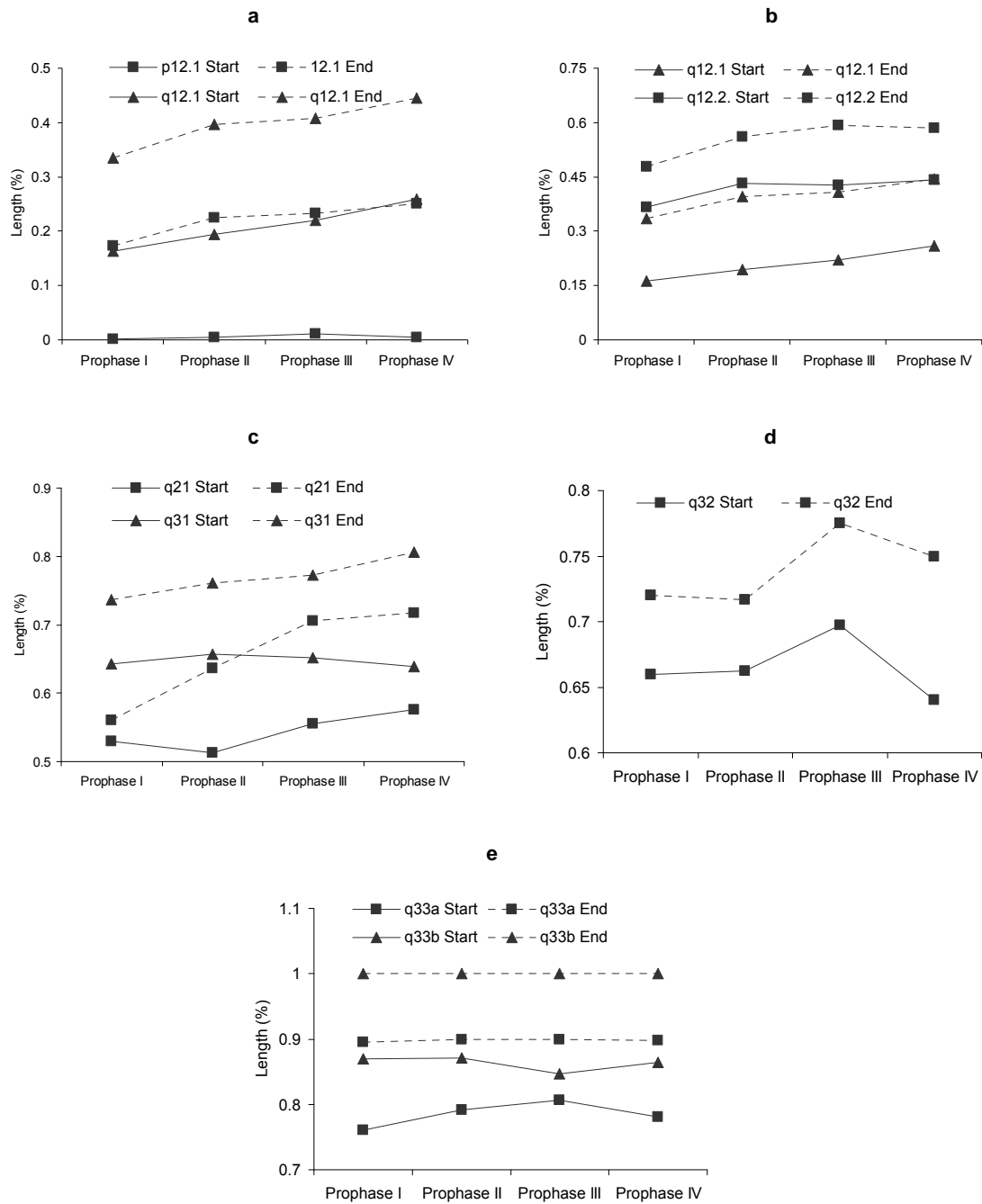


**Fig. A.2.3.** Start and end (range) of bands of chromosome 7 at fourth stages of prophase.

Additional evidence of chromosomal dynamics is seen in the position of BAC 1F2 in C1q. 1F2 is one of the few BACs for which hybridization in two places is confirmed, and data were collected from three of the four prophases. 1F2 hybridizes to both sides of band q31, which grows in both directions and is affected by the condensation and heterochromatinization occurring in subtelomeric and centromeric regions. It is clear in the ideograms that the position of the distal signal at band q41 where the BAC was mapped, does not change in different stages of prophase. However, the more proximal signal apparently follows the position of q31 (Fig. A.2.4).

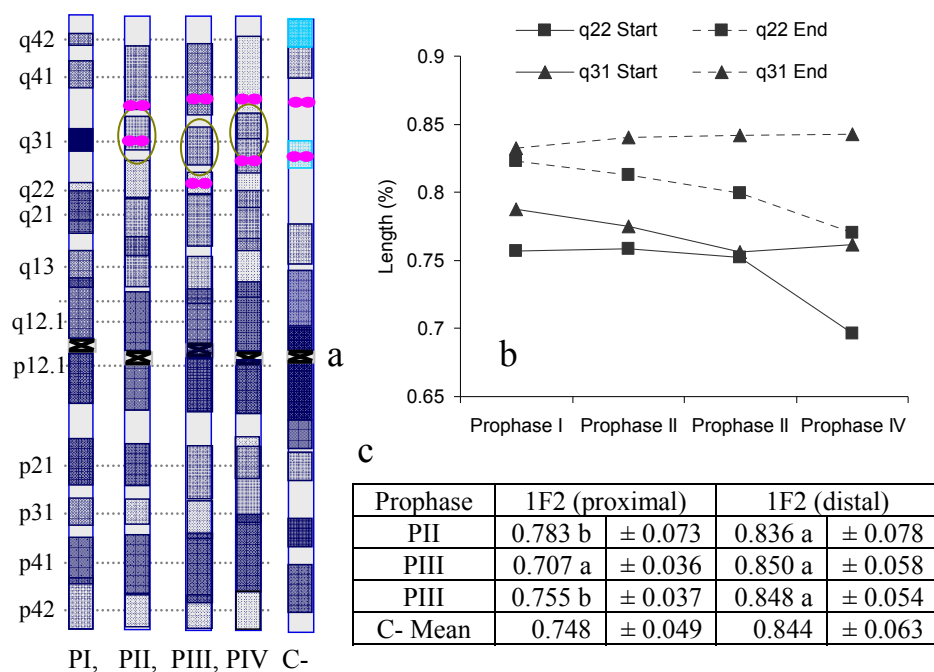


**Fig. A.2.4.** Relative position of IF2 at different stages of prophase on the DAPI- and the C-banding (C-) ideograms of C1 and. (a) Comparative ideograms showing the positions of IF2 signals during prophase (PII, PIII, and PIV), (b) graphic of bands q22 and q31 showing the dynamics of these bands. (c) Relative position of 1F2 at different prophase stages.

## Discussion

The data suggests that chromosome condensation takes uniquely in each chromosome, influenced by the banding patterns that consequently affect the length of the chromosomes and their arm ratio. The observed variation could be due to variable chromatin domains, and the nucleotide composition and proteins associated with these domains. Although chromosome length reveals a definite pattern of reduction of chromosome size, that reduction is nonlinear throughout prophase even though, the majority of the period between prophase I and prophase IV is linear with several pauses, which are vary in number and time between chromosomes, which agrees with observations by Belmont, (2006) and Kireeva et al. (2004). Chromosomes 5, 7 and 12 show a gradual decrease in arm ratio from PI to PIV, while the arm ratio of chromosomes 6, 8, 9, 11, 13 and 14 is consistently lower in PI than in PII-PIV. Banding patterns also show chromosome specific patterns of condensation (Figs. 4 and 5). In agreement with observations of Hiraoka et al. (1989) and Li et al. (1998), they banding patterns often progress from preexisted heterochromatin. In other cases preexisting heterochromatin can work as a barrier to the heterochromatinisation, as happened with the pericentromeric heterochromatin of the short arm of the C1. Some bands show variation in size that implies a particular condensation behavior through prophase. For example, band q21 of C6 and q31 in C1 remain almost static through prophase; while bands q3 and q2 of C7 are very active and increase in size throughout prophase. Other bands, such as q13 in C11 are not visible until later stages of prophase, while others, such as q21 of C12 experience reduction. The entire chromosome banding pattern shows that there are a fixed number of bands that serves as condensation and heterochromatinisation spots. Usually these bands are formed from one, two or several overlapping bands. Consistently, with some little variation in the frequency of the observed bands, the pericentromeric heterochromatin of the long arm, q12.1 and q12.2 of all chromosomes seems to be the primary spots of condensation and

heterochromatinisation. The honey bee chromosomes except for C10 and C15 showed at least two centers of condensation and heterochromatinisation. The second center is usually a middle band or several distal bands (Table A.1.1). However there are some singlet bands that work as centers, including q31 in C2 and C3 and q21 in C6. The single and overlapping bands that experience growth or reduction could be considered regulatory heterochromatin bands that could function in gene expression - silencing genes when they propagate and activating genes when they recede (Grewal and Jia., 2006).

These and other examples show that condensation of the chromosome can be expected to be variable and chromosome specific, and that the constitutive and facultative heterochromatin banding reflects this individuality. Physical evidence that condensation of heterochromatin is complex and dynamic; the process is similar to that earlier mentioned by Richer et al. (1983), Sen and Sharma (1985), and Craig and Bickmore, (1993). That complexity explains indirectly how it is possible that an alteration in control of the heterochromatinization in pre-existent bands will lead to abnormalities. In humans, aberrant DNA methylation in the 2q14.2 band alters the pattern of histone modification and leads to cancer (Smith and Costello, 2006). In mammals in general, IGF2 gene expression is controlled by chromosome modeling, and heterochromatin silencing can as a consequence result in multiple diseases, such as breast and prostate cancer (The National Cancer Institute Breast and Prostate Cancer Cohort Consortium, 2005). Alteration of heterochromatin modification in bands surrounding the IGF2 gene is characteristic of the loss of imprinting that leads to Wilms Tumor in children (Ravenel, 2001), or to important effect on meat production in domestic animals (Nezer et al., 1999). In honey bee this heterochromatin plasticity could be related to systematic change of specialization in workers throughout their lives Queller (2003).

It is generally accepted that heterochromatin protein (HP), a variant of H2A and H3 histones (Malik and Henikoff, 2003) has an important role not only in heterochromatinization (HP1) but also in epigenetic silencing of gene expression (H3 methylation / acetylation) and centromere function (CenH3s variants) (Malik and



Henikoff, 2003, Maizon and Almouzni, 2004), although not specifically chromosome banding. Molecular evidence of heterochromatin function has been reported in plants (Houben et al., 1999) and animals (Maddox et al., 2006). There is also evidence that certain segments of the chromosomes with different sequences and protein systems are involved in heterochromatin formation. Variation in that composition will shape different heterochromatin domains (Dietzel and Belmont, 2001). It is possible that an irregular distribution of these domains disrupts banding pattern morphology at later stages of prophase and metaphase, making chromosome characterization and identification difficult. Thus, the use of the prophase chromosomes, a large number of chromosome spreads, and several different banding techniques is justified and necessary in small chromosomes with irregularly banded chromosomes.

The entire chromosome banding pattern shows that there are a fixed number of bands that serves as condensation and heterochromatinization sites. Usually these bands are formed from one, two or several overlapping bands. Consistently, with some little variation in the frequency of the observed bands, the pericentromeric heterochromatin of the long arm, q12.1 and q12.2 of all chromosomes seems to be the primary center of condensation and heterochromatinization. The honey bee chromosomes except for C10 and C15 showed at least two centers of condensation and heterochromatinization. The second center is usually a middle band or several distal bands (Table A.1.2). However there are some singlet bands that work as centers, including q31 in C2 and C3 and q21 in C6. The single and overlapping bands that experience growth or reduction could be considered regulatory heterochromatin bands that function in gene expression - silencing genes when they propagate and activating genes when they recede (Grewal and Jia., 2006).

**Table A.1.2.** Bands that apparently serving as center of heterochromatinization and condensation in the honey bee chromosomes

Bands	Chromosomes
q21-q22	1, 12, 14 and 16
q21-q31	11 and 13
q31-q32	4, 6 and 8
q31-q33	5, 7 and 9
q41-q42	1, 2 and 8
q51-q52-q53	2 and 3

**Table A.1.** Summary of data for location, position, and comparisons with the location and position in the different version of NCBI-Map Viewer

BAC	Chromosome and Position				Significance for Matching Position						Expected Chromosome Locatio	Match for Position				Match for chromosome				Frequ ency	Score				
	Chro	Pos	Std Dev	N	MV1		MV2		MV3			MV4	MV1	MV2	MV3	MV4	MV1	MV2	MV3			MV4			
11A3	3	0.824	0.0113	5	0.33	***	0.795	NS	0.795	NS	0.1846 and NP	3	2	2	2 and NP		√	√		√				√√	5
1A8	1	0.242	0.024	4	0.197	NS	0.572	****			0.211	2	6		16 and NP	√			√						2
1A8	2	0.374	0.108	14	0.197	***	0.572	****			0.211	2	6		16		√		√					√√	4
1A8	3	0.472	0.068	4	0.197	***	0.572	NS			0.211	2	6		16		√								1
1A8	6	0.319	0.093	9	0.197	***	0.572	****			0.211	2	6		16				√		√			√√	4
1A8	7	0.612	0.076	4	0.197	***	0.572	NS			0.211	2	6		16		√								1
1A8	8	0.534	0.083	5	0.197	***	0.572	NS			0.211	2	6		16		√								1
1C6	1	0.545	0.193	4	0.484	NS	0.571	NS	0.417	NS	0.476	2	6	6	6		√	√	√						3
1C6	2	0.789	0.127	10	0.484	***	0.571	***	0.417	***	0.476	2	6	6	6	√				√				√√	4
1C6	3	0.825	0.107	4	0.484	****	0.571	****	0.417	****	0.476	2	6	6	6										0
1C6	6	0.758	0.160	4	0.484	****	0.571	****	0.417	****	0.476	2	6	6	6						√	√	√	√	4
1C6	7	0.904	0.053	4	0.484	****	0.571	****	0.417	****	0.476	2	6	6	6										0
1C6	8	0.703	0.154	5	0.484	****	0.571	****	0.417	****	0.476	2	6	6	6										0
1F2	1	0.795	0.091	21	0.198	****	0.868	**	0.757	NS	0.755 and NP	1	1	1	1			√	√	√	√	√	√	√	7
1F2	1	0.869	0.073	17	0.198	****	0.868	NS	0.868	NS	0.865	1	1	1	1			√	√	√	√	√	√	√	7
1F6	11a	0.883	0.0375	4	0.111	****	1E-04	****	1E-04		0.024 and NP	8	9	9	10 and NP										0
1F6	8a	0.508	0	16	0.89	****	1E-04	****	1E-04		0.024 and NP	8	9	9	10 and NP					√				√√√	4

**Table A.1. (Continued)**

BAC	Chromosome and Position				Significance for Matching Position							Expected Chromosome Locatio	Match for Position				Match for chromosome				Frequency	Score			
	Chro	Pos	Std Dev	N	MV1		MV2		MV3		MV4		MV1	MV2	MV3	MV4	MV1	MV2	MV3	MV4					
1F6	8b	0.77	0.0757	8	0.89	****	1E-04	****	1E-04		0.024 and NP	8	9	9	10 and NP					√				√√	3
1F6	11a	0.291	0.0127	4	0.111	*	1E-04		1E-04		0.024 and NP	8	9	9	10 and NP	√									1
22F1	2	0.667	0.667	2	0.467	NS	0.419	NS	0.419	NS	0.533	14	16	NP	16	√	√	√	√						4
22F1	7	0.609	0.051	31	0.467	***	0.419	***	0.419	***	0.533	14	16	NP	16									√√	2
22F1	14	0.552	0.0858	22	0.467	NS	0.419	NS	0.419	NS	0.533	14	16	NP	16	√	√	√	√	√				√√	7
22F1	16a	0.651	0.0793	37	0.467	NS	0.419	NS	0.419	NS	0.533	14	16	NP	16	√	√	√	√	√	√		√	√√√	10
22F1	16b	0.884	0.884	10	0.467	***	0.419	***	0.419	***	0.533	14	16	NP	16						√		√	√	3
26F7	4	0.539	0.090	8	0.694	NS	0.295	***	0.273	***	0.4733 and 0.7176	3	2	2	2	√								√	2
2B11	1	0.189	0.017	2	0.916	****	0.114	*	0.114	*	NP	3	2	2	NP										0
2B11	9	0.465	0.332	2	0.916	***	0.114	***	0.114	***	NP	3	2	2	NP										0
2B11	2a	0.527	0.155	2	0.916	***	0.114	***	0.114	***	NP	3	2	2	NP						√	√			2
2D1	2	0.662	0.0169	20	0.372	****	0.772	NS	0.772	NS	0.186	2	2	2	2		√	√		√	√	√	√	√√	8
2D1	3	0.3	0.071	6	0.372	NS	0.772	****	0.772	****	0.186	2	2	2	2	√									1
2D1	5	0.529	0.1075	4	0.372	NS	0.772	**	0.772	**	0.186	2	2	2	2	√									1
2D1	6	0.687	0.078	7	0.372	****	0.772	NS	0.772	NS	0.186	2	2	2	2		√	√							2
2D1	8	0.831	0.0226	8	0.372	***	0.772	NS	0.772	NS	0.186	2	2	2	2		√	√							2
2D1	9	0.651	0.0989	24	0.372	****	0.772	***	0.772	***	0.186	2	2	2	2									√√	2
2D1	2b	0.927	0.063	20	0.372	****	0.772	****	0.772	****	0.186	2	2	2	2									√√	2
35D9	2	0.66	0.166	4	0.453	NS			0.806	**	0.211	14	NP	4	4										0

**Table A.1. (Continued)**

BAC	Chromosome and Position				Significance for Matching Position							Expected Chromosome Locatio				Match for Position				Match for chromosome				Frequency	Score
	Chro	Pos	Std Dev	N	MV1		MV2		MV3		MV4	MV1	MV2	MV3	MV4	MV1	MV2	MV3	MV4	MV1	MV2	MV3	MV4		
35D9	3	0.759	0.024	7	0.453	***			0.806	NS	0.211	14	NP	4	4			√						√√	3
35D9	6	0.9	0.191	2	0.453	***			0.806	NS	0.211	14	NP	4	4			√							1
35D9	16	0.254	0.0431	8	0.453	**			0.806	NS	0.211	14	NP	4	4									√√	2
36H10	4	0.604	0.123	7	0.366	**	0.593	NS	0.63	NS	0.299	13	10	10	10			√						√	2
36H10	7(6)	0.847	0.117	5	0.366	***	0.593	**	0.63	*	0.299	13	10	10	10										0
36H10	8	0.574	0.104	2	0.366	**	0.593	NS	0.63	*	0.299	13	10	10	10			√							1
36H10	10	0.584	0.115	4	0.366	****	0.593	NS	0.63	NS	0.299	13	10	10	10		√	√			√	√	√		5
37D2	7	0.658	0.110	4	0.602	NS			0.357	***	0.488	11	NP	7	7	√						√	√	√	4
37D2	11	0.737	0.124	5	0.602	**			0.357	***	0.488	11	NP	7	7					√				√	2
3F5	1	0.893	0.006	3	0.445	****	0.705	****	0.705	****	0.268	2	2	2	2										0
3F5	2	0.844	0.068	4	0.445	***	0.705	NS	0.705	NS	0.268	2	2	2	2		√	√		√	√	√	√		6
3F5	6	0.379	0.135	6	0.445	NS	0.705	***	0.705	***	0.268	2	2	2	2	√			√					√	3
3F5	9	0.666	0.064	5	0.445	NS	0.705	NS	0.705	NS	0.268	2	2	2	2	√	√	√							3
3H8	7	0.21	0.103	5	0.329	NS	0.643	****	0.714	****	0.025 and NP	11	7	7	9 and NP	√					√	√	√		4
3H8	11	0.174	0.062	5	0.329	****	0.643	***	0.714	***	0.025 and NP	11	7 and NP	7	9 and NP	√				√			√		3
3H8	11	0.512		5	0.329	****	0.643	***	0.714	***	0.025 and NP	11	8 and NP	7	9 and NP	√	√			√					3
3H8	8	0.166		5	0.329	****	0.643	***	0.714	***	0.025 and NP	11	7 and NP	7	9 and NP										
3H8	8	0.389		5	0.329	****	0.643	***	0.714	***	0.025 and NP	11	8 and NP	7	9 and NP	√									1
3H8	15	0.704	0.157	4	0.329	***	0.643	NS	0.714	NS	0.025 and NP	11	9 and NP	7	9 and NP		√	√							2

**Table A.1. (Continued)**

BAC	Chromosome and Position				Significance for Matching Position								Expected Chromosome Locatio				Match for Position				Match for chromosome				Frequency	Score
	Chro	Pos	Std Dev	N	MV1		MV2		MV3		MV4	MV1	MV2	MV3	MV4	MV1	MV2	MV3	MV4	MV1	MV2	MV3	MV4			
44B2a	8	0.843	0.093	6	0.023	****			0.964	NS	Tel	8	NP	9	9			√		√				√	3	
44B2b	11	0.32	0.084	3	0.023	***			0.964	**	Tel	8	NP	9	9	√									1	
49H2	4	0.58	0.097	13	0.942	****					0.375 and NP	6	NP	NP	7 and NP									√√	2	
49H2	8	0.505	0.051	2	0.942	****					0.375 and NP	6	NP	NP	7 and NP										0	
49H2	9	0.957	nd	nd	0.942						0.375 and NP	6	NP	NP	7 and NP										0	
49H2	11a	0.912	0.107	9	0.942	NS					0.375 and NP	6	NP	NP	7 and NP	√								√√	3	
49H2	11b	0.635	0.066	6	0.942	****					0.375 and NP	6	NP	NP	7 and NP									√	1	
4E8.	1	0.943	0.077	20	1	NS	1		1		0.995	1	1	1	1	√	√	√	√	√	√	√	√	√	√	9
56F6	1	0.228	0.076	16	0.397	NS	0.412	***	0.412	***	0.37	1	1	1	1	√	√	√	√	√	√	√	√	√	√	9
5B10	2	0.66	0.060	4	0.376	***	0.636	NS	0.636	NS	0.354	6	3	3	3		√	√							2	
5B10	6	0.652	0.099	16	0.376	**	0.636	NS	0.636	NS	0.125	6	3	3	3		√	√		√				√√	5	
5B10	14	0.676	0.019	3	0.376	*	0.636	NS	0.636	NS	0.125	6	3	3	3		√	√							2	
5G9	4	0.496	0.109	3	0.133	*	0.846	*	0.852	**	0.13	13	10	10	10										0	
5G9	6	0.473	0.164	3	0.133	*	0.846	***	0.852	***	0.13	13	10	10	10										0	
5G9	10	0.285	0.226	4	0.133	NS	0.846	****	0.852	****	0.13	13	10	10	10	√					√	√	√	√	5	
6B8	2	0.251	0.041	12	0.963	***	0.001	*	0.001	*	0.858	12	4	4	4										0	
6B8	4	0.425	0.0424	18	0.963	NS	0.999	***	0.999		0.858	12	4	4	4	√			√		√	√	√	√	6	
6B8	11a	0.588	0.1273	41	0.963	***	0.001	***	0.001	***	0.858	12	4	4	4									√√√	3	

**Table A.1. (Continued)**

BAC	Chromosome and Position				Significance for Matching Position							MV4	Expected Chromosome Locatio				Match for Position				Match for chromosome				Frequency	Score
	Chro	Pos	Std Dev	N	MV1		MV2		MV3		MV1		MV2	MV3	MV4	MV1	MV2	MV3	MV4	MV1	MV2	MV3	MV4			
6B8	11b	0.974	0.039	14	0.963	NS	0.999	NS	0.999	NS	0.858	12	4	4	4	√	√	√	√							4
6B8	12a	0.92	0.072	15	0.963	NS	0.001	***	0.001	***	0.858	12	4	4	4	√				√						2
6B8	12b	0.59	0.184	2	0.963	***	0.001	***	0.001	***	0.858	12	4	4	4					√						1
6B8	14a	0.54	0.082	28	0.963	***	0.001	***	0.001	***	0.858	12	4	4	4									√√		2
6B8	14b	0.852	0.105	18	0.963	***	0.999	***	0.999	***	0.858	12	4	4	4				√							1
6B9	1	0.646	0.041	3	0.882	**	0.839	**	0.806	**	0.191	11	11	11	11											0
6B9	3	0.921	0.0286	80	0.882	NS	0.839	NS	0.806	NS	0.191	11	11	11	11	√	√	√	√					√√√		7
6B9	7	0.505	0.077	3	0.882	**	0.839	**	0.806	**	0.191	11	11	11	11											0
6B9	12	0.811	0.1076	22	0.882	NS	0.839	NS	0.806	NS	0.191	11	11	11	11	√	√	√	√					√√		6
6B9	15	0.763	0.093	2	0.882	**	0.839	*	0.806	NS	0.191	11	11	11	11			√	√							2
6B9	11a	0.905	0.121	11	0.882	NS	0.839	NS	0.806	*	0.191	11	11	11	11	√	√		√	√	√	√	√	√		7
6B9	11b	0.583	0.085	3	0.882	*	0.839	*	0.806	*	0.191	11	11	11	11				√	√	√	√				4
6D11	1	0.774	0.095	18	0.146	****	0.868	NS	0.897	**	0.891	1	1	1	1		√		√	√	√	√	√			6
6F1	6	0.639	0.396	4	0.269	***	0.767	NS	0.767	NS	0.773	6	13	13	13		√	√	√	√						4
6F1	11	0.674	0.063	4	0.269	***	0.767	NS	0.767	NS	0.773	6	13	13	13		√	√								2
6G8	4	0.405	0.064	2	0.44	NS	0.576	***	0.606	****	0.396	6	3	3	3	√			√							2
6G8	5	0.469	0.0156	32	0.44	NS	0.576	NS	0.606	***	0.396	6	3	3	3	√	√		√					√√√		6
6G8	5	0.429	0.1471	6	0.44	NS	0.576	***	0.606	****	0.396	6	3	3	3	√			√	√						3
6G8	7	0.495	0.0064	27	0.44	NS	0.576	NS	0.606	*	0.396	6	3	3	3	√	√		√					√√		5
6G8	10a	0.42	0.055	5	0.44	NS	0.576	***	0.606	***	0.396	6	3	3	3	√			√							2
6G8	10b	0.886	0.167	5	0.44	****	0.576	**	0.606	NS	0.396	6	3	3	3			√								1
6H3	3	0.489	0.0134	17	0.372	****	0.625	**	0.594	NS	0.591	10	5	5	5											0
6H3	5	0.543	0.0205	16	0.372	***	0.625	NS	0.594	NS	0.591	10	5	5	5		√	√	√		√	√	√	√		7
6H3	6	0.971	0.043	20	0.372	****	0.625	***	0.594	****	0.591	10	5	5	5									√		1
6H3	12	0.993	0.026	15	0.372	****	0.625	***	0.594	****	0.591	10	5	5	5											0
6H3	16	0.575	0.372	15	0.372	NS	0.625	NS	0.594	NS	0.591	10	5	5	5	√	√	√	√							4
6H3	1a	0.074	0.058	39	0.372	****	0.625	****	0.594	****	0.591	10	5	5	5									√		1

**Table A.1. (Continued)**

BAC	Chromosome and Position				Significance for Matching Position								Expected Chromosome Locatio				Match for Position				Match for chromosome				Frequ ency	Score
	Chro	Pos	Std Dev	N	MV1		MV2		MV3		MV4	MV1	MV2	MV3	MV4	MV1	MV2	MV3	MV4	MV1	MV2	MV3	MV4			
6H3	1b	0.169	0.117	13	0.372	**	0.625	****	0.594	****	0.591	10	5	5	5									0		
6H3	1c	0.903	0.041	37	0.372	****	0.625	**	0.594	**	0.591	10	5	5	5									√	1	
6H3	7a	0.572	0.0339	26	0.372	***	0.625	NS	0.594	NS	0.591	10	5	5	5		√	√	√					√√	5	
6H3	7b	0.78	0.0955	22	0.372	****	0.625	NS	0.594	NS	0.591	10	5	5	5		√	√	√					√√	5	
7B4	1	0.21	0.101	7	0.788	****	0.235	NS	0.221	NS	0.175	1	1	1	1		√	√	√	√	√	√	√	√√	9	
7B4	9	0.75	0.113	3	0.788	NS	0.235	****	0.221	****	0.205, 0.945	1	1	1	1	√									1	
82B7	1	0.441	0.199	4	0.64	NS	0.229	*	0.229	*	0.205, 0.946	2	6	6	6	√									1	
82B7	2	0.476	0.122	11	0.64	***	0.229	****	0.229	****	0.32	2	6	6	6	√			√	√			√	√√	6	
82B7	3	0.469	0.140	4	0.64	***	0.229	*	0.229	*	0.32	2	6	6	6	√									1	
82B7	6	0.45	0.103	5	0.64	**	0.229	***	0.229	***	0.32	2	6	6	6	√			√		√	√	√		5	
82B7	7	0.545	0.103	4	0.64	NS	0.229	***	0.229	***	0.32	2	6	6	6	√									1	
82B7	8	0.653	0.105	5	0.64	NS	0.229	**	0.229	**	0.32	2	6	6	6	√									1	
82B7	11	0.413	0.089	2	0.64	*	0.229	*	0.229	*	0.32	2	6	6	6										0	
8A2	4	0.456	0.096	29																				√√√	3	
8A2	8 (11)	0.65	0.151	7																				√	1	
8H7	4	0.538	0.046	11	0.689	**	0.333	***	0.407	**	0.5	13	10	10	10				√					√	2	
8H7	5	0.685	0.113	6	0.689	NS	0.333	**	0.407	***	0.5	13	10	10	10	√									1	
8H7	6	0.542	0.123	4	0.689	NS	0.333	*	0.407	NS	0.5	13	10	10	10	√		√	√						3	
8H7	7	0.753	0.115	6	0.689	**	0.333	****	0.407	***	0.5	13	10	10	10										0	
8H7	8	0.74	0.1662	3	0.689	NS	0.333	*	0.407	NS	0.5	13	10	10	10	√		√							2	
8H7	10a	0.490	0.055	7	0.689	NS	0.333	*	0.407	NS	0.5	13	10	10	10	√		√	√		√	√	√		6	
8H7	10	0.808	0.106	27	0.689	****	0.333	****	0.407	****	0.5	13	10	10	10					√	√	√	√	√√	5	
8H8	1	0.405	0.0106	72	0.386	NS	0.386	NS	0.386	NS	0.574	1	2	NP	2	√	√	√	√	√				√√√	8	
8H8	2	0.596	0.085	9	0.386	*	0.386	*	0.386	*	0.574	1	2	NP	2				√		√	√	√		4	



**Table A.1. (Continued)**

BAC	Chromosome and Position				Significance for Matching Position							Expected Chromosome Location				Match for Position				Match for chromosome				Frequency	Score
	Chro	Pos	Std Dev	N	MV1		MV2		MV3		MV4	MV1	MV2	MV3	MV4	MV1	MV2	MV3	MV4	MV1	MV2	MV3	MV4		
8H8	4a	0.528	0.121	6	0.386	NS	0.386	NS	0.386	NS	0.574	1	2	NP	2									0	
8H8	4b	0.814	0.106	16	0.386	***	0.386	**	0.386	**	0.574	1	2	NP	2									0	
97B3	1	0.143	0.078	19	0.501	****	0.367	****	0.531	****	0.453	10	5	5	5								√	1	
97B3	3	0.606	0.1372	14	0.501	NS	0.5	NS	0.531	NS	0.453	10	5	5	5	√	√	√					√	4	
97B3	4	0.427	0.0707	6	0.501	NS	0.5	NS	0.531	*	0.453	10	5	5	5	√	√		√					3	
97B3	10	0.785	0.082	16	0.501	****	0.5	****	0.531	****	0.453	10	5	5	5					√				2	
97B3	6 (3a)	0.914	0.044	10	0.501	****	0.5	****	0.531	****	0.453	10	5	5	5								√	1	
97B3	7a	0.525	0.065	22	0.501	NS	0.5	NS	0.531	NS	0.453	10	5	5	5	√	√	√	√				√√	6	
97B3	7b	0.723	0.035	9	0.501	****	0.5	****	0.531	****	0.453	10	5	5	5									0	
57E10	4	0.477	0.122	9	0.187	***	0.133	***	0.183	***	0.811	16	11	11	11								√	1	
57E10	16	0.698	0.0431	8	0.453	**			0.806	NS	0.211	16	11	11	11	√		√					√	3	
57E10	12	1.		3	0.187	***	0.133	***	0.183	***	0.811	16	11	11	11										
5E2	2	0.848	0.071	5	0.717	*	0.367	***	0.55	**	3NP	12 and 15	4 and 15	4 and 15	4 and 15									0	
5E2	3	0.923	0.101	10	8E-04	****	1	NS	1	**	Tel and NP	12 and 15	4 and 15	4 and 15	4 and 15		√		√				√	3	
a5E2	4	0.618	0.078	5	0.316	****	0.555	*	0.555	NS	0.351	12 and 15	4 and 15	4 and 15	4 and 15			√			√	√	√	4	
5E2	11	0.761	0.1803	11	0.717	NS	0.367	***	0.55	*	0.351	12 and 15	4 and 15	4 and 15	4 and 15	√							√	2	
5E2	12	0.727	0.056	5	0.717	NS	0.367	***	0.55	*	0.351	12 and 15	4 and 15	4 and 15	4 and 15	√				√				2	

**Table A.1. (Continued)**

BAC	Chromosome and Position				Significance for Matching Position				MV4	Expected Chromosome Location				Match for Position				Match for chromosome				Frequency	Score		
	Chro	Pos	Std Dev	N	MV1		MV2			MV3		MV1	MV2	MV3	MV4	MV1	MV2	MV3	MV4	MV1	MV2			MV3	MV4
5E2	15	0.559	0.0632	19	0.316	NS	0.5	NS	0.5	NS	0.351	12 and 15	4 and 15	4 and 15	4 and 15	√	√	√		√		√	√	√√	8
5E2	9 (11b)	0.234	0.124	3	0.008	****	0.636	****	0.376	NS	0.351	12 and 15	4 and 15	4 and 15	4 and 15			√	√						2
5E2	14 (15b)	0.893	0.0179	17	0.717	*	0.367	****	0.55	****	0.351	12 and 15	4 and 15	4 and 15	4 and 15									√√	2
5E2	9 (7a)	0.94	0.076	5	8E-04	****	1	NS	1	**	0.351	12 and 15	4 and 15	4 and 15	4 and 15		√								1
5E2	7b	0.513	0.154	5	0.717	NS	0.367	NS	0.55	NS	0.351	12 and 15	4 and 15	4 and 15	4 and 15	√	√	√	√						4
rDNA	1	0.314	0.0196	77																					

**VITA**

Name: Gildardo Aquino Pérez

Place of Birth: Tlacoahuaya, Oaxaca, México

Address: C Xochío MZA 54 LT 55  
Barrio Pescadores 56367  
Chimalhuacán, Estado de México, México

Email Address: jaquino@colpos.mx and dm58gap72@yahoo.com

Education: B. S. in Agronomy, Universidad Autonoma Chapingo, Texcoco,  
Edo de México, México. December 1989

M. S. in Fruticulture, Colegio de Postgraduados, Montecillo,  
Texcoco, Edo de México, México. August 1991

Ph.D. in Entomology, Texas A&M University, College Station,  
December 2007